

MONITORING THE IMPACT OF BLANKET BOG CONSERVATION IN THE SOUTH PENNINE MOORS SPECIAL AREA OF CONSERVATION USING AN UNMANNED AERIAL VEHICLE

FINAL REPORT

MoorLIFE 2020



Prepared by:



Moors for the Future Partnership, (2021)

Suggested citation:

Clutterbuck, B., Yallop, A., & Thacker, J. (2021) Monitoring the impact of blanket bog conservation in the South Pennine Moors Special Area of Conservation using an Unmanned Aerial Vehicle. Nottingham Trent University & CS Conservation Survey.



MoorLIFE 2020

Published by MoorLIFE 2020, a Moors for the Future Partnership project in the EU designated South Pennine Moors Special Area of Conservation. Delivered by the Peak District National Park Authority as the lead and accountable body (the Coordinating Beneficiary). On the ground delivery was largely undertaken by the Moors for the Future staff team with works also undertaken by staff of the National Trust High Peak and Marsden Moor Estates, the RSPB Dove Stone team and the South Pennines Park (the Associated Beneficiaries).

Funded by the EU LIFE programme and co-financed by Severn Trent Water, Yorkshire Water and United Utilities. With advice and regulation from Natural England and the Environment Agency, and local advice from landowners.

Moors for the Future Partnership

The Moorland Centre, Edale, Hope Valley, Derbyshire, S33 7ZA
e: moors@peakdistrict.gov.uk w: www.moorsforthefuture.org.uk



MFF 50 2016-17 MoorLIFE 2020

Monitoring the impact of blanket bog conservation in the South Pennine Moors Special Area of Conservation using an Unmanned Aerial Vehicle

Final Report



Dr Adrian R Yallop
ary@calopteryx.com

Dr Jonathan I Thacker
jit@calopteryx.com



Dr Ben Clutterbuck
Nottingham Trent University
ben.clutterbuck@ntu.ac.uk

Contents

Acknowledgements	vi
Executive Summary	7
SECTION 1: INTRODUCTION	9
1.1 Background	9
1.2 MFF 50 2016-17 specifications	10
1.3 General notes on image classification	11
1.4 Structure of this document	13
SECTION 2: METHODOLOGICAL CONSIDERATIONS	15
2.1 Project ethos	15
2.2 Rationale for remote sensing and field surveys approaches adopted	15
SECTION 3: PHASE 1 – UAV IMAGE CAPTURE	20
Summary introduction to Phase 1 activities	21
3.1 Methods	22
3.1.1 Image data	22
3.1.2 Field data	23
3.1.3 Supervised Classification	24
3.1.4 Spectral separability analyses	24
3.1.5 Accuracy assessment	25
3.2 Results	26
3.2.1 Geometric accuracy of DSMs and orthomosaics	26
3.2.2 Field data	27
3.2.3 Image quality and supervised classification delivery	27
3.2.4 Class Separability	28
3.2.5 Accuracy assessment	44
3.3 Summary of Phase 1	46
SECTION 4: PHASE 2 – MAV IMAGE CAPTURE I	48
Summary introduction to Phase 2 activities	49
Objectives of Phase 2	50
4.1. Data sources and associated pre-processing	51
4.1.1 Image data	51
4.1.2 Field data	51
4.2 Analytical protocols	52
4.2.1 Special consideration: Shadow	52
4.2.2 Analytical approach	53
4.2.3 Systematic approach	55
4.3 Results	57
4.3.1 Spectral separability analyses (class separability)	57
4.3.2 Canonical Correspondence Analysis	57
4.3.3 Classification accuracy	58
4.3.4 Class separability and accuracy	76



4.4	Summary of Phase 2.....	78
SECTION 5: PHASE 3 – MAV IMAGE CAPTURE II		79
	Summary introduction to Phase 3 activities.....	80
	Objectives of Phase 3.....	80
5.1	Image data.....	81
5.1.1	Orthorectification accuracy.....	81
5.1.2	Potential impact of image processing procedures on image classification.....	82
5.2	Methods.....	84
5.2.1	Spectral separability of <i>Sphagnum</i>	84
5.2.2	Image classification: All species.....	85
5.3	Results.....	87
5.3.1	Sphagnum spectral separability.....	87
5.3.2	Image classification: All species.....	91
5.4	Summary of Phase 3.....	110
SECTION 6: PHASE 4 – CLASSIFICATION OF SPECIES GROUPINGS		111
	Summary introduction to Phase 4 activities.....	112
	Objectives of Phase 4.....	112
	Approaches for identifying species clusters.....	112
6.1	Exploratory analyses: Kinder.....	114
6.1.1	Methods.....	114
6.1.2	Results.....	117
6.2	Species grouping classification across all sites.....	124
6.2.1	Method.....	124
6.2.2	Results.....	125
6.3	Machine learning– random forest classification.....	142
6.3.1	Method.....	142
6.3.2	Results.....	142
6.4	Discussion.....	143
6.4.1	MFFP-defined groups.....	144
6.4.2	Mapping bare peat.....	145
SECTION 7: PHASE 5 – COMPARISON OF UAV/MAV/EO DATA		146
	Introduction.....	147
	Objectives of extension to Phase 4.....	147
7.1	Method.....	148
7.1.1	Image data.....	148
7.1.2	Field data.....	149
7.1.3	Image classification.....	149
7.2	Results.....	150
7.2.1	Image orthorectification accuracy.....	150
7.2.2	Image classification.....	150
SECTION 8: WP 5 – MONITORING CHANGES IN SURFACE WETNESS		162
	Introduction.....	163





Work Package 5.....	163
Objectives of WP5.....	163
8.1 Method	163
8.1.1 Thermal image data	163
8.1.2 Surface peat samples	164
8.2 Results	165
8.2.1 Thermal image data	165
8.2.2 Peat samples	165
8.2.3 Relationship between soil moisture and temperature.....	169
SECTION 9: WP 6 – MONITORING CHANGES IN EROSION AND ACCUMULATION	172
Introduction	173
Work Package 6.....	173
Objectives of WP6.....	173
9.1 Method	174
9.1.1 RGB imagery and elevation data	174
9.2 Results	174
SECTION 10: DISCUSSION, CONCLUDING REMARKS AND OVERALL RECOMMENDATIONS	178
10.1 Summary conclusions from each phase	179
10.1.1 Phase 1 – UAV Image Capture	180
10.1.2 Phase 2 – MAV Image Capture II	181
10.1.3 Phase 3 – MAV Image Capture II	184
10.1.4 Phase 4 – Classification of Species Groupings	185
10.1.5 Phase 5 – Comparison of UAV/MAV/EO Data	187
10.1.6 Work Package 5 – Monitoring changes in surface wetness	189
10.1.7 Work Package 6 – Monitoring changes in peat erosion and accumulation	190
10.2 Concluding discussion and summary recommendations	190
SECTION 11: REFERENCES	192
SECTION 12: ANNEXES	196
Annex A:.....	197
Strim A: Exclusions	197
Strim B: Exclusions	197
Strim C: Exclusions.....	198
Error matrices created during development in Phase 2.....	199
Annex B:.....	215
Re-examination of field data for 2020 classification	215
Annex C:	216
Error matrices created during spectral clustering	216



Acknowledgements

At completion of this project, we would like to thank all those at MFFP who have made it possible. Tia Crouch and Diarmuid Crehan deserve special mention for their competence in managing this project and help in bringing it home to a successful conclusion. In addition, thanks must go to all the other members of the MFFP team that have made it possible, not least to those who undertook the extensive field work and surveys required during its execution.



Executive Summary

In August 2017 Moors for the Future Partnership (MFFP) contracted Nottingham Trent University and CS Conservation Survey to undertake a project assessing the potential of remote sensing imagery to map vegetation change in response to conservation intervention. This report covers all aspects of that project, describes the imagery and processes used, the results obtained, and discusses their implications. It supersedes, and replaces, all annual interim reports. To ensure relevance to those working in peatland restoration this project was undertaken using data sources, software and techniques that would be expected to be accessible to all UK conservation agencies and NGOs.

Originally predicated on the utilisation of extremely high-resolution imagery (XHR) obtained from an unmanned aerial vehicle (UAV), this project expanded to include MAV (manned aerial vehicle) and orbital earth observation (EO) data. As a result, this document reports on the results obtained using examples of the majority of remote sensing imagery types available to the conservation sector. An extensive campaign of field data acquisition was undertaken with samples being recorded at over 7000 locations, each DGPS-logged to centimetre accuracy to enable precise geo-registration with image pixels. The desire to quantitatively detect change in vegetation using XHR imagery rationally precluded inclusion of established community and habitat typologies, so this project mapped to individual species. All image classification results were tested for accuracy using ground-truth data and should therefore provide a significant body of evidence to guide future projects.

UAVs offer potential advantages over MAVs, for example the ability to fly at short notice to suit needs and/or meteorological conditions. They also offer the potential for repeated seasonal coverage allowing the incorporation of phenological change into image classification processes, something that is likely to be prohibitively expensive using MAV platforms. The results gained here suggest that such platforms are potentially able to provide imagery suitable for classification (against the criteria tested here). However, operational factors, mainly flight times for complete coverage of large areas, can result in image quality degradation owing to changes in illumination and sun angle during capture. Their use, if image classification is required, can therefore only be realistically recommended for surveys over areas that can be captured in a single flight (typically <math><0.5\text{ km}^2</math> depending on platform/sensor combination used).

Commercially contracted MAV-captured digital 4-band imagery, at 5 cm ground sample distance (GSD), proved able to map common upland *species* to accuracies that might be usually seen using far broader classes. This would make it ideally suitable for use over wide areas. However, as errors in determining change between classified images are



generally assumed to be multiplicative it would be unwise to follow such baseline assessments by more than one subsequent monitoring round, without supporting ancillary survey data. The overall consistency of this kind of imagery was generally superior to that from UAVs, although a number of caveats to this are noted.

Mapping to vegetation groups defined by MFFP as applicable for conservation management planning and monitoring purposes increased levels of accuracy much further. These groups, based as they are on unambiguous field data, fully error-checked and providing a typology suited to MFFP needs, demonstrated successful remote sensing of vegetation for monitoring using 4-band MAV imagery.

The use of EO data, with larger GSDs, resulted in a marked reduction in classification accuracies when compared to MAV, although it must be acknowledged that these results will have been affected by the typology and field sampling protocols used. Even with that caveat this does indicate the application of EO imagery data for plant species mapping (except perhaps trees) is clearly going to be problematic in most habitats as very few species form single species stands of a size resolvable in such imagery.

Within the overall project scope, a series of additional objectives were set by MFFP. WP4 required mapping of bare peat: this has been found to be readily achievable to high accuracies (>90%). This would allow for reliable baselining and identification of areas revegetating after management intervention as well as worsening situations. Demonstration of the use of thermal data for soil moisture determination was undertaken in WP5 and this showed some success under the conditions tested. However, conceptual issues severely limit the value this might serve in monitoring, because it can only provide data in patches of bare peat, a small areal component of most moorland. Attempts explored in WP6 to utilise UAV-derived data to map erosion/accumulation were unsuccessful using the protocols tested, showing further development, testing and verification are required before it can be considered as operationally deployable.

This project has tested many approaches and imagery types. It shows that remote sensing, if executed properly, with extensive field support, using repeatable typologies and with full error appraisal can deliver detailed data as a key part of a monitoring programme. However, the accuracies achievable suggest it should not be deployed alone, but rather used in conjunction with other survey data as part of an integrated monitoring programme.



Section 1: Introduction

1.1 Background

Awareness of the importance of peatlands, for both habitat provision (e.g. Lindsay *et al.*, 1988; Joosten & Clarke, 2002; Bragazza, 2009) and long-term carbon storage and sequestration (Yu *et al.*, 2011; Scharlemann *et al.*, 2014), has increased markedly over the past few decades. In the UK, around 80% of such peatlands are defined as blanket bog, where the primary peat forming taxon historically was *Sphagnum* (Lindsay *et al.*, 1988).

Most areas of blanket bog in the UK are now classified as degraded with a reduced presence or, in many places, a complete absence, of the *Sphagnum* species responsible for peat formation (Tallis, 1987). This situation arises as a result of pressures including, *inter alia*: wildfire (Yeloff *et al.*, 2006); prescribed burning (Yallop *et al.*, 2006) and atmospheric deposition (e.g. sulphur compounds: Ferguson & Lee, 1983). The presence of *Sphagnum* is considered essential to creating and maintaining the moisture regimes necessary for the accumulation of partly-decomposed plant remains as peat. Therefore, the re-establishment of these mosses is seen as an important component in restoring the functioning and resilience of upland bog ecosystems.

Since 2003 MFFP have undertaken a range of restoration techniques on blanket bog across the moorlands of the Peak District National Park (PDNP) and the South Pennine Moors (SPM) Special Area of Conservation (SAC). These activities include revegetation of bare peat (MFFP, 2013), gully-blocking (Maskill *et al.*, 2015) and more recently, the re-introduction of *Sphagnum* (Caporn *et al.*, 2018).

Under MoorLIFE 2020, MFFP aims to diversify the vegetation assemblage of areas of blanket bog that have become dominated by single species such as cotton grass, purple moor grass and heather. The approach adopted by MFFP will mainly involve, but is not restricted to, the planting of *Sphagnum* propagules. Monitoring of the establishment of *Sphagnum* will be focussed in the first instance on a series of experimental catchments ('Field Laboratories') established on different blanket bog communities. Monitoring at these field laboratories involves measurements of water flow, water table, peat accumulation/ erosion, and vegetation survey.

Specifically, the overall aims of MFF 50 2016-17 are to:

1. Monitor land cover change across the Project area, including:
 - a. Increases in the extent of *Sphagnum* moss;





- b. Reductions in the dominance of cotton grass, purple moor grass and heather;
- c. Reductions in the extent of bare peat.

2. Monitor changes in surface wetness
3. Monitor rates of peat accumulation and erosion

The project recognises that monitoring such restoration activities is key to quantifying results and developing improved strategies. Many restoration projects are monitored intensively at the local scale by researchers 'on the ground', but as the area undergoing restoration expands, there is an increasing requirement for monitoring using less labour-intensive approaches such as remote sensing. Therefore, within the overall project aims, MFFP also identified a need to utilise small UAVs to capture multi-temporal imagery to monitor the impact of blanket bog conservation actions at a 'landscape scale', rather than using traditional site-based surveys.

1.2 MFF 50 2016-17 specifications

To develop such a monitoring programme in August 2017 MFFP contracted a consortium of Nottingham Trent University and CS Conservation Survey to supply services under '*MFF 50 2016-17 MoorLIFE 2020 - monitoring the impact of blanket bog conservation in the South Pennine Moors Special Area of Conservation using an Unmanned Aerial Vehicle*'.

The requirements of this project were defined in seven 'work packages':

- 1: Design of Monitoring Programme
- 2: Design of Data Preparation and Processing Protocols
- 3: Monitor Changes in the Cover of *Sphagnum* Moss
- 4: Monitor Changes in Cover of Vegetation and Bare Peat
- 5: Monitor Changes in Surface Wetness
- 6: Monitor Rates of Peat Accumulation and Erosion
- 7: Investigate the Relationship Between Ground and Airborne Data

It should be noted that within these general specifications, MFF 50 2016-17 has developed with experience gained, so the approaches used changed as the project progressed. As such the project has transitioned from being based on an assumption of

capabilities to refining objectives as actual data and results were obtained to define what could actually be achieved.

The numerous limitations of remote sensing approaches are frequently overlooked. The potential to map broad landscape-scale habitat classes such as conifer or deciduous forest, lake waters or grassland to modest accuracies, or for tasks such as identifying zones of chlorophyll anomalies within crops for agricultural disease/nutrient-deficit monitoring is well established. However, its usefulness for conservation monitoring of change within diverse habitats comprised of many plant species in mixed swards such as those present across MFFP's sites is unclear. In the majority of published academic studies, the subject area of this project would typically comprise one, or at most two, classes within a wider landscape classification.

The mapping of numerous subdivisions of landscape-scale classes is required to deliver MFFP's monitoring objectives, so this project had to develop in an area with a dearth of pre-existing knowledge. As such, MFF 50 2016-17 has provided a wealth of information, over and beyond an original expectation of simply reporting changes. This will help guide not only future MFFP restoration monitoring projects but hopefully others in the uplands of the UK and elsewhere.

1.3 General notes on image classification

It is not within the scope of this report to provide a full grounding in remote sensing techniques, but some background is provided as a guide to the inherent limitations of the processes used, to balance expectations about what is achievable and to judge the outcomes achieved. This is far from an exhaustive description, but rather a generalisation of issues considered relevant to this project.

Owing to one primary project objective, a demonstration of the ability to map *Sphagnum* species, together with a desire to obtain the highest repeatability during field data collection, the typology used throughout this project has simply been based on individual plant species as the identification of these is unambiguous (assuming surveyor competence). This decision was also deemed optimal for the use of XHR imagery, as most pixels will represent spectral signatures from single species.

However, this inevitably leads to a very high number of classes, and it is a statistical axiom that classification accuracies decrease as the number of classes increases. Spectral space (essentially a hypervolume of n dimensions, where n equals the number of bands in the imagery), in which classification algorithms cluster and then differentiate spectral classes, is finite. Overlaps at the boundaries of clusters inevitably propagate as class numbers increase, and there are simply fewer opportunities for a class to occupy relatively



discrete space. This problem is acute in detailed conservation monitoring programmes because the great majority of classes of interest are of vegetation and most plants are green. Therefore, spectral clustering and class differentiation is largely restricted to what can be achieved in one axis. This will reduce the number of classes we might reasonably expect to extract relative to one involving other land cover types.

The summary above holds if class frequencies are relatively balanced within a scene. It is more problematic if there is considerable unevenness in this factor. Parametric classification algorithms essentially fit statistical distributions to the values recorded in the sample training data to define spectral clusters for each class. These are then used to classify unknown pixels in the rest of the image. According to the central limit theorem, this distribution will represent the true spectral space with increasing accuracy in proportion to the square root of the number of training pixels that are available. In the context of this project this impacts rarer species more as the probability of classifying and mapping these well is unlikely owing to the paucity of training data for rare species. The creation of wide spectral classes owing to limited sample numbers means a high probability of overlap with more common classes. Allocation of class membership of unknown pixels within these overlaps is based on the probability that a pixel belongs to a class based solely on geometric distance from the 'centre' of overlapping clusters. The basic equation assumes that these probabilities are equal for all classes, and that the input bands have normal distributions. Therefore, rare classes are usually over-represented or 'over-mapped' in classified map outputs. Some algorithms allow manipulation of these probabilities based on frequency of occurrence in training data. However, for this to be valid, field survey would need to random, i.e. representing true class frequency on the ground. This is not always appropriate for conservation monitoring as rare, and often desirable classes from the perspective of the conservation effort, may not be recorded using such an approach. Indeed, because of this consideration, field sampling in this project was not undertaken using a randomised approach.

An optimised remote sensing project will therefore seek to determine limits to the species to be included in a mapping/monitoring programme, essentially trading off the number of classes for mapping accuracy. In this case, however, as is usual from the perspective of a monitoring program, it is frequently the rarer species that are of greatest conservation interest e.g. *Sphagnum* sp. on degraded peatlands. Related to this issue is consideration of how to treat records of such rare species (i.e. those that do not meet minimum sample numbers in the field data). These species are clearly present, yet their mapping is unlikely to be accurate. However, if they are not utilised, the classification and error assessment processes will be 'blind' to their occurrence. The pixels in which they occur in the image will be classified as something else, *but the user will be unaware of the fact*. This can be



thought of as ‘apparent accuracy’ because accuracy measurements are in reality no more than a mathematical measure of image classification concordance with field data, and carry no information about the abundance of those species not recorded or not included in the classification because of their low frequency.

The decision to adopt a large number of classes for this project, with perhaps lower class accuracies, instead of using a smaller set with a probably higher *apparent* accuracy was therefore a difficult one and needs to be justified. The arguments underpinning this decision are presented in Section 2. In addition, such an approach would deliver data of direct application to MFFP’s requirements e.g. *Sphagnum* species mapping, so it was important to test its feasibility.

1.4 Structure of this document

During its four years of execution this project has undertaken an extensive array of analyses and, in the process, generated a large number of results and outputs. Balancing the presentation of these is difficult: trying to include sufficient information to inform transparently as well as providing the necessary evidence to justify statements made, while not including so many results as to make the whole report impenetrable and incomprehensible. Where possible, summary data are presented in each section for clarity and more complete results are supplied in the annexes for reference where required.

This document is structured in such a way as to illustrate the temporal progression of the project, how the results and experience gained each year informed the processes and imagery to be used for the following phase. It also reports on several discrete ancillary pieces of work executed during the four year period. This structure should allow the developmental reasoning behind the final concluding statements to be followed.

Section 2 summarises the background and rationale for the general methodological approaches adopted for work packages 1, 2, 3, 4 and 7. The specific methods used, their application and results obtained for each annual phase of vegetation mapping activities, are presented in each discrete section. Sections 3, 4 and 5 reprise the annual summary reports for 2018, 2019, and 2020 and effectively replace those documents as some additions to those reports are included. These sections include the recommendations arising from each round where these contribute to the *raison d’être* for the work reporting in the subsequent section. In addition to these summaries, more comprehensive conclusions and discussion from each piece of work are included in Section 10. Section 6 reports for the first time on species aggregation approaches and the results achieved. Section 7 compares the results achieved mapping species and aggregations using UAV,





MAV and orbital EO imagery. Section 8 examines the potential application of the use of UAV-derived thermal imagery for soil moisture determination and Section 9 explores the potential use of high-resolution digital surface models (DSM) to assay topographical change. Conclusions drawn from all aspects of this study, observations on lessons learned and final recommendations for the future are provided in Section 10. As these summarise all parts of the project there is some inevitable repetition between this final section and some comments made in earlier sections of the report. References and annexes conclude the report.



Section 2: Methodological considerations

2.1 Project ethos

All aspects of MFF 50 2016-17 have been predicated on the central purpose of developing and assessing practical approaches and techniques that are robust and within reach of most conservation NGO operations with limited specialist staff, computing, or financial resources. This project has therefore been restricted to the application of commercially standard GIS and remote sensing software packages (ArcGIS and ERDAS IMAGINE respectively) and mainstream classification protocols. Where more specialist approaches like multivariate mathematical analyses have been included, they are shown for illustrative purposes only and are not necessary for application.

As a result of the desire to demonstrate readily applicable processes and outputs we have not tried to extract small incremental improvements in accuracy by working exhaustively on single images, exploiting increasingly complex processes like machine-learning or developing unique code or classification hierarchies. While such approaches are common in most academic studies, and are valuable in their own right, they invariably provide unique solutions that require re-development from scratch for the next study area or require access to proprietary software. The target has been to demonstrate what non-specialist staff should reasonably be able to achieve in a conservation setting.

All aspects of this project include full error data for the results presented, as should be a default requirement in any remote sensing project of this type. There are many unsubstantiated claims of success in the use of small-scale remote-sensing in conservation, especially in the application of UAVs, and this project will not add to them. Instead, it is hoped that by undertaking the project in an objective manner, the results represent a significant body of verified evidence that is directly relevant to MFFP and other conservation bodies with similar monitoring requirements.

2.2 Rationale for remote sensing and field surveys approaches adopted

This project was purposed with obtaining data to allow the effects of restoration to be monitored and assessed. It was initially predicated on the use of imagery obtained from sensors carried on small UAVs. These provide resolutions at centimetre scale and the use of such data to deliver full accuracy-assessed monitoring of diverse habitat, over large areas, is a novel field. As such there were no 'go to' or 'off-the-shelf' solutions available to this project. The following section provides a summary background to the considerations behind the approaches adopted for MFF 50 2016-17 and broadly discusses these issues as they apply to both remote sensing and field survey components.



Typologies. All forms of survey require the usage of appropriate metrics or units for observation and comparison, commonly called a typology. A frequently overlooked, but fundamental requirement of a typology, if it is to serve for monitoring, is that it must be unambiguously identifiable in the field by all qualified surveyors, every time. We can refer to this as ‘repeatability’ i.e., any observer would get the same result, in the same place, on the same day (or within a quantifiable margin of error). If a typology does not satisfy this singular criterion, then it cannot differentiate real change from that arising from ambiguities in mapping, and the process is unsuitable for monitoring. Whatever typology this project was to use had to address this issue across two domains, field survey and image analysis. The early computer era adage ‘garbage in - garbage out’ (GIGO) is applicable here: it is manifestly pointless to provide incorrect data to image analysis algorithms, then test the results against more incorrect data.

Vegetation. Most techniques used in conservation vegetation survey have roots in the concept of plant associations or ‘communities’, the idea that, whether coincidental or edaphically determined, species aggregate into spatially recognisable groupings. Beyond an attempt to understand plant species distribution in response to environmental and stochastic events, such groupings are routinely used as general descriptors to illustrate, for example, the vegetation present in particular locations.

Within the UK the general approach adopted has latterly mostly been based on the precepts of the NVC (National Vegetation Classification: Rodwell 1991-2000) system. This is often utilised for monitoring site condition despite its well understood inapplicability to that task (Cherril & McClean 1999, Hearn et al. 2011). Less formalised approaches and descriptors may also frequently be used, for example: ‘sparse *Calluna/Eriophorum*’; ‘dense *Calluna*’ or ‘mixed dwarf-shrub heath.’ While both approaches provide some information, they are fundamentally unsuitable to any form of rigorous monitoring because:

- (i) Neither provide quantitative data and hence no valid comparison through time is possible.
- (ii) Sampling undertaken is not unbiased (e.g. random) and hence cannot be examined statistically.
- (iii) Boundaries are arbitrarily mapped by the observer, hence are not repeatable and so cannot be used to derive estimates of areal change.
- (iv) They do not collect comprehensive species listings, yet many species present will be important restoration targets or indicators of change.
- (v) Different surveyors frequently reach different interpretations of the same location.



This project required multiple field surveys, undertaken by different people, on different sites. Surveyor disagreements are frequent at a community or sub-community level, with obvious consequences.

The issues arising from the lack of repeatability in community mapping are long understood and are amply shown, for example, in Cherril & McClean (1995).

The use of plant associations for vegetation mapping also becomes problematic as they only have any derivation at an arbitrary scale at which they become apparent. It would obviously be irrational to attempt to assign plant community membership to the species within a single 10 x 10 cm quadrat, without reference to additional information, e.g. co-existing species at the 1-10 m range. At scales of only a few cm most vegetation stands or swards actually comprise a single species or even a single specimen which, of itself, contains no information with regard to any conceptual larger-scale grouping. Hence, in isolation it is impossible to define any community grouping from it, *as there is no community at that scale*. For example, the presence of a specimen of *Calluna* could be indicative of one of many NVC sub-communities (see below). Only by metaphorically, or literally, ‘standing back’ can any conceptual community be recognised.

The NVC user’s handbook (Rodwell, 2006), recommends quadrats to be taken at different scales depending on the habitat type, from 2 x 2 m for habitats like dwarf shrub heath to 50 x 50 m for woodland canopies, so the former would be the relevant size here. The handbook runs to 66 pages and has detailed instructions regarding quadrat placement – identifying ‘homogenous’ stands and avoiding ecotones. The NVC itself is described in five volumes, within which 860 sub-communities are delineated. The difficulty in manually delineating NVC communities led to the development of MAVIS (Modular Analysis of Vegetation Information System; Smart et al, 2016) which automatically assigns samples to the nearest NVC community. Nevertheless, field samples frequently have poor affinities to any of the 860 described sub-communities, in part because of the tendency of individual species to occur in more than one community. As an example, *Calluna vulgaris* is present in more than 200 sub-communities of the NVC. The community is built of individual species, whose identification is unequivocal with competent surveyors. The species is considered the only unit of vegetation that removes subjectivity from mapping. That is not to say that NVC-type communities could not in theory be built up by convolving species data.

Remote sensing typologies. Owing to the large 20-80 m ground spatial resolutions (or pixel size) available from early EO sensors, remote sensing techniques also developed using broad generic classes that are apparent at such scales e.g.: tundra, grasslands,



woodlands, littoral, urban. Land cover or vegetation types of finer typological or taxonomic resolutions were simply unresolvable and hence had to be aggregated or subsumed into spectral classes that were separable at scales larger than the individual pixels. This approach was imposed on researchers by the pixel size of the data.

An additional related factor that needs consideration when determining the potential of mapping plant communities or habitats is that as ground resolution increases so does the spectral heterogeneity visible within any defined class or community. Instead of an average class signature for a community type obtained when using pixels of a few metres in area or more, the use of pixels of a few centimetres provides many hundreds of spectral signatures from individual and mixed species. As there are very few species that, in isolation, determine a community type, many of these signatures will be occurring elsewhere in the image but *within different community types (however defined)*. It is therefore impossible, from first principles, to map communities directly from small pixels i.e. train a classifier to identify higher groupings as the component pixel level spectral data is not exclusive to any particular one (within the constraints of the process.)

It is conceivable some of these issues could potentially be overcome by 'blending' or 'blurring' XHR images to lower resolutions, perhaps to the 1-10m scale, by resampling. However, this would, at a minimum, be less capable of detecting the small-scale changes in species abundances and distribution of the types expected over short time periods. More importantly it would not be compatible with MFFP's objectives to map *Sphagnum* planting.

For completeness it would be worth discussing object or vector classifiers in the context of vegetation mapping as these, in principle, could be seen as allowing information from adjacent pixels to be integrated into a classification process that incorporated communities. This two-stage process examines similarity in spectral data from adjacent pixels, groups these and creates a bounding vector object. This latter stage is undertaken according to user-selectable 'shape' parameters. These function well to identify actual objects such as buildings or roads. In vegetation mapping this might, in principle, assist in differentiation of actual objects like trees, watercourses, or ponds. However, communities are not physical objects, they are conceptualised groupings and, even if they are discrete at all, have no defined shape parameters associated with them. This violates the fundamental principle behind object classifiers therefore these approaches were not explored in this project.

Protocol selected. With regard to addressing the above considerations, it was decided with MFFP to explore using a simple field and remote sensing typology based on plant



species. Firstly, unlike the process of trying to identify community types and extent, plant species are an unambiguous metric, and all competent surveyors will produce the same data. Secondly, the use of XHR imagery, with 10 cm resolution in Phase 1 and 5 cm in Phases 2, 3 and 4, means a large proportion of pixels will be imaging single species/specimens. Thirdly, it represents the 'best' solution in that if all species are mappable, it becomes possible to assess the finest possible responses to conservation interventions. Lastly, gathering field data in this form provides opportunity to develop other species grouping typologies by aggregation should this be desired or required, something that cannot be undertaken in reverse.





Section 3: Phase 1 – UAV Image Capture

Originally reporting in Summary report 2018

Summary introduction to Phase 1 activities.

Phase 1 was planned as an all-up deployment of MFFP's proposals to obtain UAV imagery and field data across the study areas and to produce classified products based on identification of separate species. It therefore represented the first opportunity to test these protocols, and to provide evidence to develop them for future rounds as necessary. This is an ambitious project and, perhaps not unexpectedly, some operational teething difficulties were experienced in this first year.

It had originally been projected that MFFP would undertake all data capture for the study sites, with NTU/CS undertaking subsequent analyses. However, early difficulties with the original UAV/sensor combination caused delays to the data collection, both field and imagery. As a result, MFFP decided to contract out the image capture activities for this year, and the area was flown by the NTU/CS team. This, however, necessitated a change from the planned sensor/platform to a different system, which had some consequential impact on project timing and ultimately the amount of field data acquired.

Despite these late changes, Phase 1 delivered much invaluable information and results. This was the first attempt to image large areas using UAVs and produce fully error-assessed classified imagery from those data. Analysis of these results ultimately revealed a severe limitation to the capture methodology used that, to the authors' knowledge, has not been previously noted. These results therefore not only guided a change in approach during the subsequent years of this project but should hopefully inform other projects anticipating their utilisation in the future.



3.1 Methods

3.1.1 Image data

Capture. The original project image capture specification was predicated upon the deployment of SONY A6000 and MicaSense RedEdge multispectral cameras mounted on a Quest Q-200 fixed wing UAV platform. In a single flight at around 120 m above the ground this combination would have provided RGB and 5-band (B, G, R, RE, NIR) imagery with ground resolutions of approximately 0.024 m and 0.08 m respectively. The A6000 would provide ultra-high resolution imagery for digital surface model (DSM) creation and visual assessment in a GIS, and the spatial and spectral resolution of the MicaSense imagery were deemed an optimal option to compare the outcomes of image classification approaches. However, due to issues with this platform, an alternate solution using sensors mounted on a senseFly eBee platform was subsequently adopted. The eBee can be flown independently with either a S.O.D.A. (Sensor Optimised for Drone Applications) or 'Parrot Sequoia' to collect RGB and 4-band (G, R, RE, NIR) imagery respectively. This approach requires two flights rather than one to capture both sets of imagery and must be flown lower (at approximately 60-70 m above the ground) to achieve comparable spatial resolution. This in turn increases the number of flight lines required to capture the area and therefore increases image capture time.

Pre-processing. Images from each individual flight were processed separately using Pix4Dmapper v4.0.25. Coordinates for ground control points (GCPs), distributed on a 100 m triangular grid within the area immediately surrounding the field laboratories and on a 150 m triangular grid for the remaining area of each survey site, were obtained using a Trimble Geo7x DGNSS. Positional data were post-corrected in Trimble Pathfinder Office using RINEX data from the OS Net base station nearest to each survey site. Accuracy of post-processed coordinates ranged from 0.021 m - 0.031 m in xy and from 0.033 – 0.050 m in z. GCP coordinates were loaded into Pix4D and all GCPs were marked first as control points in the RGB imagery and in each independent multispectral band for the Sequoia imagery to derive a model root mean squared error (RMSE). Subsequently five randomly selected GCPs were set to check points to report a true model RMSE, and all GCPs were returned to control points prior to running the model to create a DSM and orthomosaic.

The 0.02 m RGB orthomosaic derived from the S.O.D.A. imagery was resampled to the resolution of the respective multispectral data and combined with the multispectral mosaics to form a 7-band (B, G, R, G, R, RE, NIR) image stack using ERDAS Imagine. Owing to the presence of visible 'striping' in the orthomosaics (section 4.3) that is inconsistent between RGB and multispectral data, and the potential for misalignment of



pixels between the RGB and multispectral data, 4-band image stacks derived solely from the multispectral sensor (G, R, RE, NIR) were used for classification.

For all study sites, the area of the orthomosaic produced outside of the location of GCPs will contain unquantified (and likely higher) error due to the lack of ground control information for the model. The outermost 50 m of all images were therefore clipped out and are excluded from analysis here.

3.1.2 Field data

Field observations were supplied by MFFP as separate files for each taxonomic group for each image capture area in ESRI shapefile format. Prior to exploration and classification, several preliminary operations were executed. These are summarised in Table 3:1 below.

Table 3:1. Preliminary data operations

- i.* New shapefile: separate taxon point files for each site merged to single shapefile for each sample area;
- ii.* New shapefile: resultant data from above merged to create single vector file of 'all vegetation- all sites'
- iii.* New shapefile: 'imagery extent' polygons created identifying the spatial limits of image capture each sample area field, sample area field added and populated;
- iv.* New Shapefile: resultant 'image extent' intersected with 'all vegetation' shapefile to provide locale name to each record;
- v.* Add field: for veg - populate as concatenation of all veg fields, LTrim remove extraneous preceding spaces;
- vi.* Add field; 'all Sphag' merge to genus and populate;
- vii.* New Shapefile: buffer each point to 10cm;
- viii.* New Shapefile: convert circular buffer to square aligned with pixels;
- ix.* Delete all extraneous fields;
- x.* Add field: create unique ID field populated as concatenation of image extent and species;
- xi.* Add field: create 'use' field: randomly select 50% within each image-extent populate 'use' field;
- xii.* New Shapefile: dissolve on site, fields 'veg_all', 'veg_spmg' and 'use';
- xiii.* New Shapefiles (7): select by image name export for each image area;
- xiv.* New Shapefiles (7x2): select by field 'use' to export training and error subsets.

Subsequent to the decision to utilise all data for training purposes, step xiv was not applied and outputs from step xiii were utilised. Following these operations, the data were imported into ERDAS Imagine 'signature editor' and spectral signatures were collected.



3.1.3 Supervised Classification

Stacked image mosaics covering seven test areas: Bleaklow Penguins; Derwent Howden heather sites; Birchinlee (1&2); Rowlee; and Kinder Scout (Firmin & Olaf Nogson) were classified using the maximum likelihood algorithms within ERDAS Imagine. Training data comprised field data supplied by MFFP. No *a priori* probabilities were applied given the non-random nature of sampling. For Phase 1 all field data were used for training the classifier algorithm for the delivered products.

3.1.4 Spectral separability analyses

Supervised image classification, such as that used here and presented in section 4.3, is a two-stage process. Firstly, clusters within multispectral space, for each of the surveyed classes, are defined using 'training' data comprising the spectral characteristics of image pixels corresponding to each field sample point. Secondly, the 'unknown' pixels comprising the rest of the image are then assigned a membership to one of the surveyed classes according to their spectral similarity or 'closeness' to these clusters, using a range of rules or algorithms. Testing the results of such a classification is undertaken by comparing a random subset of classified pixels to another set of field survey 'ground-truth' data.

This accuracy testing is a post hoc process, i.e. occurs after the actual classification process. However, the results can be used to refine rules used in assigning membership to the 'training clusters', or any class deletions or amalgamations that can be usefully made, before additional rounds of classification are undertaken to attempt to produce a more accurate final product. Only in this way is it possible to differentiate effects caused by poor image data from the use of inappropriate methodological approaches.

Such an 'iterative' approach to working was planned in this phase of the project to assess the suitability of low-cost UAV/sensors to MFFP needs, and to design optimal survey and classification processes to be used in the future. This was not possible due to the limited number of samples available, and therefore an alternative approach has been adopted to help answer this aspect of the project.

Separability analyses are a series of preliminary procedures that can guide the classification process to be applied by testing the spectral signatures of the field classes collected to assess the probability of them being identified correctly during a supervised classification. Separability statistics were obtained using the following method. For each survey site the 4-band image stack was loaded into Imagine. The dissolved shapefiles of single-species samples were loaded into the signature editor. Each field sample collects 4-9 pixels from the raster. For example, the 308 field samples from Firmin picked up 1406



pixels from the image. The separability tool of the signature editor was used to calculate two measures of spectral separability, transformed divergence and Jeffries-Matusita distance (Hexagon Geospatial, undated), for every class. It was not possible to calculate separability for classes with only one sample. Thus, for the example of Firmin, of 22 collected signatures, it was possible to calculate separability statistics for 21. The 22nd signature only contained one sample and was excluded. In this case the excluded class was *Sphagnum spp.* The other sample sites had 1-2 classes removed from the spectral separability analysis for this reason.

According to Hexagon Geospatial (undated),

“Both transformed divergence and Jeffries-Matusita distance have upper and lower bounds. If the calculated divergence is equal to the appropriate upper bound, then the signatures can be said to be totally separable in the bands being studied. A calculated divergence of zero means that the signatures are inseparable.”

The upper bound for transformed divergence is 2.000 and that for Jeffries-Matusita is 1.414 ($\sqrt{2}$). For transformed divergence, separability values of above 1.900 indicate good separability, and values below 1.700 show poor separability (Jensen, 1996).

3.1.5 Accuracy assessment

Owing to the overall low number of samples recorded, there were in general too few data available to enable reserving 50% for accuracy assessments. However, at Firmin, the number of samples for many species present approached the minimum needed and it was decided to undertake an exploratory error check.

At this site there were initially 308 samples available across 22 classes. Once classes with fewer than ten samples were removed, there were a total of 16 classes and 290 samples. These 290 samples were divided between training and test data on a random basis, resulting in 151 training samples and 139 test samples.

The training data shapefile was used together with the relevant 4-band image stack for supervised classification in Imagine with default settings (maximum likelihood). Point data at the positions of the 139 test samples were then intersected with the classified map. The predicted class at each location was then compared with the known class as identified during field data collection using a confusion matrix; overall accuracy and kappa were calculated from the confusion matrix.



3.2 Results

3.2.1 Geometric accuracy of DSMs and orthomosaics

Appropriate target design, highly accurate GCP coordinates obtained using the Trimble Geo7x DGNSS and well-distributed GCPs on each site enabled Pix4D to process the imagery and report consistently low mean error.

For RGB data from the S.O.D.A. camera the mean overall RMSE (in x, y and z) was consistently comparable to and often lower than the pixel size (Table 3:2). The error in the height (z) was frequently lower than the horizontal error (x and y). The resultant RGB orthomosaics (Figures 1-7) and DSMs therefore provide ultra-high resolution data covering the experimental plots and surrounding areas that can be used for visual assessment, hydrological modelling and potentially for identifying future morphological change (e.g. erosion).

Table 3:2. Geometric accuracy of RGB imagery

Survey site	Images	Resolution (m)	Control RMSE (m)		Check RMSE (m)	
			(x, y)	(x, y, z)	(x, y)	(x, y, z)
Derwent/Howden	803	0.022	0.033	0.025	0.024	0.026
Penguins	690	0.021	0.031	0.024	0.048	0.042
Birchinlee 1	851	0.021	0.019	0.018	0.020	0.035
Birchinlee 2	1040	0.019	0.017	0.016	0.023	0.024
Rowlee	750	0.022	0.031	0.025	0.029	0.037
Firmin	1179	0.020	0.016	0.018	0.022	0.032
Olaf Nogson	821	0.021	0.019	0.018	0.026	0.030

For the multispectral data from the Sequoia camera, the mean overall RMSE was less than half the pixel size (Table 3:3). It is however worth considering the way in which low-cost multispectral cameras developed for UAVs, including the RedEdge and Sequoia, capture images. These types of cameras have independent sensors for each spectral band. Manufacturing tolerances mean that each sensor will be oriented to some extent at different angles to each other giving slightly different fields of view (FOV). This approach means that GCPs have to be marked in imagery for each band so that the resultant orthomosaic is aligned with each other. Although the mean RMSE achieved for the multispectral data was consistently lower than the pixel size, Pix4D support have advised that the RMSE reported is the average for all bands (it is not possible to assess the error of each band individually). There will, therefore, be an inevitable slight displacement in the alignment of pixels between all bands. Although this is reported as less than half the width of a pixel, it is not clear at this point to what degree this impacts on the success of image classification.



Table 3:3. Geometric accuracy of RGB imagery

Survey site	Images	Resolution (m)	Control RMSE (m)		Check RMSE (m)	
			(x, y)	(x, y, z)	(x, y)	(x, y, z)
Derwent/Howden	1158	0.096	0.063	0.058	0.024	0.031
Penguins	999	0.093	0.033	0.028	0.047	0.048
Birchinlee 1	1207	0.090	0.013	0.020	0.013	0.035
Birchinlee 2	1170	0.089	0.023	0.026	0.023	0.028
Rowlee	993	0.093	0.043	0.037	-	-
Firmin	1203	0.087	0.024	0.021	0.034	0.031
Olaf Nogson	1193	0.089	0.019	0.024	0.024	0.042

3.2.2 Field data

The initial field data target was for 20 field samples to be collected for each species present at each site. This would have allowed 10 samples to be used for image classification while withholding 10 further samples for error assessment. This target could not be achieved for most species at most of the seven field sites, so there were insufficient data for traditional classification/error assessment procedures.

3.2.3 Image quality and supervised classification delivery

Without formal error assessment it is difficult to assess the classification accuracies achieved by the supervised classification. However, for some sites such as Derwent Howden (Figure 3:1) and Firmin (Figure 3:6), the identified distributions of outlier classes like bare peat and rock seem to match visual interpretation of RGB imagery. A limited exploration of classification accuracy for Firmin (the site with the most available field data) is provided in section 4.5.

There is little evidence for the accuracy of other classes. A number of artefacts are visible in the multispectral image stacks that undoubtedly affect classification accuracy. As the multispectral data for each site were collected over a period of 1-2 hours, sun-angle and illumination changed during this time creating visible striping in the data. These stripes have been identified as single taxa in the classified product (e.g. *Vaccinium myrtillus* in Penguins and Birchinlee 1; Figures 2-3). In addition, the proportion of the same taxa identified in the classified data for adjacent survey areas appears unrealistic. For example, at Birchinlee 2 around 20% of the area was classified as Feather Moss (Figure 3:4), while in the overlapping Birchinlee 1, the cover of Feather Moss was <3% (Figure 3:3).

The resultant thematic maps are considered the delivered products for Phase 1 and are supplied separately as reported in Table 3:4.



Table 3:4. Phase 1 delivered products

Site name	Classified output
Derwent Howden	dw_hw_20180718_classified.img
Penguins	penguins_20180718_classified.img
Birchinlee 1	brch_site_1_20180723_classified.img
Birchinlee 2	brch_site_2_20180719_classified.img
Rowlee	rowlee_20180802_classified.img
Firmin	firmin_20180830_classified.img
Olaf Nogson	olaf_nogson_20180831_classified.img

3.2.4 Class Separability

In the absence of data on class accuracies it is possible to explore class separability and the reported cover of certain classes in the output data. Unsurprisingly the two measures of separability are highly correlated (see Tables 3:6-3:12). However, transformed divergence appears to asymptote to its maximum value earlier than Jeffries-Matusita, making the latter measure more useful for discriminating relative differences at higher separabilities.

In general, there are two obvious patterns in the separability statistics. The first is that certain classes are more separable than others across survey sites. Thus, where bare peat, rock, or *Pteridium aquilinum* occur, these classes are highly separable from other classes. Conversely some classes tend to have low separability, principally the grass or grass-like classes: *Deschampsia flexuosa*, *Eriophorum spp.* and *Juncus spp.* as examples. Some classes (e.g. *Calluna*) have variable average separability between sites, from 1.956 (TD) at Derwent Howden to only 1.547 (TD) at Firmin.

The second pattern is that small classes are more separable according to the statistics than are large classes. This does not appear to be due to the formulae for calculating the separability. Rather, it seems to be because small classes have correspondingly few pixels and by chance these often have low variability between samples. This is then an artefact and does not represent the “true” separability of these classes, which would be more accurately known with more available data.

As an example of these patterns, the average separability statistics for classes collected at Firmin are shown in Table 3:5.



Table 3:5. Average separability statistics by class at Firmin.

Classes ranked from most to least separable.

Class	Sample count	Pixel count	Average separability	
			Transformed divergence	Jeffries-Matusita
<i>Betula</i> spp	2	10	2.00	1.38
Water	2	8	2.00	1.41
Rock	10	42	2.00	1.40
Bare peat	27	127	1.96	1.34
<i>Holcus mollis</i>	5	24	1.92	1.32
Feather moss	4	18	1.89	1.30
<i>Abies</i> spp	4	16	1.89	1.32
<i>Nardus stricta</i>	11	50	1.80	1.27
Cushion moss	21	90	1.79	1.27
<i>Vaccinium myrtillus</i>	22	111	1.74	1.25
<i>Empetrum nigrum</i>	17	76	1.74	1.24
<i>Eriophorum angustifolium</i>	21	94	1.74	1.23
<i>Salix</i>	13	56	1.72	1.25
<i>Juncus squarrosus</i>	21	101	1.70	1.23
<i>Polytrichum</i> spp	13	61	1.69	1.22
<i>Agrostis</i> spp	13	58	1.66	1.22
<i>Eriophorum vaginatum</i>	20	92	1.64	1.21
<i>Chamaenerion angustifolium</i>	17	86	1.64	1.16
<i>Juncus effusus</i>	21	90	1.62	1.17
<i>Calluna vulgaris</i>	21	96	1.55	1.17
<i>Deschampsia flexuosa</i>	22	100	1.52	1.12



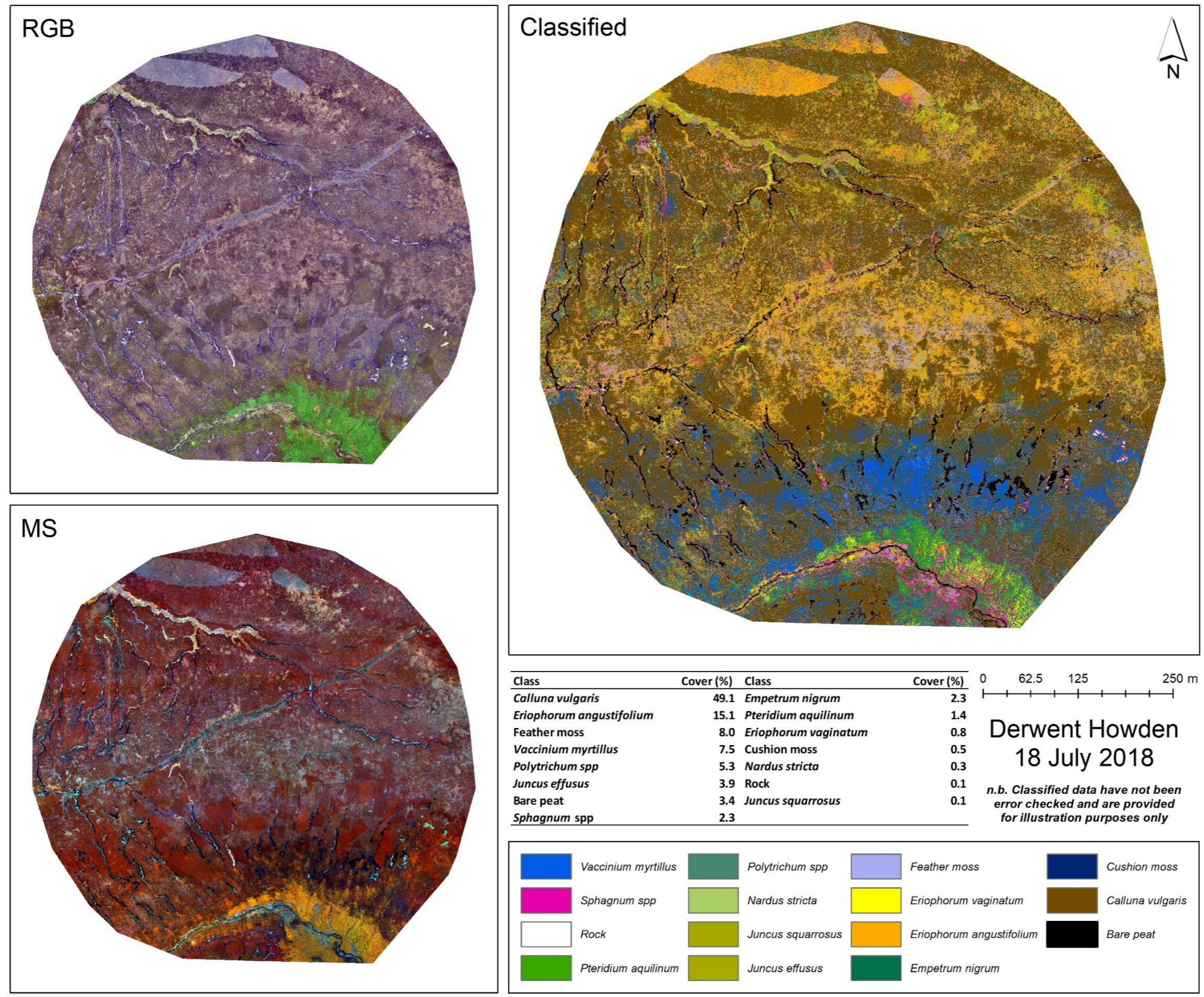


Figure 3:1. Processed RGB and multispectral (MS: NIR, G, R) imagery and classified output for Derwent Howden study area

Table 3:6. Spectral separability analysis: Derwent Howden.

Above: Transformed Divergence. Values nearer to 2.0 mean an increasing probability of good separation. Breakpoints taken as <1.0 poor separability; 1.0 – 1.9 moderate separation (Jenson 1996).

Below: Jeffries-Matusita Distance. Values nearer to 1.414 mean an increasing probability of good separation.

	Bare peat	<i>Calluna vulgaris</i>	Cushion moss	<i>Empetrum nigrum</i>	<i>E. angustifolium</i>	<i>E. vaginatum</i>	Feather moss	<i>Juncus effusus</i>	<i>Juncus squarrosus</i>	<i>Nardus stricta</i>	<i>Polytrichum spp</i>	<i>Pteridium aquilinum</i>	Rock	<i>Sphagnum spp</i>	<i>Vaccinium myrtillus</i>
Bare peat	0.000	2.000	2.000	2.000	1.987	2.000	2.000	2.000	2.000	2.000	2.000	2.000	2.000	2.000	2.000
<i>Calluna vulgaris</i>		0.000	2.000	2.000	1.936	2.000	1.999	1.992	2.000	2.000	1.729	2.000	2.000	2.000	1.733
Cushion moss			0.000	2.000	2.000	2.000	2.000	2.000	2.000	2.000	2.000	2.000	2.000	2.000	2.000
<i>Empetrum nigrum</i>				0.000	2.000	2.000	2.000	2.000	2.000	2.000	2.000	2.000	2.000	2.000	2.000
<i>E. angustifolium</i>					0.000	1.979	1.957	1.620	1.993	1.970	1.839	2.000	2.000	1.962	2.000
<i>E. vaginatum</i>						0.000	2.000	1.798	1.618	0.889	1.811	2.000	2.000	1.769	1.985
Feather moss							0.000	1.997	2.000	2.000	2.000	2.000	2.000	2.000	2.000
<i>Juncus effusus</i>								0.000	1.833	1.745	1.822	2.000	2.000	1.831	1.999
<i>Juncus squarrosus</i>									0.000	1.689	1.956	2.000	2.000	1.980	1.968
<i>Nardus stricta</i>										0.000	1.967	2.000	2.000	1.439	2.000
<i>Polytrichum spp</i>											0.000	2.000	2.000	1.990	1.921
<i>Pteridium aquilinum</i>												0.000	2.000	2.000	1.759
Rock													0.000	2.000	2.000
<i>Sphagnum spp</i>														0.000	2.000
<i>Vaccinium myrtillus</i>															0.000
Bare peat	0.000	1.337	1.398	1.414	1.313	1.414	1.407	1.414	1.414	1.414	1.402	1.414	1.414	1.406	1.411
<i>Calluna vulgaris</i>		0.000	1.395	1.336	1.292	1.413	1.320	1.390	1.414	1.414	1.154	1.406	1.414	1.375	1.178
Cushion moss			0.000	1.402	1.354	1.414	1.406	1.414	1.414	1.414	1.412	1.414	1.414	1.402	1.412
<i>Empetrum nigrum</i>				0.000	1.409	1.414	1.393	1.414	1.414	1.414	1.390	1.414	1.414	1.402	1.398
<i>E. angustifolium</i>					0.000	1.399	1.294	1.211	1.407	1.395	1.272	1.414	1.414	1.340	1.410
<i>E. vaginatum</i>						0.000	1.403	1.282	1.234	0.862	1.257	1.362	1.414	1.197	1.372
Feather moss							0.000	1.368	1.414	1.385	1.396	1.414	1.410	1.282	1.404
<i>Juncus effusus</i>								0.000	1.317	1.244	1.210	1.388	1.414	1.221	1.357
<i>Juncus squarrosus</i>									0.000	1.274	1.321	1.393	1.414	1.348	1.389
<i>Nardus stricta</i>										0.000	1.369	1.394	1.414	1.092	1.406
<i>Polytrichum spp</i>											0.000	1.285	1.414	1.304	1.110
<i>Pteridium aquilinum</i>												0.000	1.414	1.391	1.260
Rock													0.000	1.406	1.414
<i>Sphagnum spp</i>														0.000	1.340
<i>Vaccinium myrtillus</i>															0.000

n.b. Owing to small sample sizes these figures should be treated with caution.

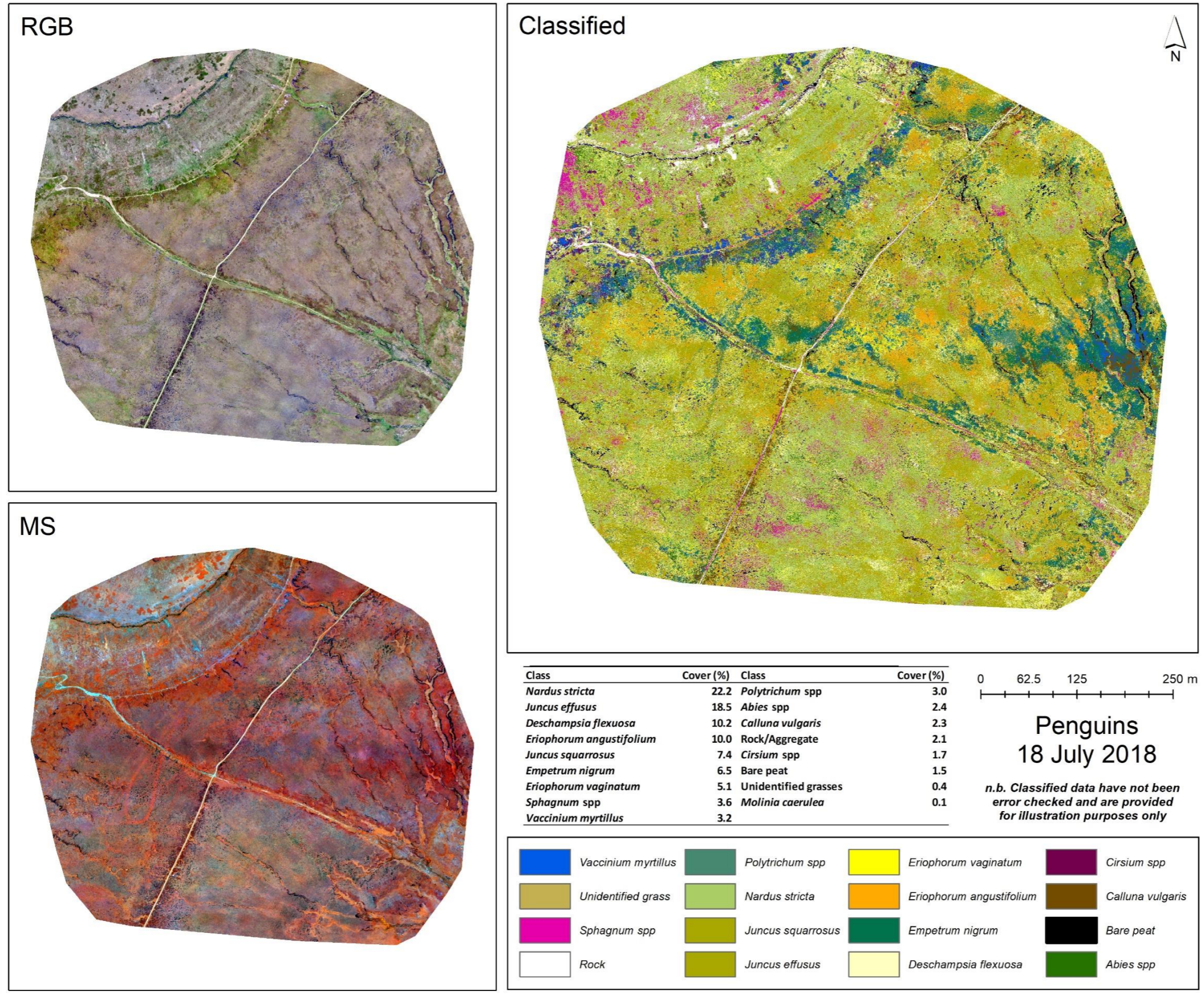


Figure 3:2. Processed RGB and multispectral (MS: NIR, G, R) imagery and classified output for Penguins study area

Table 3:7. Spectral separability analysis: Penguins.

Above: Transformed Divergence. Values nearer to 2.0 mean an increasing probability of good separation. Breakpoints taken as <1.0 poor separability; 1.0 – 1.9 moderate separation (Jenson 1996).

Below: Jeffries-Matusita Distance. Values nearer to 1.414 mean an increasing probability of good separation.

	Abies spp	Aggregate	Bare peat	Calluna vulgaris	Cirsium spp	Deschampsia flexuosa	Empetrum nigrum	E. angustifolium	E. vaginatum	Juncus effusus	Juncus squarrosus	Molinia caerulea	Nardus stricta	Polytrichum spp	Rock	Sphagnum spp	Unidentified grasses	Vaccinium myrtillus
Abies spp	0.000	2.000	2.000	2.000	1.915	1.958	1.999	1.998	1.509	1.996	1.841	1.974	1.907	1.996	2.000	2.000	1.997	1.994
Aggregate		0.000	2.000	2.000	2.000	2.000	2.000	2.000	2.000	2.000	2.000	2.000	2.000	2.000	2.000	2.000	2.000	2.000
Bare peat			0.000	2.000	2.000	2.000	2.000	2.000	2.000	2.000	2.000	2.000	2.000	2.000	2.000	2.000	2.000	2.000
Calluna vulgaris				0.000	1.930	1.910	1.745	1.793	1.915	1.873	1.811	1.998	1.999	1.967	2.000	2.000	1.889	1.406
Cirsium spp					0.000	1.937	1.981	1.992	1.598	1.990	1.557	2.000	1.996	1.999	2.000	2.000	1.955	1.741
Deschampsia flexuosa						0.000	1.917	0.925	1.233	1.190	1.236	1.999	1.414	1.290	1.990	1.401	1.990	1.455
Empetrum nigrum							0.000	1.579	1.930	1.922	1.725	1.998	2.000	1.486	2.000	2.000	1.996	1.186
E. angustifolium								0.000	1.569	0.765	1.151	1.997	1.699	1.138	1.999	1.818	1.981	1.570
E. vaginatum									0.000	1.783	0.716	1.458	1.656	1.842	2.000	1.936	1.880	1.552
Juncus effusus										0.000	1.261	2.000	1.610	1.787	2.000	1.860	1.970	1.822
Juncus squarrosus											0.000	1.896	1.736	1.637	2.000	1.974	1.759	1.429
Molinia caerulea												0.000	2.000	1.995	2.000	2.000	1.984	1.945
Nardus stricta													0.000	1.987	2.000	1.402	2.000	1.991
Polytrichum spp														0.000	2.000	1.970	2.000	1.444
Rock															0.000	1.926	2.000	2.000
Sphagnum spp																0.000	2.000	1.998
Unidentified grasses																	0.000	1.929
Vaccinium myrtillus																		0.000
Abies spp	0.000	1.414	1.414	1.414	1.210	1.250	1.412	1.402	1.108	1.396	1.304	1.365	1.268	1.407	1.408	1.347	1.404	1.323
Aggregate		0.000	1.414	1.414	1.414	1.414	1.414	1.414	1.414	1.414	1.414	1.414	1.414	1.414	1.389	1.414	1.414	1.414
Bare peat			0.000	1.328	1.414	1.397	1.411	1.394	1.411	1.414	1.414	1.414	1.412	1.413	1.344	1.405	1.414	1.414
Calluna vulgaris				0.000	1.352	1.195	1.298	1.185	1.354	1.262	1.331	1.394	1.387	1.288	1.371	1.290	1.319	1.085
Cirsium spp					0.000	1.281	1.362	1.374	1.063	1.379	1.167	1.316	1.344	1.368	1.414	1.362	1.347	1.157
Deschampsia flexuosa						0.000	1.196	0.864	0.958	0.956	1.014	1.358	1.040	1.035	1.384	0.983	1.342	1.112
Empetrum nigrum							0.000	1.130	1.315	1.334	1.281	1.362	1.401	0.987	1.398	1.328	1.400	0.952
E. angustifolium								0.000	1.219	0.805	1.051	1.369	1.241	1.010	1.362	1.073	1.330	1.155
E. vaginatum									0.000	1.222	0.789	1.090	1.115	1.298	1.385	1.243	1.288	1.200
Juncus effusus										0.000	1.051	1.389	1.149	1.259	1.390	1.103	1.284	1.254
Juncus squarrosus											0.000	1.245	1.243	1.226	1.408	1.245	1.247	1.132
Molinia caerulea												0.000	1.397	1.368	1.414	1.399	1.374	1.339
Nardus stricta													0.000	1.396	1.375	0.983	1.399	1.368
Polytrichum spp														0.000	1.405	1.206	1.380	1.088
Rock															0.000	1.363	1.413	1.405
Sphagnum spp																0.000	1.373	1.292
Unidentified grasses																	0.000	1.270
Vaccinium myrtillus																		0.000

n.b. Owing to small sample sizes these figures should be treated with caution.

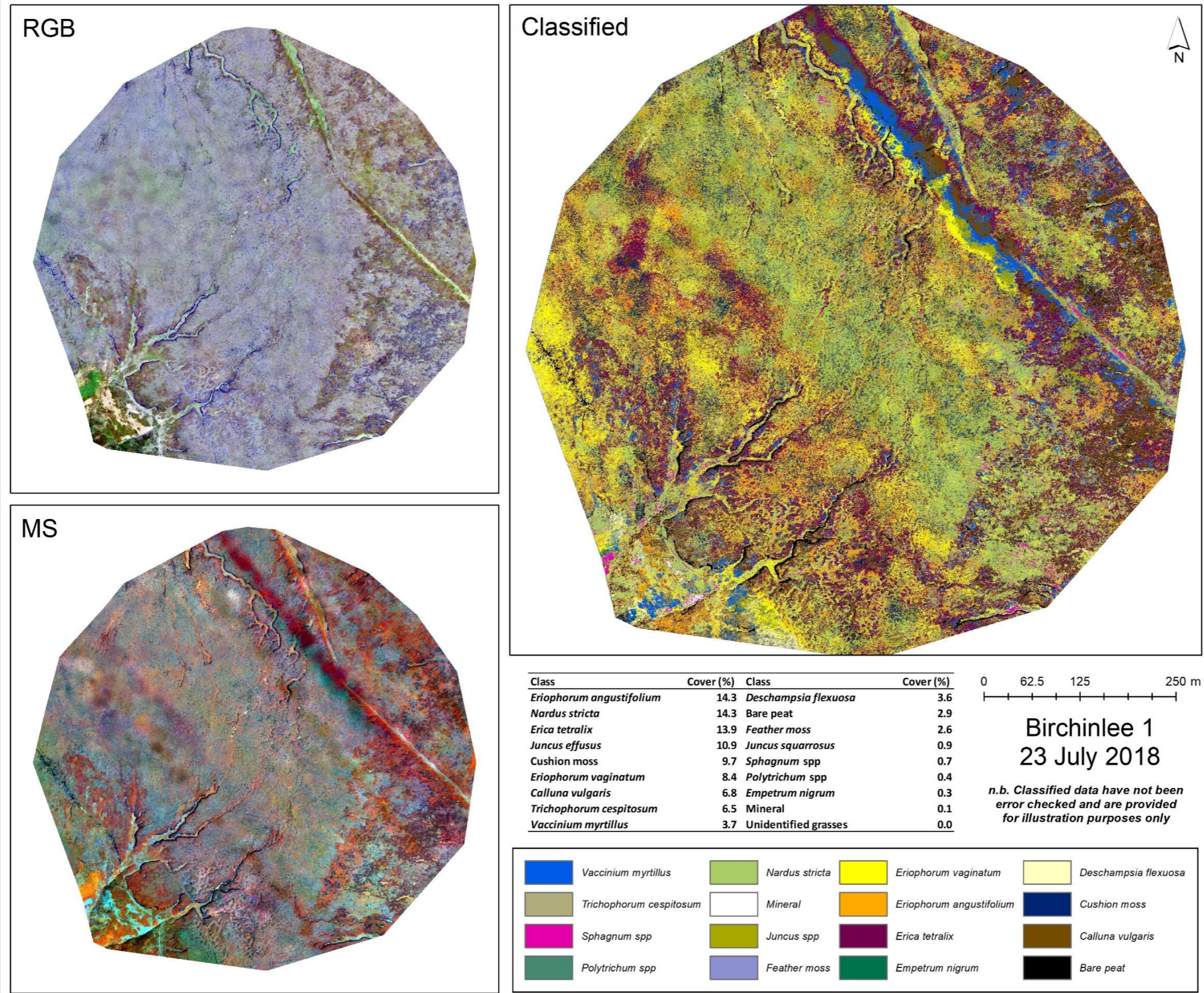


Figure 3:3. Processed RGB and multispectral (MS: NIR, G, R) imagery and classified output for Birchinlee 1 study area.
n.b. the very clear 'striping' apparent in the MS image and its effects in the classified output. The causes of this are discussed in text.

Table 3:8. Spectral separability analysis: Birchinlee 1.

Above: Transformed Divergence. Values nearer to 2.0 equals an increasing probability of good separation. Breakpoints taken as <1.0 poor separability; 1.0 – 1.9 moderate separation (Jenson 1996).

Below: Jeffries-Matusita Distance. Values nearer to 1.414 equals an increasing probability of good separation.

	Bare peat	<i>Calluna vulgaris</i>	Cushion moss	<i>Deschampsia flexuosa</i>	<i>Empetrum nigrum</i>	<i>Erica tetralix</i>	<i>E. angustifolium</i>	<i>E. vaginatum</i>	Feather moss	<i>Juncus effusus</i>	<i>Juncus squarrosus</i>	Mineral	<i>Nardus stricta</i>	<i>Polytrichum</i> spp	<i>Sphagnum</i> spp	<i>Trichophorum cespitosum</i>	Unidentified grasses	<i>Vaccinium myrtillus</i>
Bare peat	0.000	1.589	2.000	1.849	2.000	1.759	1.837	1.949	2.000	1.822	1.986	2.000	1.978	1.951	2.000	1.812	2.000	1.930
<i>Calluna vulgaris</i>		0.000	1.935	1.981	1.978	1.388	1.845	1.988	2.000	1.947	1.997	2.000	1.998	1.997	2.000	1.757	2.000	1.797
Cushion moss			0.000	2.000	2.000	1.950	1.981	2.000	1.997	1.993	2.000	2.000	2.000	2.000	2.000	1.999	2.000	2.000
<i>Deschampsia flexuosa</i>				0.000	2.000	1.632	1.229	0.478	2.000	1.599	1.993	2.000	0.648	1.672	1.498	1.501	2.000	1.414
<i>Empetrum nigrum</i>					0.000	1.936	1.999	2.000	2.000	1.999	2.000	2.000	2.000	1.989	2.000	1.999	2.000	1.889
<i>Erica tetralix</i>						0.000	1.302	1.758	2.000	1.392	1.991	2.000	1.865	1.941	1.999	1.289	2.000	1.568
<i>E. angustifolium</i>							0.000	1.789	2.000	1.727	2.000	2.000	1.556	1.771	1.720	1.934	2.000	1.653
<i>E. vaginatum</i>								0.000	2.000	1.782	1.943	2.000	1.251	1.853	1.985	1.287	2.000	1.475
Feather moss									0.000	2.000	2.000	2.000	2.000	2.000	1.998	2.000	2.000	2.000
<i>Juncus effusus</i>										0.000	1.974	2.000	1.490	1.870	1.878	1.422	2.000	1.536
<i>Juncus squarrosus</i>											0.000	2.000	2.000	2.000	2.000	1.417	2.000	1.790
Mineral												0.000	2.000	2.000	2.000	2.000	2.000	2.000
<i>Nardus stricta</i>													0.000	1.919	1.570	1.861	2.000	1.888
<i>Polytrichum</i> spp														0.000	1.997	1.956	2.000	1.267
<i>Sphagnum</i> spp															0.000	2.000	2.000	1.996
<i>T. cespitosum</i>																0.000	2.000	1.267
Unidentified grasses																	0.000	2.000
<i>Vaccinium myrtillus</i>																		0.000
Bare peat	0.000	1.119	1.332	1.289	1.413	1.263	1.282	1.364	1.372	1.260	1.380	1.414	1.366	1.366	1.338	1.257	1.412	1.365
<i>Calluna vulgaris</i>		0.000	1.302	1.295	1.399	1.097	1.154	1.379	1.363	1.292	1.390	1.414	1.409	1.329	1.358	1.269	1.414	1.217
Cushion moss			0.000	1.301	1.405	1.294	1.205	1.376	1.298	1.262	1.414	1.414	1.367	1.361	1.344	1.386	1.414	1.375
<i>Deschampsia flexuosa</i>				0.000	1.384	1.125	1.018	0.634	1.341	1.051	1.235	1.408	0.756	1.160	1.075	1.053	1.411	1.118
<i>Empetrum nigrum</i>					0.000	1.333	1.326	1.407	1.408	1.409	1.413	1.414	1.413	1.320	1.393	1.409	1.414	1.244
<i>Erica tetralix</i>						0.000	0.945	1.255	1.400	1.071	1.381	1.414	1.348	1.155	1.279	1.095	1.414	1.086
<i>E. angustifolium</i>							0.000	1.236	1.253	1.124	1.372	1.402	1.213	1.067	1.151	1.231	1.414	1.212
<i>E. vaginatum</i>								0.000	1.405	1.236	1.201	1.414	1.041	1.253	1.273	1.060	1.412	1.166
Feather moss									0.000	1.348	1.414	1.414	1.339	1.372	1.241	1.409	1.414	1.403
<i>Juncus effusus</i>										0.000	1.255	1.409	1.131	1.209	1.132	1.068	1.414	1.175
<i>Juncus squarrosus</i>											0.000	1.414	1.348	1.248	1.364	1.055	1.414	1.155
Mineral												0.000	1.408	1.411	1.383	1.414	1.414	1.414
<i>Nardus stricta</i>													0.000	1.334	0.984	1.256	1.409	1.345
<i>Polytrichum</i> spp														0.000	1.288	1.258	1.414	1.010
<i>Sphagnum</i> spp															0.000	1.283	1.410	1.318
<i>T. cespitosum</i>																0.000	1.409	1.082
Unidentified grasses																	0.000	1.413
<i>Vaccinium myrtillus</i>																		0.000

n.b. Owing to small sample sizes these figures should be treated with caution.

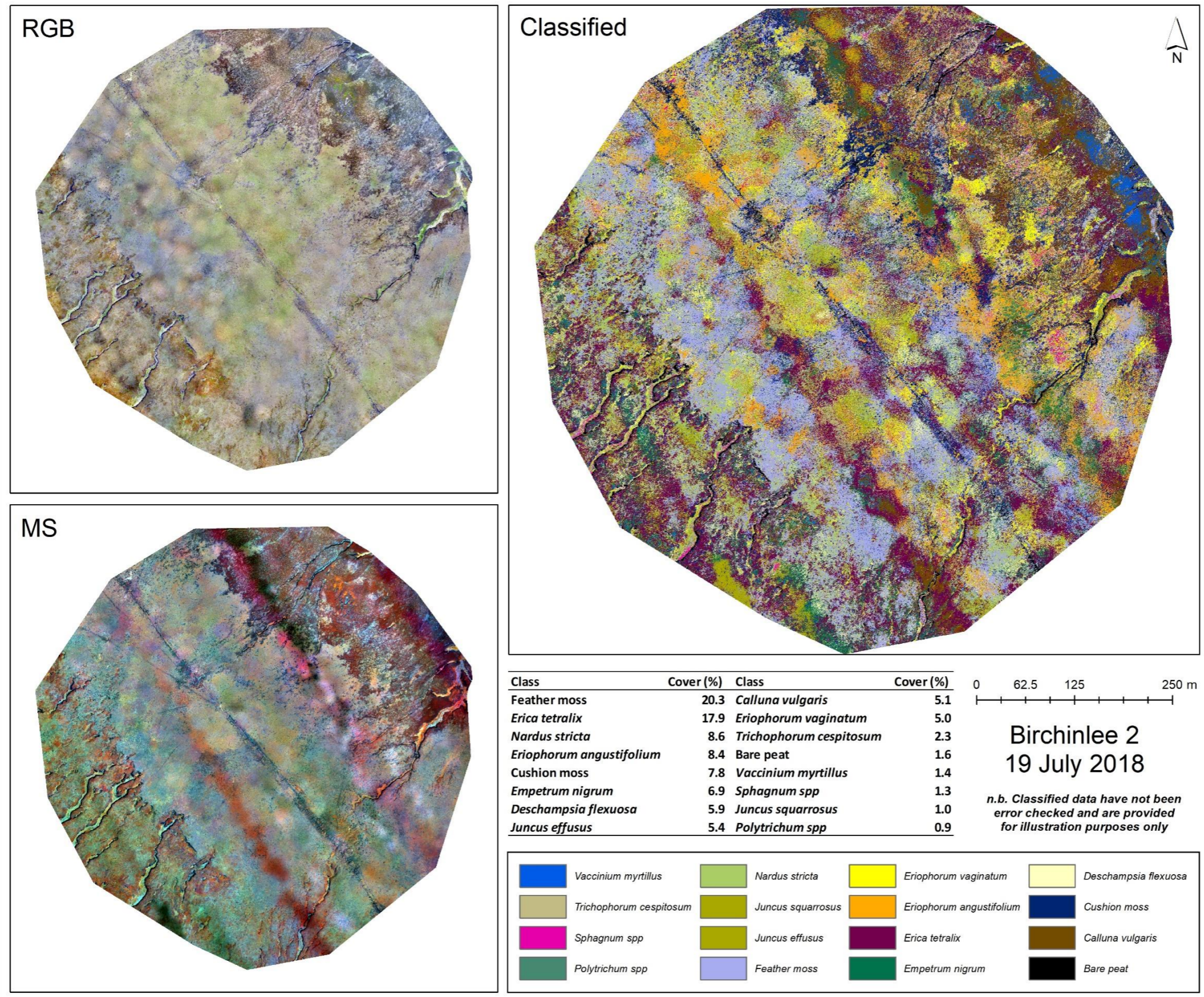


Figure 3:4. Processed RGB and multispectral (MS: NIR, G, R) imagery and classified output for Birchinlee 2 study area.
n.b. the very clear 'striping' apparent in the MS image and its effects in the classified output. The causes of this are discussed in text.

Table 3:9. Spectral separability analysis: Birchinlee 2 Note: Owing to small sample sizes these figures should be treated with caution.

Above: Transformed Divergence. Values nearer to 2.0 mean an increasing probability of good separation. Breakpoints taken as <1.0 poor separability; 1.0 – 1.9 moderate separation (Jenson 1996).

Below: Jeffries-Matusita Distance. Values nearer to 1.414 mean an increasing probability of good separation.

	Bare peat	<i>Calluna vulgaris</i>	Cushion moss	<i>Deschampsia flexuosa</i>	<i>Empetrum nigrum</i>	<i>Erica tetralix</i>	<i>E. angustifolium</i>	<i>E. vaginatum</i>	Feather moss	<i>Juncus effusus</i>	<i>Juncus squarrosus</i>	<i>Nardus stricta</i>	<i>Polytrichum</i> spp	<i>Sphagnum</i> spp	<i>Trichophorum cespitosum</i>	<i>Vaccinium myrtillus</i>
Bare peat	0.000	2.000	1.910	2.000	2.000	2.000	1.999	2.000	1.999	2.000	2.000	2.000	2.000	2.000	2.000	2.000
<i>Calluna vulgaris</i>		0.000	1.888	1.958	1.110	1.307	1.617	1.992	1.855	1.778	1.998	1.999	1.717	2.000	1.693	1.562
Cushion moss			0.000	1.921	1.913	1.438	1.289	1.992	1.603	1.887	2.000	1.955	1.999	1.992	1.978	2.000
<i>Deschampsia flexuosa</i>				0.000	1.475	1.627	1.702	0.467	1.252	1.327	1.996	0.690	1.432	1.174	1.745	1.983
<i>Empetrum nigrum</i>					0.000	0.964	1.545	1.691	1.611	1.856	1.998	1.900	1.576	1.946	1.579	1.418
<i>Erica tetralix</i>						0.000	1.466	1.779	1.602	1.525	1.983	1.829	1.942	1.989	1.446	1.819
<i>E. angustifolium</i>							0.000	1.906	1.248	1.755	2.000	1.957	1.943	1.973	1.893	1.997
<i>E. vaginatum</i>								0.000	1.591	1.449	1.992	0.705	1.520	1.251	1.819	1.990
Feather moss									0.000	1.826	2.000	1.431	1.969	1.724	1.955	1.999
<i>Juncus effusus</i>										0.000	1.696	1.568	1.717	1.488	1.242	1.829
<i>Juncus squarrosus</i>											0.000	1.997	1.998	2.000	1.473	1.804
<i>Nardus stricta</i>												0.000	1.900	1.252	1.942	1.999
<i>Polytrichum</i> spp													0.000	1.793	1.487	1.791
<i>Sphagnum</i> spp														0.000	1.999	2.000
<i>T. cespitosum</i>															0.000	1.083
<i>Vaccinium myrtillus</i>																0.000
Bare peat	0.000	1.322	1.302	1.363	1.385	1.395	1.379	1.412	1.307	1.396	1.414	1.407	1.389	1.382	1.409	1.396
<i>Calluna vulgaris</i>		0.000	1.114	1.263	0.888	1.044	1.068	1.360	1.241	1.270	1.406	1.393	1.157	1.273	1.213	1.067
Cushion moss			0.000	1.222	1.255	1.122	1.006	1.386	1.108	1.281	1.413	1.363	1.298	1.272	1.328	1.352
<i>Deschampsia flexuosa</i>				0.000	1.119	1.127	1.149	0.628	0.953	1.043	1.297	0.786	1.130	0.922	1.164	1.288
<i>Empetrum nigrum</i>					0.000	0.899	1.091	1.220	1.149	1.303	1.384	1.303	1.099	1.284	1.075	1.045
<i>Erica tetralix</i>						0.000	1.107	1.250	1.181	1.114	1.376	1.277	1.231	1.255	1.025	1.193
<i>E. angustifolium</i>							0.000	1.331	1.026	1.284	1.413	1.363	1.064	1.188	1.289	1.349
<i>E. vaginatum</i>								0.000	1.166	1.178	1.286	0.813	1.187	1.033	1.159	1.289
Feather moss									0.000	1.189	1.406	1.103	1.242	1.167	1.345	1.379
<i>Juncus effusus</i>										0.000	1.208	1.174	1.164	1.024	1.021	1.257
<i>Juncus squarrosus</i>											0.000	1.354	1.277	1.322	1.073	1.231
<i>Nardus stricta</i>												0.000	1.338	0.930	1.331	1.378
<i>Polytrichum</i> spp													0.000	1.148	1.052	1.097
<i>Sphagnum</i> spp														0.000	1.231	1.324
<i>T. cespitosum</i>															0.000	0.968
<i>Vaccinium myrtillus</i>																0.000

n.b. Owing to small sample sizes these figures should be treated with caution.

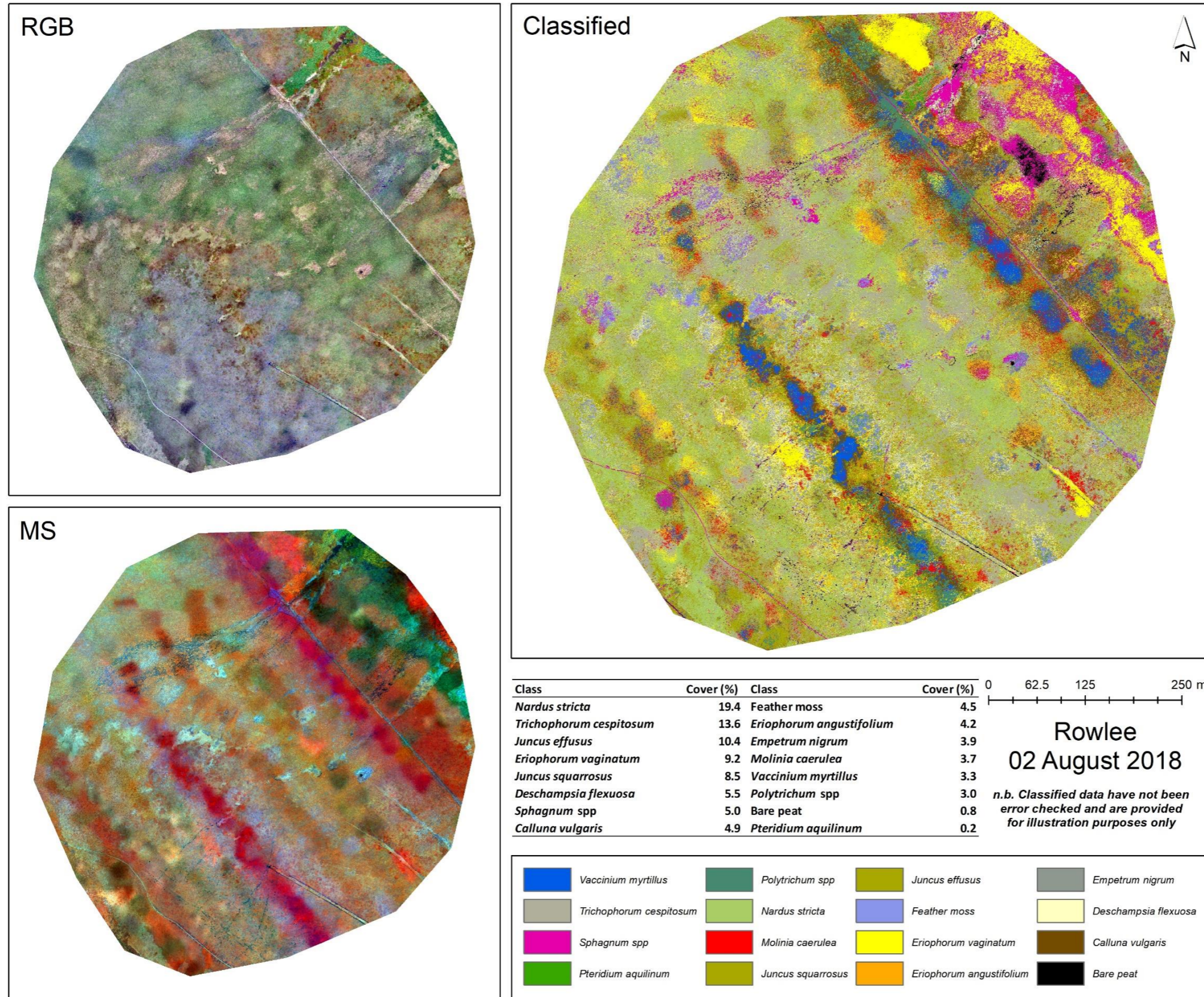


Figure 3:5. Processed RGB and multispectral (MS: NIR, G, R) imagery and classified output for Rowlee study area
n.b. the very clear 'striping' apparent in the MS image and its effects in the classified output. The causes of this are discussed in text.

Table 3:10. Spectral separability analysis: Rowlee.

Above: Transformed Divergence. Values nearer to 2.0 mean an increasing probability of good separation. Breakpoints taken as <1.0 poor separability; 1.0 – 1.9 moderate separation (Jenson 1996).

Below: Jeffries-Matusita Distance. Values nearer to 1.414 mean an increasing probability of good separation.

	Bare peat	<i>Calluna vulgaris</i>	<i>D. flexuosa</i>	<i>Empetrum nigrum</i>	<i>E. angustifolium</i>	<i>E. vaginatum</i>	Feather moss	<i>Juncus effusus</i>	<i>Juncus squarrosus</i>	<i>Molinia caerulea</i>	<i>Nardus stricta</i>	<i>Polytrichum</i> spp	<i>Pteridium aquilinum</i>	<i>Sphagnum</i> spp	<i>T. cespitosum</i>	<i>Vaccinium myrtillus</i>
Bare peat	0.000	2.000	1.982	1.999	1.991	2.000	2.000	1.998	1.999	2.000	1.998	1.994	2.000	1.999	1.999	2.000
<i>Calluna vulgaris</i>		0.000	1.998	1.098	1.503	1.905	2.000	1.873	1.268	1.406	1.918	1.898	2.000	2.000	1.955	1.620
<i>Deschampsia flexuosa</i>			0.000	1.996	1.877	1.965	2.000	1.908	1.999	2.000	1.948	1.985	2.000	2.000	1.996	2.000
<i>Empetrum nigrum</i>				0.000	0.717	1.852	1.998	1.738	1.420	1.583	1.747	1.632	2.000	2.000	1.923	1.806
<i>Eriophorum angustifolium</i>					0.000	1.358	1.899	1.528	1.293	1.308	1.548	1.492	2.000	1.988	1.435	1.954
<i>Eriophorum vaginatum</i>						0.000	1.889	1.930	1.901	0.758	1.760	1.928	2.000	1.935	1.176	1.951
Feather moss							0.000	1.797	1.963	1.969	1.686	1.872	2.000	1.767	1.910	2.000
<i>Juncus effusus</i>								0.000	0.852	1.658	1.355	1.140	2.000	1.943	1.659	1.981
<i>Juncus squarrosus</i>									0.000	1.163	1.587	1.544	2.000	1.992	1.731	1.798
<i>Molinia caerulea</i>										0.000	1.511	1.875	1.999	1.973	1.035	1.378
<i>Nardus stricta</i>											0.000	1.848	2.000	1.918	1.017	1.971
<i>Polytrichum</i> spp												0.000	2.000	1.784	1.880	1.971
<i>Pteridium aquilinum</i>													0.000	2.000	2.000	1.998
<i>Sphagnum</i> spp														0.000	1.980	2.000
<i>T. cespitosum</i>															0.000	1.956
<i>Vaccinium myrtillus</i>																0.000
Bare peat	0.000	1.413	1.312	1.400	1.390	1.414	1.414	1.412	1.411	1.411	1.411	1.399	1.414	1.378	1.409	1.412
<i>Calluna vulgaris</i>		0.000	1.390	0.982	1.125	1.201	1.411	1.234	0.950	1.040	1.327	1.282	1.414	1.362	1.206	1.166
<i>Deschampsia flexuosa</i>			0.000	1.278	1.184	1.276	1.349	1.179	1.313	1.305	1.216	1.282	1.414	1.304	1.280	1.412
<i>Empetrum nigrum</i>				0.000	0.774	1.188	1.399	1.166	1.073	1.112	1.229	1.122	1.414	1.320	1.214	1.297
<i>Eriophorum angustifolium</i>					0.000	1.039	1.346	1.025	0.970	1.016	1.132	1.110	1.414	1.263	1.066	1.332
<i>Eriophorum vaginatum</i>						0.000	1.318	1.258	1.243	0.825	1.110	1.361	1.413	1.330	0.939	1.269
Feather moss							0.000	1.314	1.398	1.359	1.264	1.313	1.414	1.117	1.343	1.414
<i>Juncus effusus</i>								0.000	0.884	1.181	1.063	1.047	1.414	1.299	1.134	1.351
<i>Juncus squarrosus</i>									0.000	0.984	1.230	1.180	1.414	1.353	1.037	1.208
<i>Molinia caerulea</i>										0.000	1.114	1.316	1.402	1.349	0.923	1.030
<i>Nardus stricta</i>											0.000	1.315	1.414	1.274	0.926	1.367
<i>Polytrichum</i> spp.												0.000	1.414	1.255	1.281	1.356
<i>Pteridium aquilinum</i>													0.000	1.414	1.408	1.406
<i>Sphagnum</i> spp														0.000	1.350	1.405
<i>T. cespitosum</i>															0.000	1.313
<i>Vaccinium myrtillus</i>																0.000

n.b. Owing to small sample sizes these figures should be treated with caution.

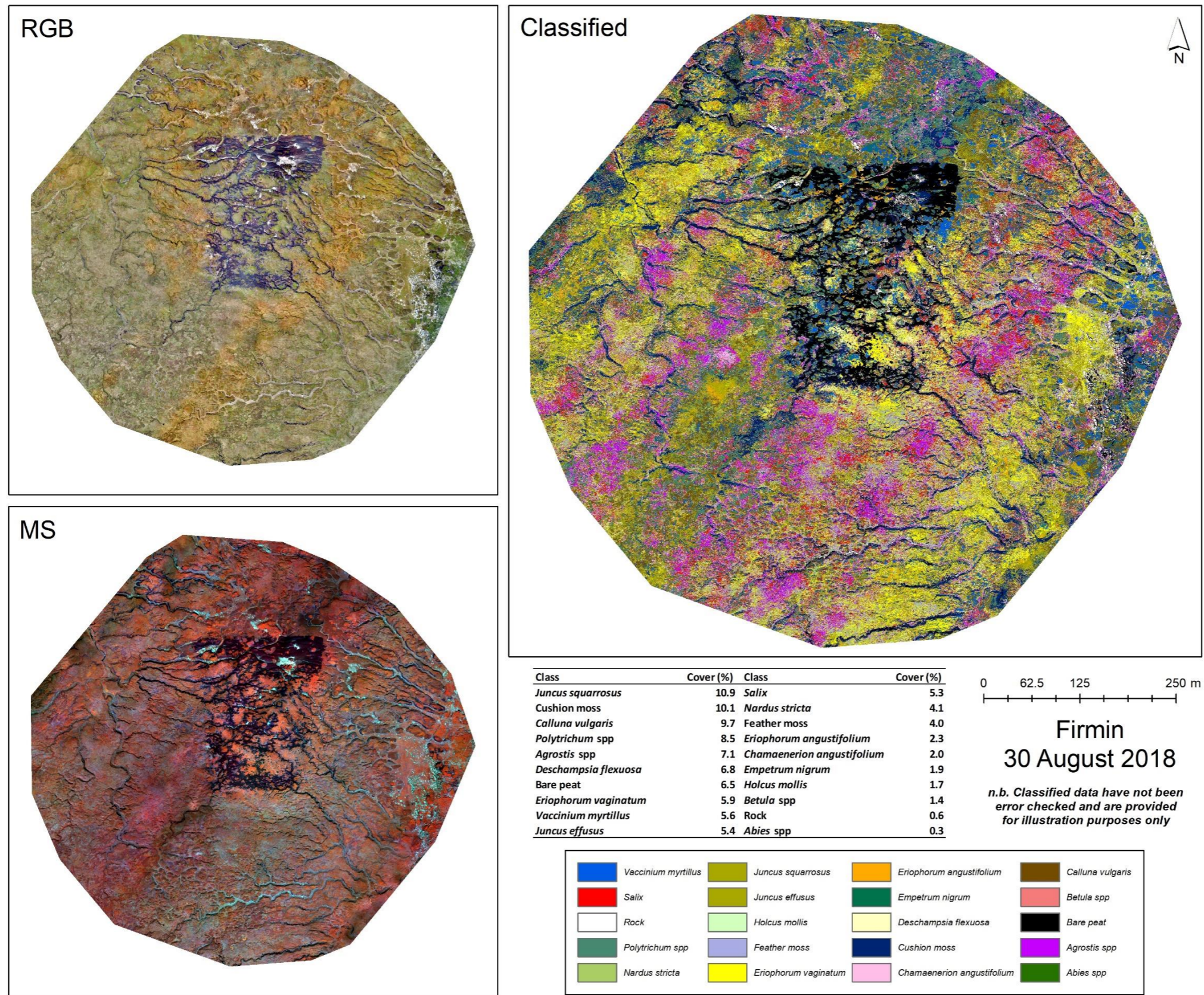


Figure 3:6. Processed RGB and multispectral (MS: NIR, G, R) imagery and classified output for Firmin study area
n.b. the very clear 'striping' apparent in both RGB and MS images and their effects in the classified output. The causes of this are discussed in text.

Table 3:11. Spectral separability analysis: Firmin.

Above: Transformed Divergence. Values nearer to 2.0 mean an increasing probability of good separation. Breakpoints taken as <1.0 poor separability; 1.0 – 1.9 moderate separation (Jenson 1996).

Below: Jeffries-Matusita Distance. Values nearer to 1.414 mean an increasing probability of good separation.

	Abies spp	Agrostis spp	Bare peat	Betula spp	Calluna vulgaris	C. angustifolium	Cushion moss	Deschampsia flexuosa	Empetrum nigrum	E. angustifolium	E. vaginatum	Feather moss	Holcus mollis	Juncus effusus	Juncus squarrosus	Nardus stricta	Polytrichum spp	Rock	Salix	Vaccinium myrtillus	Water
Abies spp	0.000	2.000	2.000	2.000	1.871	1.465	1.999	1.990	1.582	2.000	1.887	2.000	2.000	2.000	1.999	2.000	1.953	2.000	1.413	1.551	2.000
Agrostis spp		0.000	1.874	2.000	1.717	1.756	1.710	0.775	1.966	1.554	1.747	1.226	1.722	0.763	1.712	1.042	1.838	1.994	1.876	1.997	2.000
Bare peat			0.000	2.000	1.990	2.000	1.849	1.917	2.000	1.835	1.999	2.000	1.998	1.874	1.995	1.997	1.982	1.972	2.000	2.000	2.000
Betula spp				0.000	2.000	2.000	2.000	2.000	2.000	2.000	2.000	2.000	2.000	2.000	2.000	2.000	2.000	2.000	2.000	2.000	2.000
Calluna vulgaris					0.000	1.306	1.679	0.977	1.585	1.284	1.267	1.938	1.994	1.314	0.947	1.793	0.671	2.000	1.456	1.153	2.000
C. angustifolium						0.000	1.966	1.465	0.814	1.921	0.888	1.997	2.000	1.917	1.863	1.857	1.700	2.000	0.726	1.173	2.000
Cushion moss							0.000	1.302	1.995	1.622	1.704	1.993	1.382	1.439	1.801	1.984	1.434	2.000	1.971	1.973	2.000
Deschampsia flexuosa								0.000	1.772	1.296	1.242	1.734	1.742	0.803	1.190	1.312	1.338	2.000	1.629	1.888	2.000
Empetrum nigrum									0.000	1.988	1.329	2.000	2.000	1.978	1.957	1.978	1.879	2.000	1.301	0.641	2.000
Eriophorum angustifolium										0.000	1.845	1.964	1.994	1.155	1.360	1.796	1.134	2.000	1.967	1.990	2.000
Eriophorum vaginatum											0.000	1.922	1.990	1.753	1.426	1.527	1.590	2.000	1.269	1.470	2.000
Feather moss												0.000	1.951	1.573	1.918	1.598	1.988	1.999	1.990	2.000	2.000
Holcus mollis													0.000	1.716	1.991	1.983	1.970	2.000	2.000	2.000	2.000
Juncus effusus														0.000	1.147	1.455	1.547	1.992	1.929	1.990	2.000
Juncus squarrosus															0.000	1.754	1.263	2.000	1.856	1.897	2.000
Nardus stricta																0.000	1.979	1.948	1.910	1.998	2.000
Polytrichum spp																	0.000	2.000	1.809	1.796	2.000
Rock																		0.000	2.000	2.000	2.000
Salix																			0.000	1.291	2.000
Vaccinium myrtillus																				0.000	2.000
Water																					0.000
Abies spp	0.000	1.401	1.411	1.353	1.300	1.065	1.396	1.355	1.123	1.400	1.342	1.401	1.409	1.396	1.400	1.397	1.346	1.414	1.066	1.101	1.413
Agrostis spp		0.000	1.232	1.405	1.278	1.236	1.286	0.816	1.363	1.137	1.233	0.969	1.136	0.801	1.264	0.973	1.315	1.396	1.334	1.394	1.414
Bare peat			0.000	1.414	1.373	1.368	1.143	1.237	1.399	1.277	1.378	1.335	1.263	1.266	1.404	1.323	1.330	1.338	1.413	1.412	1.407
Betula (not specified)				0.000	1.311	1.345	1.396	1.363	1.364	1.402	1.384	1.393	1.411	1.384	1.397	1.407	1.339	1.414	1.329	1.324	1.414
Calluna vulgaris					0.000	0.985	1.223	0.933	1.149	1.082	1.095	1.333	1.356	1.066	0.893	1.288	0.772	1.414	1.183	1.016	1.414
C. angustifolium						0.000	1.284	1.044	0.812	1.230	0.868	1.328	1.370	1.193	1.130	1.259	1.124	1.414	0.751	0.967	1.414
Cushion moss							0.000	1.069	1.356	1.100	1.264	1.368	1.055	1.075	1.286	1.381	1.112	1.414	1.396	1.383	1.401
Deschampsia flexuosa								0.000	1.235	1.008	1.031	1.155	1.104	0.796	0.987	1.028	1.061	1.403	1.215	1.238	1.414
Empetrum nigrum									0.000	1.360	1.027	1.376	1.402	1.329	1.289	1.333	1.304	1.414	0.940	0.719	1.414
Eriophorum angustifolium										0.000	1.265	1.324	1.237	0.946	1.045	1.267	0.979	1.410	1.392	1.369	1.413
Eriophorum vaginatum											0.000	1.274	1.369	1.157	1.079	1.146	1.223	1.414	1.105	1.132	1.414
Feather moss												0.000	1.335	1.093	1.344	0.971	1.370	1.394	1.361	1.391	1.414
Holcus mollis													0.000	1.181	1.396	1.378	1.340	1.407	1.411	1.409	1.414
Juncus effusus														0.000	0.982	1.153	1.081	1.397	1.362	1.351	1.414
Juncus squarrosus															0.000	1.242	1.010	1.414	1.341	1.301	1.414
Nardus stricta																0.000	1.353	1.364	1.321	1.356	1.414
Polytrichum spp																	0.000	1.414	1.321	1.271	1.413
Rock																		0.000	1.414	1.414	1.414
Salix																			0.000	1.016	1.414
Vaccinium myrtillus																				0.000	1.414
Water																					0.000

n.b. Owing to small sample sizes these figures should be treated with caution.

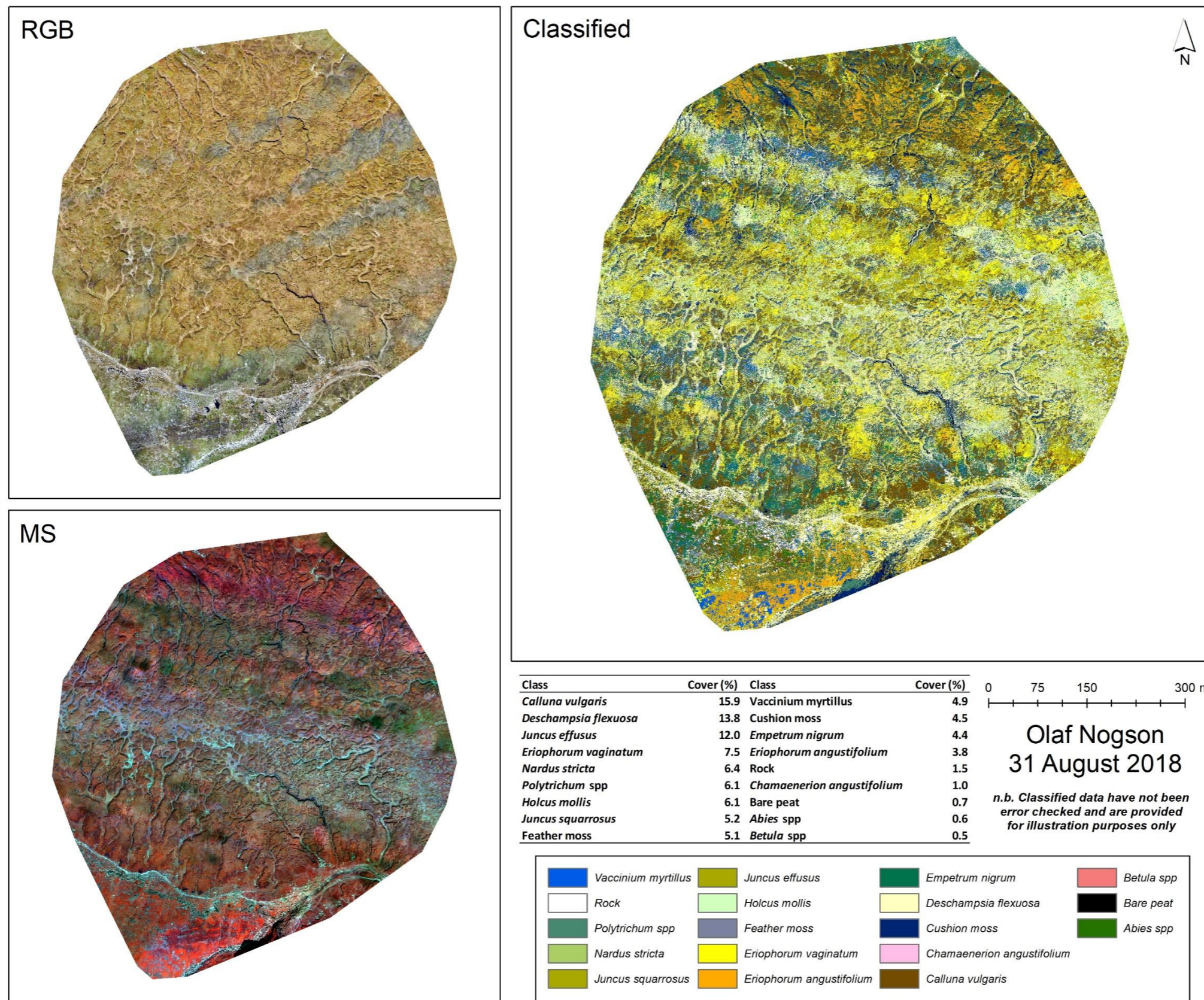


Figure 3:7. Processed RGB and multispectral (MS: NIR, G, R) imagery and classified output for Olaf Nogson study area
n.b. the very clear 'striping' apparent in both RGB and MS images and their effects in the classified output. The causes of this are discussed in text.

Table 3:12. Spectral separability analysis: Olaf Nogson.

Above: Transformed Divergence. Values nearer to 2.0 mean an increasing probability of good separation. Breakpoints taken as <1.0 poor separability; 1.0 – 1.9 moderate separation (Jenson 1996).

Below: Jeffries-Matusita Distance. Values nearer to 1.414 mean an increasing probability of good separation.

	<i>Abies</i> spp	Bare peat	<i>Betula</i> spp	<i>Calluna vulgaris</i>	<i>C. angustifolium</i>	Cushion moss	<i>Deschampsia flexuosa</i>	<i>Empetrum nigrum</i>	<i>E. angustifolium</i>	<i>E. vaginatum</i>	Feather moss	<i>Holcus mollis</i>	<i>Juncus effusus</i>	<i>Juncus squarrosus</i>	<i>Nardus stricta</i>	<i>Polytrichum</i> spp	Rock	<i>Vaccinium myrtillus</i>	Water
<i>Abies</i> spp	0.000	2.000	2.000	1.995	2.000	2.000	2.000	1.233	2.000	1.946	2.000	2.000	2.000	2.000	2.000	1.996	2.000	1.575	2.000
Bare peat		0.000	2.000	2.000	2.000	1.986	2.000	2.000	2.000	2.000	2.000	2.000	2.000	2.000	2.000	2.000	2.000	2.000	1.999
<i>Betula</i> spp			0.000	2.000	2.000	2.000	2.000	2.000	2.000	1.989	2.000	2.000	2.000	2.000	2.000	2.000	2.000	1.999	2.000
<i>Calluna vulgaris</i>				0.000	1.999	1.857	1.477	1.830	1.194	1.606	1.882	1.996	0.990	1.124	1.978	0.854	2.000	1.427	2.000
<i>C. angustifolium</i>					0.000	2.000	2.000	1.998	1.999	1.996	2.000	2.000	2.000	1.999	2.000	2.000	2.000	1.999	2.000
Cushion moss						0.000	1.995	2.000	1.924	2.000	1.997	1.988	1.841	1.924	2.000	1.737	2.000	2.000	1.983
<i>Deschampsia flexuosa</i>							0.000	1.994	1.754	1.074	1.994	1.670	0.985	1.654	1.852	1.690	1.983	1.588	2.000
<i>Empetrum nigrum</i>								0.000	1.959	1.763	2.000	2.000	1.986	1.960	2.000	1.884	2.000	1.270	2.000
<i>Eriophorum angustifolium</i>									0.000	1.497	1.999	1.999	1.220	0.585	2.000	0.931	2.000	1.626	2.000
<i>Eriophorum vaginatum</i>										0.000	1.969	1.974	1.560	1.443	1.989	1.721	2.000	0.908	2.000
Feather moss											0.000	2.000	1.990	1.992	2.000	1.994	2.000	1.999	1.991
<i>Holcus mollis</i>												0.000	1.756	1.987	1.985	1.998	2.000	2.000	2.000
<i>Juncus effusus</i>													0.000	0.931	1.898	1.354	1.988	1.773	1.993
<i>Juncus squarrosus</i>														0.000	1.998	1.137	1.999	1.689	2.000
<i>Nardus stricta</i>															0.000	2.000	2.000	2.000	2.000
<i>Polytrichum</i> spp																0.000	2.000	1.528	2.000
Rock																	0.000	2.000	2.000
<i>Vaccinium myrtillus</i>																		0.000	2.000
Water																			0.000
<i>Abies</i> spp	0.000	1.414	1.405	1.378	1.402	1.413	1.307	1.035	1.381	1.260	1.414	1.398	1.398	1.385	1.406	1.359	1.414	1.079	1.414
Bare peat		0.000	1.414	1.408	1.414	1.393	1.387	1.414	1.367	1.412	1.414	1.414	1.412	1.406	1.414	1.297	1.406	1.403	1.322
<i>Betula</i> spp			0.000	1.411	1.305	1.414	1.377	1.412	1.391	1.295	1.414	1.414	1.413	1.404	1.414	1.409	1.414	1.361	1.414
<i>Calluna vulgaris</i>				0.000	1.406	1.267	1.103	1.303	1.063	1.187	1.307	1.401	0.955	1.002	1.348	0.810	1.409	1.042	1.341
<i>C. angustifolium</i>					0.000	1.414	1.355	1.372	1.398	1.223	1.413	1.414	1.408	1.384	1.414	1.401	1.414	1.301	1.414
Cushion moss						0.000	1.250	1.414	1.240	1.391	1.373	1.328	1.273	1.250	1.414	1.116	1.366	1.360	1.196
<i>Deschampsia flexuosa</i>							0.000	1.258	1.276	0.963	1.229	1.145	0.918	1.185	1.142	1.163	1.345	1.106	1.259
<i>Empetrum nigrum</i>								0.000	1.319	1.113	1.412	1.392	1.353	1.301	1.387	1.301	1.414	0.962	1.414
<i>Eriophorum angustifolium</i>									0.000	1.172	1.390	1.395	1.022	0.713	1.405	0.915	1.403	1.173	1.345
<i>Eriophorum vaginatum</i>										0.000	1.359	1.317	1.155	1.126	1.300	1.250	1.412	0.881	1.386
Feather moss											0.000	1.379	1.300	1.343	1.381	1.332	1.387	1.352	1.294
<i>Holcus mollis</i>												0.000	1.167	1.326	1.300	1.406	1.367	1.392	1.377
<i>Juncus effusus</i>													0.000	0.870	1.245	1.093	1.389	1.225	1.252
<i>Juncus squarrosus</i>														0.000	1.372	0.991	1.396	1.187	1.303
<i>Nardus stricta</i>															0.000	1.389	1.404	1.365	1.382
<i>Polytrichum</i> spp																0.000	1.405	1.132	1.295
Rock																	0.000	1.410	1.405
<i>Vaccinium myrtillus</i>																		0.000	1.368
Water																			0.000

3.2.5 Accuracy assessment

An accuracy assessment was only undertaken for one site, Firmin, which although lacking adequate data for an optimal error assessment, nevertheless was the site with the most species with greater than 20 field samples. The overall classification accuracy at Firmin was measured at 43%, with kappa 39%. The accuracies for different classes vary from very good for a few classes to very poor for others. Unambiguously “good” classes were bare peat and rock, which is unsurprising given their clear NIR responses. “Poor” classes included species like *Juncus effusus* (10% user accuracy), *Empetrum nigrum* and *Chamaenerion angustifolium* (13%). *Juncus effusus* was confused by the classifier with *Agrostis*, cushion moss, *Deschampsia flexuosa*, *Eriophorum angustifolium* and *Polytrichum* spp.

The estimates of spectral separability are largely reflected in the user accuracy of the classified map at Firmin, although the three classes with the lowest user accuracies were not those with the lowest separabilities (Figure 3:8). Thus spectral separability seems to be a generally useful guide for eventual classified accuracies, accepting the caveats above regarding low sample sizes (Table 3:13).

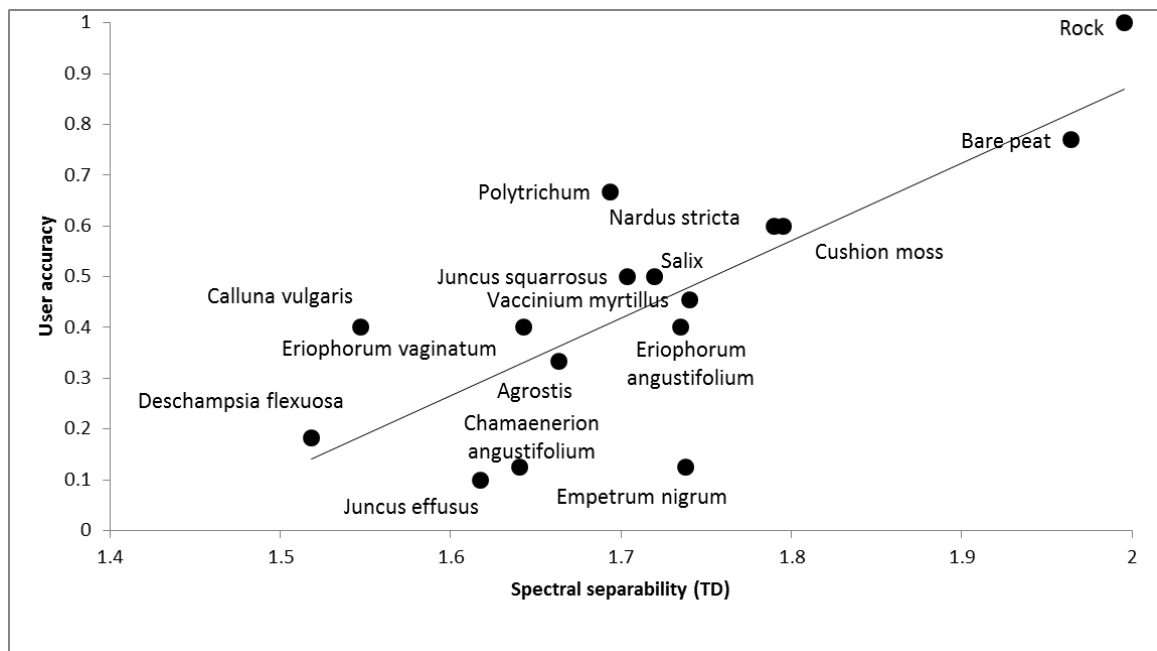


Figure 3:8. The relationship between average spectral separability and user accuracy at Firmin.



Table 3:13. Confusion matrix for image classification at Firmin.

	Agrostis spp.	Bare peat	Calluna vulgaris	Chamaenerion angustifolium	Cushion moss	Deschampsia flexuosa	Empetrum nigrum	Eriophorum angustifolium	Eriophorum vaginatum	Juncus effusus	Juncus squarrosus	Nardus stricta	Polytrichum spp.	Rock	Salix	Vaccinium myrtillus	Total	User accuracy
Agrostis spp.	2	1					1			2							6	0.33
Bare peat		10			1			1						1			13	0.77
Calluna vulgaris			4			1					1		1			3	10	0.40
Chamaenerion angustifolium				1	1				1	1	1				3		8	0.13
Cushion moss	1				6				1	1			1				10	0.60
Deschampsia flexuosa	1				2	2		1		2	1				1	1	11	0.18
Empetrum nigrum				1			1								1	5	8	0.13
Eriophorum angustifolium	1		1		1			4					3				10	0.40
Eriophorum vaginatum							2		4	1	3						10	0.40
Juncus effusus	2				3	1		1		1			2				10	0.10
Juncus squarrosus									1	3	5	1					10	0.50
Nardus stricta	1									1		3					5	0.60
Polytrichum spp.			1										4				6	0.67
Rock														5			5	1.00
Salix							1								3	2	6	0.50
Vaccinium myrtillus			1				2		1		1				1	5	11	0.45
Total	8	11	7	2	14	4	7	7	8	12	13	4	11	6	9	16	139	
Producer accuracy	0.25	0.91	0.57	0.50	0.43	0.50	0.14	0.57	0.50	0.08	0.38	0.75	0.36	0.83	0.33	0.31		
N (total observations)				139				Overall accuracy				0.43						
X (Sum of all correct)				60				Kappa				0.39						
Y (Sum of total user x sum of total producer)				1263														

3.3 Summary of Phase 1

Two main lessons were learned from Phase 1: problems of flying large areas using UAVs, and difficulties in capturing sufficient ground truth data for classifier training and error assessment. As these both adversely effected the ability of the project to meet MFFPs needs, two parallel approaches were proposed for Phase 2:

- i. Use of 'traditional' airborne digital image capture via a contractor such as Bluesky*, Cyient (Blom aerofilm), GetMapping, or similar. These can be obtained at close to, and often better than, the resolution originally anticipated for the UAV multispectral data capture so will be essentially comparable from that aspect. (*eventually used for this project after closed-tender bids).

Moreover, airborne photography covers large areas quickly and the images required to cover each MFFP field laboratory, and surrounding area, will be captured essentially instantaneously in comparison to using a UAV. This overcomes many of the potential concerns associated with the slow process required to 'build' coverage of large areas with UAVs, e.g. transitions in light intensity, changes in light angle, potential for image blur in strong wind, incomplete capture in a single flight due to change in weather or equipment failure.

Airborne photography also removes risks to image capture associated with site access restrictions. This increases the likelihood of finding 'windows' of good weather for flying. Site visits to collect field data can be undertaken at other times as access regimes allow and are at low risk of failure as they are weather independent.

Equally importantly, use of airborne photography reduces surveyor time commitments enabling them to conduct higher quality research and field work.

- ii. The success of the first round of image classification was regrettably limited by small sample numbers, as well as incomplete spatial coverage across the imaged areas. Alongside that issue it also became apparent during processing that target sample numbers for each species needed increasing beyond the original estimations.

Field data collection therefore needs a significant expansion during future rounds of monitoring. Given the image resolutions a target of 100 'pure' samples per species is recommended. There is high intrageneric spectral variation in some taxa like *Sphagnum spp.* and *Polytrichum spp.* Survey timing will have a large role in determining whether *Sphagnum spp.* can be differentiated spectrally. There



may also be difficulty in obtaining enough samples of some taxa, and this may become a particular issue where these are those of most interest, e.g. *Sphagnum* spp.





Section 4: Phase 2 – MAV Image Capture I

Originally reporting in Summary report 2020

Summary introduction to Phase 2 activities.

Following the lessons of Phase 1, the objectives of MFF 50 2016-17 were expanded to examine the application of alternate image data sources to address MFFP monitoring needs. Therefore, in lieu of performing repeat mapping using UAV-derived imagery, Phase 2 assessed the use of 'conventional' commercial MAV 4-band digital imagery capture.

In principle, conventionally flown airborne data provides several potential benefits over UAV capture for MFFP:

- i. Staff-time commitments to UAV flying and establishing ground control targets are removed.
- ii. Image processing-time overheads are minimised, expediting mapping components of the project.
- iii. Photogrammetric cameras used on recent commercial MAV platforms easily match the GSD achieved by UAVs flown at 100-120 m (above ground level) while capturing a significantly larger swath.
- iv. Image capture is effectively instantaneous over each site, and all are covered within a period of minutes; hence sun-angle and illumination are essentially the same across each study area. Additionally, this means that phenological differences between each site are minimised to those naturally present within populations at the time of capture, rather than potentially arising as a product of differing dates of survey. Both factors allow images from all sites to share field observations for training and error assessment. Execution of image classification and associated accuracy determinations can be executed in one go.

However, this project has been predicated on mapping individual species using extremely-high-resolution imagery to identify changes in abundances of *Sphagnum* spp. and cover of bare peat at a fine scale, and this remains a prime objective. Accommodating a shift to alternate high-resolution imagery in this case brings potential challenges. The most significant of these is that airborne data are generally orthorectified using sensor and aircraft orientation parameters with few or even no ground control data localised to the study sites. While this process can be expected to still yield a high degree of accuracy, the co-registration between image and ground data will not be as 'tight' as that originally expected, or achieved, using UAV capture. In this case, the airborne data had a reported orthorectification accuracy (RMSE) of 12 cm and 16 cm in x and y respectively (representing a potential horizontal image shift of 1-2 pixels) compared to <1 pixel achieved by the UAV in Phase 1. This project is heavily dependent on obtaining spectral data from individual pixels matched to field data recorded by DGNS with a location



typically accurate to 2-3 cm. Any relaxation of spatial co-registration between image and field data increases the probability of spectral information being assigned to the wrong species and degrading classification accuracy. This can be partially mitigated in classification by using field (training) samples of a minimum size (here 50 cm in x and y dimensions).

Objectives of Phase 2

Despite the change of imagery utilised, the overall objectives of Phase 2 are essentially the same as Phase 1: to assess the application of remotely sensed data to MFFP needs, i.e. to monitor changes in the cover of *Sphagnum* species, other vegetation types, and bare peat.

To help define a suite of species that can be reliably mapped from 4-band digital imagery three main approaches were adopted during Phase 2:

1. Spectral separability analyses
2. Multivariate spectral clustering analysis via canonical correlation analysis
3. Supervised image classification and error-assessment

Each of these analyses were iterated to examine:

- i.* How rare species influence individual and overall accuracy by progressive removal.
- ii.* Possible negative consequences arising from utilising a different image type and registration accuracy.

To allow, as far as possible, comparison with results in Phase 1, the classification protocols adopted here are essentially the same, i.e. supervised pixel classification. As an extensive campaign of field survey was undertaken in 2019 in support of Phase 2 image capture, full formal error assessments of all classified products are reported.



4.1. Data sources and associated pre-processing

4.1.1 Image data

The five study sites, containing eleven experimental catchments (Table 4:1), were flown on 02/10/2019 by Bluesky International. Imagery was captured using an Ultracam Eagle 100 with a 100.5mm lens at an altitude of 2400 m to yield an ultimate ground resolution of 10cm in both axes. RGB and NIR bands were supplied fully orthorectified as 1 km² tiles (aligned with the Ordnance Survey National Grid) in TIFF format. The only additional processing applied to the supplied imagery was the creation of mosaics in .img format.

Table 4:1. Image coverage supplied by study site

Survey site	Image area (km ²)	Experimental catchments
Birchinlee	2	Eriophorum (Con); Eriophorum (Spha)
Derwent Howden	1	Calluna (Con); Calluna (Spha); Calluna (Spha GB)
Penguins	2	P (Ref)
Moss Moor	2	Molinia (Con); Molinia (Spha)
Kinder	3	F (Con); N (Veg Spha GB); O (Veg)

Intervention: Con = control; GB = gully blocking; Ref = intact reference; Spha = Sphagnum; Veg = revegetation.

Problems with data supply. Owing to problems with gaining permission to fly in the airspace required (as reported by Bluesky) the date of image capture was finally very late in the year and well outside the period specified. This had adverse consequences for both the phenological state of many species at time of imaging as well as low sun angles, the latter resulting in the presence of considerable amounts of shadow in the imagery. Both factors that could be expected to reduce classification accuracies below what might be anticipated. However, given the option of not progressing at all in 2019, and considering both: the extensive field data collection already completed and; that much of MFF 50 2016-17 is developmental in nature and hence considerable information could still be gained, it was decided to continue with image classification.

Inclusion of imagery with large amounts of shadow has necessitated some changes from what might be considered 'standard' remote sensing practices. Where this has occurred, and the consequences they might cause, a note has been made in the text.

4.1.2 Field data

During 2019 a comprehensive field survey effort was undertaken by MFFP. To ensure good spatial coverage of the area of interest within each image a virtual grid comprising 100 points was created within a GIS and transferred to the field data-logging equipment. Field surveyors searched within an approximate 30 m radius centred on these predetermined sample locations to identify single species stands with a minimum extent of 0.5 m x 0.5 m. The species present and the location of the 'patch' was recorded using



post-processed differential GNSS. A 'running tally' of each species was kept and additional samples recorded if species with a low number of records were observed in transit to each sample location. The overall aim of the sampling effort was to attempt to identify 100 examples of all species present at each study site. At the cessation of field survey the target of 100 samples at each site was only achieved for some species, either as a result of absolute scarcity or the lack of single stands of adequate size.

The field data comprised 7104 field samples providing a total of 55 vegetation classes. Samples of *Calluna vulgaris* and *Empetrum nigrum* recorded as being dead in field notes were assigned as new sub-classes (*Calluna* dead and *Empetrum* dead). The remaining *Calluna* samples were split into four further classes for classification: *Calluna* without flowers, *Calluna* in flower, *Calluna* cut and *Calluna* burnt.

At the time of image capture phenological variation across the study sites was particularly noticeable in *Pteridium aquilinum* due to the stage of senescence. As senescence has marked impact on reflectance in the NIR part of the spectrum, all *Pteridium* samples were visually assessed and split into *Pteridium aquilinum* (green) and *Pteridium aquilinum* senescent. These were mapped separately. The addition of these sub-classes increased the total class number for analysis to 61.

4.2 Analytical protocols

4.2.1 Special consideration: Shadow

Background. As outlined in 4.1.1 the imagery supplied was significantly affected by low sun-angle and associated shadow. As it is temporally-variable, and no matching field data will be available, dealing with shadow during classification of remotely sensed imagery is highly problematical, i.e. there are no real solutions, except to ensure it doesn't occur. The issues it causes will also propagate through subsequent monitoring rounds. Interestingly the impact of shadow in manual image interpretation is not the same, indeed it can be useful. The reason is simply that an observer *knows* what a shadow is and can *understand* what it covers. Classification algorithms cannot conceptualise, they essentially just compare digital numbers with other digital numbers.

Shadow reduces the absolute reflectance values returned to the sensor. However, the colour temperature of the reflected or scattered light illuminating the shadows also 'colour shifts' reflected values (usually predominantly blue owing to atmospheric Rayleigh scattering). The outcome of this is that cover classes in shadow have their spectral response shifted to impinge on the colour space of actual low-reflectance classes, e.g. bare peat and water. Ironically these are classes that are usually mapped at high accuracy owing to their distinct spectral reflectance.



Solutions. One approach that might be considered is the removal areas of deep shadow from the imagery. However, amongst other issues, having ‘holes’ in the classified output will remove those areas from subsequent monitoring rounds. More importantly, while this may appear effective at the large-scale for topographically-induced shadow, it does not deal satisfactorily with small, or even single-pixel, shadows caused by vegetation. An additional issue with this approach is the need to identify the shadow using a prior round of classification, although this can be added into a single model if required. However, the issue here is again that of confusion with other low reflectance classes. Misclassification will simply reduce the actual accuracy whichever approach is adopted.

An alternate approach is to treat the shadow as an independent class, training it by using manual aerial photographic interpretation (API) of the image, either by altering field observations that can be seen to lie in shadow and/or by the creation of additional training pixels. A major conceptual issue with this approach is related to error determination, i.e. shadow is not a land cover class so the accuracy of this class should not be counted in the overall accuracy of classification. Yet, leaving the shadow class out of an error matrix excludes all classes that are ‘confused’ with it and again misrepresents true accuracy estimates.

Balancing these objections the latter approach was adopted here for the simple reason that a considerable fraction of the image was effected by shadow and this approach also delivers information about confusion with other classes. It does however mean that a caveat is applied to the classified outputs. All field samples were visually assessed in the imagery and those in shadow (433) were used to provide the spectral ‘signature’ of shadow in the classification.

4.2.2 Analytical approach

As summarised above the project aims to develop opportunities for monitoring change related to MFFP restoration activities. During Phase 2 the image data utilised was sourced from ‘conventional’ commercial airborne digital sensors. As with Phase 1 a full appraisal of the suitability of these data to this purpose several approaches have been adopted.

Spectral separability. Separability analyses can guide the classification approaches to be adopted in remote sensing projects by testing spectral signatures of field classes to assess the probability of them being identified correctly during a supervised classification. However, in this case they have been undertaken primarily to determine how these separations translate through to final classification accuracies and to guide the choices described in ‘*systematic approach*’ below. Separability analyses were conducted in



ERDAS Imagine with both transformed divergence and Jeffries-Matusita distances being extracted.

Canonical Correspondence Analysis (CCA). Multivariate analyses identify associations, or relationships, within large datasets comprising many samples and variables. This is achieved, very simplistically, by considering the sample data as occupying multidimensional space defined by axes of the frequencies of each class and/or quantities in environmental variables. This is then reduced to 4 dimensions, or axes, while retaining the spatial associations in the data. Generally, the first two of these axes (the most 'important') are used to visualise these associations in the form of an x, y plot. In such graphs the proximity of plotted variables is a measure of the distribution of their co-occurrences within the data.

As this process has numerous analogies to the way class data is projected in multispectral space, we explored its use here to examine the effectiveness of visual interpretation of separability of classes compared to conventional statistics.

Classification – choice of algorithm. MFFP's objectives are to assess restoration success by the application of remote sensing techniques and defined this as best achieved by producing entire or complete vegetation maps of sample areas at each monitoring round. This has influenced the choice of preferred classification protocol to be applied.

Classification options fall into two major categories, non-parametric and parametric. The former has some advantages, such as computational speed, and also make no assumptions about statistical normality of the data forming the class signatures. However, this is offset by the fact that these rules alone will invariably produce 'unclassified' pixels. All else being equal, depending on method, this can increase apparent class and overall accuracies, by effectively 'throwing away' pixels that do not fit within rigidly fixed spectral class boundaries, and thus not classifying all of the image. Such unclassified pixels/gaps in the mapped outputs cannot contribute to monitoring, or change assessment, either this round or the next. ERDAS Imagine software, selected for this project owing to its wide-distribution and common availability within the NGO sector, does allow a decision tree approach to addressing unclassified pixels, however this does mean that class composition results consist of pixels derived from a mix of rules. To avoid the problem of unclassified pixels while retaining a one-step classification approach we have adopted parametric classification algorithms, despite some expected concomitant reductions in individual and overall classification.



Within supervised parametric algorithms numerous options exist for the way unknown pixels are allocated to defined (trained) spectral classes. A full discussion of these is felt to be unnecessary here, although further details can be provided if desired. In this instance the team opted to utilise a maximum likelihood or Bayesian classifier. These do assume that the data are parametric (i.e. that the distribution of classes is normally distributed in each spectral band) and tend to overclassify signatures with wide dispersion in the training data. They are also complex, creating the greatest computational demands. However, they are also likely to produce the most accurate results. During classification, comparison was also made with the Mahalanobis distance classifier (an additional parametric algorithm that allocates classes based on Euclidean distance).

4.2.3 Systematic approach

Given the objectives of Phase 2, i.e. assess the mapping success achievable using an alternative data source, both spectral analyses and classifications were undertaken using sequentially reducing subsets of the field data. These were extracted to address two primary questions: i: what consequences/difficulties might arise from using image data with lower geolocation accuracies than expected and achieved for UAV capture; ii: which species can be reliably mapped, especially with regard to rarer taxa. These groups were as follows (see Annex A for a full lists of exclusions):

Strim A:

The initial reason for sample exclusions leading to *Strim A* were those judged unsuitable on the following grounds: i: samples comprising very low areal extent (<20 cm); ii: those marked as obscured (i.e. over-showed) mixed or mislabelled; iii: samples with a very low residual frequency after *i*: and *ii*: were applied (here <5 samples, with the exception of those deemed worth still examination e.g. heather brash, which could potentially confuse with bare peat and information on this would be useful).

Sample size: 6889 (70:30; 4825 training, 2064 validation); Class number: 51. Note only 48 of these are included in separability analyses as values for n were below the minimum to create the invertible matrices required.

Strim B:

Subset of strim A.

All samples with areal extents of <40cm were excluded. Residuals with very low frequency after criteria applied also deleted.

Sample size: 6350 (70:30; 4447 training, 1903 validation); Number of classes: 45.

Strim C:

Subset of strim B.



Trees species including *Rhododendron* deleted because of low sample size (note *Salix* retained). Also deleted: *S. cuspidatum* (16), *denticulatum* (5), *papillosum* (10), *squarrosus* (2), *subnitens* (15) *Erica cinerea* (10) and heather brash (4).

Sample size: 6110 (70:30; 4283 training, 1827 validation); Number of classes: 34.

Strim D:

Subset of strim C.

Only samples with >70 records. The exclusion criteria for *Strim D* were chosen as this essentially fits with the guidance for sample sizes to be used suggested by Congalton & Green (2019).

Sample size: 5712 (50:50; 2855 training, 2857 validation); Number of classes: 23.

It was considered that geolocation accuracies could interact not only with the areal extent of field samples considered above but also the area used for extracting spectral information during class signature determination. To investigate this a series of replicated analyses of Strims A-C were also executed using circular training samples of 20 cm, 10 cm and 5 cm diameter.



4.3 Results

4.3.1 Spectral separability analyses (class separability)

Separability between all combinations of the 48 classes in the near complete dataset (strim A) are shown in Tables 4:2&4:3 and between all combinations of the 34 classes in the subset (strim C) in Tables 4:4 & 4:5. The latter show the limited improvement in class separation resulting from the removal of smaller and less frequently recorded field samples to be explored. This exercise was not undertaken on samples between Strim A and B as the small difference in sample and class number were considered unlikely to change spectral signatures to any degree. Separability was not examined for samples in Strim D as the minimum sample number of 70 excluded some classes, e.g. *Calluna* cut and *Calluna* burn that only occurred in single sites. The values for both analyses are colour coded using the breakpoints described below to show separability as green (separable), orange (fairly good separability) and red (poor probability of separability).

The upper bound for transformed divergence is 2.000 and that for Jeffries-Matusita is 1.414 ($\sqrt{2}$). For transformed divergence, separability values of above 1.900 indicate that classes can be separated, values between 1.7 and 1.9 indicate the separation is fairly good, and values below 1.700 show poor class separability (Jensen, 1996). These separability values have been used to scale comparable breakpoints for Jeffries-Matusita (1.3 and 1.2).

There are too many classes in both datasets to provide iterative reporting of separability for each class. However, some key observations for all 48 classes are:

- i. Transformed divergence indicates that heather brash, *Calluna* cut, *Calluna* burnt and flagstone are separable classes, and Jeffries-Matusita indicates that the same four classes plus rock and mineral soil are also separable;
- ii. Water, bare peat and shadow exhibit poor class separability from each other;
- iii. All species of *Sphagnum* show poor class separability from each other; however, CCA identified clusters of *Sphagnum* species in ordination space (see section 4.3.4).

The same observations hold for the 34 classes compared in the refined strim C dataset, although heather brash was excluded and only three species of *Sphagnum* were assessed (*fallax*, *fimbriatum* and *palustre*).

4.3.2 Canonical Correspondence Analysis

The location of the classes plotted in ordination space presents a number of interesting observations (Figure 4:1). Flagstone, Rock and Mineral soil are located discretely from



other classes and were indicated to be separable by the Jeffries-Matusita distance. However, other classes noted to be separable, namely heather brash, *Calluna* cut and *Calluna* burnt, are not located as discretely. The *Calluna* cut and burn classes are located in the same region as bare peat, shadow and water, which all exhibit very low NIR reflectance.

Other classes that are located discretely in ordination space including *Empetrum* dead, *Eriophorum angustifolium*, *Calluna*, *Pteridium aquilinum* and *Polytrichum* spp. were all identified as showing fairly good separation by both transformed divergence and Jeffries-Matusita distances. Classes that plotted discretely in ordination space generally showed higher classification accuracies (section 4.3.4).

Sphagnum squarrosum plotted discretely from all other species of *Sphagnum* examined, but the remaining species appear to plot in three clusters:

1. *magellanicum*, *capillifolium*, *denticulatum*, *cuspidatum*, *subnitens* and *tenellum*;
2. *papillosum* and *palustre*;
3. *fimbriatum* and *fallax*.

4.3.3 Classification accuracy

The systematic progression of classifications undertaken and the effect on classification accuracy are presented in error matrices (Annex A; Tables A:2-A:15). Classification accuracies achieved using the most refined sample set are presented below in Tables 4:6-4:7. For each step in classification all classes are reported first and then subsequently with sub-classes of *Calluna* and *Pteridium aquilinum* classes merged (i.e. *Calluna* + *Calluna* dead + *Calluna* flower; *Pteridium aquilinum* + *Pteridium aquilinum* senesced).

The size of the training sample used (20 cm, 10 cm and 5 cm) appeared to have minimal effect on the classification accuracy. The most noticeable change in accuracy related to the progressive reduction in class number. Reported for classifications using a 10 cm training sample area, the overall accuracy ranged from 35% with strim A (51 classes), through 38% (strim B; 45 classes), 42% (strim C; 34 classes) to 46% (strim D; 23 classes). Merging *Calluna* and *Pteridium aquilinum* classes produced a 2% improvement for each step (e.g. from 46% to 48%).

The use of the Mahalanobis classification algorithm (Annex A; Tables A:16-A:17) produced an overall accuracy 2% lower than that produced using the maximum likelihood algorithm.

Classified outputs for all sites are shown in Figures 4:2-4:11.



Table 4:4. Strim C: Separability analysis - Transformed divergence
Red to green graphically illustrate increasing probability of good classification accuracy
Values shown are multiplied by 1000 for consistency of decimal place.

	Calluna cut	Flagston	Calluna burnt	Bare peat	Calluna	Calluna dead	Calluna flower	Chamerion angustifolium	Cladonia spp	Cushion moss	Deschampsia flexuosa	Empetrum dead	Empetrum nigrum	Erica tetralix	Eriophorum angustifolium	Eriophorum vaginatum	fallax	Feather moss	fimbriatum	Juncus effusus	Juncus squarros	Mineral soil	Molinia caerulea	Nardus stricta	palustre	Polytrich spp	Pteridium aquilinum	Pteridium aquilinum sen	Rock	Salix spp	Shadow	Trichophorum cespitosum	Vaccinium myrtillus	Water					
Calluna cut	1995	1710	1999	2000	1916	2000	2000	2000	1999	2000	1942	2000	2000	2000	2000	2000	2000	2000	2000	1997	1993	1993	1999	1968	2000	2000	2000	2000	2000	2000	2000	2000	1999	2000	2000				
Flagston		2000	1992	2000	1917	2000	1996	1508	1988	1705	2000	1999	1998	1998	1999	1977	1999	1838	1990	1931	1940	1634	1983	1442	1936	2000	2000	1997	1549	1963	1992	1969	1994	1995					
Calluna burnt			1871	2000	1676	2000	2000	1983	1996	1985	1996	1999	1997	2000	2000	2000	2000	2000	2000	1995	1997	1996	1995	1998	2000	2000	2000	2000	2000	2000	1999	1999	1998	2000	1985				
Bare peat				1891	1121	1852	1942	1742	1455	1510	1454	1667	1931	1811	1940	1986	1702	1988	1592	1825	1790	1611	1784	1982	1990	2000	1965	1887	1999	760	1951	1673	475						
Calluna					1689	325	1745	1961	1281	1791	1992	1122	1539	1538	1698	1854	1739	1897	1315	1409	1997	1719	1932	1888	1877	1762	1300	1996	1793	1908	1372	958	1715						
Calluna dead						1505	1758	1345	1241	1128	1280	1498	1327	1583	1771	1984	1608	1973	1092	1232	1610	1010	1526	1908	1989	1996	1763	1799	1907	1815	1242	1591	1514						
Calluna flower							1732	1939	1307	1794	1963	1116	1261	1049	1714	1928	1751	1939	1282	1370	1996	1570	1937	1908	1935	1839	1092	1996	1811	1922	966	993	1750						
Chamerion angustifolium								1955	951	1403	1724	661	1128	1856	701	1439	1069	1329	462	367	1995	660	1482	1300	1457	1717	1137	1995	955	1980	1131	818	1874						
Cladonia spp									1753	1372	1941	1928	1809	1907	1777	1961	1531	1877	1694	1805	1534	1720	1338	1832	1971	1997	1935	1291	1884	1682	1865	1871	1782						
Cushion moss										883	1612	644	1027	1686	993	1319	672	1390	535	839	1907	900	1252	1432	1376	1909	1366	1920	1618	1532	1339	689	1307						
Deschampsia flexuosa											1732	1531	1717	1806	1408	1730	827	1605	756	826	1284	1407	421	1239	1855	1988	1732	1368	1636	1562	1517	1579	1576						
Empetrum dead												1644	1773	1802	1849	1952	1771	1949	1515	1616	1997	1390	1928	1928	1978	1998	1888	2000	1949	1859	1653	1875	1474						
Empetrum nigrum														834	1412	729	1241	1229	506	715	1993	546	1732	1688	1128	1568	943	1991	1412	1731	911	198	1395						
Erica tetralix															1624	1016	1812	1529	694	855	1997	567	1808	1814	1781	1731	1009	1998	1180	1993	699	854	1933						
Eriophorum angustifolium																1689	1837	1729	1651	1737	1975	1644	1969	1798	1916	1897	1123	1992	1887	1915	1226	1576	1753						
Eriophorum vaginatum																						639	1525	1093	684	1167	862	1976	443	1934	1189	715	1834						
fallax																						825	975	1988	639	1525	1093	684	1167	862	1976	443	1934	1189	715	1834			
Feather moss																						1071	1017	588	825	975	1988	639	1525	1093	684	1167	862	1976	443	1934	1189	715	1834
fimbriatum																																							
Juncus effusus																																							
Juncus squarros																																							
Mineral soil																																							
Molinia caerulea																																							
Nardus stricta																																							
palustre																																							
Polytrich spp																																							
Pteridium aquilinum																																							
Pteridium aquilinum sen																																							
Rock																																							
Salix spp																																							
Shadow																																							
Trichophorum cespitosum																																							
Vaccinium myrtillus																																							
Water																																							

Table 4:5. Strim C: Separability analysis - Jefferies-Matusita.
Red to green graphically illustrate increasing probability of good classification accuracy
Values shown are multiplied by 1000 for consistency of decimal place.

	Calluna cut	Flagstone	Calluna burnt	Bare peat	Calluna	Calluna dead	Calluna flower	Chamerion angustifolium	Cladonia spp	Cushion moss	Deschampsia flexuosa	Empetrum dead	Empetrum nigrum	Erica tetralix	Eriophorum angustifolium	Eriophorum vaginatum	fallax	Feather moss	fimbriatum	Juncus effusus	Juncus squarros	Mineral soil	Molinia caerulea	Nardus stricta	palustre	Polytrich spp	Pteridium aquilinum	Pteridium aquilinum sen	Rock	Salix spp	Shadow	Trichophorum cespitosum	Vaccinium myrtillus	Water		
Calluna cut		1389	1258	1388	1413	1258	1413	1412	1326	1379	1278	1411	1411	1413	1412	1407	1412	1377	1410	1390	1376	1228	1408	1330	1410	1414	1414	1414	1414	1362	1412	1401	1408	1413	1410	
Flagstone			1410	1406	1413	1374	1412	1407	1169	1396	1280	1411	1410	1404	1412	1392	1409	1318	1395	1382	1384	1253	1392	1130	1377	1412	1414	1411	1146	1390	1400	1401	1408	1411		
Calluna burnt				1321	1412	1183	1413	1414	1308	1380	1322	1406	1410	1412	1410	1409	1412	1384	1412	1403	1402	1231	1400	1389	1413	1414	1414	1414	1379	1414	1391	1412	1413	1392		
Bare peat					1341	992	1336	1366	1224	1163	1193	1144	1253	1337	1331	1358	1345	1199	1373	1239	1301	1161	1213	1323	1393	1373	1411	1380	1289	1401	850	1318	1278	672		
Calluna						1262	563	1253	1378	1122	1306	1345	989	1141	1172	1231	1172	1227	1252	1092	1156	1401	1169	1365	1291	1282	1221	1048	1400	1322	1322	1079	912	1271		
Calluna dead							1203	1296	1062	1015	1001	1028	1136	1092	1196	1233	1296	1098	1314	1024	1096	1127	936	1221	1328	1358	1398	1276	1296	1338	1252	1050	1230	1174		
Calluna flower								1283	1364	1120	1303	1330	1018	1063	964	1244	1198	1222	1267	1092	1159	1400	1150	1375	1258	1316	1280	968	1402	1329	1331	927	969	1284		
Chamerion angustifolium									1392	922	1066	1293	797	1032	1324	796	1003	912	1011	656	585	1404	771	1095	1044	1115	1283	1037	1378	913	1319	1042	878	1304		
Cladonia spp										1249	1123	1348	1354	1248	1357	1271	1368	1143	1330	1272	1325	1091	1234	1085	1332	1385	1392	1352	1063	1314	1250	1343	1344	1299		
Cushion moss											901	1206	763	892	1229	924	1015	733	1055	685	841	1300	837	1032	1134	1101	1258	1064	1271	1098	1137	1041	777	1121		
Deschampsia flexuosa												1207	1138	1193	1313	1109	1223	851	1186	832	870	1063	1028	626	1045	1314	1361	1206	1141	1133	1226	1157	1182	1217		
Empetrum dead													1189	1311	1211	1310	1321	1269	1354	1181	1213	1310	1118	1339	1365	1371	1413	1352	1380	1382	1309	1221	1324	1159		
Empetrum nigrum														875	1162	805	904	962	1018	665	784	1379	692	1249	1185	990	1152	887	1375	1127	1228	883	427	1152		
Erica tetralix															1178	936	1166	1073	1161	789	898	1397	725	1291	1200	1246	1279	956	1393	1060	1319	783	885	1324		
Eriophorum angustifolium																1275	1264	1264	1311	1210	1245	1379	1192	1383	1262	1361	1358	1039	1404	1350	1360	991	1204	1310		
Eriophorum vaginatum																	784	924	682	826	884	1390	759	1181	967	806	1001	912	1384	626	1315	1023	814	1326		
fallax																		947	490	1043	1087	1394	1065	1260	1015	538	1064	1063	1385	1051	1305	1164	919	1267		
Feather moss																			899	786	892	1272	898	831	806	1133	1313	1109	1206	1023	1152	1091	931	1152		
fimbriatum																				1059	1099	1397	1061	1204	850	684	1067	1080	1381	897	1331	1185	1003	1331		
Juncus effusus																					408	1351	490	996	1045	1189	1285	945	1338	981	1227	814	743	1175		
Juncus squarros																						1355	620	962	1075	1229	1280	966	1339	1003	1294	810	889	1262		
Mineral soil																							1356	1156	1394	1406	1414	1409	849	1406	1238	1387	1390	1262		
Molinia caerulea																								1171	1112	1183	1281	966	1367	974	1257	741	804	1184		
Nardus stricta																										1096	1330	1388	1317	1055	1153	1285	1274	1260	1318	
palustre																											1217	1218	932	1372	963	1366	1167	1146	1380	
Polytrich spp																												1061	1203	1397	1118	1331	1293	1038	1314	
Pteridium aquilinum																													1067	1413	1105	1391	1295	1122	1392	
Pteridium aquilinum sen																														1405	1067	1347	851	853	1320	
Rock																															1394	1250	1392	1376	1299	
Salix spp																																1366	1138	1073	1392	
Shadow																																	1331	1202	694	
Trichophorum cespitosum																																			961	1270
Vaccinium myrtillus																																				1143
Water																																				

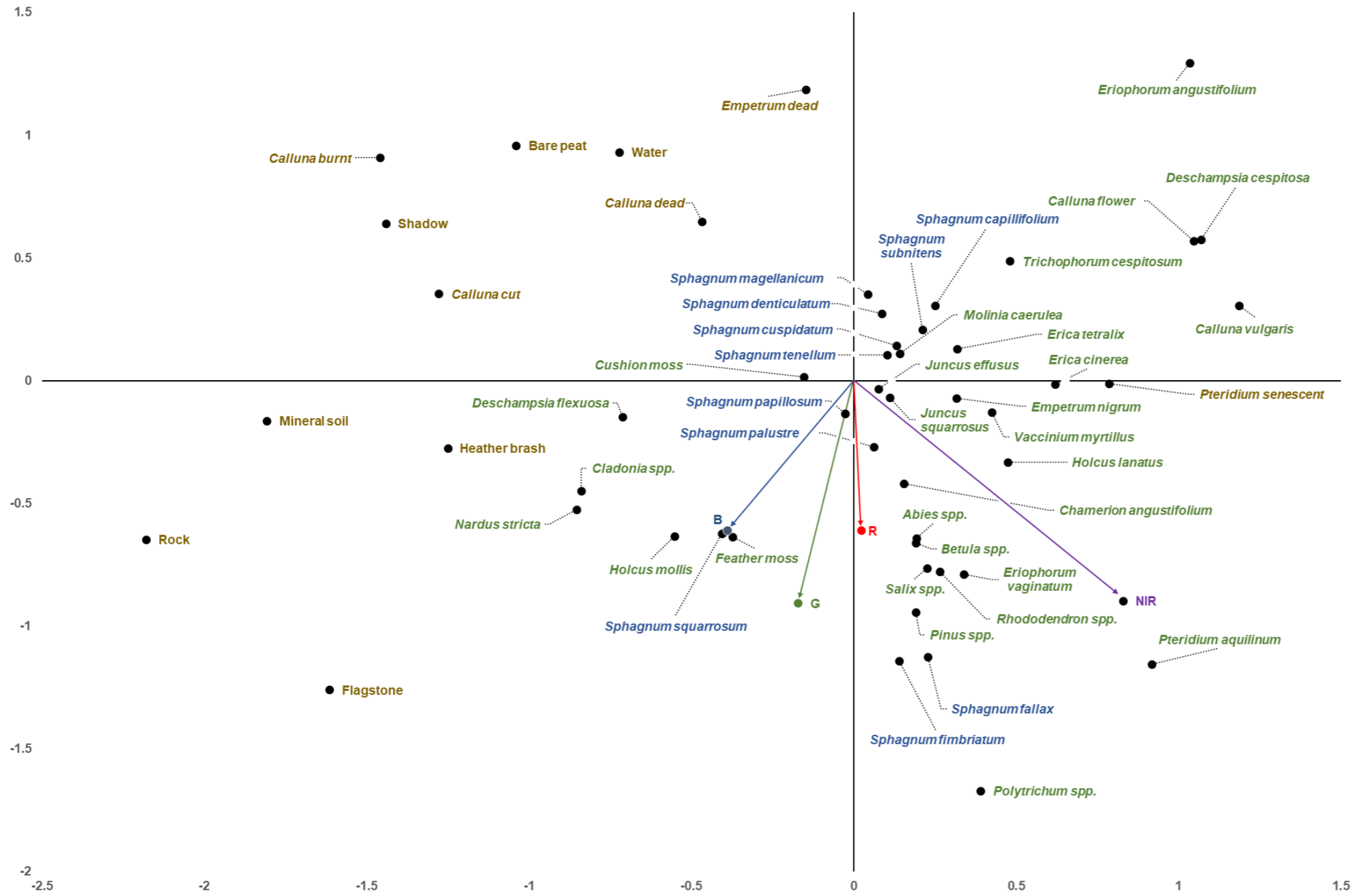


Figure 4:1. Strim A. CCA ordination of spectral data with R, G, B and NIR vectors highlighted. Axis 1 and 2 Eigenvalues shown.
Class names coloured to highlight live vegetation (green), dead or senescent vegetation and non-vegetation (brown), and *Sphagnum* spp. (blue).

Table 4.6. Strim D: Sample numbers >70 Error matrix. Maximum likelihood classification. 20cm search area. All classes.

	Bare peat	Calluna	Calluna dead	Calluna flower	Deschampsia flexuosa	Empetrum nigrum	Eriophorum angustifolium	Eriophorum vaginatum	fallax	fimbriatum	Juncus effusus	Juncus squarrosus	Mineral soil	Molinia caerulea	Nardus stricta	Polytrichum spp.	Pteridium aquilinum	Pteridium aquilinum sen	Rock	Shadow	Trichophorum cespitosum	Vaccinium myrtillus	Water	Total	User accuracy	
Bare peat	104		11		1		1	1			1		1	1	2				2	12				26	163	0.64
Calluna	1	129	1	18		2	4	1			8	1					1	1		1		14	3	185	0.70	
Calluna dead	16	4	72		3	2	6	3			14	3	6	5	2					1	3	2	2	144	0.50	
Calluna flower	1	47	4	53			30		2	1								2		1	10	10		161	0.33	
Deschampsia flexuosa	1		1		18		1				7	1	2	1	8				1	1			2	44	0.41	
Empetrum nigrum	4	2	1	2		11	1	12	2	1	4			4		6				2		17	3	72	0.15	
Eriophorum angustifolium			2	7			190	2			1		1		2			2			3		1	210	0.90	
Eriophorum vaginatum						4	1	63	3	2	5	2		2	2	6	1	2		2	1	9	1	106	0.59	
fallax								1	13	9						16				3			1	43	0.30	
fimbriatum					2	1		27	8	11	1				3	11	2					2	1	69	0.16	
Juncus effusus	1		1		3	2	1	5	1	1	16	4	1	3	1			1		1		2		44	0.36	
Juncus squarrosus		5	4	4	7	8		26	4	1	53	23		11	7	1		3	1	1	3	14	2	178	0.13	
Mineral soil	1		1										43		5				8	1			1	60	0.72	
Molinia caerulea	1	1	4	3	5	6		15	1		29	4		9	1	3		4		1	7	8		102	0.09	
Nardus stricta	3		5		9			5		3	11	3		2	78	1			4	8	1		3	136	0.57	
Polytrichum spp.		1				9		51	19	8	1					95	4				1	6		195	0.49	
Pteridium aquilinum		3				4		29	1	4	1	1		2		13	27	6				14		105	0.26	
Pteridium aquilinum sen		5		2		1	9	9	1		2	2						24			3	5		63	0.38	
Rock			1							1			8		14				60	8				92	0.65	
Shadow	17	1			2			1	2		4		5			1			4	127		2	23	189	0.67	
Trichophorum cespitosum		11	9	11		12	17	14	1		24	4		13				1			23	9	1	150	0.15	
Vaccinium myrtillus		19		8		34	1	22	3	1	20	5		5		9	2	7		2	1	62	1	202	0.31	
Water	21	5			1	2	1	2	1		4			1		1		2	1	41		11	50	144	0.35	
Total	171	233	117	108	51	99	263	289	62	43	206	53	67	59	123	163	37	55	81	213	56	187	121	2857		
Producer accuracy	0.61	0.55	0.62	0.49	0.35	0.11	0.72	0.22	0.21	0.26	0.08	0.43	0.64	0.15	0.63	0.58	0.73	0.44	0.74	0.60	0.41	0.33	0.41			
N (total observations)					2857				Overall accuracy				0.46													
X (Sum of all correct)					1301				Kappa				0.43													
Y (Sum of total user x sum of total producer)					401789																					

Table 4.7. Strim D: Sample numbers >70 Error matrix. Maximum likelihood classification. 20cm search area. *Calluna* (includes *Calluna*, *Calluna* flower and *Calluna* dead); *Pteridium* (includes *Pteridium* and *Pteridium* sen) folded.

	Bare peat	Calluna	Deschampsia flexuosa	Empetrum nigrum	Eriophorum angustifolium	Eriophorum vaginatum	fallax	fimbriatum	Juncus effusus	Juncus squarrosus	Mineral soil	Molinia caerulea	Nardus stricta	Polytrichum spp.	Pteridium aquilinum	Rock	Shadow	Trichophorum cespitosum	Vaccinium myrtillus	Water	Total	User accuracy	
Bare peat	104	11	1		1	1			1		1	1	2			2	12				26	163	0.64
Calluna	18	328	3	4	40	4	2	1	22	4	6	5	2		4		3	13	26		5	490	0.67
Deschampsia flexuosa	1	1	18		1				7	1	2	1	8			1	1				2	44	0.41
Empetrum nigrum	4	5		11	1	12	2	1	4			4		6			2		17	3		72	0.15
Eriophorum angustifolium		9			190	2			1		1				2			3		1		210	0.90
Eriophorum vaginatum				4	1	63	3	2	5	2		2	2	6	3		2	1	9	1		106	0.59
fallax						1	13	9						16			3				1	43	0.30
fimbriatum			2	1		27	8	11					3	11	2					2	1	69	0.16
Juncus effusus	1	1	3	2	1	5	1	1	16		1	3	1		1		1			2		44	0.36
Juncus squarrosus		13	7	8		26	4	1	53	23		11	7	1	3	1	1	3	14	2		178	0.13
Mineral soil	1	1									43		5			8	1				1	60	0.72
Molinia caerulea	1	8	5	6		15	1		29	4		9	1	3	4		1	7	8			102	0.09
Nardus stricta	3	5	9			5		3	11	3		2	78	1		4	8	1		3		136	0.57
Polytrichum spp.		1		9		51	19	8	1					95	4				1	6		195	0.49
Pteridium aquilinum		10		5	9	38	2	4	3	3		2		13	57			3	19			168	0.34
Rock		1						1			8		14			60	8					92	0.65
Shadow	17	1	2			1	2		4		5			1		4	127			2	23	189	0.67
Trichophorum cespitosum		31		12	17	14	1		24	4		13		1	1			23	9	1		150	0.15
Vaccinium myrtillus		27		34	1	22	3	1	20	5		5		9	9		2	1	62	1		202	0.31
Water	21	5	1	2	1	2	1		4			1		1	2	1	41		11	50		144	0.35
Total	171	458	51	99	263	289	62	43	206	53	67	59	123	163	92	81	213	56	187	121	2857		
Producer accuracy	0.61	0.72	0.35	0.11	0.72	0.22	0.21	0.26	0.08	0.43	0.64	0.15	0.63	0.58	0.62	0.74	0.60	0.41	0.33	0.41			
N (total observations)						2857						Overall accuracy	0.48										
X (Sum of all correct)						1381						Kappa	0.45										
Y (Sum of total user x sum of total producer)						556974																	

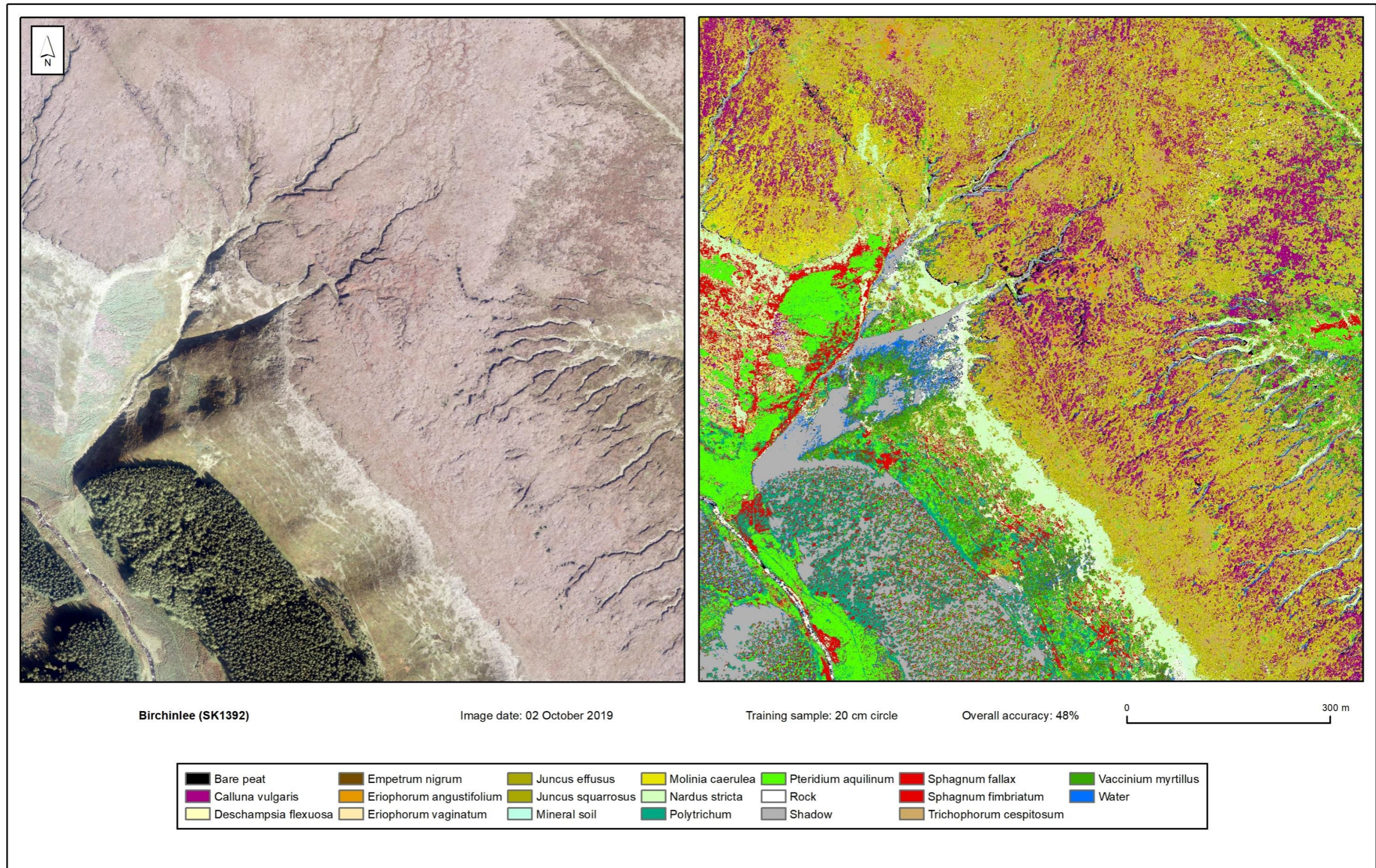


Figure 4:2. Classified output for Birchinlee (SK1392) using strim D. 20cm training area. *Calluna* and *Pteridium aquilinum* sub-classes merged.

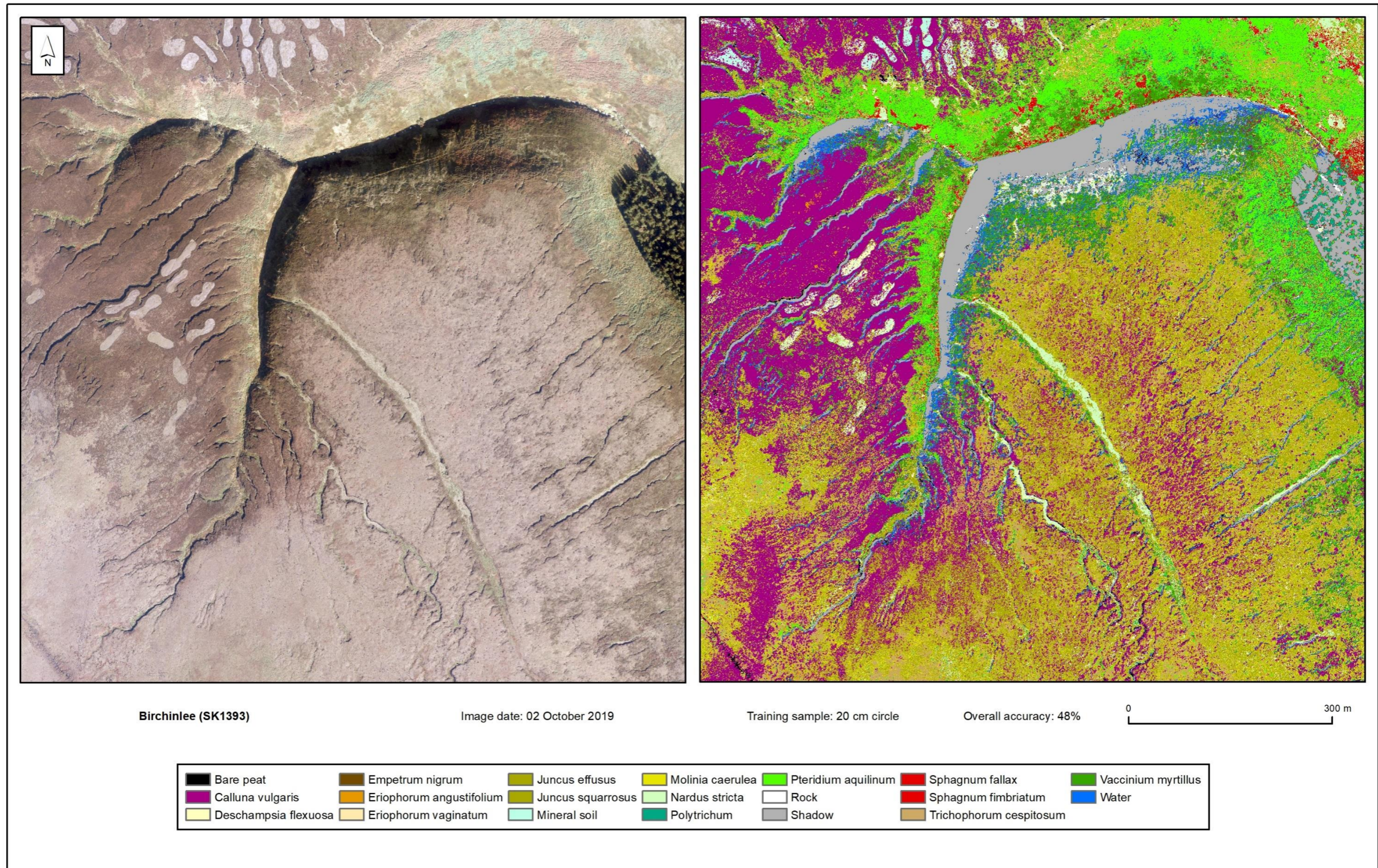


Figure 4:3. Classified output for Birchinlee (SK1393) using strim D. 20cm training area. *Calluna* and *Pteridium aquilinum* sub-classes merged.

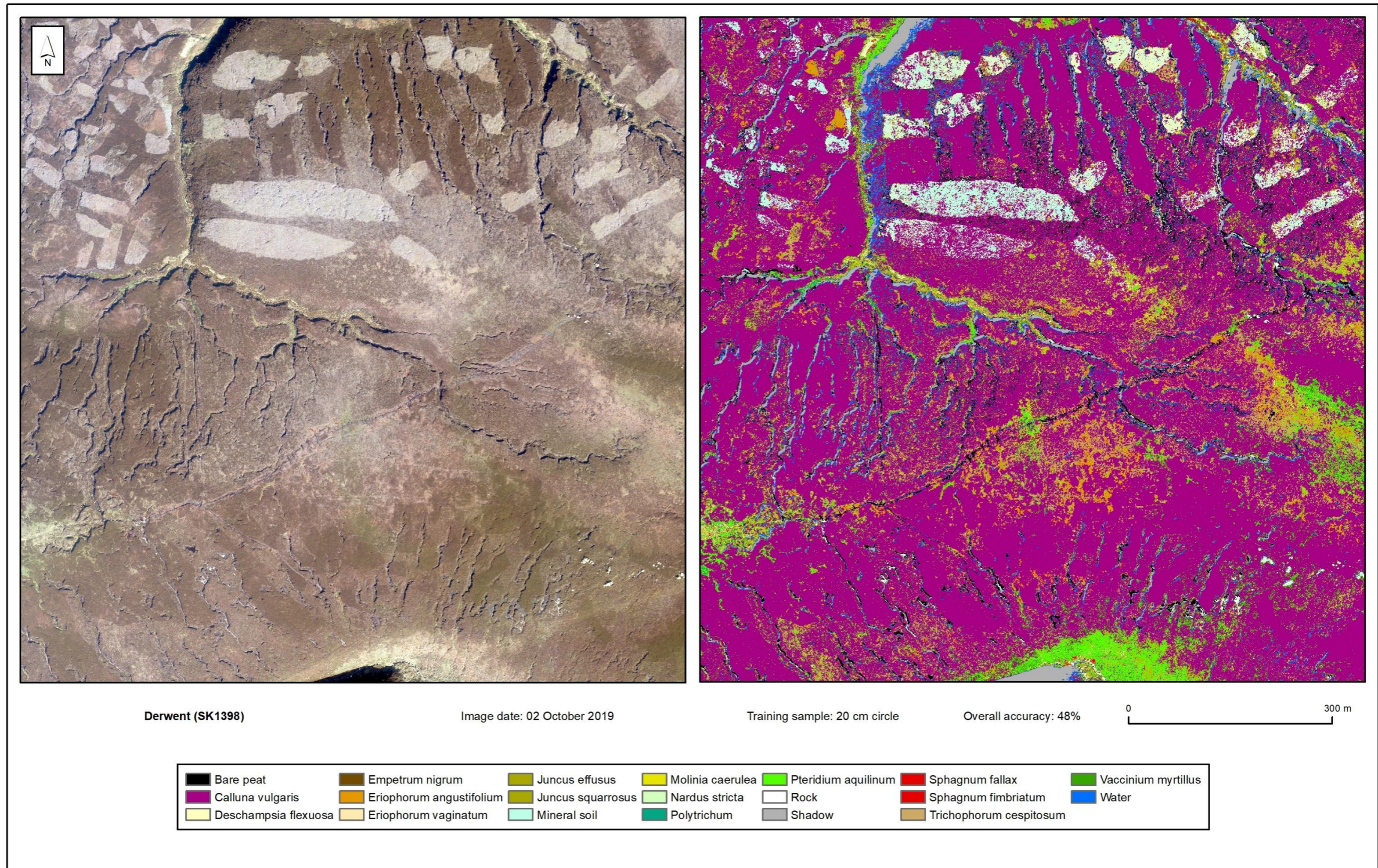


Figure 4.4. Classified output for Derwent Howden (SK1398) using strim D. 20cm training area. *Calluna* and *Pteridium aquilinum* sub-classes merged.

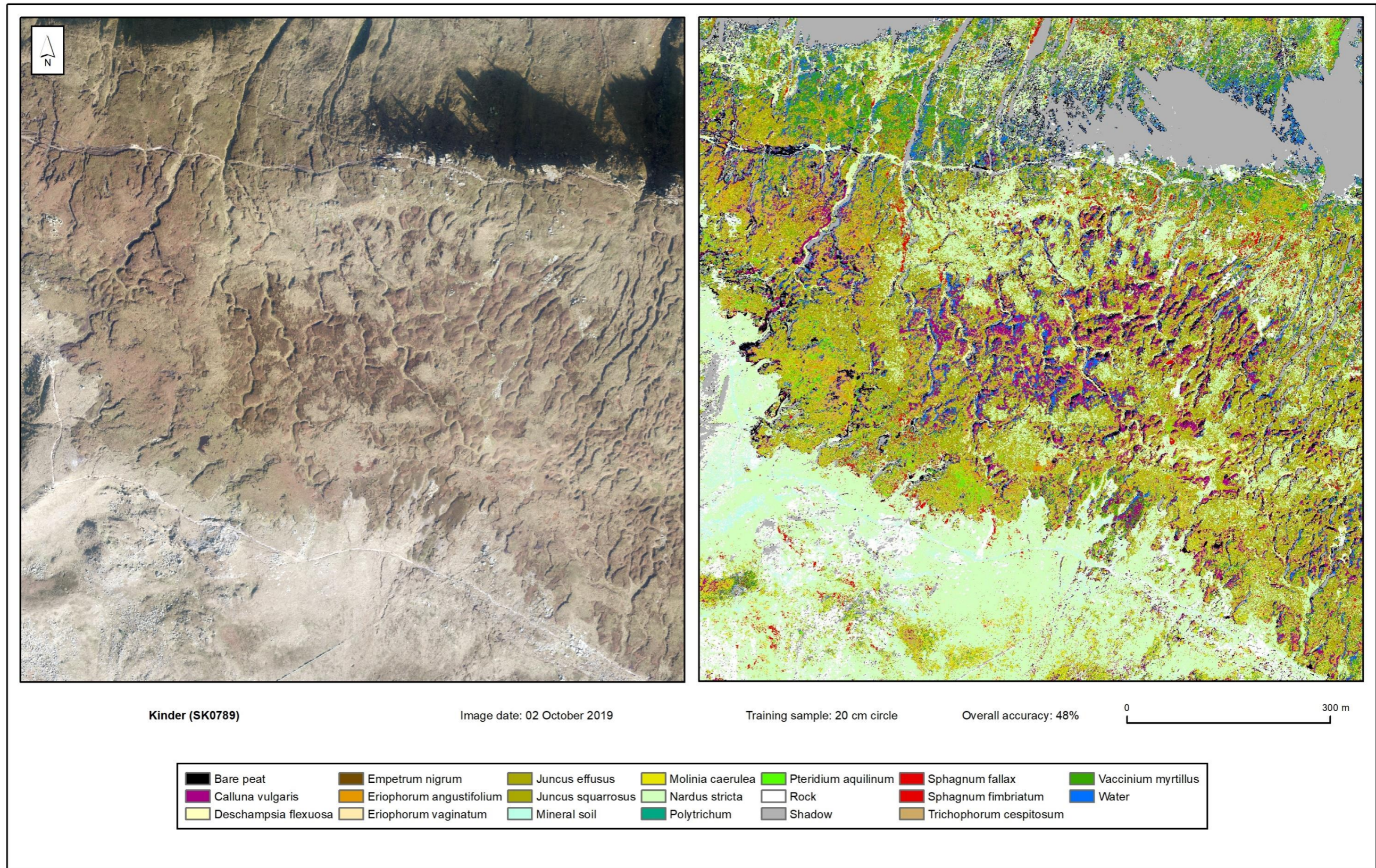


Figure 4:5. Classified output for Kinder (SK0789) using strim D. 20cm training area. *Calluna* and *Pteridium aquilinum* sub-classes merged.

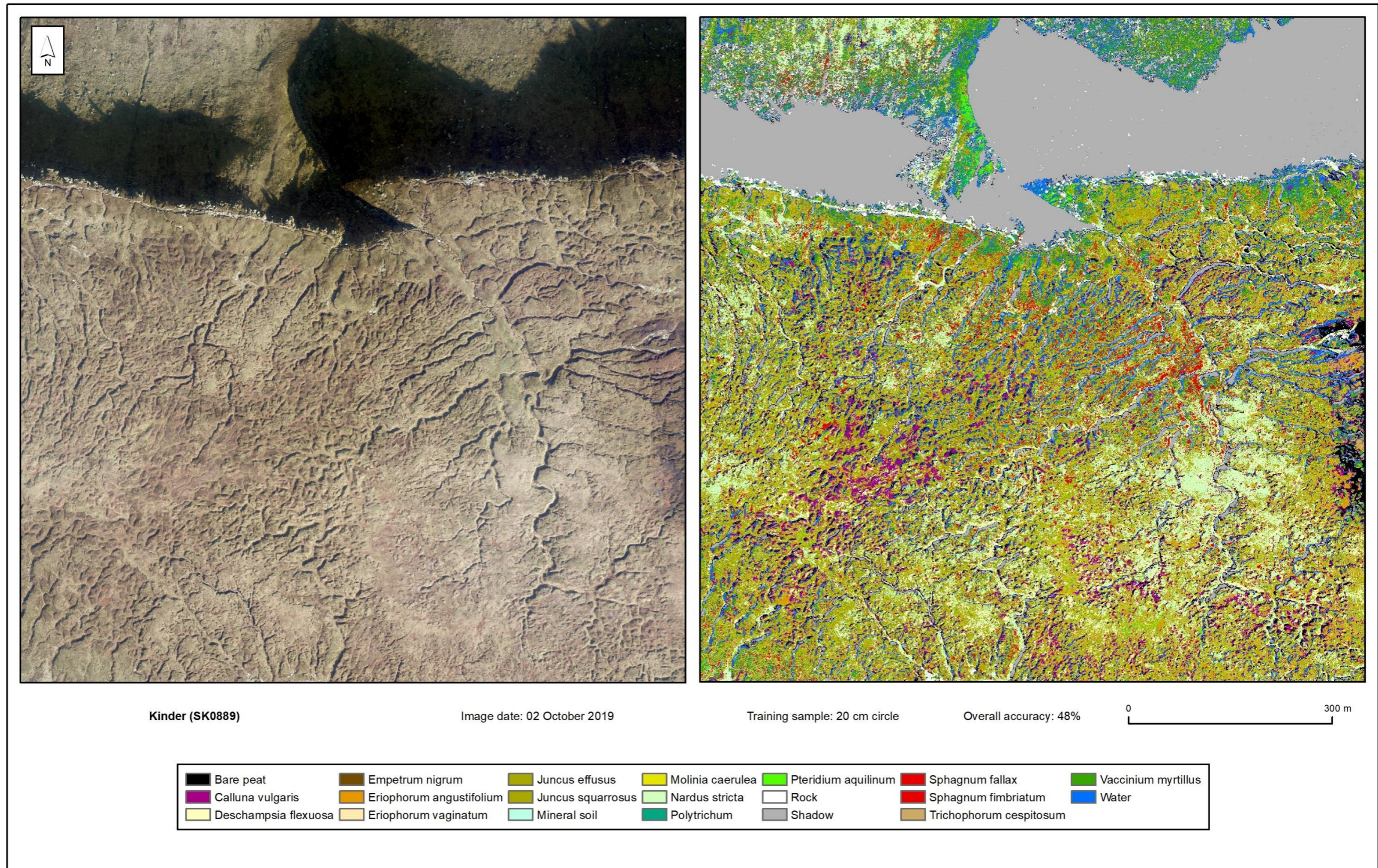


Figure 4:6. Classified output for Kinder (SK0889) using strim D. 20cm training area. *Calluna* and *Pteridium aquilinum* sub-classes merged.

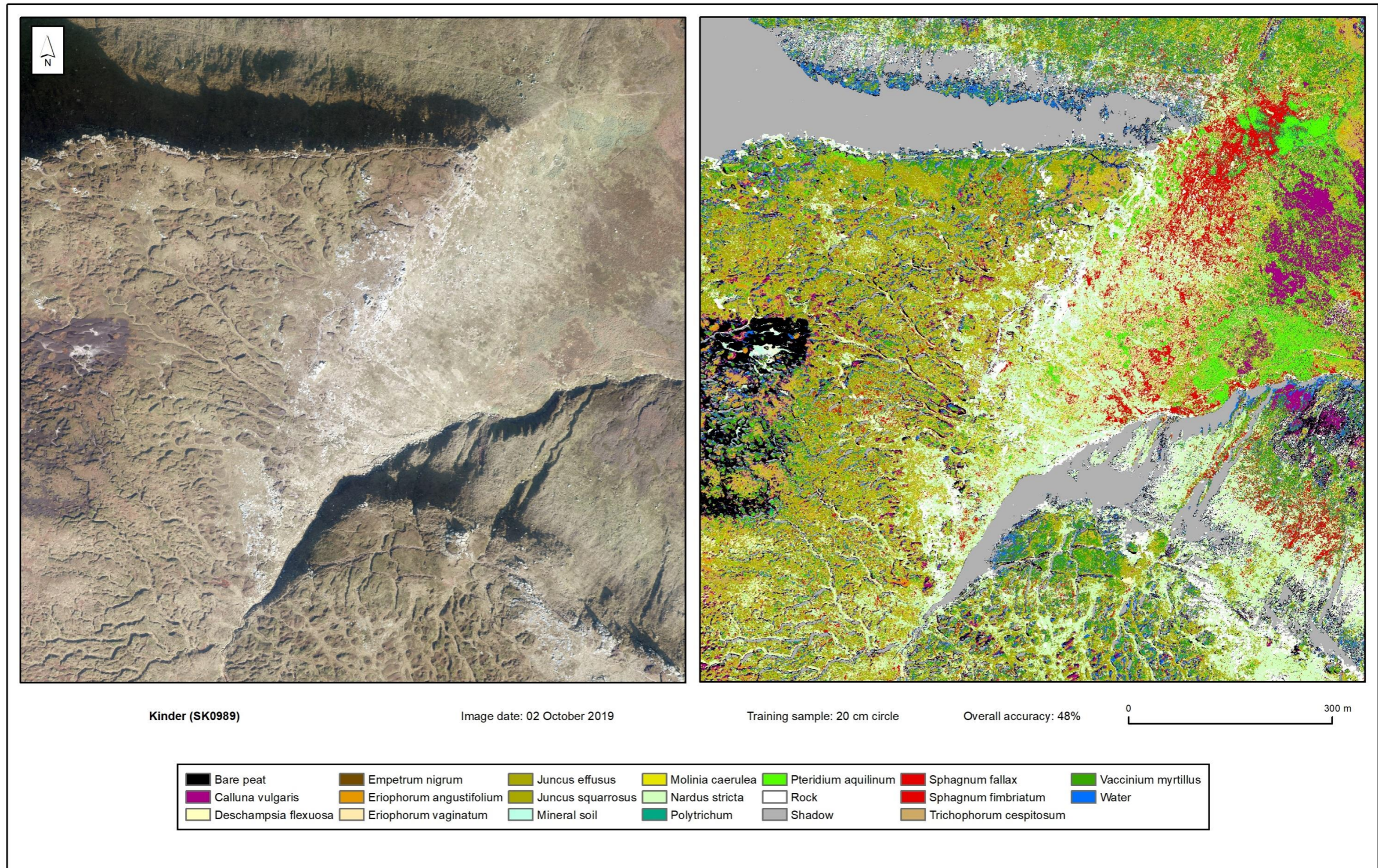


Figure 4:7. Classified output for Kinder (SK0989) using strim D. 20cm training area. *Calluna* and *Pteridium aquilinum* sub-classes merged.

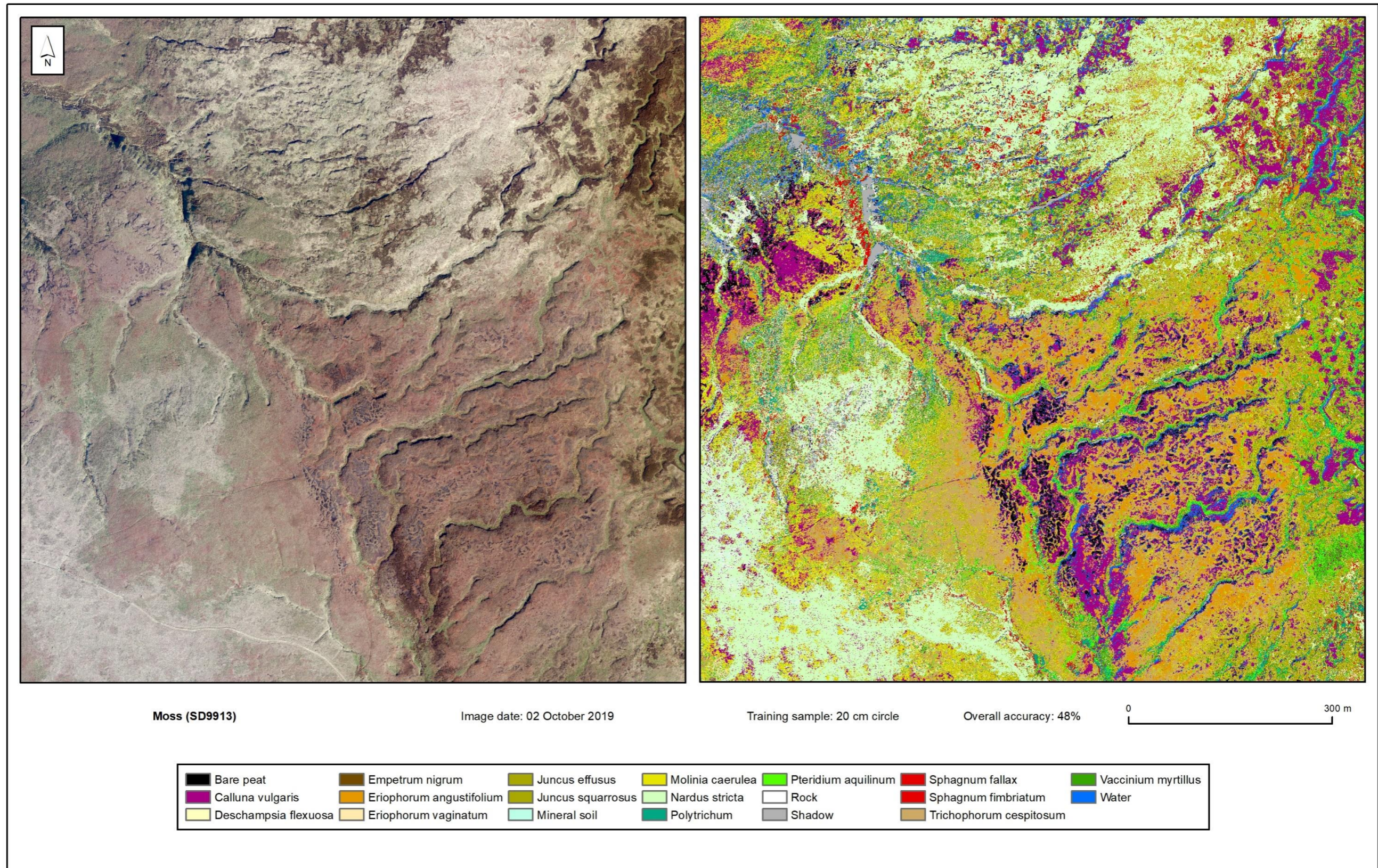


Figure 4:8. Classified output for Molinia (SD9913) using strim D. 20cm training area. *Calluna* and *Pteridium aquilinum* sub-classes merged.

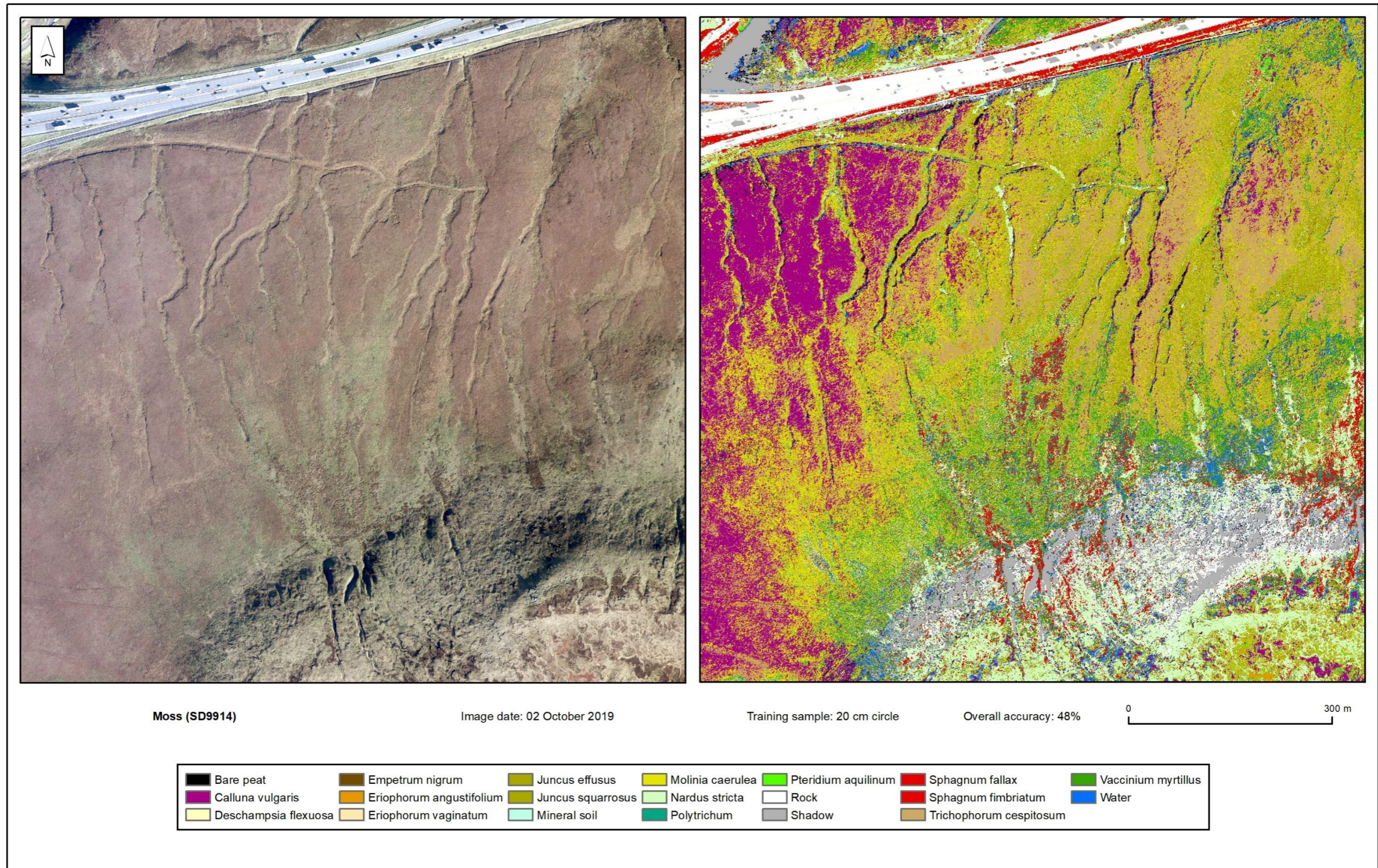


Figure 4:9. Classified output for Molinia (SD9914) using strim D. 20cm training area. *Calluna* and *Pteridium aquilinum* sub-classes merged.

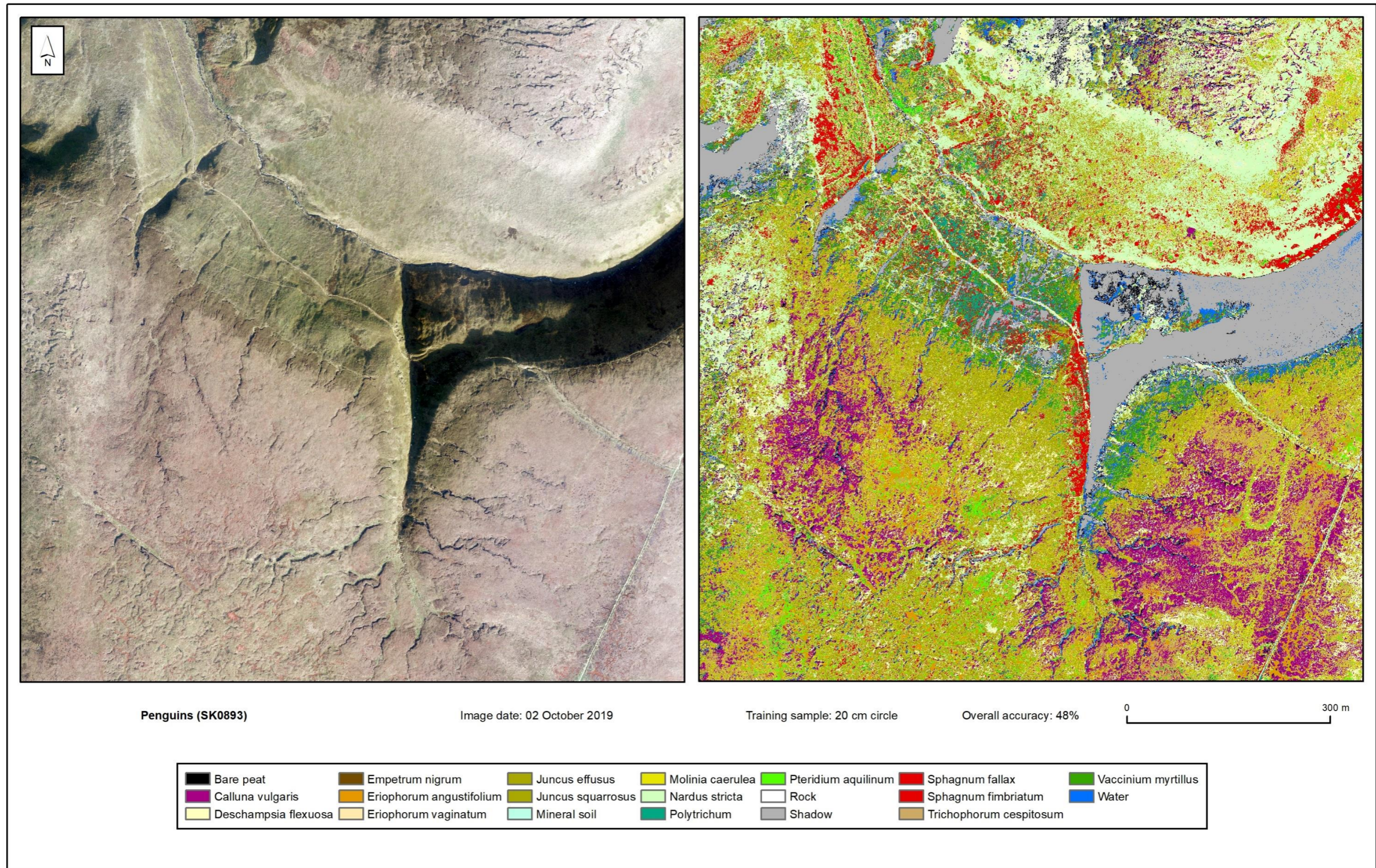


Figure 4:10. Classified output for Penguins (SK0893) using strim D. 20cm training area. *Calluna* and *Pteridium aquilinum* sub-classes merged.

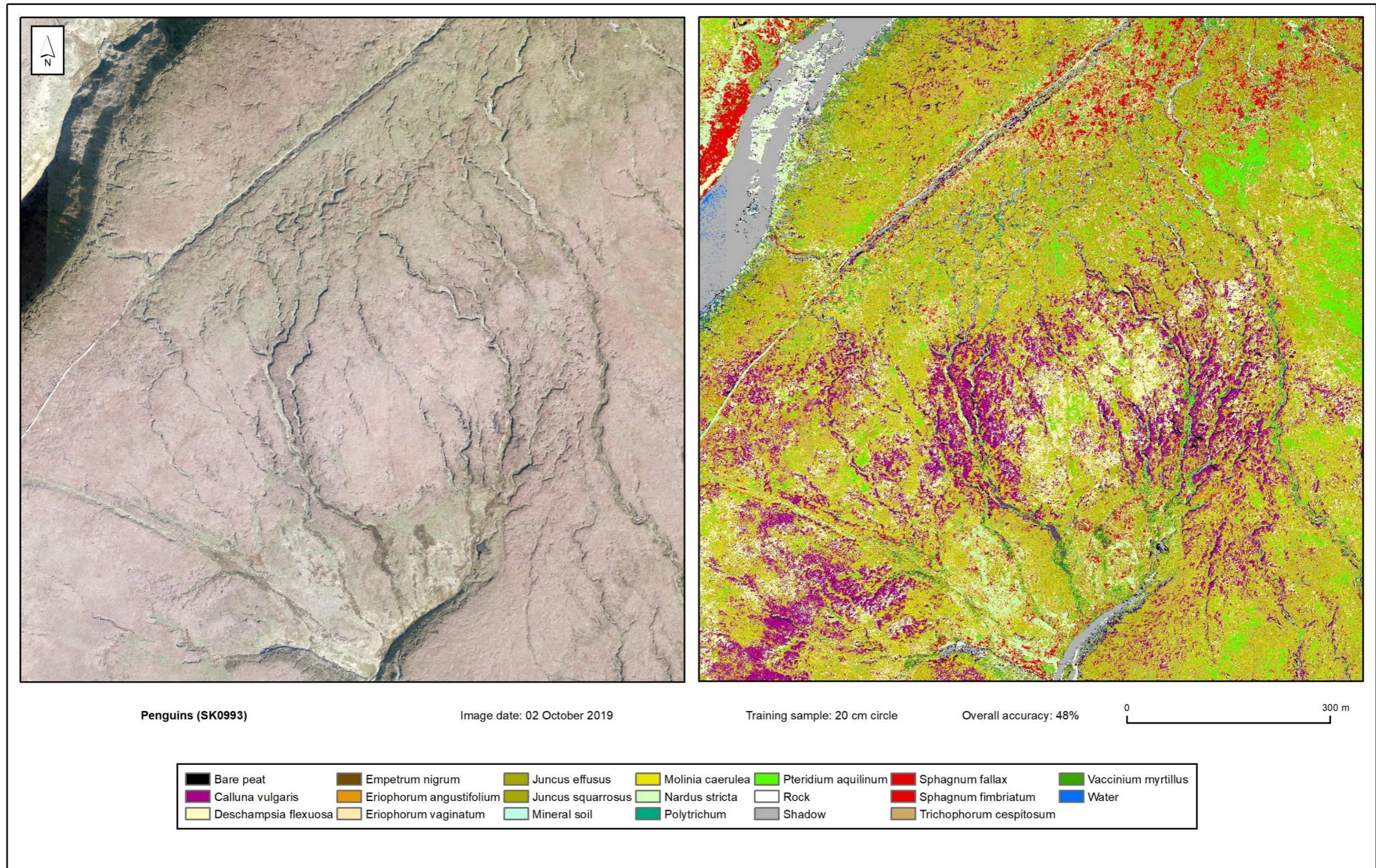


Figure 4:11. Classified output for Penguins (SK0993) using strim D. 20cm training area. *Calluna* and *Pteridium aquilinum* sub-classes merged.

4.3.4 Class separability and accuracy

Ranked values of spectral separability determined by transformed divergence and Jeffries-Matusita distance indicate very similar potential for class separation (and therefore accuracy) in classification (Table 4:24). There is a clear correlation between the separability values and class accuracy (producer accuracy), but it is worth noting that some classes that obtained relatively high classification accuracies, particularly *Pteridium aquilinum* (86%) and *Eriophorum angustifolium* (74%) were only identified as having fairly good or even poor separability. It is interesting that these two classes plotted in discrete locations in ordination space (Figure 4:1) and indicates that CCA of class signatures provides additional insight to conventional spectral separability statistics.





Table 4:24. Ranked class separability (transformed divergence and Jeffries-Matusita distances) and class accuracy

Class	Mean transformed divergence	Producer accuracy	Class	Mean Jeffries-Matusita	Producer accuracy
Heather Brash	2.000	0.50	Heather Brash	1.408	0.50
<i>Calluna</i> cut	1.989	0.50	<i>Calluna</i> burnt	1.386	0.40
<i>Calluna</i> burnt	1.981	0.40	<i>Calluna</i> cut	1.382	0.50
Flagstone	1.920	0.75	Flagstone	1.369	0.75
Mineral soil	1.867	0.55	Rock	1.315	0.57
Rock	1.835	0.57	Mineral soil	1.313	0.55
Shadow	1.800	0.61	<i>Pteridium aquilinum</i>	1.272	0.86
<i>Erica cinerea</i>	1.773	0.33	<i>Cladonia</i> spp	1.265	0.44
<i>Pteridium aquilinum</i>	1.759	0.86	Shadow	1.262	0.61
<i>Empetrum</i> dead	1.745	0.00	<i>Empetrum</i> dead	1.259	0.00
<i>Holcus mollis</i>	1.737	0.00	Bare peat	1.253	0.67
<i>Cladonia</i> spp	1.737	0.44	<i>Eriophorum angustifolium</i>	1.235	0.74
Bare peat	1.718	0.67	<i>Erica cinerea</i>	1.235	0.33
<i>Eriophorum angustifolium</i>	1.670	0.74	Water	1.228	0.53
Water	1.665	0.53	<i>Holcus mollis</i>	1.222	0.00
<i>Calluna</i>	1.628	0.59	<i>Calluna</i>	1.205	0.59
<i>Polytrichum</i> spp	1.609	0.54	<i>Polytrichum</i> spp	1.203	0.54
<i>Calluna</i> flower	1.562	0.40	<i>Calluna</i> flower	1.182	0.40
<i>Calluna</i> dead	1.531	0.35	<i>Nardus stricta</i>	1.170	0.35
<i>Nardus stricta</i>	1.527	0.35	<i>Calluna</i> dead	1.150	0.35
<i>Abies</i> spp	1.467	0.00	<i>Abies</i> spp	1.106	0.00
<i>fallax</i>	1.395	0.12	<i>Pteridium aquilinum</i> senesced	1.095	0.33
<i>Deschampsia flexuosa</i>	1.384	0.16	<i>Deschampsia flexuosa</i>	1.093	0.16
<i>Pteridium aquilinum</i> senesced	1.354	0.33	<i>Salix</i> spp	1.061	0.11
<i>Salix</i> spp	1.322	0.11	<i>Chamaenerion angustifolium</i>	1.050	0.50
<i>Erica tetralix</i>	1.309	0.25	<i>Pinus</i> spp	1.049	0.24
<i>Pinus</i> spp	1.293	0.24	<i>Erica tetralix</i>	1.047	0.25
<i>Chamaenerion angustifolium</i>	1.273	0.50	<i>Trichophorum cespitosum</i>	1.039	0.26
<i>Trichophorum cespitosum</i>	1.271	0.26	<i>fallax</i>	1.027	0.12
<i>fimbriatum</i>	1.269	0.10	<i>Vaccinium myrtillus</i>	1.021	0.29
Feather moss	1.262	0.11	Feather moss	1.016	0.11
<i>magellanicum</i>	1.254	0.25	<i>magellanicum</i>	1.013	0.25
<i>palustre</i>	1.228	0.00	<i>Empetrum nigrum</i>	1.008	0.11
<i>Empetrum nigrum</i>	1.214	0.11	<i>Eriophorum vaginatum</i>	0.999	0.05
<i>Vaccinium myrtillus</i>	1.208	0.29	<i>fimbriatum</i>	0.989	0.10
<i>Rhododendron</i> spp	1.206	0.00	<i>palustre</i>	0.988	0.00
<i>Eriophorum vaginatum</i>	1.187	0.05	<i>Rhododendron</i> spp	0.985	0.00
<i>Juncus squarrosus</i>	1.165	0.18	<i>Juncus squarrosus</i>	0.982	0.18
<i>papillosum</i>	1.153	0.06	<i>Betula</i> spp	0.980	0.00
<i>tenellum</i>	1.144	0.08	<i>capillifolium</i>	0.972	0.00
<i>Betula</i> spp	1.139	0.00	Cushion moss	0.969	0.07
<i>Molinia caerulea</i>	1.138	0.06	<i>papillosum</i>	0.967	0.06
<i>capillifolium</i>	1.131	0.00	<i>Molinia caerulea</i>	0.961	0.06
Cushion moss	1.131	0.07	<i>tenellum</i>	0.960	0.08
<i>Juncus effusus</i>	1.072	0.02	<i>Juncus effusus</i>	0.934	0.02
<i>denticulatum</i>	1.065	0.00	<i>denticulatum</i>	0.928	0.00
<i>cuspidatum</i>	1.043	0.00	<i>cuspidatum</i>	0.919	0.00
<i>subnitens</i>	1.019	0.06	<i>subnitens</i>	0.911	0.06

4.4 Summary of Phase 2

In the second project year (summer 2019) commercial airborne 4-band digital imagery were assessed. The approach of using airborne imagery demonstrated a number of advantages:

- i.* No MFFP staff-time requirement for flying sites or post-flight processing of imagery;
- ii.* Spatial resolution of the delivered 4-band imagery is comparable to that of multi-spectral data collected by the UAV in 2018;
- iii.* All sites were collected in a short space of time minimising potential for any change in light angle

The use of MAV imagery to address data acquisition requirements for mapping vegetation in the project appears to provide a satisfactory alternative to that from UAVs. However, this has to be tempered with at least one caveat, a loss of physical control over which the dates on which imagery is captured.

It was nevertheless decided that MAV acquired data would form the primary image data collection during summer 2020. To help address the issues experienced with time of capture, several suggestions were made to the commercial supplier: all sites should be captured with 4-band airborne imagery on a day as close to 01 July 2020 as possible, and within a maximum window of 4 weeks either side of this date. In addition, a slight variation in the contractually specified GSD would be acceptable. This would allow alternate altitudes to be requested to air traffic control (ATC) thereby improving chances of acquisition within the desired timeframe.



Section 5: Phase 3 – MAV Image Capture II

Originally reporting in Summary report 2021

This phase of the project also experienced issues with MAV data supply. Although, in this case, the capture dates were appropriate, and the imagery supplied by Bluesky International appeared on visual examination to be of good quality, it exhibited variation in spectral balancing between each site, especially in the NIR band.

As this issue initially went unseen, the interim 2021 annual report contains potentially misleading results and statements. That report should therefore be considered withdrawn, and under no circumstances should it be quoted or cited.

The major analyses contained within that report have been re-executed here and the new results should be considered a fairer test of the use of such imagery.

Summary introduction to Phase 3 activities

Objectives of Phase 3

As part of the overall project aim of defining techniques for, and determining the successes of, the use of remote sensing for monitoring MFFP's conservation efforts, several objectives were defined for Phase 3:

- i. Test the approaches adopted in Phase 2 but using imagery with much higher spatial resolution (5 cm vs \cong 10 cm in Phases 1 and 2).

This potentially provides improvement in the ability to differentiate between *Sphagnum* spp. compared to Phase 1 and 2 by allowing the utilisation of many dimensionally smaller planted 'plug' samples previously excluded. However, for this benefit to accrue, greater accuracy in the co-registration of imagery and field samples than used previously is required. These are explored in section 5.1.

- ii. Determine the actual impact of low sun-angle induced shadow experienced with Phase 2 imagery on classification accuracies by repeating the classification using the same field data.

As the majority of mapped species are both essentially slow-growing and perennial it was considered that the utilisation of field data from the previous year would not be overly problematic. During Phase 2 these data provided in total 61 vegetation classes for image classification and were examined through a systematic series of classifications, using progressive exclusions of some samples and species. This was undertaken to remove both samples smaller than the target area of 0.25 m² and to exclude those with a low number of occurrences. In the fourth iteration, the effects of combining some taxa with high levels of spectral confusion was also tried. Even using this final set of samples overall accuracy was still relatively low (\approx 46%). To avoid unnecessary repetition of this process for Phase 3, and allow resource for exploration of *Sphagnum* mapping, it was agreed with MFFP that initial classification of 2020 imagery should commence with this final vegetation dataset of 23 classes (Strim D). Only if the accuracy of this classification was markedly higher than in Phase 2 then the progressive inclusion of further classes would be examined. In effect Phase 3 would work 'in reverse' of Phase 2 to seek an optimal trade-off of taxonomic resolution against accuracy for the new image data.



5.1 Image data

The five study sites, containing 11 experimental catchments (Table 5:1), were flown on 02/06/2020 by Bluesky International Ltd. Imagery was captured using an Ultracam Eagle, with a 79.8 mm focal length lens, and flown at an altitude of 1500 m to yield an ultimate ground resolution of 5 cm. RGB and NIR bands were supplied fully orthorectified as 1 km² tiles (aligned with the Ordnance Survey National Grid) in TIFF format. An individual mosaic for each site was created in .img format.

Table 5:1. Image coverage supplied by study site

Survey site	Image area (km ²)	Experimental catchments
Birchinlee	2	Eriophorum (Con); Eriophorum (Spha)
Derwent Howden	1	Calluna (Con); Calluna (Spha); Calluna (Spha GB)
Penguins	2	P (Ref)
Moss Moor	2	Molinia (Con); Molinia (Spha)
Kinder	3	F (Con); N (Veg Spha GB); O (Veg)

Intervention: Con = control; GB = gully blocking; Ref = intact reference; Spha = Sphagnum; Veg = revegetation.

5.1.1 Orthorectification accuracy

Metadata supplied by Bluesky International reported a RMSE of 0.091m (1.8 pixels) and 0.066m (1.3 pixels) in x and y dimensions respectively for these data. As a result of both increased image resolution and *Sphagnum* ‘plug’ growth since Phase 2, individual *Sphagnum* plugs that were not obscured by either vegetation or water were visible as discrete bright features within the imagery (see Figure 5:1). These provided good visual references with which to assess image registration with field sample loci determined using DGNS (RMSE in x and y 0.024 m). In some places *Sphagnum* plugs were mis-registered by 4-5 pixels in the imagery (see Figure 5:1). While this is not unexpected as RMSE is an average error, and orthorectification cannot account for local topographical variation, it clearly shows the potential issues in achieving fine-scale co-registration of image and field data, something not commonly discussed. It is for this reason the field survey protocols for this project were defined to only utilise patches of vegetation with areas exceeding 0.25 m².

To improve the accuracy of orthorectification, and thereby allow for classification of the smaller areas of *Sphagnum* spp., 28 field samples collected in 2019 evenly distributed across all images (including *Sphagnum* plugs, small rocks, small discrete *Calluna* shrubs and tussocks of *Eriophorum vaginatum*) were identified and their locations supplied to Bluesky International. Orthorectification was then repeated by the supplier using these ground control data and the imagery resupplied to MFFP. Although the reported mean RMSE in x (0.059 m; 1.2 pixels) and y (0.066 m; 1.3 pixels) dimensions only appeared to



improve in x, visual assessment showed an acceptable improvement in alignment between the reprocessed imagery and *Sphagnum* plugs (Figure 5:1).

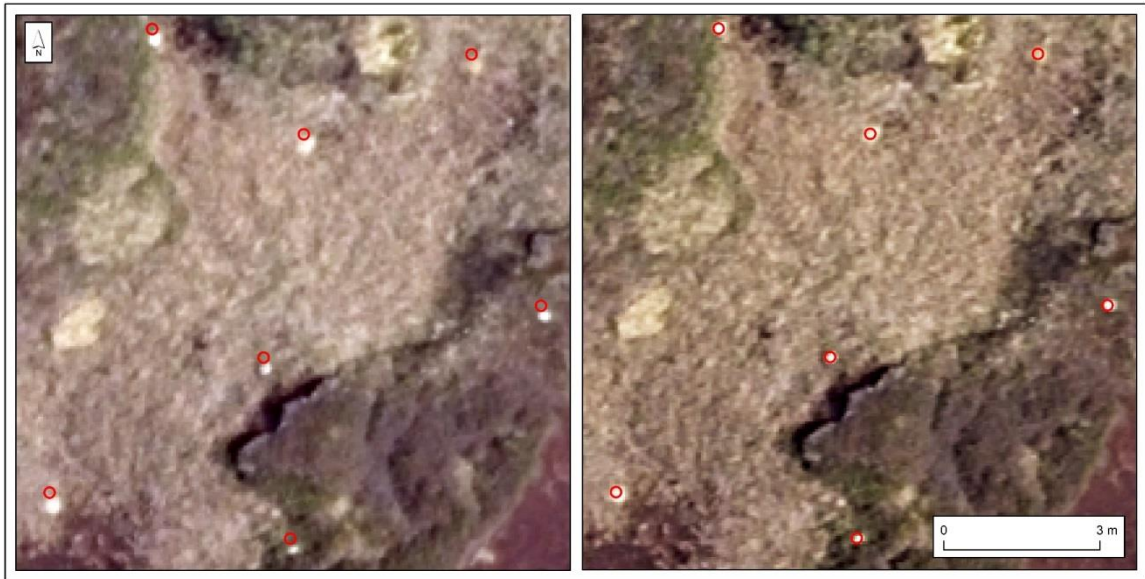


Figure 5:1. Alignment between imagery and example *Sphagnum* plug samples
left: original right: reprocessed imagery

red shows GNSS field samples as 10 cm radius spectral sampling loci

5.1.2 Potential impact of image processing procedures on image classification

Initial image classifications (originally contained in the Phase 3 preliminary report) shown here in Table 5:10, shows only marginally increased overall classification accuracies of 47% compared to those reported for Phase 2 at 46%. This improvement, considering the substantive reduction in shadow and some phenotypic variability, was considerably lower than might be reasonably anticipated. As the entire study area had been imaged over a short period (<1 hr.) it is not considered probable that this arose from the issues of changing sun angle/irradiance experienced in Phase 1. Therefore, another potential cause was sought.

As described earlier the 11 km² of this study are not a continuous area, rather it comprises 5 disjunct sites of varying size: Moss Moor, Penguins, Kinder, Birchinlee and Derwent, spread over an area of approximately 400 km². Each of these sites was imaged separately. Upon receipt of the data visual examination of these blocks showed that the images appeared to be of good quality and much better than those from 2019 given the absence of excessive shadow and higher spatial resolution. However, following the first unsatisfactory attempts to classify these as a single block (i.e. using training data gathered across all images to create a single spectral signature file), the imagery was examined more closely. This revealed substantive differences in 'balancing' between, but

not within, each of the 5 discrete blocks of imagery. This affected all spectral bands to some extent but was most marked in the NIR.

Hence, pixel sampling during classifier training would collect examples of 5 different spectral distributions for each species, generating wider class boundaries for each than would be the case if this image artefact did not exist. The potential magnitude of this effect was considered sufficient to have had impact on classification, possibly leading to the underwhelming improvements noted over 2019. This concern was communicated to Bluesky International and further image data were supplied using revised processing procedures. However, none of these were able to improve the NIR imbalance to any notable degree.

As a result of this the procedures adopted for Phase 3 were changed from those originally planned for this project and a complete re-analysis undertaken. As such there is a mismatch in reporting between the Phase 3 interim annual report and that presented here. The early report should be discarded.

To mitigate, as far as possible, the potential impact of the differences between image groups on accuracy, image classification was undertaken independently for each of the 5 image/site groups, instead of as a 'whole'. It should be noted that the original project protocols, including field sampling and determining minimum sample numbers gathered, were based on treating the field areas and imagery as a single unit. Hence dividing training and verification data into separate groups is not without introducing potential problems of its own, e.g. small numbers of samples for certain species at some site-groups (see Table 5:3). Although it might be expected to affect classification outcomes to some extent, it still represented the best option for assessing this round of image capture.



5.2 Methods

5.2.1 Spectral separability of *Sphagnum*

One of the overall aims of the project is to provide information on the ability of a remote sensing solution to identify individual *Sphagnum* species. In addition to quantifying taxonomic separability, the project seeks to differentiate peat-forming from non-peat forming species. The enhanced visibility of the *Sphagnum* plugs in the 2020 imagery provided the opportunity to extract the spectral response of individual *Sphagnum* sp. with greater confidence than in previous phases. Spectral separability analyses were undertaken to explore the potential to differentiate between species and groups of species.

***Sphagnum* sample selection.** All *Sphagnum* plugs were surveyed in July/August 2020 by MFFP staff. Although these observations are not contemporaneous with image capture, the field notes provided were used to review samples for analysis. Potential issues identified from field records included examples of plugs of mixed species (37), those obscured by other vegetation (58), sparse (11) or submerged (4). These were excluded from analysis leaving 507 of the 617 plugs with potential for collection of ‘pure’ spectral signatures (i.e. single species). All were examined in the reprocessed imagery to assess visibility and image alignment identifying 412 where a high degree of confidence could be placed on the species (Table 5:2).

Table 5:2. *Sphagnum* plugs identifiable in 2020 imagery

Species	Birchinlee	Derwent	Kinder	Moss	Penguins	Total
<i>capillifolium</i>	9	8	10	1	5	33
<i>cuspidatum</i>	10	10	10	0	4	34
<i>denticulatum</i>	12	16	13	0	4	45
<i>fallax</i>	11	11	13	1	3	39
<i>fimbriatum</i>	12	11	8	2	3	36
<i>magellanicum</i>	11	16	8	0	3	38
<i>palustre</i>	11	14	11	5	5	46
<i>papillosum</i>	12	13	14	0	4	43
<i>squarrosus</i>	10	2	6	0	0	18
<i>subnitens</i>	11	13	10	0	4	38
<i>tenellum</i>	11	16	10	0	5	42
Total	120	130	113	9	40	412

Separability analyses. Owing to the low number of *Sphagnum* ‘plugs’ visible at Moss Moor and Penguins (i.e. those not ‘masked or over-topped’ by other vegetation), samples at these two sites were excluded leaving in total 363 samples (Birchinlee, Derwent and Kinder) for testing. The spectral signature of each plug was extracted using a 20 cm circular pixel averaging area. Separability analyses were undertaken using the algorithms in ERDAS Imagine and transformed divergence values were extracted. This was firstly



undertaken to compare the separability of all species within each individual site and subsequently to compare the separability of same species between sites to ascertain consequences resulting from any phenological variability between them.

5.2.2 Image classification: All species

Field data. The final field data used in Phase 2 (strim D) comprised 5712 samples, and these were chosen as the basis for re-examination using 2020 imagery. However, a large number of samples had been excluded in 2019 owing to extensive areas of shadow caused by the low sun angle at time of capture. The higher sun angle during 2020 capture (32° - 39°) meant far fewer patches of shadow were present, except for a few areas of large changes in topography (e.g., on Kinder). As this potentially meant that additional samples could be added to the analysis, all those previously excluded owing to presence of shadow (427) were examined using 2020 imagery. All but 13 of these were noted as shadow-free and were added to the data for analysis (see Annex B).

Phenological variation in *Calluna vulgaris* (i.e. presence or absence of flowers) and in *Pteridium aquilinum* (i.e. chlorophyllous or senesced) at the time of image capture in 2019 meant that each of these species had been separated into two classes prior to classification during Phase 2. No such variation was evident in 2020 and these species were kept as single classes for analysis in Phase 3. Samples of 'dead' *Calluna* were, however, retained as a discrete class.

Very little, if any, standing water was present on the sampled areas at the time of image capture in 2020, so field samples identified as such were excluded. *Sphagnum* plugs of both *fallax* and *fimbriatum* originally in strim D (n=4), were removed to leave only naturally occurring *Sphagnum* samples for classification. This provided 5377 samples of 19 classes for classification in total (Table 5:8), and these were randomly separated 50:50 into training (2690) and validation (2687) samples.

Training data for image classification were determined using 20 cm circular pixel averaging areas. Supervised maximum likelihood classification was then performed using imagery for each image block.



Table 5:3. Classes and sample sizes used in supervised classification

Class	Birchinlee	Derwent	Kinder	Moss	Penguins	Total
Bare peat	93	105	80	62	109	449
<i>Calluna vulgaris</i>	173	125	125	150	118	691
<i>Calluna dead</i>	45	61	54	7	67	234
<i>Deschampsia flexuosa</i>	8	5	58	8	30	109
<i>Empetrum nigrum</i>	7	9	96	48	44	204
<i>Eriophorum angustifolium</i>	109	100	104	110	129	552
<i>Eriophorum vaginatum</i>	111	116	105	136	131	599
<i>fallax</i>	33	28	28	2	44	135
<i>fimbriatum</i>	12	40	10	4	28	94
<i>Juncus effusus</i>	59	52	104	108	103	426
<i>Juncus squarrosus</i>	23	16	36	12	24	111
Mineral soil	21	38	24	18	74	175
<i>Molinia caerulea</i>	3			111	5	119
<i>Nardus stricta</i>	49	23	47	100	40	259
<i>Polytrichum spp</i>	23	35	99	133	59	349
<i>Pteridium aquilinum</i>	125	60		5		190
Rock	1	54	86	31	6	178
<i>Trichophorum cespitosum</i>	90	16		1	6	113
<i>Vaccinium myrtillus</i>	113	48	68	75	86	390
Total	1098	931	1124	1121	1103	5377

5.3 Results

5.3.1 Sphagnum spectral separability

The upper bound for transformed divergence is 2.000 and separability values of above 1.900 indicate that classes should separate well, those between 1.7 and 1.9 indicate the probability should be fairly good, with values of <1.700 suggesting poor class separability is likely (Jensen, 1996).

The results of this analysis, for all combinations of *Sphagnum* species within each site are shown in Tables 5:4-5:6. The values of transformed divergence have been colour coded using the breakpoints described above to show separability as green (separable), orange (fairly good separability) and red (poor separability). Transformed divergence values for all species of *Sphagnum* at Birchinlee and Derwent, and all species except *cuspidatum* at Kinder, showed poor class separability (values typically below 1.0). At Kinder, transformed divergence values indicated that *cuspidatum* is separable from *magellanicum*, *squarrosom* and *tenellum*, and shows fairly good separation from *capillifolium*, *fallax*, *fimbriatum*, *palustre* and *subnitens*.

These observations indicate that *Sphagnum* sp. differentiation, or grouping of species, is unlikely to be successful using classification of 4-band aerial imagery. It is possible that environmental conditions at the time of image capture presented a confounding factor as the *Sphagnum* was bleached and this may be a reason why the plugs were highly visible in the imagery. However, it must be noted that this is a common occurrence for this taxon.



Table 5:4. Birchinlee *Sphagnum* plugs: Separability analysis - Transformed divergence
Red to green graphically illustrate increasing probability of good classification accuracy.

	capillifolium	cuspidatum	denticulatum	fallax	fimbriatum	magellanicum	palustre	papillosum	squarrosum	subnitens	tenellum
capillifolium		597	351	440	366	90	259	286	130	88	380
cuspidatum			401	534	571	694	748	602	600	653	600
denticulatum				311	421	356	617	438	379	415	326
fallax					479	603	526	371	450	445	488
fimbriatum						449	489	358	474	370	426
magellanicum							351	381	214	176	410
palustre								164	226	127	846
papillosum									360	167	698
squarrosum										157	467
subnitens											560
tenellum											

n.b. Values shown are *10³ for consistency of decimal place.

Table 5:5. Derwent *Sphagnum* plugs: Separability analysis - Transformed divergence
Red to green graphically illustrate increasing probability of good classification accuracy.

	capillifolium	cuspidatum	denticulatum	fallax	fimbriatum	magellanicum	palustre	papillosum	squarrosum	subnitens	tenellum
capillifolium		678	332	522	457	342	266	295	901	268	515
cuspidatum			537	432	373	766	655	702	1446	845	524
denticulatum				227	319	429	229	357	1050	443	204
fallax					95	639	357	317	1307	795	339
fimbriatum						839	356	298	1439	795	486
magellanicum							437	443	819	313	455
palustre								229	1080	468	459
papillosum									854	484	537
squarrosum										930	1124
subnitens											489
tenellum											

n.b. Values shown are *10³ for consistency of decimal place.



Table 5:6. Kinder *Sphagnum* plugs: Separability analysis - Transformed divergence
Red to green graphically illustrate increasing probability of good classification accuracy.

	capillifolium	cuspidatum	denticulatum	fallax	fimbriatum	magellanicum	palustre	papillosum	squarrosum	subnitens	tenellum
capillifolium	1801	598	732	341	525	687	510	484	591	742	
cuspidatum		1683	1832	1722	1978	1892	1199	1972	1844	1945	
denticulatum			267	420	525	908	575	572	919	422	
fallax				482	632	947	617	545	883	243	
fimbriatum					363	430	292	360	450	425	
magellanicum						968	875	186	484	478	
palustre							554	682	1035	862	
papillosum								733	445	779	
squarrosum									438	251	
subnitens										785	
tenellum											

n.b. Values shown are *10³ for consistency of decimal place.

Potential impact of phenological variability. Comparing the separability of *Sphagnum* species between sites indicates that all species at Birchinlee exhibit poor class separability from the same species at Derwent (Table 5:7). Interestingly, except for *denticulatum* and *tenellum*, all other *Sphagnum* species at Birchinlee and Derwent exhibit fairly good separation, or are separable from the same species at Kinder (Table 5:7).

The reason for the projected separability between the majority of *Sphagnum* sp. examined on Kinder and the same species on the other two sites is not clear. It is possible that some plugs on Kinder were more exposed and hence subject to increased bleaching, but no field evidence is available to support this conjecture.



Table 5:7. *Sphagnum* plugs: Separability analysis between sites - Transformed divergence

Red to green graphically illustrate increasing probability of good classification accuracy.

		Derwent	Kinder
capillifolium	Birchinlee	1065	1879
	Derwent		1806
cuspidatum	Birchinlee	1396	1963
	Derwent		1984
denticulatum	Birchinlee	1642	1690
	Derwent		1437
fallax	Birchinlee	1693	1847
	Derwent		1834
fimbriatum	Birchinlee	1198	1740
	Derwent		1903
magellanicum	Birchinlee	1195	1776
	Derwent		1747
palustre	Birchinlee	1216	1829
	Derwent		1979
papillosum	Birchinlee	1286	1871
	Derwent		1978
squarrosom	Birchinlee	1644	1881
	Derwent		1992
subnitens	Birchinlee	1104	1964
	Derwent		1704
tenellum	Birchinlee	1529	1899
	Derwent		1371

n.b. Values shown are *10³ for consistency of decimal place.



5.3.2 Image classification: All species

Overall, the accuracies achieved when treating each site individually, despite the potential issues of reduced sample numbers, were markedly higher than either those in Phase 2, or the preliminary results in Phase 3 when the complete study area had been classified as single unit. The latter can readily be seen in comparing Table 5:10 (all sites classified as a whole) with 5:11 (combined error matrices for sites classified separately).

Bare peat and rock achieved high accuracies >90% (92% and 91% respectively). The former is of key importance to MFFP's objectives and, as such, this result is satisfying. Earlier phases, affected by below par imagery, did not demonstrate this potential well despite the fact these should be differentiated readily. Other classes achieving relatively high producer accuracies were *Calluna vulgaris* (79%), *Calluna* dead (77%), mineral soil (76%) and *Vaccinium myrtillus* (67%). Worthy of note is the mapping of surfaces within moorland burn 'scars' which is commonly mapped as mineral soil. In actuality such scars contain a mix of burned 'stick', bare peat, and sparse regrowth of several species. This undoubtedly erroneous identification as mineral soil possibly arises from an absence of training data from within these areas. Regrettably, no actual data on the ground cover present in regenerating burns were collected during the field survey so no definitive statement on this phenomenon can be made. The occurrence of burn management is almost ubiquitous in upland *Calluna* moorland (Yallop *et al.*, 2006) so the inability to provide further detail on the ability to map species regeneration in these scars represent something of a lacuna in this study. The automated mapping of burn 'scars' as objects is readily achieved (Yallop *et al.*, 2008) but this does not directly provide detail on any regenerating vegetation present. Further exploration of this topic could therefore be usefully included in further research.

Examination of the classification results (Tables 5:12-5:16) highlights considerable variation in both overall and individual classification accuracies across sites for a number of classes. For example:

- i. A 10% difference in overall accuracy from 51% to 61% at Penguins compared to Kinder;
- ii. *Calluna vulgaris*, where present as large continuous areas, exhibits producer accuracy of >90% at Birchinlee and Derwent, but at the other three sites this is markedly lower at 63%-77%.
- iii. Producer accuracy for mineral soil at Birchinlee, Kinder and Penguins range from 73%-89% whereas at Derwent and Moss, this is notably lower at 56%-60%



While it would be incorrect to propose any definitive cause for these phenomena without further investigation, it is not unreasonable to assume it arises, at least in part, as a consequence of the wide disparity in both numbers of species and samples between sites. This arises as a consequence of the need to classify each image separately as a result of the spectral issues within the image data. The field survey campaign was planned and executed to provide data for training and error assessment for the study area *as a whole*. The necessary division of these data into 5 sub-groups created imbalances in n for many site/species combinations.

Classified outputs from Phase 3 classifications are shown in Figures 5:2-5:11.



Table 5:10. Error matrix from training and classifying all 2020 images as one group. Maximum likelihood classification. 20cm search area.

	Bare peat	Calluna	Calluna dead	Deschampsia flexuosa	Empetrum nigrum	Eriophorum angustifolium	Eriophorum vaginatum	fallax	fimbriatum	Juncus effusus	Juncus squarrosus	Mineral soil	Molinia caerulea	Nardus stricta	Polytrichum spp.	Pteridium aquilinum	Rock	Trichophorum cespitosum	Vaccinium myrtillus	Total	User accuracy		
Bare peat	188	6	8		10	5		1		10	1	5		1	9				1	245	0.77		
Calluna	2	257	2	6	20	2	2	2	1	7	5		1	6	12	1			4	330	0.78		
Calluna dead	13	6	59	3	5	28	3			9	2	8	2	3	7			4		152	0.39		
Deschampsia flexuosa		21		11	2	3	20		4	2	6		1	10	3				5	88	0.13		
Empetrum nigrum	13	21	22	2	46	11	2	2	1	26	7				35				8	196	0.23		
Eriophorum angustifolium		1	6		2	86	8	3	1	31	3	3		2	2	1		2	2	153	0.56		
Eriophorum vaginatum	1			11	1	26	87	6	5	6	1	1	1	12		5		6	1	170	0.51		
fallax				4		1	8	11	3	1				6	1	1			1	37	0.30		
fimbriatum			1	2			7	9	10	1		1		2	1	2				36	0.28		
Juncus effusus	4	5	1		4	15	2			45	4				26			2	1	109	0.41		
Juncus squarrosus		13	2	4	5	4	15	3	1	9	7		2	14	8	4		1	20	112	0.06		
Mineral soil	1	1	8	1			3	3	3	1		58	6	1	1		13			100	0.58		
Molinia caerulea		1	4	1		2	51	8	4	4	4	7	34	38		3	3	1	4	169	0.20		
Nardus stricta	1			2			13				4		7	16	1	1	2			47	0.34		
Polytrichum spp.		1	2		2	2		2	3	8				1	45	1			3	70	0.64		
Pteridium aquilinum	1			3		19	36	7	4	4	6		3	10	2	60		4	10	169	0.36		
Rock			1				6	1		1		6	2				71			88	0.81		
Trichophorum cespitosum		1	2		4	70	36		3	48	4		1	7	14	16		37	10	253	0.15		
Vaccinium myrtillus		10		5	1		1	8	3					1	7	2			125	163	0.77		
Total	224	344	118	55	102	274	300	66	46	213	54	89	60	130	174	97	89	57	195	2687			
Producer accuracy	0.84	0.75	0.50	0.20	0.45	0.31	0.29	0.17	0.22	0.21	0.13	0.65	0.57	0.12	0.26	0.62	0.80	0.65	0.64				
N (total observations)						2687						Overall accuracy	0.47										
X (Sum of all correct)						1253						Kappa	0.43										
Y (Sum of total user x sum of total producer)						445214																	

Table 5:11. Merged error matrix classifying images by sites independently. Maximum likelihood classification. 20cm search area.

	Bare peat	Calluna	Calluna dead	Deschampsia flexuosa	Empetrum nigrum	Eriophorum angustifolium	Eriophorum vaginatum	fallax	fimbriatum	Juncus effusus	Juncus squarrosus	Mineral soil	Molinia caerulea	Nardus stricta	Polytrichum spp.	Pteridium aquilinum	Rock	Trichophorum cespitosum	Vaccinium myrtillus	Total	User accuracy	
Bare peat	207		6					1				6		1					1	222	0.93	
Calluna		272	2	2	18		2	1	1	4	3		1	3	6	2			2	319	0.85	
Calluna dead	10	7	91	3	12	11	4			6	2	5			1			1	2	155	0.59	
Deschampsia flexuosa		7		11	3	3	18		1	2	5			7	3	1		4	8	73	0.15	
Empetrum nigrum	1	16	5		33	5	2		1	16	2			1	22				7	111	0.30	
Eriophorum angustifolium	2	3	2	1	4	139	18	2	3	42	3	1	1	1	3	6		7		238	0.58	
Eriophorum vaginatum				11	1	24	130	5	4	15	1		9	19	1	18		8	4	250	0.52	
fallax				2		4	7	19	8	5	1	2		2		3			1	54	0.35	
fimbriatum		2		3	1	4	23	12	12		2			8		4				71	0.17	
Juncus effusus		4	3	1	6	25	3	4	1	72	6				22	7		9	8	171	0.42	
Juncus squarrosus		13	3	4	11	12	25	2	2	19	16			13	13	4			18	155	0.10	
Mineral soil	2	1	4				1	2	1	1		68		2	1		8			91	0.75	
Molinia caerulea							13			1	1		31	7						53	0.58	
Nardus stricta		3		9	1	2	34	3		1	6		12	57	3	3		1	2	137	0.42	
Polytrichum spp.	1	10	2	1	11	9		2	3	19	2			1	88	1			9	159	0.55	
Pteridium aquilinum							11	6	2		2			4		38		1	2	66	0.58	
Rock	1											7	2				78			88	0.89	
Trichophorum cespitosum						35	7			10				1	2	3		21		79	0.27	
Vaccinium myrtillus		6		4	1	1	2	6	5		2			3	9	4		1	131	175	0.75	
Total	224	344	118	52	102	274	300	65	44	213	54	89	56	130	174	94	86	53	195	2667		
Producer accuracy	0.92	0.79	0.77	0.21	0.32	0.51	0.43	0.29	0.27	0.34	0.30	0.76	0.55	0.44	0.51	0.40	0.91	0.40	0.67			
N (total observations)						2667						Overall accuracy	0.57									
X (Sum of all correct)						1514						Kappa	0.54									
Y (Sum of total user x sum of total producer)						493138																

Table 5:12. Error matrix for Birchinlee. Maximum likelihood classification. 20cm search area.

	Bare peat	Calluna	Calluna dead	Deschampsia flexuosa	Empetrum nigrum	Eriophorum angustifolium	Eriophorum vaginatum	fallax	fimbriatum	Juncus effusus	Juncus squarrosus	Mineral soil	Nardus stricta	Polytrichum spp.	Pteridium aquilinum	Trichophorum cespitosum	Vaccinium myrtillus	Total	User accuracy
Bare peat	42												1					43	0.98
Calluna		79			2					1	1							83	0.95
Calluna dead	2	1	23			1	1					1				1		30	0.77
Deschampsia flexuosa						1	9			2	2		1	1	1	4	2	23	0.00
Empetrum nigrum		2			1					1				1				5	0.20
Eriophorum angustifolium						23			1	2					4	7		37	0.62
Eriophorum vaginatum				3		3	29	3		3			2		8	5	3	59	0.49
fallax								2		3		2			3			10	0.20
fimbriatum		1			1	1	2	3	2				3		4			19	0.11
Juncus effusus		3		1		10	1	1		10	2			4	5	7	4	48	0.21
Juncus squarrosus							1				1		1	1			8	12	0.08
Mineral soil	2											8		1	1			12	0.67
Nardus stricta						2	1				2		11			1	1	18	0.61
Polytrichum spp.									1	1			1	3	1		2	9	0.33
Pteridium aquilinum							5	4	2		1		1		35	1	2	51	0.69
Trichophorum cespitosum						14	5			7			1		1	18		46	0.39
Vaccinium myrtillus						1	1	2					2		1	1	35	43	0.81
Total	46	86	23	4	4	54	56	16	6	30	11	11	25	11	63	45	57	548	
Producer accuracy	0.91	0.92	1.00	0.00	0.25	0.43	0.52	0.13	0.33	0.33	0.09	0.73	0.44	0.27	0.56	0.40	0.61		
N (total observations)						548						Overall accuracy						0.59	
X (Sum of all correct)						322						Kappa						0.55	
Y (Sum of total user x sum of total producer)						25481													

Table 5:13. Error matrix for Derwent. Maximum likelihood classification. 20cm search area.

	Bare peat	Calluna	Calluna dead	Empetrum nigrum	Eriophorum angustifolium	Eriophorum vaginatum	fallax	fimbriatum	Juncus effusus	Juncus squarrosus	Mineral soil	Nardus stricta	Polytrichum spp.	Pteridium aquilinum	Rock	Trichophorum cespitosum	Vaccinium myrtillus	Total	User accuracy
Bare peat	50		5				1				3						1	60	0.83
Calluna		56	1											2				59	0.95
Calluna dead			21	1	1						2							25	0.84
Empetrum nigrum		2		3				1	1				4				1	12	0.25
Eriophorum angustifolium	2				16	3		2	4					2				29	0.55
Eriophorum vaginatum					4	32	1	2	3			1	1	10		3		57	0.56
fallax					2	2	4	4									1	13	0.31
fimbriatum		1			1	2	1	4				1						10	0.40
Juncus effusus					4	2	1	1	11				2	2		2	1	26	0.42
Juncus squarrosus		2				3				3		2	3	4			5	22	0.14
Mineral soil		1	4				1	1			12				3			22	0.55
Nardus stricta						5	1			1		5		3				15	0.33
Polytrichum spp.	1						1	2	4	1			4				6	19	0.21
Pteridium aquilinum						6	2			1		3		3				15	0.20
Rock											3				25			28	0.89
Trichophorum cespitosum					21	2			3				2	2		3		33	0.09
Vaccinium myrtillus								2		1			2	3			9	17	0.53
Total	53	62	31	4	49	57	13	19	26	7	20	12	18	31	28	8	24	462	
Producer accuracy	0.94	0.90	0.68	0.75	0.33	0.56	0.31	0.21	0.42	0.43	0.60	0.42	0.22	0.10	0.89	0.38	0.38		
N (total observations)					462					Overall accuracy					0.56				
X (Sum of all correct)					261					Kappa					0.53				
Y (Sum of total user x sum of total producer)					16403														

Table 5:14. Error matrix for Kinder. Maximum likelihood classification. 20cm search area.

	Bare peat	Calluna	Calluna dead	Deschampsia flexuosa	Empetrum nigrum	Eriophorum angustifolium	Eriophorum vaginatum	fallax	fimbriatum	Juncus effusus	Juncus squarrosus	Mineral soil	Nardus stricta	Polytrichum spp.	Rock	Vaccinium myrtillus	Total	User accuracy	
Bare peat	40											1					41	0.98	
Calluna		42		2	9						1			2			56	0.75	
Calluna dead		4	20		9	1	1			2	1						38	0.53	
Deschampsia flexuosa		2		8	2		6				1		4	1		2	26	0.31	
Empetrum nigrum		4	2		13					3	1		1	2			26	0.50	
Eriophorum angustifolium		1			2	37	3			12	2						57	0.65	
Eriophorum vaginatum				4	1	8	24		1	7	1		4				50	0.48	
fallax				1			3	8	2				1				15	0.53	
fimbriatum				1		2	6	4	2				3				18	0.11	
Juncus effusus			2		1	1				18	2			3		1	28	0.64	
Juncus squarrosus		4	1	3	3	2	9			9	7		1	1		4	44	0.16	
Mineral soil								1				10	1		4		16	0.63	
Nardus stricta				6									8			1	15	0.53	
Polytrichum spp.		5	2		8	1				1	1			40			58	0.69	
Rock												1			39		40	0.98	
Vaccinium myrtillus				4			1	1			1			1		26	34	0.76	
Total	40	62	27	29	48	52	53	14	5	52	18	12	23	50	43	34	562		
Producer accuracy	1.00	0.68	0.74	0.28	0.27	0.71	0.45	0.57	0.40	0.35	0.39	0.83	0.35	0.80	0.91	0.76			
N (total observations)						562	Overall accuracy		0.61										
X (Sum of all correct)						342	Kappa		0.58										
Y (Sum of total user x sum of total producer)						22615													

Table 5:15. Error matrix for Moss. Maximum likelihood classification. 20cm search area.

	Bare peat	Calluna	Calluna dead	Deschampsia flexuosa	Empetrum nigrum	Eriophorum angustifolium	Eriophorum vaginatum	Juncus effusus	Juncus squarrosus	Mineral soil	Molinia caerulea	Nardus stricta	Polytrichum spp.	Rock	Vaccinium myrtillus	Total	User accuracy
Bare peat	26									1						27	0.96
Calluna		58			3			1			1	3			1	67	0.87
Calluna dead	4	1		1	1	2		1					1			11	0.00
Deschampsia flexuosa		3		1		1			1			1				7	0.14
Empetrum nigrum		4	2		15	2	1	10	1				13			48	0.31
Eriophorum angustifolium		1	1	1	1	25	5	13	1		1	1	1			51	0.49
Eriophorum vaginatum						6	32	1			9	8				56	0.57
Juncus effusus					1	3		8	1					5	1	19	0.42
Juncus squarrosus					2	7	5	10				3	5			32	0.00
Mineral soil										5				1		6	0.83
Molinia caerulea							13	1	1		31	7				53	0.58
Nardus stricta		3		1	1	2	12	1	1		12	27	3			63	0.43
Polytrichum spp.		2				7		8					35			52	0.67
Rock	1									3	2			14		20	0.70
Vaccinium myrtillus		3											3		35	41	0.85
Total	31	75	3	4	24	55	68	54	6	9	56	50	66	15	37	553	
Producer accuracy	0.84	0.77	0.00	0.25	0.63	0.45	0.47	0.15	0.00	0.56	0.55	0.54	0.53	0.93	0.95		
N (total observations)						553	Overall accuracy		0.56								
X (Sum of all correct)						312	Kappa		0.52								
Y (Sum of total user x sum of total producer)						26327											

Table 5:16. Error matrix for Penguins. Maximum likelihood classification. 20cm search area.

	Bare peat	Calluna	Calluna dead	Deschampsia flexuosa	Empetrum nigrum	Eriophorum angustifolium	Eriophorum vaginatum	fallax	fimbriatum	Juncus effusus	Juncus squarrosus	Mineral soil	Nardus stricta	Polytrichum spp.	Vaccinium myrtillus	Total	User accuracy	
Bare peat	49		1									1				51	0.96	
Calluna		37	1		4		2	1	1	2	1			4	1	54	0.69	
Calluna dead	4	1	27	2	1	6	2			3	1	2			2	51	0.53	
Deschampsia flexuosa		2		2	1	1	3		1		1		1	1	4	17	0.12	
Empetrum nigrum	1	4	1		1	3	1			1				2	6	20	0.05	
Eriophorum angustifolium		1	1		1	38	7	2		11		1		2		64	0.59	
Eriophorum vaginatum				4		3	13	1	1	1			4		1	28	0.46	
fallax				1		2	2	5	2	2	1		1			16	0.31	
fimbriatum				2			13	4	4				1			24	0.17	
Juncus effusus		1	1		4	7		2		25	1			8	1	50	0.50	
Juncus squarrosus		7	2	1	6	3	7	2	2		5		6	3	1	45	0.11	
Mineral soil							1			1		33				35	0.94	
Nardus stricta				2			15	1			2		6			26	0.23	
Polytrichum spp.		3		1	3	1		1		5				6	1	21	0.29	
Vaccinium myrtillus		3			1			3	3				1	3	26	40	0.65	
Total	54	59	34	15	22	64	66	22	14	51	12	37	20	29	43	542		
Producer accuracy	0.91	0.63	0.79	0.13	0.05	0.59	0.20	0.23	0.29	0.49	0.42	0.89	0.30	0.21	0.60			
N (total observations)						542						Overall accuracy						0.51
X (Sum of all correct)						277						Kappa						0.47
Y (Sum of total user x sum of total producer)						22235												

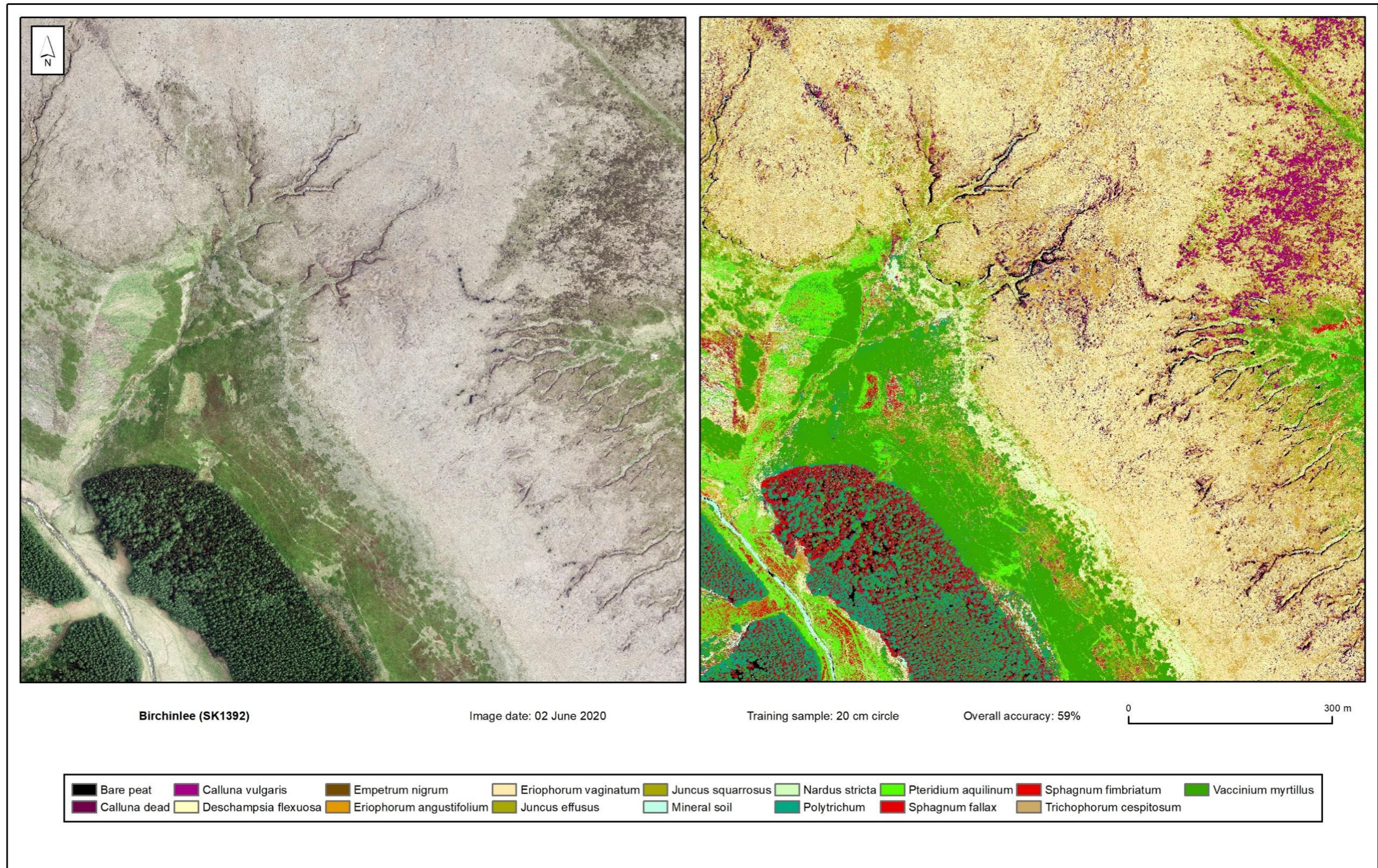


Figure 5:2. Classified output for Birchinlee (SK1392).

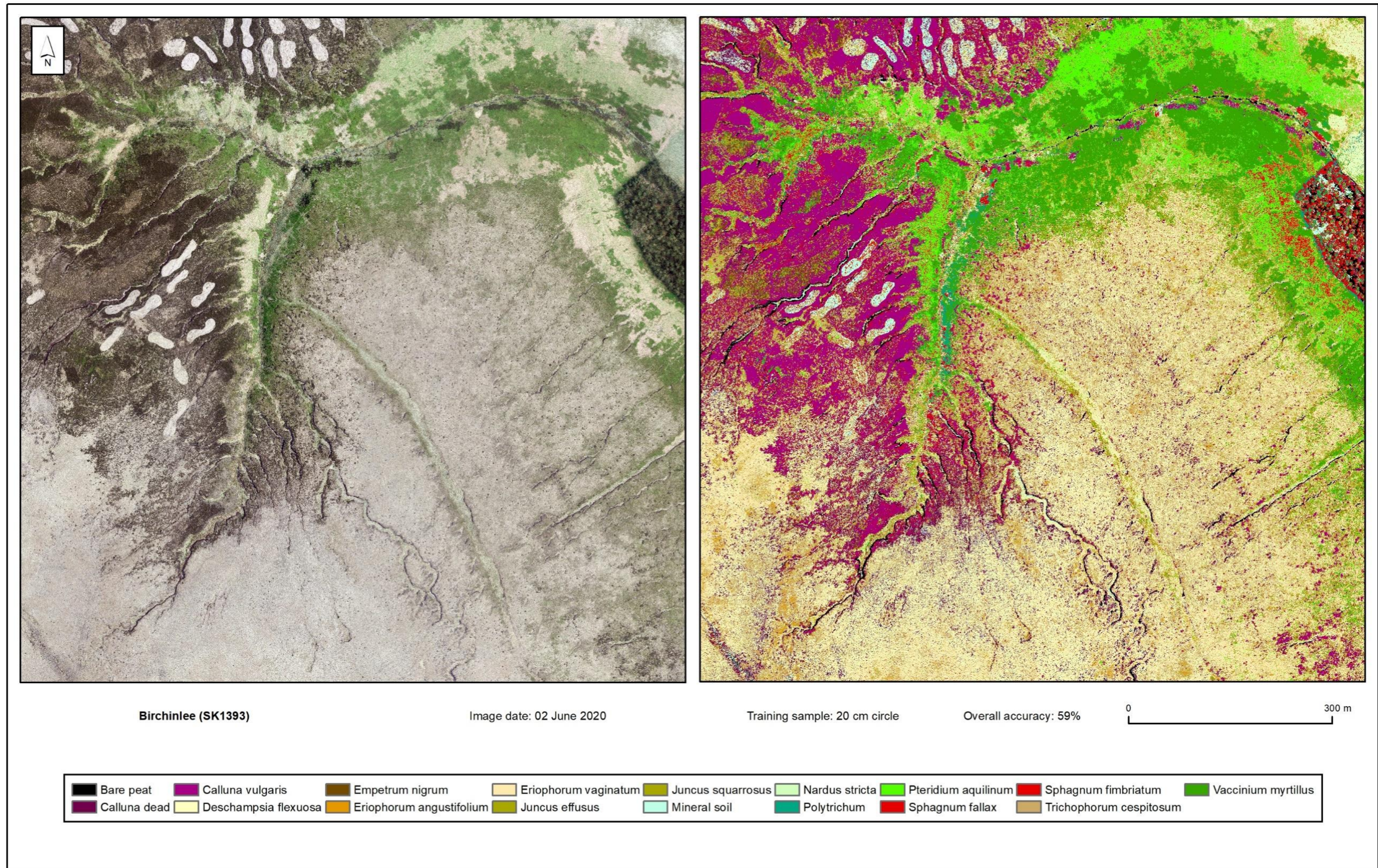


Figure 5:3. Classified output for Birchinlee (SK1393).

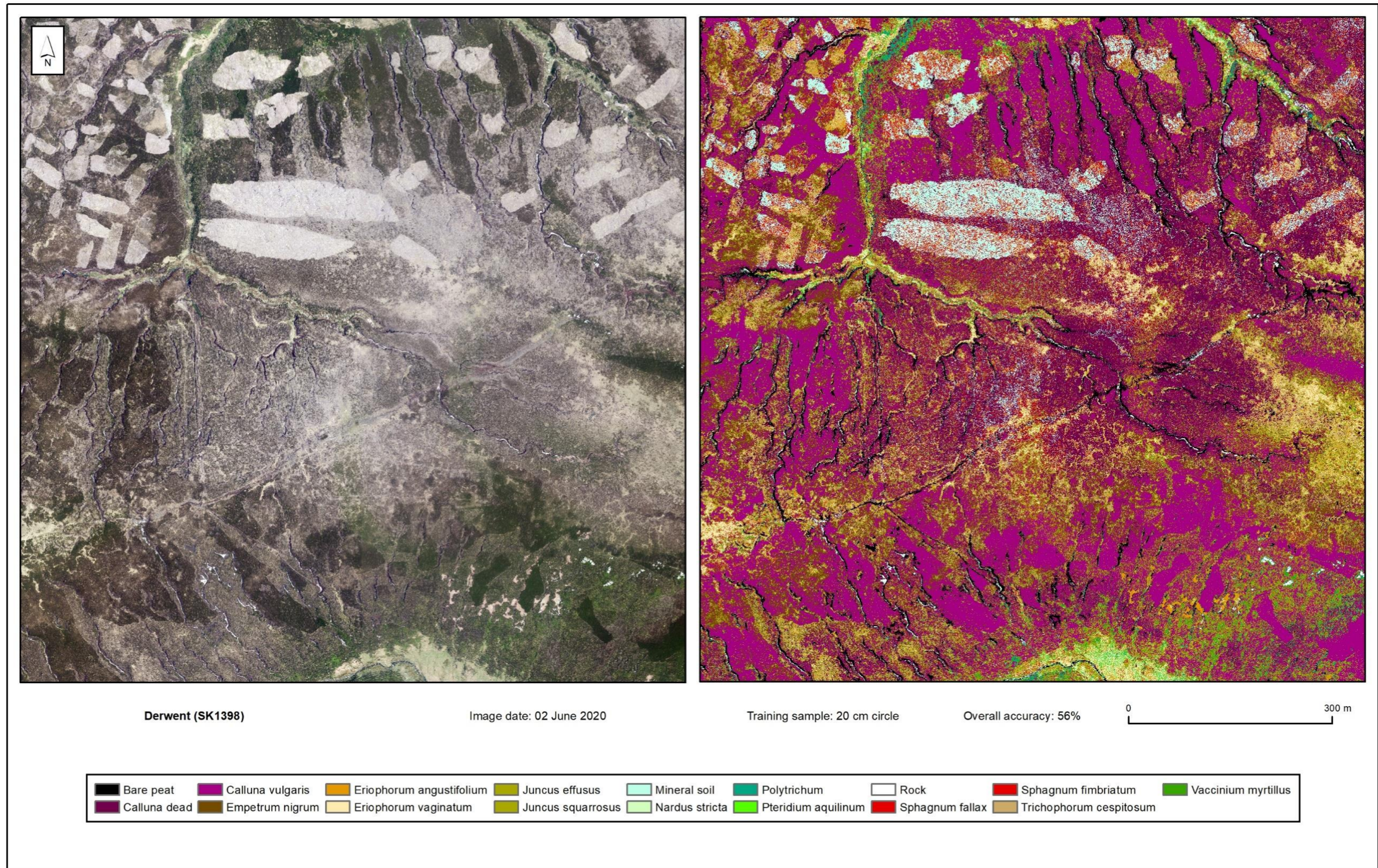


Figure 5:4. Classified output for Derwent Howden (SK1398).

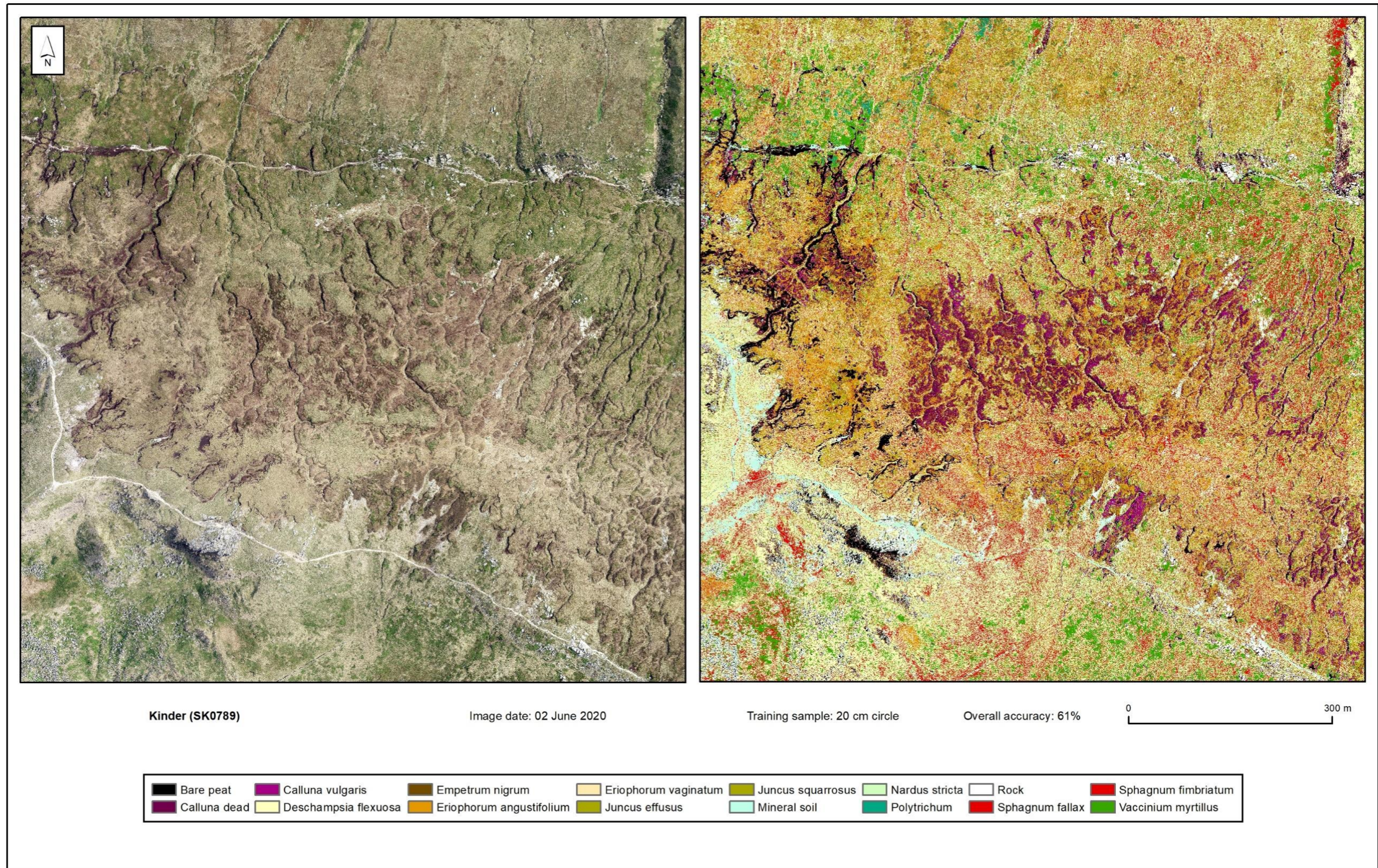


Figure 5:5. Classified output for Kinder (SK0789).

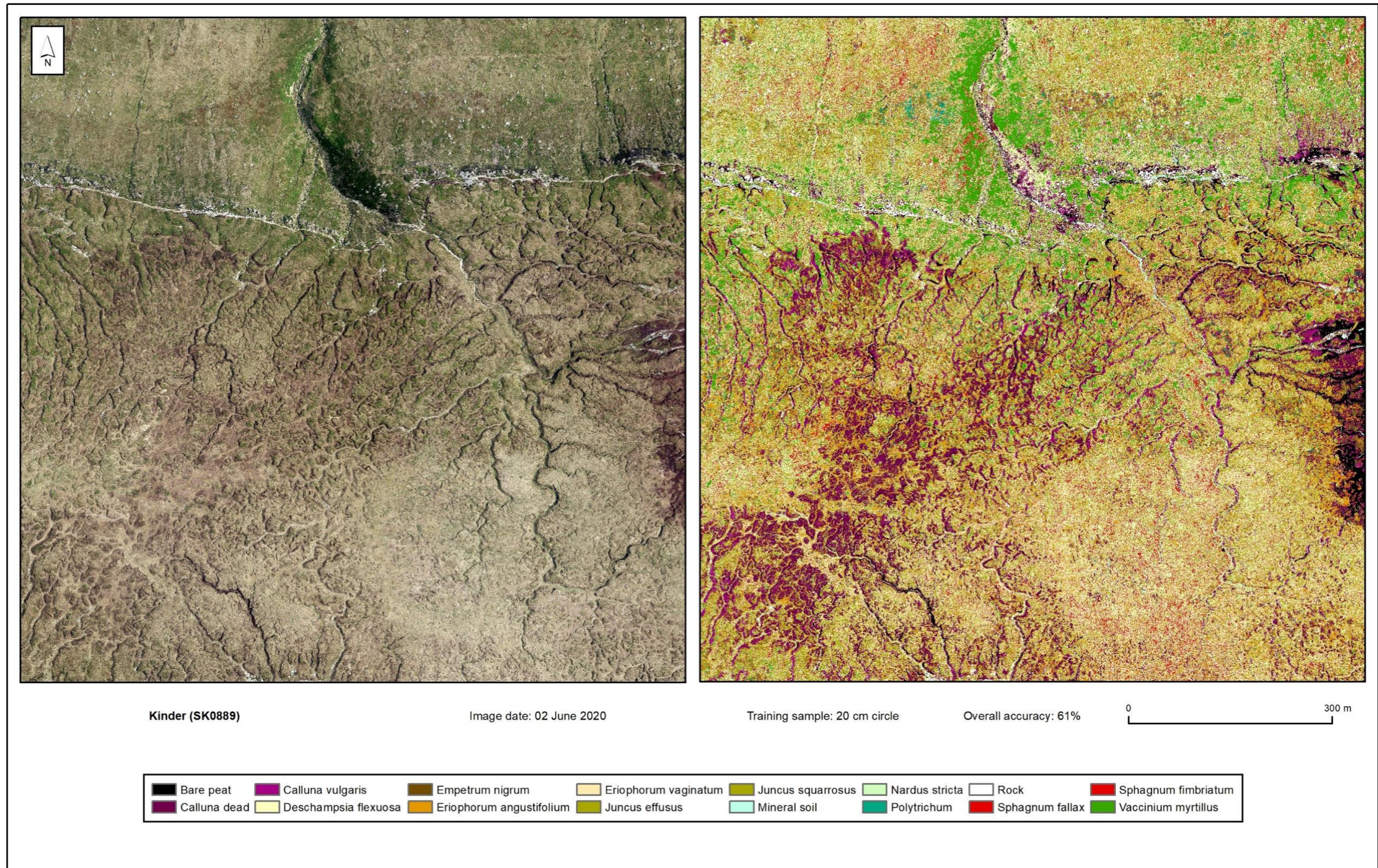


Figure 5:6. Classified output for Kinder (SK0889).

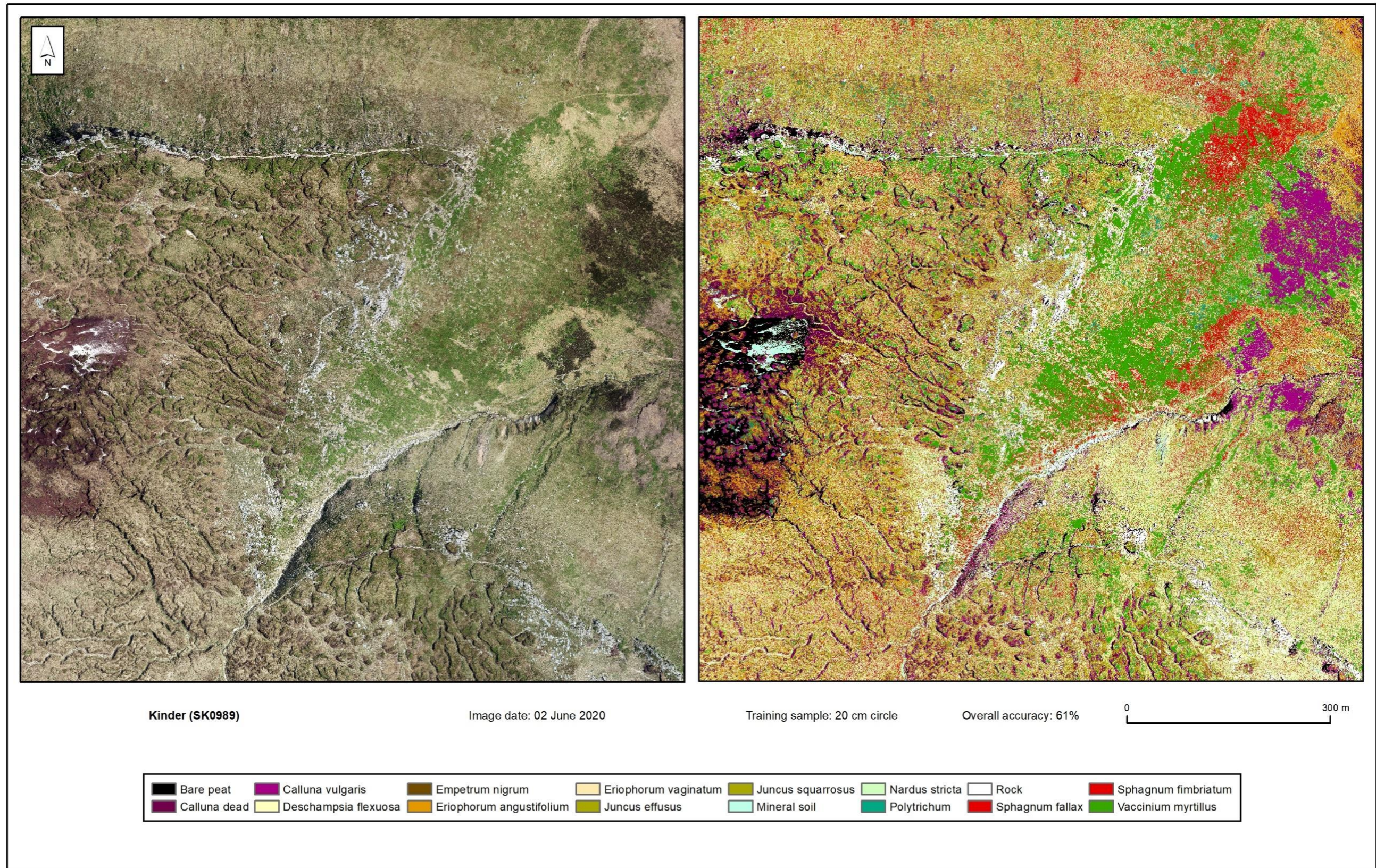


Figure 5.7. Classified output for Kinder (SK0989).

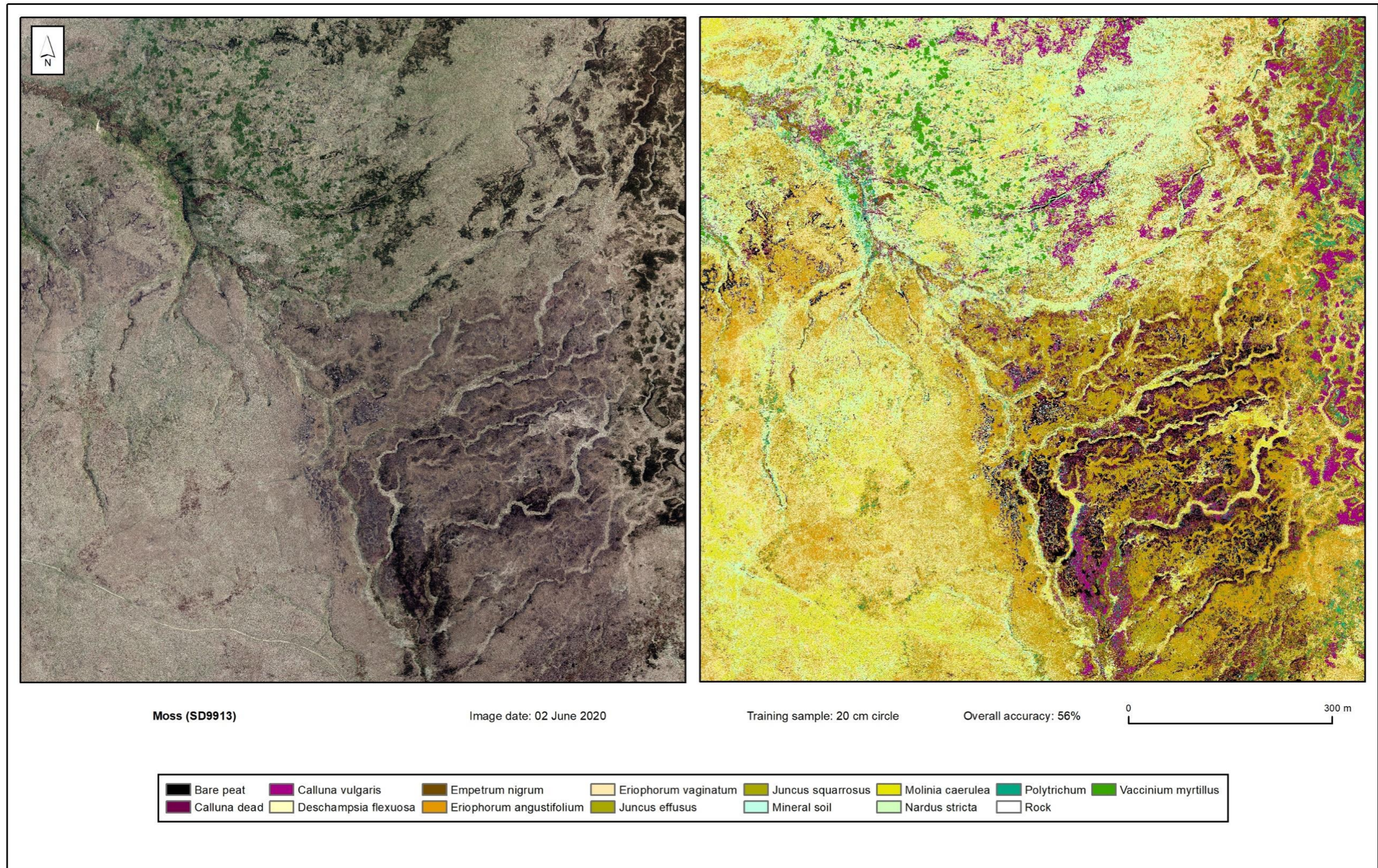


Figure 5:8. Classified output for Molinia (SD9913).

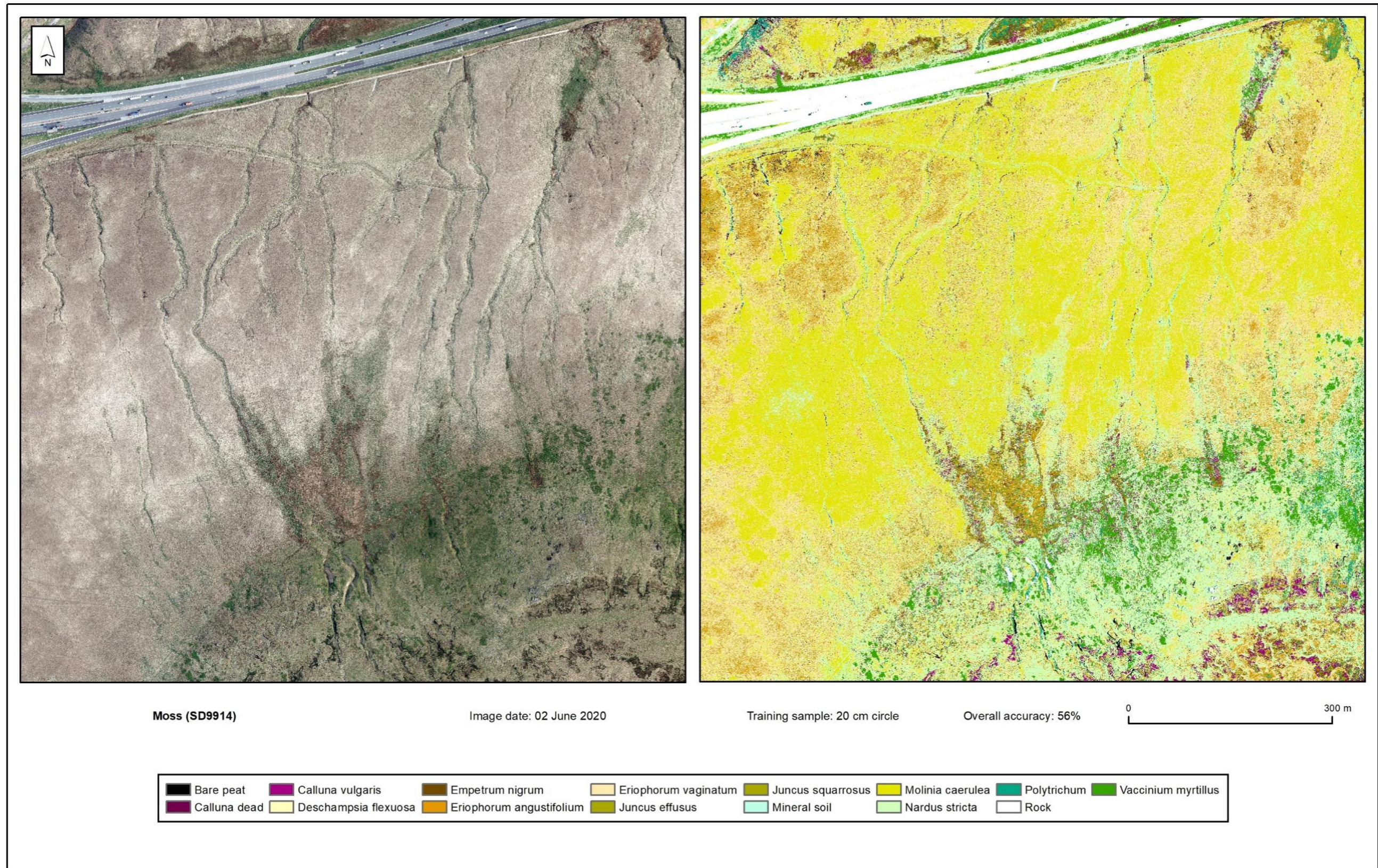


Figure 5:9. Classified output for Molinia (SD9914).

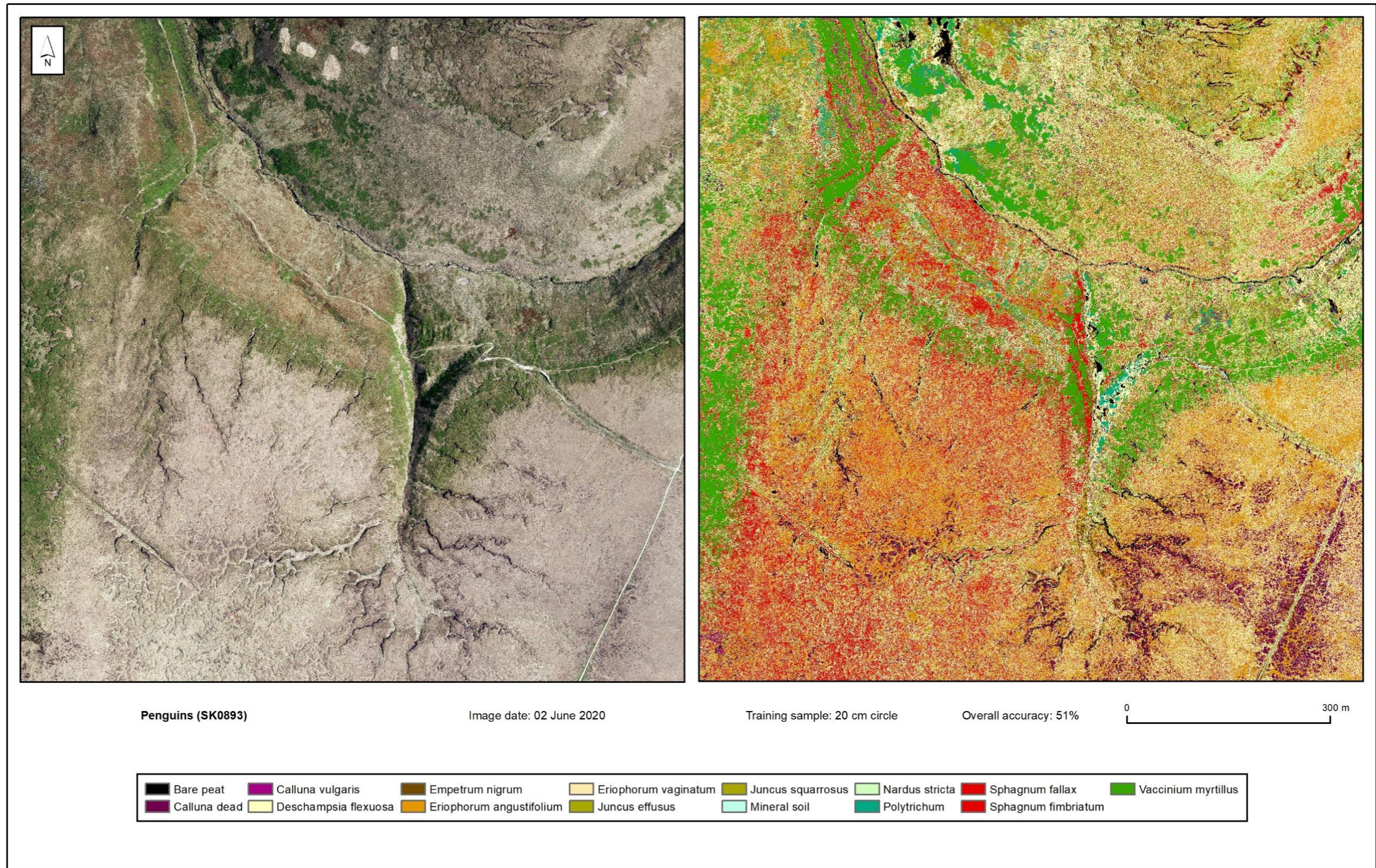


Figure 5:10. Classified output for Penguins (SK0893).

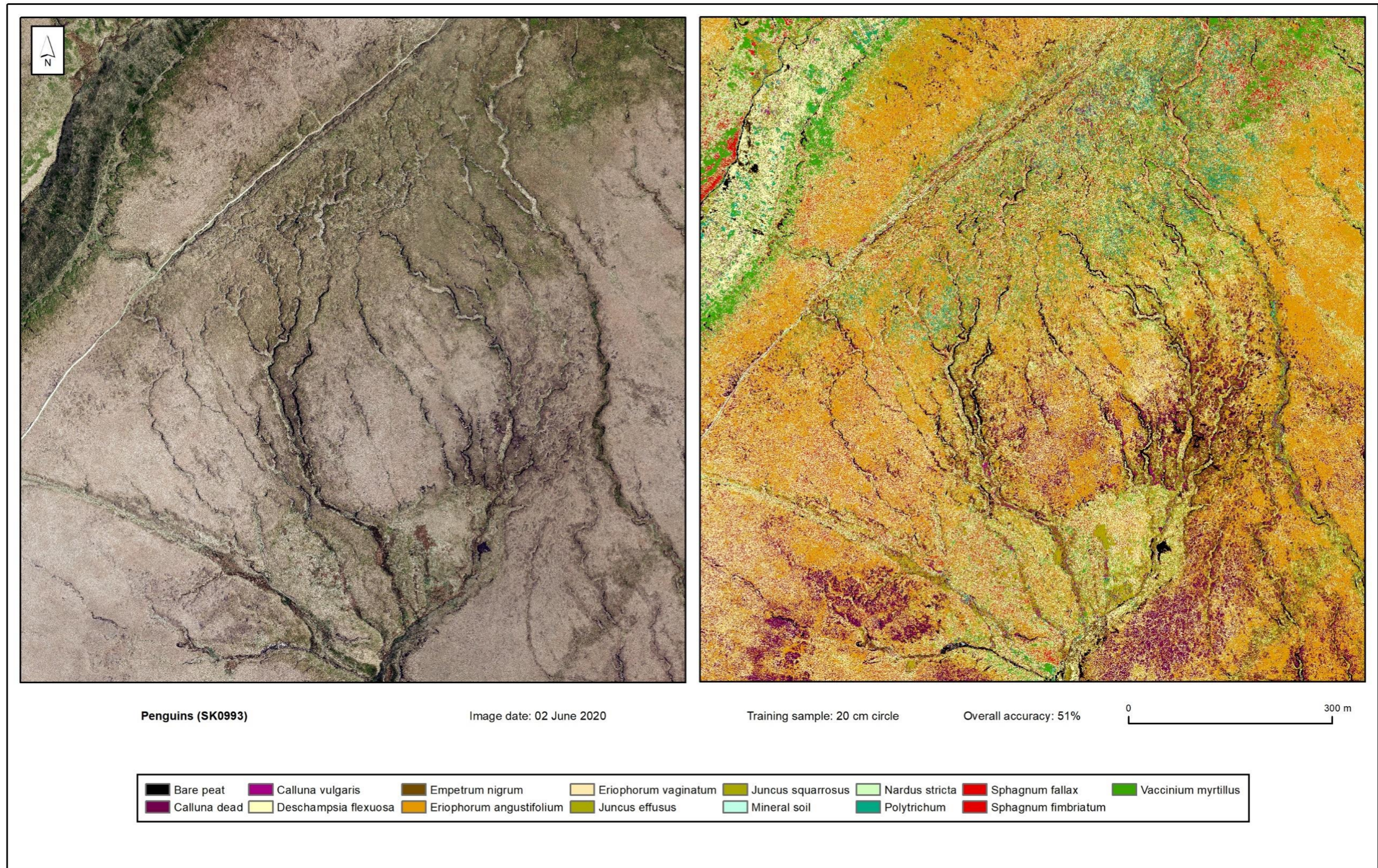


Figure 5:11. Classified output for Penguins (SK0993).

5.4 Summary of Phase 3

Once an approach to, as far as possible, mitigate the issues with the supplied imagery had been undertaken, Phase 3 can be considered as utilising the best ‘standard’ or ‘off the shelf’ imagery available from commercial sources. It therefore represents a definitive test of the original project objectives to map to species. The results achieved using this typology approaches the accuracy that might be expected when using far broader (and probably less repeatable) habitat or community approaches.

As such, providing limitations of the outputs are understood, a typology based on species would provide an initial product suitable for landscape scale assessment and planning. The results are as good as other approaches, and it removes the issues with field survey ambiguities that inevitably reduce the value of all alternate habitat or community descriptor approaches. In addition, many classes e.g. bare peat and *Calluna*, can be classified to the level that they both provide reliable assessment of peatland condition.

However, the overall accuracies achieved would be unsuitable, *on their own*, for undertaking a monitoring programmes for all species as the multiplicative nature of accuracy determination for change between two or more images would be too low. Such a process would require higher overall accuracies.

Many of the reductions in overall accuracy arise as a consequence of ‘confusion’ between many species of little conservation management importance and each other. It is possible that combining these into aggregate classes would therefore both increase overall accuracies to the level temporal change monitoring is possible, while still meeting MFFP’s needs.

Phase 4 therefore was tasked with trying this approach.





Section 6: Phase 4 – Classification of Species Groupings

Summary introduction to Phase 4 activities

Phase 4 is the final part of the original MFF 50 2016-17 specification dealing with the potential application of remote sensing to monitor upland vegetation change using XHR imagery. Following the experience and results gained during earlier phases it was decided to broaden the project to consider the application of differing classification protocols.

Objectives of Phase 4

1. Investigate the possibility of using species aggregations to improve overall classification accuracies. These aggregate classes were to be defined by two processes:
 - i. A pair of species groups were to be defined by MFFP based solely on their relevance to monitoring requirements;
 - ii. The NTU/CS team were to explore what groups could be derived using species spectral characteristics.

Owing to the spectral balancing issues with the 2020 imagery described in Phase 3 these approaches were to be developed and tested using Kinder imagery and field data. The 'best' performing of the two approaches would then be deployed across the remaining 4 sites. In addition, the groups would form the basis of an extension to the original project viz. a direct comparison of classification using imagery from satellite EO, UAV and airborne sources. Methods and results of the latter are presented in section 7.
2. Examine the potential of alternate classification algorithms, in this case machine learning techniques, to improve classification accuracies. This project has intentionally restricted itself to software and techniques most likely to be accessible to conservation NGOs and agencies. However, it was considered important to test recent advances in classification procedures to ensure continuing relevance of the conclusions drawn in this report.

Approaches for identifying species clusters

Two contrasting methods for 'grouping' or 'merging' species to determine their potential for improving classification accuracies were adopted during Phase 4. The first utilised simple taxonomic groups determined by MFFP to be of direct relevance to conservation monitoring. As this approach makes no regard to the spectral characteristics of each species it was not expected to produce substantial increases in classification accuracies over species mapping. However, given the direct relevance of the data produced to monitoring this method might still provide worthwhile products, if the gain in accuracy was significant.



The second method sought to identify similarities in spectral reflectance of each species to create 'natural' combinations that would minimise spectral overlap. This approach might be anticipated to exhibit higher classification accuracies but identify less immediately interpretable species groups of unpredictable applicability for conservation monitoring. The method might nevertheless prove to be of merit if it produced significantly higher accuracy than the species or other grouping approaches.

Clarification with regard to meaning of 'species grouping.' To avoid potential confusion, it should be noted that the grouping of species in 1: above, i.e. by association of spectral or taxonomic relationships is not analogous to deriving groups of species according to ecological field survey 'community' or 'habitat' concepts. The processes used here do not assume, or utilise, any spatial relationships in the groups of species identified. It cannot imply any 'community' types that might be recognisable by field survey as the latter are based solely on spatial associations.

The proposed processes in Phase 4 therefore do not run counter to the direct objections raised in Section 2.2 with regard to the use of community descriptors for any form of mapping or monitoring. Field survey data used here consists solely of species data, free of any *a priori* assumptions of associations. Any groupings therefore arise from either intrinsic spectral characteristics, or perceived monitoring role alone, and are determined *post hoc* of field data collection. This means that species groups defined here, and in Section 7, do not identify any associations 'on the ground', they are merely co-mapped species sharing a common typology and accuracy metrics.



6.1 Exploratory analyses: Kinder

6.1.1 Methods

Image specification. The experimental development of species groupings was undertaken using 4-band aerial imagery (RGB NIR) with a GSD of 5 cm captured on 02/06/2020 by Bluesky International Ltd. Owing to the observed impact of NIR imbalance across the image groups on classification accuracy (section 5.1), development and testing of groupings was undertaken at Kinder (the largest area) before the best approach was deployed across the remaining sites.

Field data. The final field data used in Phase 3 comprised a subset of all field data that excluded classes with low sample numbers (5377 samples, 19 classes: Strim D). The approach of *a priori* grouping means that those species with low sample numbers could now be added to the analysis. The original field data (7104 samples) were therefore re-examined and a larger subset comprising 6519 samples of 59 classes were extracted for development of species grouping methods (Table 6:1). A subset of these data was used for MFFP-defined groups, i.e. species that were not part of these were removed prior to that part of the analysis, resulting in 5919 samples of 39 species/classes entering the analysis.

Species aggregations using MFFP-defined classes. Two groups of 7 and 12 classes were defined and provided by MFFP (Table 6:1). Samples of each class were randomly separated 50:50 into training and validation samples. Training data for image classification were extracted for each site using 20 cm circular pixel averaging. Supervised maximum likelihood classification was then performed.

Table 6:1 Classes and sample size used for MFFP groups at Kinder

Group 1	n	Group 2	n
Bare peat	80	Bare peat	80
Bryophytes	306	Bilberry	68
Dwarf shrubs	309	Cotton grasses	209
Ferns	0	Ferns	0
Grass, sedge & rush	463	Heather	125
Mineral soil	24	Mineral soil	24
Rock *	86	Other bryophytes	141
		Other dwarf shrubs	116
		Other grass, sedge & rush	254
		Purple moor grass	0
		Rock *	86
		<i>Sphagnum</i>	165
Totals	1268		1268

Species aggregations using spectral similarity. The methods used here for assigning species to groups were all based on measures of the spectral distance between them.

Three exploratory approaches for identifying these distances were tested: transformed divergence, Euclidean distance in spectral space and unsupervised classification (ISODATA) (Table 6:2). It should be noted that the process of identifying species groups by these methods was complex, with many intermediary stages. For clarity only the summary outcomes are presented in this section. A fuller presentation of the results is shown in Annex C.

Table 6:2 Classes and sample size used for spectral clustering groups at Kinder

Note: for consistency with other methods all species are shown, only those with a value for *n* were actually present at Kinder.

Species/class	n	Species/class	n
<i>Abies</i> spp.	6	<i>Juncus squarrosus</i>	38
<i>Agrostis</i> spp.	1	<i>Molinia caerulea</i>	
Bare peat	80	<i>Nardus stricta</i>	47
<i>Betula</i> spp.	21	<i>Phragmites</i> spp.	2
<i>Calluna</i> burnt		<i>Pinus</i> spp.	68
<i>Calluna</i> cut		<i>Leucanthemum vulgare</i>	1
<i>Calluna</i> dead	54	Mineral soil	24
<i>Calluna vulgaris</i>	125	<i>Polytrichum</i> spp.	99
<i>Chamaenerion angustifolium</i>	23	<i>Pteridium aquilinum</i>	
<i>Cladonia</i> spp.	4	<i>Rhododendron groenlandicum</i>	
Cushion moss	24	<i>Rhododendron</i> spp.	1
<i>Deschampsia cespitosa</i>		Rock	86
<i>Deschampsia flexuosa</i>	58	<i>Salix</i> spp.	12
<i>Empetrum</i> dead	5	<i>Sorbus aucuparia</i>	
<i>Empetrum nigrum</i>	98	<i>Sphagnum capillifolium</i>	10
<i>Epilobium</i> spp.		<i>Sphagnum cuspidatum</i>	11
<i>Erica cinerea</i>		<i>Sphagnum denticulatum</i>	13
<i>Erica tetralix</i>	18	<i>Sphagnum fallax</i>	41
<i>Eriophorum angustifolium</i>	104	<i>Sphagnum fimbriatum</i>	19
<i>Eriophorum vaginatum</i>	105	<i>Sphagnum flexuosum</i>	2
Feather moss	18	<i>Sphagnum magellanicum</i>	8
Fern		<i>Sphagnum palustre</i>	18
Flagstone		<i>Sphagnum papillosum</i>	16
<i>Ulex</i> spp	1	<i>Sphagnum squarrosus</i>	6
Heather Brash		<i>Sphagnum subnitens</i>	11
<i>Holcus lanatus</i>		<i>Sphagnum tenellum</i>	10
<i>Holcus mollis</i>	6	<i>Trichophorum cespitosum</i>	
<i>Juncus bulbosus</i>		<i>Vaccinium myrtillus</i>	68
<i>Juncus effusus</i>	104	<i>Vaccinium vitis-idaea</i>	
		Total	1466

Transformed divergence. The transformed divergence measure is frequently used to test class separability, and in this instance it was implemented in the 'Erdas Imagine' software suite. It produces a maximum value of 2000 and gives an exponentially decreasing weight to increasing distances between the classes (Jensen, 1996). The higher the value of transformed divergence between two classes, the more likely they are to classify separately. Good separation is described as being reached at values of 1900 or above. In reality, most plant class pairs are likely to have lower divergences, showing less than perfect separation. The method of clustering by transformed divergence used here uses the dissimilarity matrix to manually group species with high similarity.



First, species with fewer than 10 samples were removed, leaving 30 species (including non-biological classes: bare peat, mineral soil, rock) to enter the first stage. Species pairs with transformed divergence values of below 500 were grouped at the first stage. At the second stage, species pairs with transformed divergence values of below 750 were grouped. The third and final stage was of species pairs with transformed divergence values of below 1400. The class sets produced by the latter two stages were tested for classification accuracy, which is presented in the results.

Spectral space. The centroid of a species' spectral position is simply its average value in n -dimensional space where n represents the number of image bands available. The Euclidean distance between two species can be calculated by Pythagoras. It is also possible to utilise the variability around each species' mean position to calculate the distance between them in terms of standard deviations. Conceptually the overlap between two species in spectral space can be seen as a function of how far apart their average position is and how variable they are around that average position.

In a standard normal distribution, 95% of a species' distribution would be expected to be within 2 standard deviations of the mean. Thus, species or classes that were 2 standard deviations apart in spectral space would be very well separated. 50% of a species' distribution would be expected to be within 0.67 standard deviations of its mean. Species' spectral responses tend to be quite similar, so that large separation of plant species within communities is the exception rather than the rule.

As for the other methods, species with fewer than 10 samples were removed, leaving 30 species (including non-biological classes: bare peat, mineral soil, rock) to enter the first stage. The first stage of species groups compiled here joined species that were within 0.1 standard deviations of one another in spectral space. Subsequent iterations grouped species that were 0.2 standard deviations and 0.4 standard deviations apart. All three stages were tested for classification accuracy and the results are reported below.

Iterative Self Organizing Data Analysis Technique (ISODATA). ISODATA is a form of unsupervised classification that divides the spectral space of an image into classes without reference to any other data. Such derived classes may therefore represent only part of, or more than, one actual species.

The method employed here for identifying natural species spectral groupings used the ISODATA algorithm in 'Erdas Imagine' to extract 20 classes. As before species with fewer than 10 samples were removed. The remaining species ($n=30$) were tested to see whether they were significantly associated with 1 or more of the unsupervised classes using a binomial function. At stage 1, species were merged if they only occurred in the



same unsupervised class(es) as other species. For example, if species A and species B only occurred in unsupervised class 1, they were merged into a single group. This process was then expanded from single unsupervised classes to multiple, for example if species A and species B both only occurred in unsupervised class 1 and unsupervised class 2, they were merged into a single class.

Testing classification accuracy. Individual samples were labelled with their derived class and were divided into a training and testing set using alternate samples (50:50 train: test). Spectral signatures for training classes were extracted using a 20 cm circular sampling area and these were used to classify the image (maximum likelihood). Test samples were intersected with the classified image, and the actual and predicted classes were compared using error matrices.

6.1.2 Results

MFFP-defined groups. The smaller of the two groups of species defined by MFFP (Group 1) produced an overall classification accuracy of 0.75, reducing to 0.64 for the second, larger group (Table 6:3); *c.f.* the average accuracy of 0.61 for classification to species at Kinder (Table 5:14).



Table 6:3. Classification accuracies for MFFP classes at Kinder
 Top: Group 1. Bottom: Group 2

	Bare peat	Bryophytes	Dwarf shrubs	Grass, sedge & rush	Mineral soil	Rock	Total	User accuracy	
Bare peat	40	1	3		1		45	0.89	
Bryophytes		74	8	15	1		98	0.76	
Dwarf shrubs		22	133	33			188	0.71	
Grass, sedge & rush		34	11	177			222	0.80	
Mineral soil		19		5	8	2	34	0.24	
Rock		3		1	2	41	47	0.87	
Total	40	153	155	231	12	43	634		
Producer accuracy	1.00	0.48	0.86	0.77	0.67	0.95			
N (total observations)							634	Overall accuracy	0.75
X (Sum of all correct)							473		
Y (Sum of total user x sum of total producer)							99645	Kappa	0.66

	Bare peat	Bilberry	Cotton grasses	Heather	Mineral soil	Other bryophytes	Other dwarf shrubs	Other grasses, sedge & rush	Rock	Sphagnum	Total	User accuracy
Bare peat	40			1	1	1	1				44	0.9
Bilberry		30	1	2		2	3	9			47	0.6
Cotton grasses			80	1		3	2	43		10	139	0.5
Heather				49		1	13	3			67	0.7
Mineral soil					6			1	2	14	23	0.2
Other bryophytes		1	3	1		39	5	16			65	0.6
Other dwarf shrubs		1	2	7		10	31	9			60	0.5
Other grasses, sedge & rush		2	6	2		7	2	36		2	57	0.6
Rock					2	1			40	1	44	0.9
Sphagnum			11		3	6	1	10	1	56	88	0.6
Total	40	34	104	63	12	70	58	127	43	83	634	
Producer accuracy	1.00	0.88	0.77	0.78	0.50	0.56	0.53	0.28	0.93	0.67		
N (total observations)							634	Overall accuracy			0.64	
X (Sum of all correct)							407					
Y (Sum of total user x sum of total producer)							46776	Kappa			0.59	



Kinder Spectral groupings

Transformed divergence. Few species fell within 500 units of one another on the transformed divergence scale. At the first stage, two groups each of two species were derived. At the second (transformed divergence within 750 units), three additional groups were derived, and one existing class expanded. At the third (transformed divergence within 1400 units), most species were members of groups, and earlier groups had been merged (Table 6:4).

Ungrouped species/classes at this stage were: Bare peat, *Chamaenerion angustifolium*, Feather moss, *Juncus squarrosus*, *Polytrichum* spp., Rock, *Salix* spp., *Sphagnum capillifolium* and *S. tenellum*. Further grouping beyond this stage was not productive because some species' range of similarity spanned almost the entire range of plants. For example, *Eriophorum angustifolium* was found to be within 1800 TD units of 16 other species.

Table 6:4 Groups derived from each stage of Transformed Divergence clustering

Group	Species
Stage 1	
1	<i>Eriophorum angustifolium</i> , <i>Juncus effusus</i>
2	<i>Sphagnum fimbriatum</i> , <i>S. papillosum</i>
Stage 2	
1	<i>Betula</i> spp., <i>Deschampsia flexuosa</i>
2	<i>Calluna vulgaris</i> , <i>Erica tetralix</i>
3	<i>Eriophorum angustifolium</i> , <i>Juncus effusus</i>
4	<i>Eriophorum vaginatum</i> , <i>Nardus stricta</i>
5	<i>Sphagnum fallax</i> , <i>S. fimbriatum</i> , <i>S. palustre</i> , <i>S. papillosum</i>
Stage 3	
1	<i>Betula</i> spp., <i>D. flexuosa</i> , <i>E. angustifolium</i> , <i>E. vaginatum</i> , <i>Juncus effusus</i> , <i>Nardus stricta</i>
2	<i>Calluna</i> dead, Cushion moss
3	<i>Calluna vulgaris</i> , <i>Empetrum nigrum</i> , <i>Erica tetralix</i>
4	Mineral soil, <i>Sphagnum denticulatum</i>
5	<i>Pinus</i> spp., <i>Vaccinium myrtillus</i>
6	<i>Sphagnum cuspidatum</i> , <i>S. fallax</i> , <i>S. fimbriatum</i> , <i>S. palustre</i> , <i>S. papillosum</i> , <i>S. subnitens</i>
<i>Note: species not listed for each stage did not group and remained discrete</i>	



Spectral space. At the first stage, four groups were identified by merging species within 0.1 standard deviation. A visual representation of the distribution of species in two of the four dimensions of spectral space available is shown in Figure 6:1.

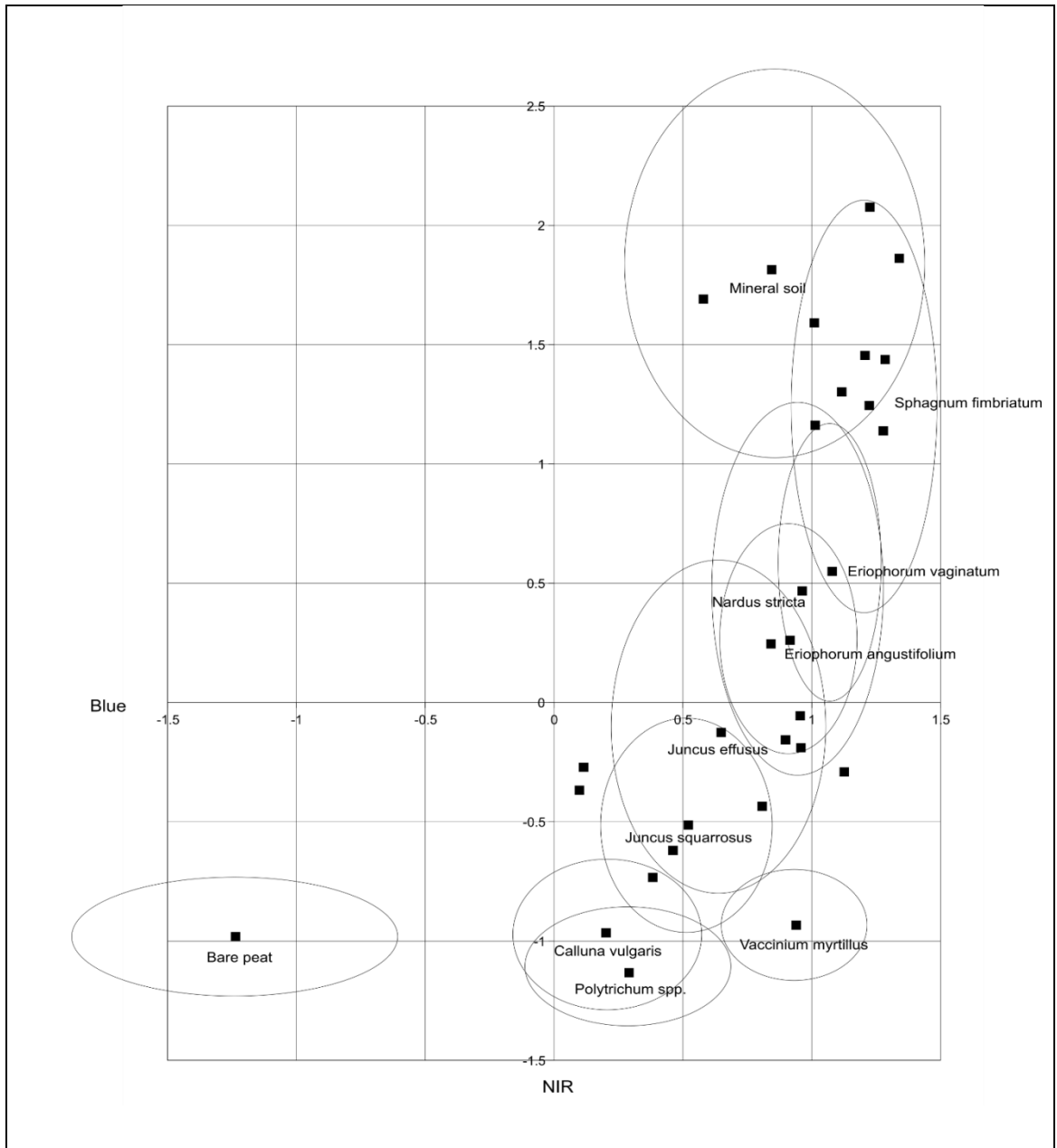


Figure 6:1. Example of species/classes in distribution in spectral space at Kinder.

Eleven key species are highlighted. Ellipses represent a radius of one standard deviation around the 2-d centroid in NIR/blue bands.



At the second stage, initial *Sphagnum* groups were merged, and further groups added. Considering species pairs where separation was below 0.4 standard deviations, almost all species were included in groups. At this stage only Bare peat and *Vaccinium myrtillus* remained as single species classes (Table 6:6; c.f. Figure 6:1).

Table 6:6 Groups derived from each stage of Spectral Space clustering

Group	Species
Stage 1	
1	<i>Betula</i> spp., <i>Deschampsia flexuosa</i>
2	<i>Eriophorum angustifolium</i> , Feather moss, <i>Nardus stricta</i>
3	<i>Sphagnum capillifolium</i> , <i>S. fallax</i> , <i>S. fimbriatum</i> , <i>S. subnitens</i>
4	<i>Sphagnum palustre</i> , <i>S. papillosum</i> , <i>S. tenellum</i>
Stage 2	
1	<i>Betula</i> spp., <i>Chamaenerion angustifolium</i> , <i>Deschampsia flexuosa</i>
2	<i>Calluna</i> dead, Cushion moss
3	<i>Calluna vulgaris</i> , <i>Polytrichum</i> spp.
4	<i>Empetrum nigrum</i> , <i>Erica tetralix</i>
5	<i>Eriophorum angustifolium</i> , <i>E. vaginatum</i> , Feather moss, <i>Nardus stricta</i>
6	Mineral soil, Rock
7	<i>S. capillifolium</i> , <i>S. fallax</i> , <i>S. fimbriatum</i> , <i>S. palustre</i> , <i>S. papillosum</i> , <i>S. subnitens</i> , <i>S. tenellum</i>
8	<i>Sphagnum cuspidatum</i> , <i>S. denticulatum</i>
Stage 3	
1	<i>Betula</i> spp., <i>Calluna</i> dead, <i>Chamaenerion angustifolium</i> , Cushion moss, <i>D. flexuosa</i> , <i>Juncus effusus</i> , <i>Juncus squarrosus</i> , <i>Pinus</i> spp., <i>Salix</i> spp.
2	<i>Calluna vulgaris</i> , <i>Polytrichum</i> spp.
3	<i>Empetrum nigrum</i> , <i>Erica tetralix</i>
4	<i>Eriophorum angustifolium</i> , <i>E. vaginatum</i> , Feather moss, <i>Nardus stricta</i>
5	Mineral soil, Rock, <i>Sphagnum capillifolium</i> , <i>S. cuspidatum</i> , <i>S. denticulatum</i> , <i>S. fallax</i> , <i>S. fimbriatum</i> , <i>S. palustre</i> , <i>S. papillosum</i> , <i>S. subnitens</i> , <i>S. tenellum</i>
Note: species not listed for each stage did not group and remained discrete	

ISODATA. The association of species with ISODATA classes ($n=20$) generally shows little grouping, with a large proportion of species being represented across more than half of the classes. Only a limited number of species/classes represent distinct ISODATA classes, the most notable of these being bare peat and many of the *Sphagnum* present (Table 6:7).



Table 6:7 Proportional species make up of artificial classes derived from Unsupervised Classification clustering

ISO class	1	2	3	4	5	6	7	8	9	10	11	12	13	14	15	16	17	18	19	20
Species																				
Bare peat	0.59	0.05	0.26																	
<i>Betula</i> spp.					0.03	0.06			0.07				0.10		0.07					
<i>Calluna</i> dead		0.03	0.21			0.04	0.19	0.12			0.28									
<i>Calluna vulgaris</i>	0.20	0.37	0.09	0.09	0.10	0.06	0.06							0.08						
<i>Chamaenerion angustifolium</i>				0.06					0.17	0.14			0.14						0.03	
Cushion moss			0.06				0.11	0.06			0.10									
<i>Deschampsia flexuosa</i>		0.03		0.09	0.08	0.04				0.14		0.05	0.10		0.21	0.10	0.08	0.04	0.03	0.01
<i>Empetrum nigrum</i>	0.03	0.12	0.15	0.10	0.19	0.24	0.17	0.08	0.07			0.09								
<i>Erica tetralix</i>		0.03			0.07	0.08														
<i>Eriophorum angustifolium</i>			0.02					0.25			0.21	0.07		0.28		0.38	0.14	0.28	0.13	0.01
<i>Eriophorum vaginatum</i>							0.04			0.14	0.05	0.18	0.07		0.10	0.20	0.21	0.26	0.23	0.06
Feather moss			0.02									0.07					0.05	0.03	0.02	0.01
<i>Juncus effusus</i>		0.04	0.07		0.06	0.14	0.26	0.22		0.07	0.15	0.23			0.10	0.08	0.06	0.08	0.09	0.03
<i>Juncus squarrosus</i>		0.02	0.02	0.03	0.05	0.08	0.07	0.12		0.07		0.09								
Mineral soil																			0.03	0.09
<i>Nardus stricta</i>			0.02		0.02	0.06				0.07		0.07		0.12	0.10	0.04	0.08	0.05	0.09	0.03
<i>Pinus</i> spp.	0.04	0.04	0.02	0.09	0.02	0.08	0.04		0.17	0.14			0.38		0.10	0.04	0.17	0.04		
<i>Polytrichum</i> spp.	0.11	0.25	0.02	0.11	0.25	0.06														
Rock														0.28				0.05	0.14	0.29
<i>Salix</i> spp.										0.07		0.05			0.10	0.06				
<i>Sphagnum capillifolium</i>																				0.03
<i>Sphagnum cuspidatum</i>																				0.05
<i>Sphagnum denticulatum</i>																				0.06
<i>Sphagnum fallax</i>													0.10					0.03	0.13	0.09
<i>Sphagnum fimbriatum</i>																	0.08		0.02	0.05
<i>Sphagnum palustre</i>																	0.03	0.04	0.02	0.05
<i>Sphagnum papillosum</i>																	0.03	0.03		0.05
<i>Sphagnum subnitens</i>																			0.03	0.02
<i>Sphagnum tenellum</i>																				0.04
<i>Vaccinium myrtillus</i>		0.03		0.41	0.08				0.50											

Given the generally wide distribution of most species to ISODATA classes it is perhaps unsurprising that only three groups could be derived using this approach (Table 6:8) and that these are comprised of those few that cluster to a restricted numbers of classes.

Table 6:8 Groups derived from unsupervised classification clustering

Group	Species
1	Bare peat, <i>Calluna</i> dead
2	<i>Calluna vulgaris</i> , <i>Empetrum nigrum</i> , <i>Erica tetralix</i>
3	<i>Sphagnum capillifolium</i> , <i>S. cuspidatum</i> , <i>S. denticulatum</i> , <i>S. fimbriatum</i> , <i>S. palustre</i> , <i>S. papillosum</i> , <i>S. subnitens</i> , <i>S. tenellum</i>

Note: species not listed did not group and remained discrete

The *Sphagnum* group included all *Sphagnum* spp. present except *S. fallax*.

Comparative classification accuracy. Despite an intuitive expectation that taxonomic aggregation would perform less well than those based on spectral characteristics, the MFFP-defined groups produced the best results of the approaches tested. Note though that spectral clustering algorithms incorporated additional species not represented in the MFFP-defined groups (like *Pinus* sp.). That is because the only criterion for inclusion in the algorithms was that the number of samples available was at least 10. Such species are silently misclassified in the MFFP groupings, so the comparison is not strictly direct (c.f. Section 1.3). Spectral grouping stage 3 was the most successful of the ‘natural’ grouping methods, in fact producing a marginally higher average accuracy than MFFP Group 2, albeit with only 7 classes compared to 10. A summary of the classification accuracies achieved for each method are shown below (Table 6:9). Individual error matrices for all development stages are shown in Annex C.

Table 6:9 Accuracy of different clustering methods: Kinder

Grouping method	Class <i>n</i>	Accuracy
None (species)	30	0.46
MFFP group class 1	6	0.75
MFFP group class 2	10	0.64
Transformed divergence stage 2	23	0.51
Transformed divergence stage 3	15	0.54
ISODATA groups + ungrouped species	18	0.58
Spectral position stage 1	22	0.50
Spectral position stage 2	13	0.56
Spectral position stage 3	7	0.65



6.2 Species grouping classification across all sites

6.2.1 Method

Given the results arising in 6.1, together with the direct utility of MFFP's groups making them the 'preferred option', it was decided to progress by using these across all the study sites. For easy reference and comparison the results from Kinder are repeated here.

Species aggregations using MFFP-defined classes. Sample sizes for each group/site combination are shown in Table 6:10. These were randomly assigned into training and validation groups in a 50:50 ratio. *Molinia caerulea* (purple moor grass) was excluded from Birchinlee and Penguins in the second MFFP class grouping as the number of samples was <10 (3 and 6 respectively).

Training data for image classification were extracted for each site using 20 cm circular pixel sampling. Supervised maximum likelihood classification was then performed using imagery covering each site independently.

Table 6:10 Classes and sample size used for MFFP groups

	Birchinlee	Derwent	Kinder	Moss	Penguins
Group 1					
Bare peat	93	105	80	62	109
Bryophytes	197	287	306	175	199
Dwarf shrubs	360	194	309	279	261
Ferns	126	61			
Grass, sedge & rush	453	337	463	587	475
Mineral soil	21	38	24	18	74
Rock *		54	86	31	55
Total	1250	1076	1268	1152	1173
Group 2					
Bare peat	93	105	80	62	109
Bilberry	113	48	68	77	89
Cotton grasses	221	219	209	246	261
Ferns	126	61			
Heather	173	125	125	150	118
Mineral soil	21	38	24	18	74
Other bryophytes	27	66	141	151	75
Other dwarf shrubs	74	21	116	52	54
Other grass, sedge & rush	229	118	254	230	208
Purple moor grass				31	
Rock *		54	86	111	55
<i>Sphagnum</i>	170	221	165	24	124
Total	1247	1076	1268	1152	1167
* Samples of flagstone at Penguins are labelled as rock.					



6.2.2 Results

MFFP Group 1. Group 1, the smaller of two MFFP groups, defines just 7 classes and classification using this typology across all sites produced consistently higher overall accuracies than Phase 3 using species. Error matrices for site each are shown in Figures 6:11a to f. with mapped outputs for each site (as 1 km² tiles) in Figures 6:13a to j.

Table 6:11a. Error matrices for MFFP class group 1
Birchinlee

	Bare peat	Bryophytes	Dwarf shrubs	Ferns	Grass, sedge & rush	Mineral soil	Total	User accuracy
Bare peat	45				1	3	49	0.92
Bryophytes		65	1		20		86	0.76
Dwarf shrubs		11	155	3	17		186	0.83
Ferns		8	3	49	30		90	0.54
Grass, sedge & rush		13	22	10	158		203	0.78
Mineral soil	1	1		1		8	11	0.73
Total	46	98	181	63	226	11	625	
Producer accuracy	0.98	0.66	0.86	0.78	0.70	0.73		
N (total observations)						625	Overall accuracy 0.77	
X (Sum of all correct)						480		
Y (Sum of total user x sum of total producer)						96017	Kappa 0.69	





Table 6:11b. Error matrices for MFFP class group 1

Derwent

	Bare peat	Bryophytes	Dwarf shrubs	Ferns	Grass, sedge & rush	Mineral soil	Rock	Total	User accuracy
Bare peat	48	3	1			3		55	0.87
Bryophytes		48		1	26	1	1	77	0.62
Dwarf shrubs		8	83	2	4			97	0.86
Ferns		18	7	21	36			82	0.26
Grass, sedge & rush	3	27	5	6	103			144	0.72
Mineral soil	1	36	1		1	14	5	58	0.24
Rock		3				1	21	25	0.84
Total	52	143	97	30	170	19	27	538	
Producer accuracy	0.92	0.34	0.86	0.70	0.61	0.74	0.78		
N (total observations)						538	Overall accuracy		0.63
X (Sum of all correct)						338	Kappa		0.55
Y (Sum of total user x sum of total producer)						51997			

Table 6:11c. Error matrices for MFFP class group 1

Kinder

	Bare peat	Bryophytes	Dwarf shrubs	Grass, sedge & rush	Mineral soil	Rock	Total	User accuracy	
Bare peat	40	1	3		1		45	0.89	
Bryophytes		74	8	15	1		98	0.76	
Dwarf shrubs		22	133	33			188	0.71	
Grass, sedge & rush		34	11	177			222	0.80	
Mineral soil		19		5	8	2	34	0.24	
Rock		3		1	2	41	47	0.87	
Total	40	153	155	231	12	43	634		
Producer accuracy	1.00	0.48	0.86	0.77	0.67	0.95			
N (total observations)						634	Overall accuracy		0.75
X (Sum of all correct)						473	Kappa		0.66
Y (Sum of total user x sum of total producer)						99645			



Table 6:11d. Error matrices for MFFP class group 1

Moss

	Bare peat	Bryophytes	Dwarf shrubs	Grass, sedge & rush	Mineral soil	Rock	Total	User accuracy	
Bare peat	28	3	1		2		34	0.82	
Bryophytes	1	57	13	43			114	0.50	
Dwarf shrubs		6	118	13			137	0.86	
Grass, sedge & rush		21	8	235			264	0.89	
Mineral soil	1			1	5	1	8	0.63	
Rock	1			1	2	15	19	0.79	
Total	31	87	140	293	9	16	576		
Producer accuracy	0.90	0.66	0.84	0.80	0.56	0.94			
N (total observations)							576	Overall accuracy	0.80
X (Sum of all correct)							458		
Y (Sum of total user x sum of total producer)							107880	Kappa	0.70

Table 6:11e. Error matrices for MFFP class group 1

Penguins

	Bare peat	Bryophytes	Dwarf shrubs	Flagstone	Grass, sedge & rush	Mineral soil	Total	User accuracy	
Bare peat	50		2		7	2	61	0.82	
Bryophytes	1	52			39	1	93	0.56	
Dwarf shrubs	1	21	112		33		167	0.67	
Flagstone		2		23		15	40	0.58	
Grass, sedge & rush	1	22	15		158	1	197	0.80	
Mineral soil	2	2	1	4	1	18	28	0.64	
Total	55	99	130	27	238	37	586		
Producer accuracy	0.91	0.53	0.86	0.85	0.66	0.49			
N (total observations)							586	Overall accuracy	0.70
X (Sum of all correct)							413		
Y (Sum of total user x sum of total producer)							83274	Kappa	0.61



Table 6:11f. Error matrices for MFFP class group 1

Merged: all sites

	Bare peat	Bryophytes	Dwarf shrubs	Ferns	Grass, sedge & rush	Mineral soil	Rock	Total	User accuracy
Bare peat	211	7	7		8	11		244	0.86
Bryophytes	2	296	22	1	143	3	1	468	0.63
Dwarf shrubs	1	68	601	5	100			775	0.78
Ferns		26	10	70	66			172	0.41
Grass, sedge & rush	4	117	61	16	831	1		1030	0.81
Mineral soil	5	58	2	1	8	53	12	139	0.38
Rock	1	8			2	20	100	131	0.76
Total	224	580	703	93	1158	88	113	2959	
Producer accuracy	0.94	0.51	0.85	0.75	0.72	0.60	0.88		
N (total observations)					2959	Overall accuracy			0.73
X (Sum of all correct)					2162	Kappa			0.65
Y (Sum of total user x sum of total producer)					2106692				

MFFP Group 2. Group 2 defines 12 classes and these produce lower overall accuracies than Group 1 across all sites, although generally still higher than Phase 3 using species. Error matrices for each site, are shown in Figure 6:12a to f.

Table 6:12a. Error matrices for MFFP class group 2

Birchinlee

	Bare peat	Bilberry	Cotton grasses	Ferns	Heather	Mineral soil	Other bryophytes	Other dwarf shrubs	Other grasses, sedge & rush	Sphagnum	Total	User accuracy
Bare peat	45					3			1		49	0.92
Bilberry		37	5	3	2		1	2	6	2	58	0.64
Cotton grasses		2	70	11			1		42	5	131	0.53
Ferns		2	9	44			1		11	6	73	0.60
Heather		2			79			3	3	4	91	0.87
Mineral soil	1			1		8	1				11	0.73
Other bryophytes		6	5		1		7		16	2	37	0.19
Other dwarf shrubs		2	3		5		1	32	9		52	0.62
Other grasses, sedge & rush		5	11	4			1	1	22	2	46	0.48
Sphagnum			7						5	64	76	0.84
Total	46	56	110	63	87	11	13	38	115	85	624	
Producer accuracy	0.98	0.66	0.64	0.70	0.91	0.73	0.54	0.84	0.19	0.75		
N (total observations)					624	Overall accuracy			0.65			
X (Sum of all correct)					408	Kappa			0.61			
Y (Sum of total user x sum of total producer)					46756							



Table 6:12b. Error matrices for MFFP class group 2
Derwent

	Bare peat	Bilberry	Cotton grasses	Ferns	Heather	Mineral soil	Other bryophytes	Other dwarf shrubs	Other grasses, sedge & rush	Rock	Sphagnum	Total	User accuracy
Bare peat	47	1				3	2				1	54	0.87
Bilberry		17	2	5			2		9		1	36	0.47
Cotton grasses	3		71	8			3	2	17		18	122	0.58
Ferns			16	13			2		6		7	44	0.30
Heather				1	59			1	1		1	63	0.94
Mineral soil	1		1		1	14				5	21	43	0.33
Other bryophytes	1	3	2			1	7		1		3	18	0.39
Other dwarf shrubs		1	1		3		4	5	3		1	18	0.28
Other grasses, sedge & rush		2	6				8	2	16		2	36	0.44
Rock						1				21	1	23	0.91
Sphagnum			11	3			5		7	1	54	81	0.67
Total	52	24	110	30	63	19	33	10	60	27	110	538	
Producer accuracy	0.90	0.71	0.65	0.43	0.94	0.74	0.21	0.50	0.27	0.78	0.49		
N (total observations)						538	Overall accuracy						0.60
X (Sum of all correct)						324	Kappa						0.55
Y (Sum of total user x sum of total producer)						35663							

Table 6:12c. Error matrices for MFFP class group 2
Kinder

	Bare peat	Bilberry	Cotton grasses	Heather	Mineral soil	Other bryophytes	Other dwarf shrubs	Other grasses, sedge & rush	Rock	Sphagnum	Total	User accuracy	
Bare peat	40			1	1	1	1				44	0.91	
Bilberry		30	1	2		2	3	9			47	0.64	
Cotton grasses			80	1		3	2	43		10	139	0.58	
Heather			1	49		1	13	3			67	0.73	
Mineral soil					6			1	2	14	23	0.26	
Other bryophytes		1	3	1		39	5	16			65	0.60	
Other dwarf shrubs		1	2	7		10	31	9			60	0.52	
Other grasses, sedge & rush		2	6	2		7	2	36		2	57	0.63	
Rock					2	1			40	1	44	0.91	
Sphagnum			11		3	6	1	10	1	56	88	0.64	
Total	40	34	104	63	12	70	58	127	43	83	634		
Producer accuracy	1.00	0.88	0.77	0.78	0.50	0.56	0.53	0.28	0.93	0.67			
N (total observations)						634	Overall accuracy						0.64
X (Sum of all correct)						407	Kappa						0.59
Y (Sum of total user x sum of total producer)						46776							



Table 6:12d. Error matrices for MFFP class group 2
Moss

	Bare peat	Bilberry	Cotton grasses	Heather	Mineral soil	Other bryophytes	Other dwarf shrubs	Other grasses, sedge & rush	Purple moor grass	Rock	Sphagnum	Total	User accuracy
Bare peat	28				2	3	1					34	0.82
Bilberry		37		3		1						41	0.90
Cotton grasses			58	1		3	1	21	5		1	90	0.64
Heather		2		64		2	3	8	1			80	0.80
Mineral soil	1				5				1	1		8	0.63
Other bryophytes	1		6			40	1	12	1			61	0.66
Other dwarf shrubs			6	7		16	17	19				65	0.26
Other grasses, sedge & rush			12			3	2	20	5		1	43	0.47
Purple moor grass			21			1	1	27	30		3	83	0.36
Rock	1				2					15		18	0.83
Sphagnum			20			6		7	13		7	53	0.13
Total	31	39	123	75	9	75	26	114	56	16	12	576	
Producer accuracy	0.90	0.95	0.47	0.85	0.56	0.53	0.65	0.18	0.54	0.94	0.58		
N (total observations)						576	Overall accuracy		0.55				
X (Sum of all correct)						314	Kappa		0.49				
Y (Sum of total user x sum of total producer)						35898							

Table 6:12e. Error matrices for MFFP class group 2
Penguins

	Bare peat	Bilberry	Cotton grasses	Flagstone	Heather	Mineral soil	Other bryophytes	Other dwarf shrubs	Other grasses, sedge & rush	Sphagnum	Total	User accuracy
Bare peat	50					2		1	3		56	0.89
Bilberry	1	29	3		2		4	2	12	5	58	0.50
Cotton grasses		1	68			1	2	2	22	4	100	0.68
Flagstone				23		15				2	40	0.58
Heather		3	1		51		5	5	6	1	72	0.71
Mineral soil	2		1	4	1	18				2	28	0.64
Other bryophytes	1					1	5		4		11	0.45
Other dwarf shrubs		10	18		5		5	16	21	3	78	0.21
Other grasses, sedge & rush			13				8	1	24	3	49	0.49
Sphagnum	1	1	27				8		12	42	91	0.46
Total	55	44	131	27	59	37	37	27	104	62	583	
Producer accuracy	0.91	0.66	0.52	0.85	0.86	0.49	0.14	0.59	0.23	0.68		
N (total observations)						583	Overall accuracy		0.56			
X (Sum of all correct)						326	Kappa		0.50			
Y (Sum of total user x sum of total producer)						38347						

Table 6:12f. Error matrices for MFFP class group 2
Merged: all sites

	Bare peat	Bilberry	Cotton grasses	Ferns	Heather	Mineral soil	Other bryophytes	Other dwarf shrubs	Other grasses, sedge & rush	Purple moor grass	Rock	Sphagnum	Total	User accuracy
Bare peat	210	1			1	11	6	3	4			1	237	0.89
Bilberry	1	150	11	8	9		10	7	36			8	240	0.63
Cotton grasses	3	3	347	19	2	1	12	7	145	5		38	582	0.60
Ferns		2	25	57			3		17			13	117	0.49
Heather		7	2	1	302		8	25	21	1		6	373	0.81
Mineral soil	5		2	1	2	51	1		1	1	12	37	113	0.45
Other bryophytes	3	10	16		2	2	98	6	49	1		5	192	0.51
Other dwarf shrubs		14	30		27		36	101	61			4	273	0.37
Other grasses, sedge & rush		9	48	4	2		27	8	118	5		10	231	0.51
Purple moor grass			21				1	1	27	30		3	83	0.36
Rock	1					20	1				99	4	125	0.79
Sphagnum	1	1	76	3		3	25	1	41	13	2	223	389	0.57
Total	224	197	578	93	347	88	228	159	520	56	113	352	2955	
Producer accuracy	0.94	0.76	0.60	0.61	0.87	0.58	0.43	0.64	0.23	0.54	0.88	0.63		
N (total observations)						2955	Overall accuracy						0.60	
X (Sum of all correct)						1786	Kappa						0.56	
Y (Sum of total user x sum of total producer)						950024								

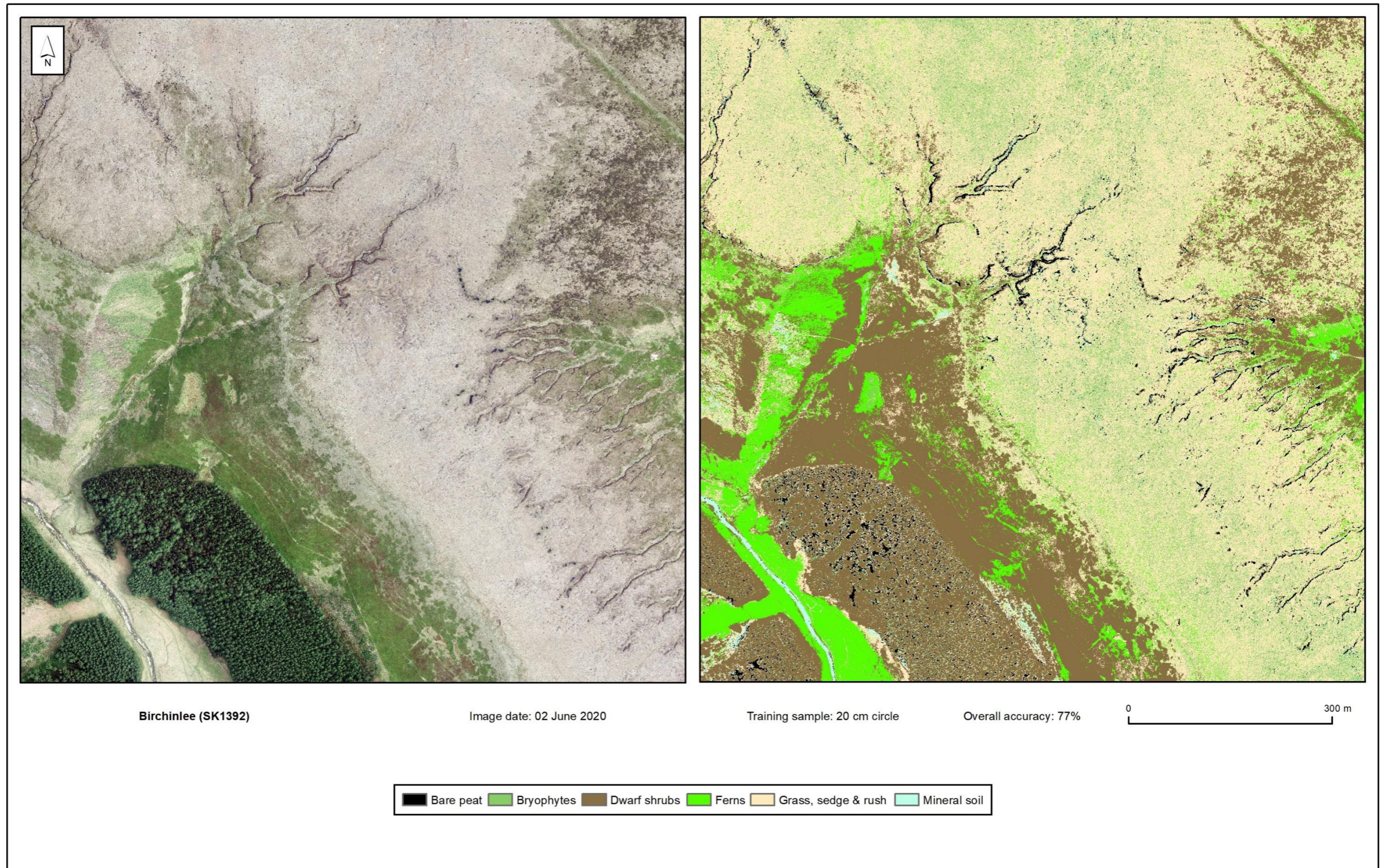


Figure 6:13a. Classified output for Birchinlee (SK1392) – MFFP class group 1.

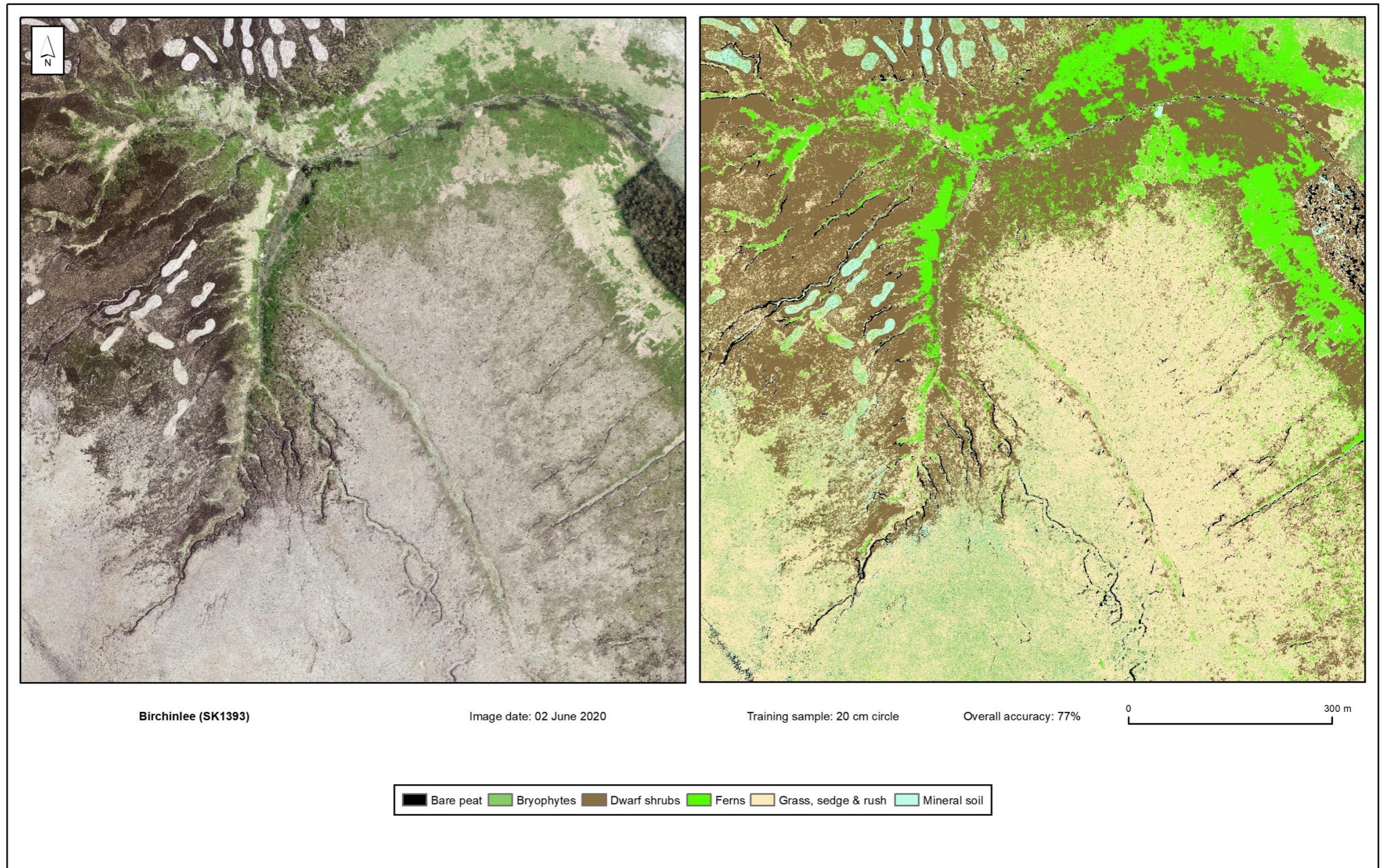


Figure 6:13b. Classified output for Birchinlee (SK1393) – MFFP class group 1.

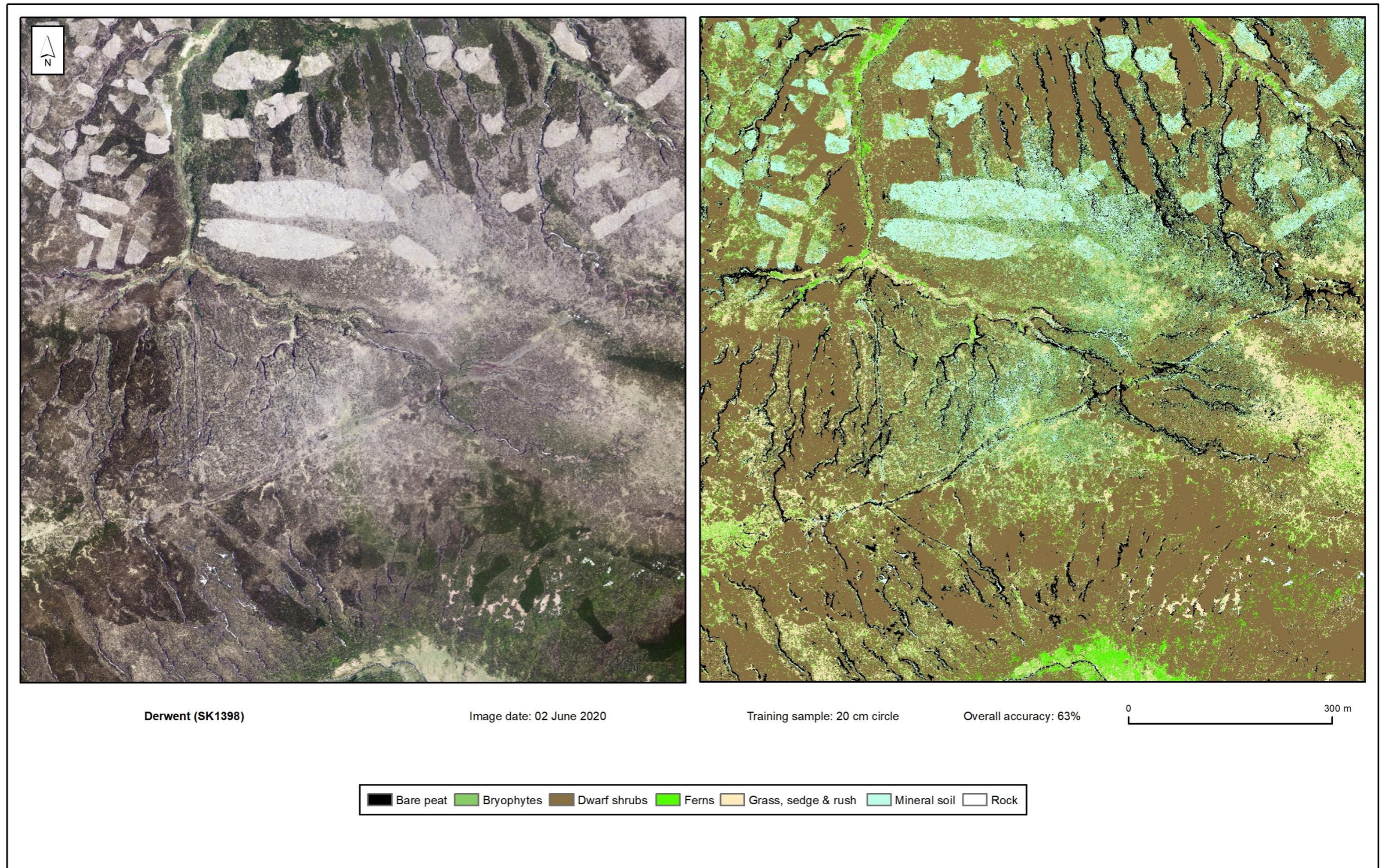


Figure 6:13c Classified output for Derwent (SK1398) – MFFP class group 1.

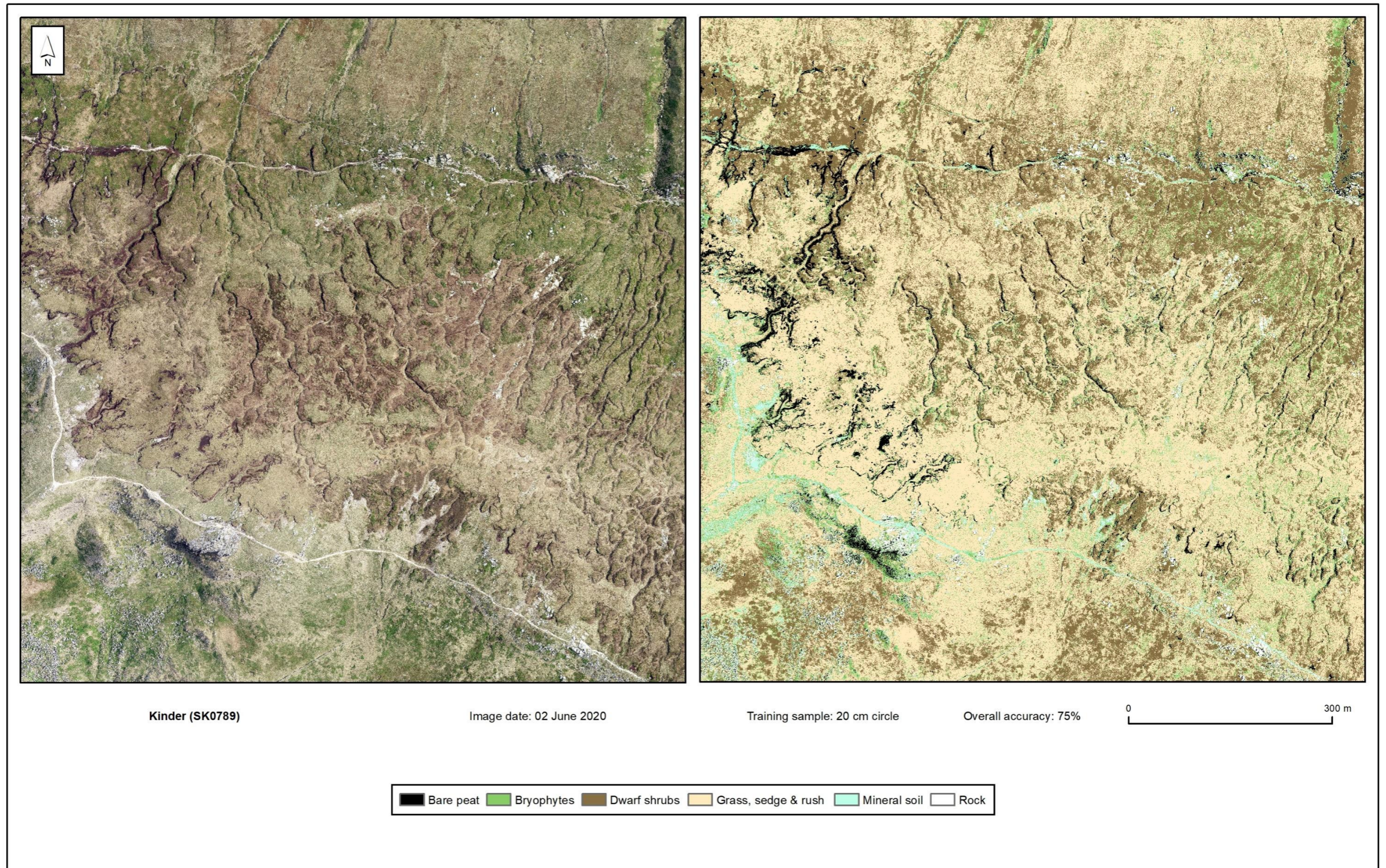


Figure 6:13d. Classified output for Kinder (SK0789) – MFFP class group 1.

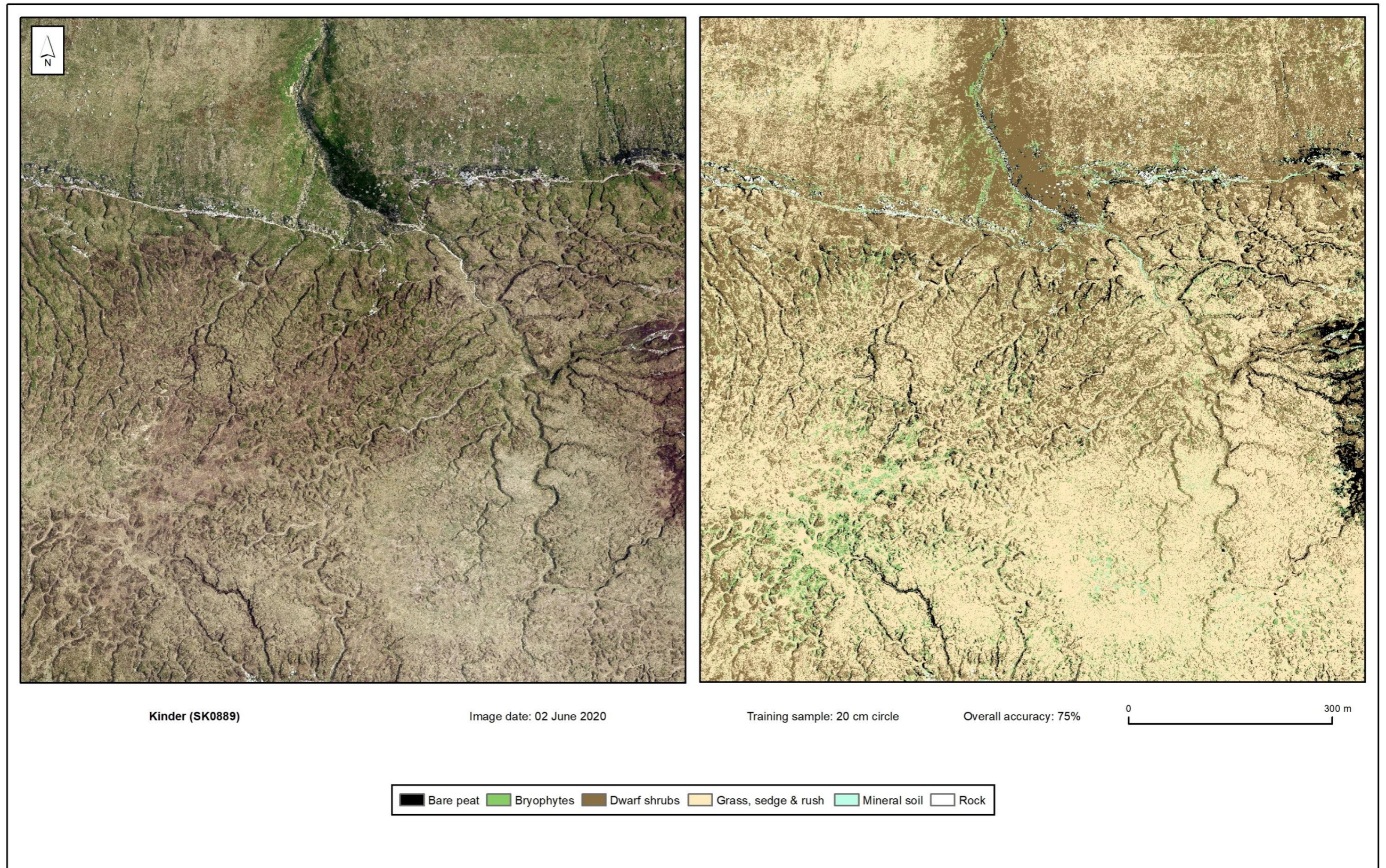


Figure 6:13e. Classified output for Kinder (SK0889) – MFFP class group 1.

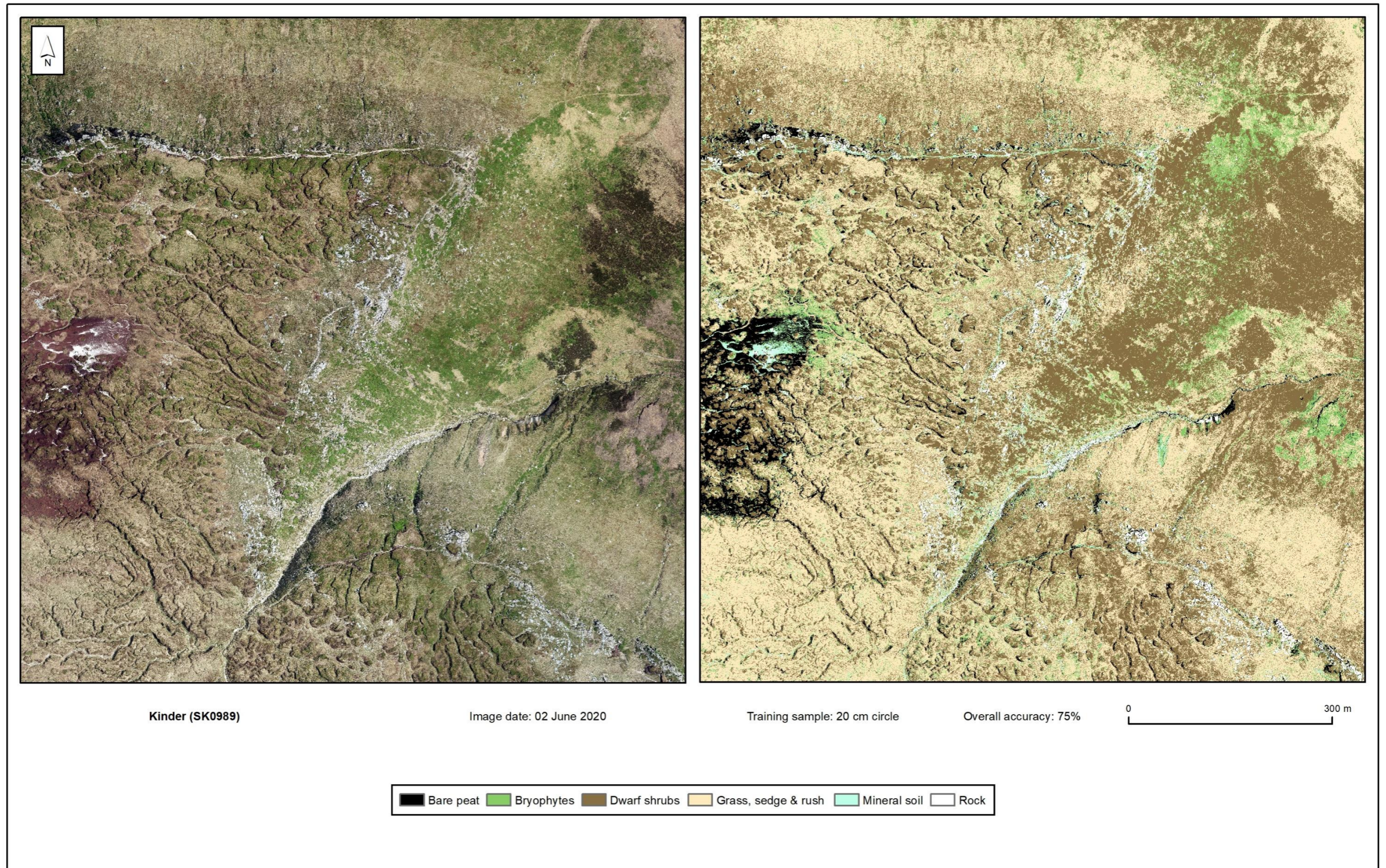


Figure 6:13f. Classified output for Kinder (SK0989) – MFFP class group 1.

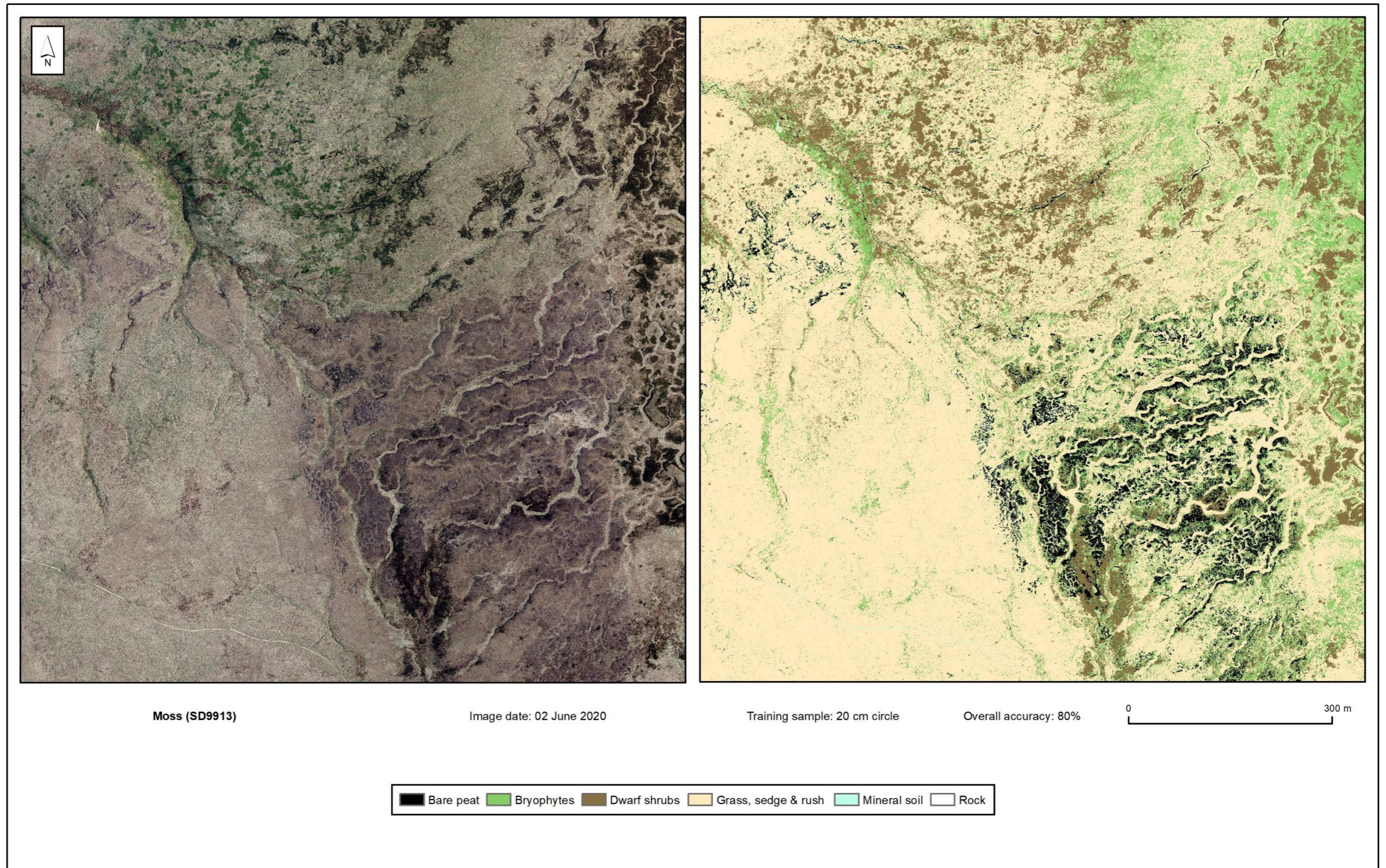


Figure 6:13g. Classified output for Moss (SD9913) – MFFP class group 1.

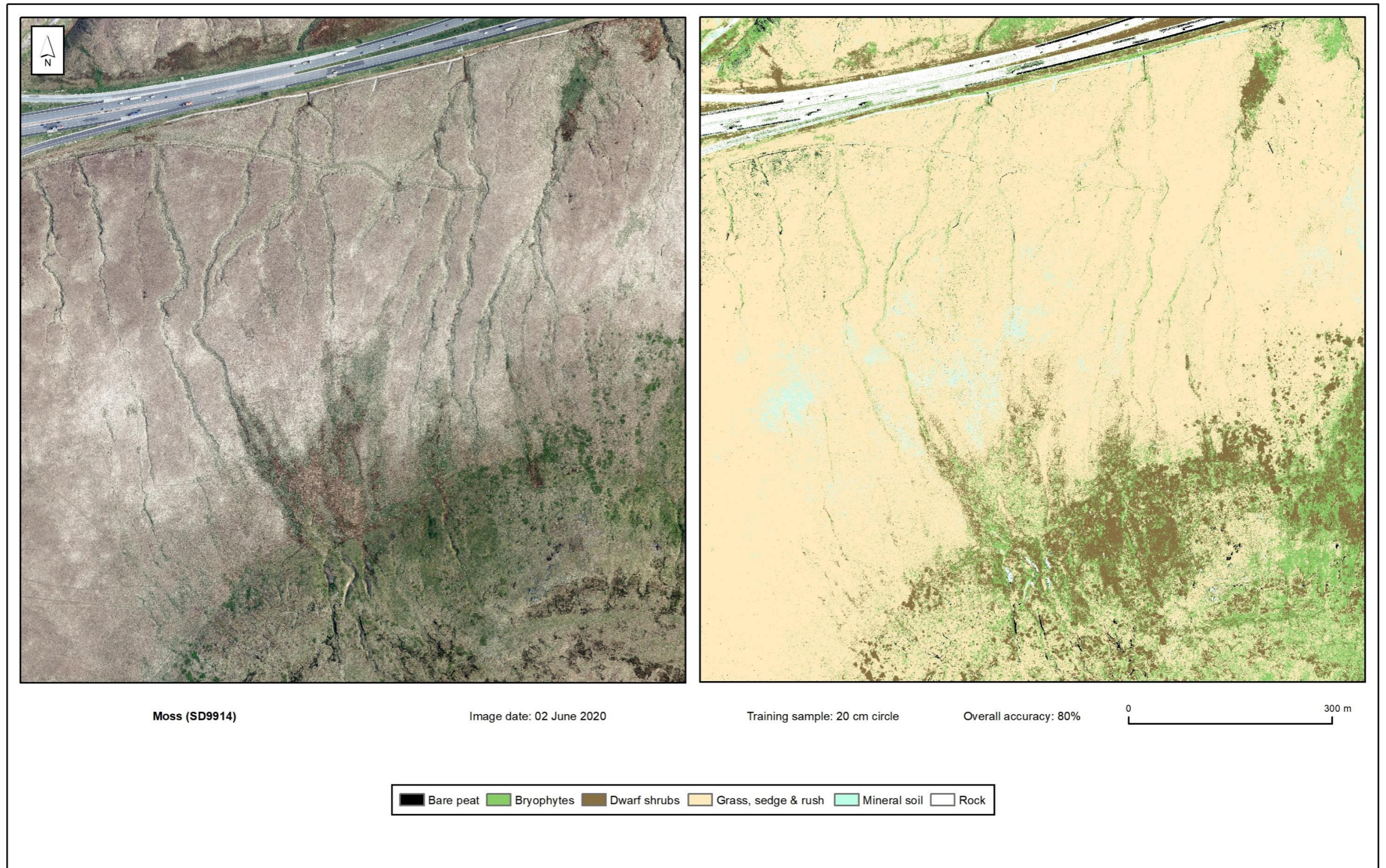


Figure 6:13h. Classified output for Moss (SD9914) – MFFP class group 1.

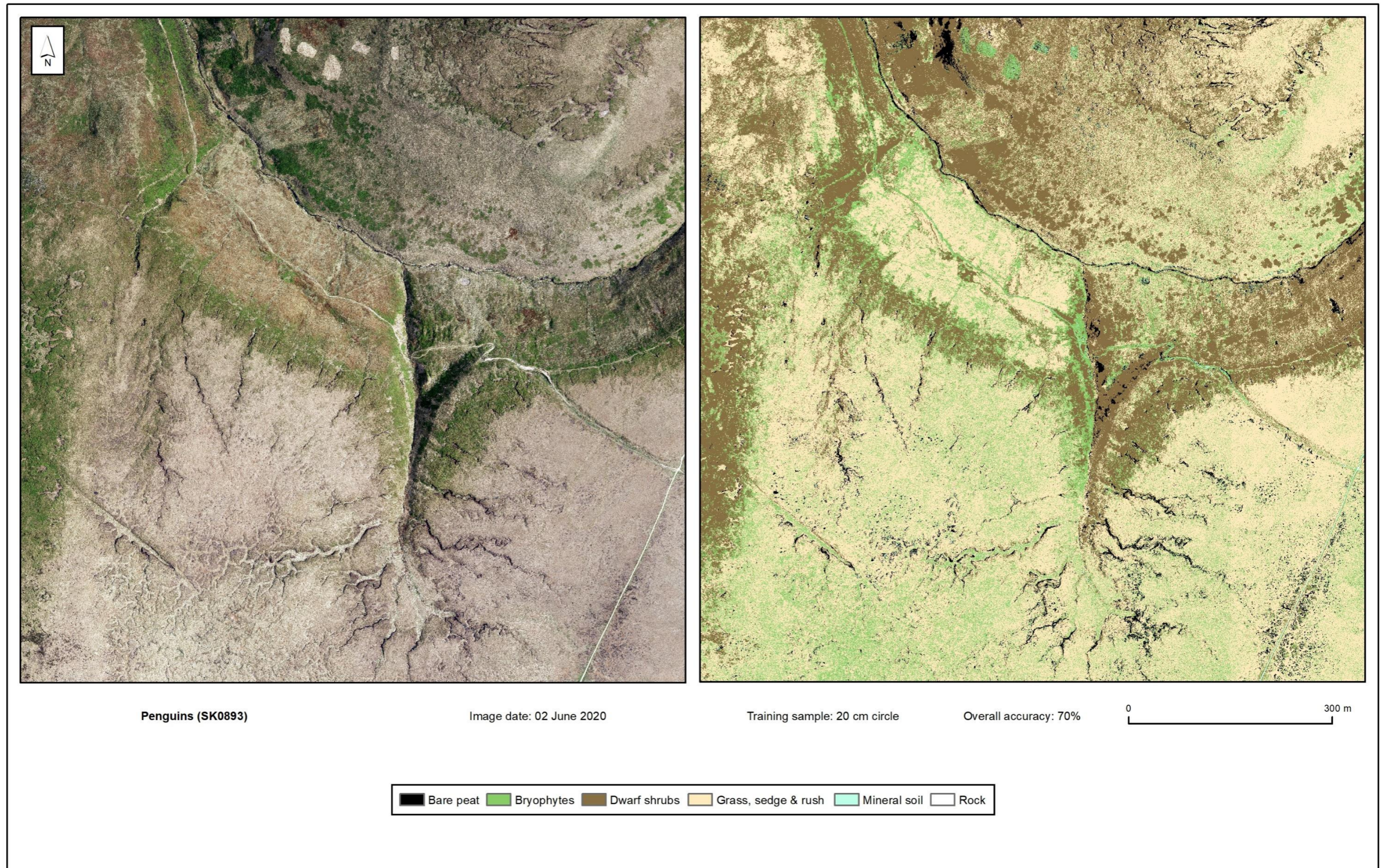


Figure 6:13i. Classified output for Penguins (SK0893) – MFFP class group 1.

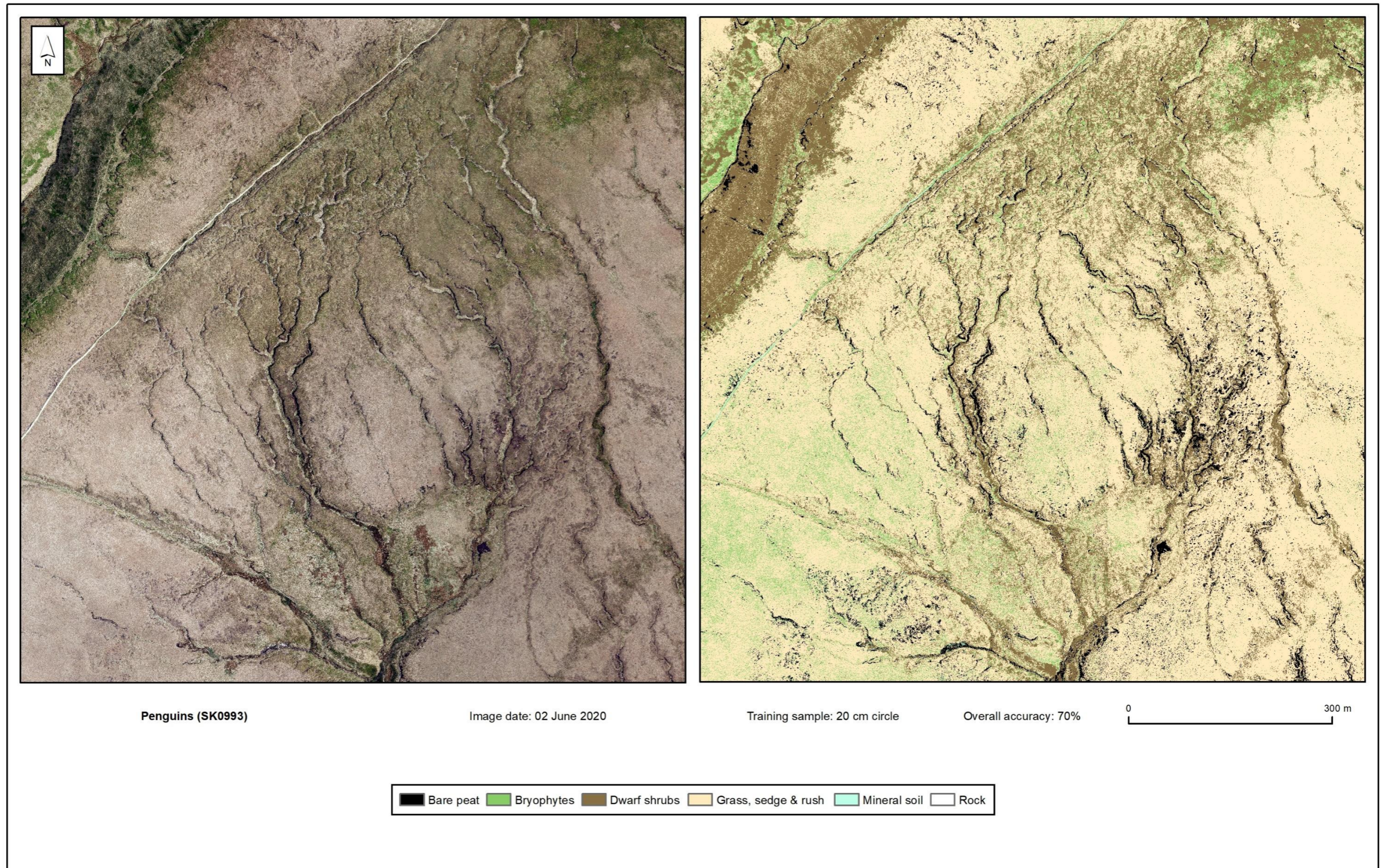


Figure 6:13j. Classified output for Penguins (SK0993) – MFFP class group 1.

6.3 Machine learning– random forest classification

Image classification algorithms such as maximum likelihood combine information from all training samples to produce a single n -dimensional spectral signature for each class. Untrained pixels are subsequently assigned to the class that their spectral signature best fits. Random Forest (RF) classification comprises an ensemble of decision trees, where each ‘tree’ uses a different selection of the training samples to create class signatures. This results in each tree possessing a different set of spectral signatures for all classes. Each tree in the forest assigns a pixel to a class (votes) and untrained pixels are assigned to the class that has the most votes. By using a different selection of training samples in each tree this classification approach might remove the influence of outliers or erroneous training data (such as incorrectly labelled field samples).

The method was developed by Ho (1995) for character recognition and expanded into a range of different applications by Breiman (2001). The technique was soon in use for remote sensing (e.g. Pal, 2005) and has seen some application for mapping peatland vegetation communities (e.g. Beyer et al., 2019). Given that these approaches are sometimes seen to be ‘modern’ compared to more traditional methods used in this project it was decided to briefly assess the results they can achieve.

6.3.1 Method

RF classification was tested on the best performing set of class groups for Kinder as this site has the highest number of field samples. Classification was undertaken using the Spatial Model Editor in ERDAS Imagine with the number of decision trees being unconstrained.

6.3.2 Results

The overall accuracy of 73% (Table 6:14) was marginally lower than results using the supervised classification approached adopted in 6.2 (at 75%) and elsewhere in this project.



Table 6:14. Error matrix for Kinder – RF classification. MFFP class group 1

	Bare peat	Bryophytes	Dwarf shrubs	Grass, sedge & rush	Mineral soil	Rock	Total	User accuracy	
Bare peat	39	2	4		1		46	0.85	
Bryophytes		103	17	35	6	3	164	0.63	
Dwarf shrubs	1	18	113	27			159	0.71	
Grass, sedge & rush		24	21	168		1	214	0.79	
Mineral soil		2		1	2		5	0.40	
Rock		4			3	39	46	0.85	
Total	40	153	155	231	12	43	634		
Producer accuracy	0.98	0.67	0.73	0.73	0.17	0.91			
N (total observations)							634	Overall accuracy	0.73
X (Sum of all correct)							464		
Y (Sum of total user x sum of total producer)							103049	Kappa	0.64

6.4 Discussion

The two MFFP grouping approaches showed the best results here, with both producing higher overall accuracies compared to classification of single species. Group 1 performed significantly better giving on average around a 25% improvement for all sites combined. The higher number of classes in group 2 however only provided for an improvement of around 5% (Table 6:15). It is worth noting that *Sphagnum* spp. were treated as a separate class in these groupings, and at three sites (Birchinlee, Kinder and Penguins) *Sphagnum* achieved producer accuracies (67-75%) at least 10% higher than that achieved for classification of individual species in Phase 3 (13-57%). For Derwent and Moss the producer accuracy of *Sphagnum* ranged from 49-58%.

Table 6:15. Summary classification accuracies of species and MFFP groups by site

	Species		MFFP Group 1		MFFP Group 2	
	n	accuracy	n	accuracy	n	accuracy
Birchinlee	17	0.59	6	0.77	10	0.65
Derwent	17	0.56	7	0.63	11	0.60
Kinder	16	0.61	6	0.75	10	0.64
Moss	15	0.56	6	0.80	11	0.55
Penguins	15	0.51	6	0.70	10	0.56
Combined	19	0.57	7	0.73	12	0.60



6.4.1 MFFP-defined groups

The two groupings of species and classes provided by MFFP were based solely on their monitoring requirements. Given that no spectral information was used to guide definitions it is interesting to note that group 1 performed better than any tested spectral aggregation. In part this highlights the influence of the number of classes, as the iterative reduction of class number in spectral aggregation resulted in higher classification accuracy. However, because no *a priori* conditions were placed on the species entering the spectral clustering algorithm, a larger pool of species was used than for the MFFP-defined groups. The two methods are therefore not directly comparable.

The success or applicability of remote sensing outputs are typically judged by their accuracy. This approach has been adopted in this project to fully test and develop classification performance. However, as noted in Phase 3, some classes of interest map with high accuracy. It may therefore be more useful to estimate the proportional cover of the classes mapped, and classes with high mapping accuracy may provide an indicator of site condition.

Adopting this approach using MFFP group 1 (Table 6:16) indicates that Birchinlee, Kinder, Moss and Penguins are grass, sedge & rush dominated sites (46-67%) and that Derwent is dwarf shrub dominated (51%). These observations do not appear at odds with visual assessment of the aerial photography. Further breakdown using MFFP group 2 might indicate that for Birchinlee and Penguins a large proportion of grass/sedge is cotton grass. For Kinder grass/sedge is divided approximately 50:50 between cotton grass and 'other' grass/sedge, while for Moss it is divided approximately 50:50 between cotton grass and *Molinia caerulea*, and for Derwent a large proportion of dwarf shrub is heather (Table 6:17).

Table 6:16. Proportional vegetation cover for MFFP class group 1

Group	Birchinlee	Derwent	Kinder	Moss	Penguins
Bare peat	0.02	0.07	0.04	0.03	0.03
Bryophytes	0.11	0.17	0.10	0.15	0.14
Dwarf shrubs	0.29	0.51	0.34	0.12	0.24
Ferns	0.10	0.05			
Grass, sedge & rush	0.46	0.12	0.49	0.67	0.59
Mineral soil	0.02	0.06	0.01	0.01	0.00
Rock		0.01	0.02	0.02	0.00



Table 6:17. Proportional vegetation cover for MFFP class group 2

Group	Birchinlee	Derwent	Kinder	Moss	Penguins
Bare peat	0.02	0.06	0.03	0.03	0.02
Bilberry	0.15	0.06	0.13	0.02	0.15
Cotton grasses	0.32	0.07	0.28	0.26	0.41
Ferns	0.08	0.02			
Heather	0.08	0.32	0.07	0.05	0.03
Mineral soil	0.01	0.06	0.01	0.00	0.00
Other bryophytes	0.06	0.05	0.06	0.07	0.03
Other dwarf shrubs	0.08	0.21	0.10	0.08	0.13
Other grass, edge & rush	0.11	0.03	0.22	0.12	0.10
Purple moor grass				0.23	
Rock		0.01	0.02	0.02	0.00
<i>Sphagnum</i>	0.08	0.11	0.08	0.12	0.14

6.4.2 Mapping bare peat

Because bare peat is a key component of condition monitoring and restoration efforts, it is important that mapping bare peat is possible at high accuracy. Bare peat is never grouped by any of the automatic grouping algorithms, and is clearly separate from all other classes spectrally (c.f. Figure 6:1). It is always among the most accurate classes in all the image classifications done in this work. Examples for combined sites are shown in Table 6:18.

Table 6:18. Accuracy of bare peat in a range of classifications

Classification	Accuracy		Principal confusion classes
	Producer	User	
Strim D, all species	0.92	0.93	Dead <i>Calluna</i> , mineral soil
MFFP Groups 1	0.94	0.86	Mineral soil
MFFP Groups 2	0.94	0.89	Mineral soil
Spectral Space	0.94	0.84	Mineral soil, dead <i>Calluna</i>

The slight variation in accuracy is due to the different suite of species/classes in each classification, but it is uniformly high. Other confusion classes of minor importance include cushion moss and dead *Empetrum* (spectral space), bryophytes (MFFP Groups 1 and 2) and very occasionally cotton grasses including *Eriophorum angustifolium*.

Maps of bare peat are likely to be very accurate and therefore highly useful for informing conservation objectives.





Section 7: Comparison of UAV/MAV/EO data

Introduction

MFF 50 2016-17 was originally planned on the utilisation of UAV imagery. Owing to a paucity of field data available during Phase 1 this was never fully explored, and in later phases emphasis shifted to the application of only one source of imagery, that from MAVs.

As such this project can provide little evidence on the suitability of alternate data sources potentially available for conservation monitoring. MFFP therefore, under an extension to the original project specification, requested a direct comparison of the capabilities of three main image sources suitable to their needs, Satellite Earth Observation (EO), UAV and MAV.

Objectives of extension to Phase 4

1: Employ the best performing aggregated classes developed in Phase 4 to classify imagery from satellite, UAV and airborne sources to provide a direct comparison of results.



7.1 Method

7.1.1 Image data

UAV. UAV imagery covering the Kinder experimental sites Firmin and Olaf Nogson were captured on consecutive days in August 2018. Both flights with the multispectral sensor were undertaken around solar noon (Firmin: 11:49-13:00 GMT; Olaf Nogson: 11:18-12:32 GMT) and the extent of ground captured in the surveys overlaps by approximately 5 ha. All MS images were therefore re-processed as one capture using Pix4Dmapper v4.7.5. All ground control points (GCPs; n=52) were marked as control points in each independent multispectral band to derive a model root mean squared error (RMSE) of orthorectification.

The orthomosaics derived for each band were stacked to create a 4-band image (G, R, RE, NIR) covering an area of 153 ha. The image stack was clipped to the extent of the aerial imagery from Phase 3 (captured in 2020) producing a UAV-derived MS image covering an area of 129 ha (Figure 7:1 A). The larger image footprint from the combined flight data enabled a greater number of ground truth observations to be used in classification.

Aerial imagery (MAV). The 4-band aerial imagery from 2020 covering Kinder were clipped to the min/max extent of the UAV imagery (Figure 7:1 B).

Satellite. A WorldView-2 (WV-2) satellite scene captured on 23 July 2019 was obtained from Airbus Defence and Space Intelligence. The footprint of the imagery covers four of the MFFP sites (Birchinlee, Derwent, Kinder and Penguins). The data were provided as a 1.55 m resolution 8-band multispectral stack (coastal, B, G, Y, R, RE, NIR1, NIR2) and a 0.38 m resolution panchromatic band. All data were provided in Ortho Ready Standard format (i.e. no prior image processing had been undertaken).

The WV-2 panchromatic band collects information from the electromagnetic spectrum across wavelengths 450-800 nm (DigitalGlobe, 2009). As this overlaps the bandwidth of six of the multispectral bands (G to NIR1: 450-895 nm), it was decided to pansharpener all eight MS bands to the spatial resolution of the panchromatic band. The modified IHS (intensity, hue, saturation) resolution merge function (Siddiqui, 2003) was undertaken using ERDAS Imagine. The 0.38 m resolution 8-band pansharpened data were then stacked with the native 1.55 m resolution 8-band MS data.

Phase 3 aerial imagery from 2020 and Ordnance Survey Terrain 5 data (5 m resolution digital terrain model (DTM)) were used to identify 15 GCPs across the four MFFP sites. The 16-band image stack was orthorectified in ERDAS Imagine using all GCPs to derive



a model RMSE. The orthorectified pansharpened data were extracted to an 8-band stack at 0.38 m resolution, and the orthorectified MS data were extracted to an 8-band stack resampled to the native 1.55 m. All image resampling was undertaken using the nearest neighbour algorithm.

The orthorectified pansharpened and MS data were then clipped to the min/max extent of the UAV imagery (Figure 7:1 C-D).

7.1.2 Field data

The footprint of the UAV imagery, comprising the smallest area of the data available, was used to select a subset of the field data for Kinder used in Phase 4. As the *Sphagnum* plugs were not present in 2018, these were excluded leaving 827 samples for classification (Table 7:1).

Table 7:1. Classes and sample sizes for classification

Species	n	Group 1	n
<i>Agrostis</i> spp.	1	Bare peat	53
Bare peat	53	Bryophytes	146
<i>Calluna vulgaris</i>	84	Dwarf shrubs	226
Cushion moss	20	Grass, sedge & rush	333
<i>Deschampsia flexuosa</i>	39	Mineral soil	13
<i>Empetrum nigrum</i>	79	Rock	56
<i>Erica tetralix</i>	17		
<i>Eriophorum angustifolium</i>	78		
<i>Eriophorum vaginatum</i>	78	Group 2	
Feather moss	13		
<i>Holcus mollis</i>	6	Bare peat	53
<i>Juncus effusus</i>	78	Bilberry	46
<i>Juncus squarrosus</i>	30	Cotton grasses	156
Mineral soil	13	Heather	84
<i>Nardus stricta</i>	23	Mineral soil	13
<i>Polytrichum</i> spp.	78	Other bryophytes	111
Rock	56	Other dwarf shrubs	96
<i>Sphagnum cuspidatum</i>	1	Other grasses, sedge & rush	177
<i>Sphagnum fallax</i>	25	Rock	56
<i>Sphagnum fimbriatum</i>	3	<i>Sphagnum</i>	35
<i>Sphagnum flexuosum</i>	2		
<i>Sphagnum palustre</i>	3		
<i>Sphagnum subnitens</i>	1		
<i>Vaccinium myrtillus</i>	46		
Total	827		

7.1.3 Image classification

As species classification was not fully tested on UAV imagery in Phase 1, a species level classification was performed for all image types for comparison. For species and each set of groups, samples were randomly separated 50:50 into training and validation samples.



Training data for image classification were extracted for each image type using 20 cm circular pixel averaging areas. Supervised maximum likelihood classification was then performed on each image type. Note that for species classification, classes with only one sample (*Agrostis* spp., *Sphagnum cuspidatum* and *S. subnitens*) were excluded.

7.2 Results

7.2.1 Image orthorectification accuracy

The reported RMSE of orthorectification for the UAV MS data was around one quarter of the pixel size in both x and y (Table 7:2). For both MAV and satellite imagery the reported RMSE was typically equal to or slightly larger than the pixel size. This difference likely arises because a greater number and density of GCPs were used to orthorectify the UAV imagery. Assessment of the MAV imagery in Phase 3 demonstrated that the co-registration between ground sample loci and image pixels was of sufficient precision for reliable image classification (section 5.3.2). Owing to the larger pixel size (0.38 m) it was not possible to undertake a similar assessment of co-registration for the WV-2 imagery.

Table 7:2. Image resolution and orthorectification accuracy

Image source	Ground resolution (m)	Control point RMSE (m)	
		x	y
UAV	0.088	0.023	0.020
MAV	0.05	0.059	0.066
Satellite	1.55 (MS); 0.38 (pan)	0.29	0.43

7.2.2 Image classification

The overall accuracy of species and group classifications achieved for MAV data here are highly comparable to the accuracies achieved with the larger field dataset used in Phases 3 and 4 (Table 7:3). This highlights that the field sample protocol and classification approach is appropriate and provides confidence in the comparative performance of classification presented for each image type.

Classified outputs for all image types tested are shown in Figure 7:2 for MFFP Group 1. All error matrices are presented in Tables 7:4-7:11.



Table 7:3. Classification accuracy of image types

Image source	Classification accuracy		
	Species	MFFP Group 1	MFFP Group 2
MAV – Phase 3 & 4	0.61	0.75	0.64
<i>This phase</i>			
MAV	0.57	0.80	0.65
UAV	0.40	0.63	0.54
Satellite - MS	0.23	0.38	0.25
Satellite - pansharpened	0.24	0.44	0.29

Satellite. From all image types tested, the native resolution MS and pansharpened satellite imagery provided the least accurate classifications. At species level, overall accuracies achieved were <25% (Table 7:3). Bare peat and *Calluna vulgaris*, classes that achieved high accuracies in previous rounds, mapped with between 24-31% accuracy in native resolution MS data and 38-42% accuracy in the pansharpened data (Tables 7:10-7:11). Even when species were grouped, the highest overall accuracy achieved with satellite data was still lower than the overall accuracy of species classification for MAV data in Phase 3 (Table 7:3).

UAV. Despite the increased number of field samples used, the species level classification accuracy achieved for UAV derived MS data here (40%) was slightly lower than that reported in Phase 1 (43%; Table 3:13). Bare peat was the only class that achieved a high producer accuracy (89%; Table 7:8). Grouping species resulted in a clear improvement in overall accuracy, and it is worth noting that bare peat, heather and *Sphagnum* classes all achieved relatively high accuracies (85%, 76% and 71% respectively; Table 7:8).

MAV. Direct comparison of the image types assessed clearly demonstrates that MAV derived MS data provide the best classification performance at all levels examined. Species and group classification performance have already been examined in detail in Phases 3 and 4. However, the results here provide additional valuable insight. The overall classification accuracy of MFFP group 1 classes is 5% higher than that reported in Phase 4 (80% vs 75%). One clear difference in the training and validation data used here is that *Sphagnum* plugs were excluded. The producer accuracy of *Sphagnum* achieved here is 11% higher than in Phase 4 (88% vs 67%; Table 7:9). As this represents the accuracy with which naturally occurring *Sphagnum* can be mapped this is extremely encouraging.



Table 7:4. Error matrix for Kinder. UAV derived MS data - species.

	Bare peat	Calluna vulgaris	Cushion moss	Deschampsia flexuosa	Empetrum nigrum	Erica tetralix	Eriophorum angustifolium	Eriophorum vaginatum	Feather moss	Holcus mollis	Juncus effusus	Juncus squarrosus	Mineral soil	Nardus stricta	Polytrichum spp.	Rock	Sphagnum fallax	Sphagnum fimbriatum	Sphagnum flexuosum	Sphagnum palustre	Vaccinium myrtillus	Total	User accuracy
Bare peat	24		1	1																		26	0.92
Calluna vulgaris		21			2		8	1			3	1			10						2	48	0.44
Cushion moss	1	3	6				1				5	1	1		4							22	0.27
Deschampsia flexuosa				1					1	1	5	2			2							12	0.08
Empetrum nigrum				1	17	4		4													7	33	0.52
Erica tetralix		1			8	4		2				1			1		1				5	23	0.17
Eriophorum angustifolium		4	1		1	17	1	1			1	3			10							38	0.45
Eriophorum vaginatum			1	2	4	1	19	1				2			3		1		1		3	38	0.50
Feather moss	1			3				2						1			1					8	0.25
Holcus mollis			1						1		2											4	0.25
Juncus effusus			1	1			3			1	10			2								18	0.56
Juncus squarrosus		1		1			3	3			5	1		1	2							17	0.06
Mineral soil	1								1		1		3			11						17	0.18
Nardus stricta				6	1		1	1			3			3			1					16	0.19
Polytrichum spp.		8			2		5	3			2	4			6						1	31	0.19
Rock														3	1	18						22	0.82
Sphagnum fallax				1	1				1	1				1			8	2		1		16	0.50
Sphagnum fimbriatum																						0	0.00
Sphagnum flexuosum		2													1						1	4	0.00
Sphagnum palustre				1										2								3	0.00
Vaccinium myrtillus		1		1	4			5			1										4	16	0.25
Total	27	41	11	19	39	9	39	39	6	4	38	15	7	11	39	29	12	2	1	1	23	412	
Producer accuracy	0.89	0.51	0.55	0.05	0.44	0.44	0.44	0.49	0.33	0.25	0.26	0.07	0.43	0.27	0.15	0.62	0.67	0.00	0.00	0.00	0.17		
N (total observations)						412	Overall accuracy					0.40											
X (Sum of all correct)						165	Kappa					0.36											
Y (Sum of total user x sum of total producer)						11310																	

Table 7:5. Error matrix for Kinder. MAV derived MS data - species.

	Bare peat	Calluna vulgaris	Cushion moss	Deschampsia flexuosa	Empetrum nigrum	Erica tetralix	Eriophorum angustifolium	Eriophorum vaginatum	Feather moss	Holcus mollis	Juncus effusus	Juncus squarrosus	Mineral soil	Nardus stricta	Polytrichum spp.	Rock	Sphagnum fallax	Sphagnum fimbriatum	Sphagnum flexuosum	Sphagnum palustre	Vaccinium myrtillus	Total	User accuracy
Bare peat	25	1													1							27	0.93
Calluna vulgaris	2	28		2	4	4						3			1							44	0.64
Cushion moss			8		1		5				6			1								21	0.38
Deschampsia flexuosa		1		2	1			2	1			2		1					1		1	12	0.17
Empetrum nigrum		2			14						1				5							22	0.64
Erica tetralix		8			6	5																19	0.26
Eriophorum angustifolium			2	1			25	1			11	2										42	0.60
Eriophorum vaginatum			1	1			3	21			5			3		1					1	36	0.58
Feather moss					1		2	1	3		2			2		1	1	1				14	0.21
Holcus mollis										2											1	3	0.67
Juncus effusus								1			4											5	0.80
Juncus squarrosus				2	2		2	4			5	5										20	0.25
Mineral soil									1				6			2						9	0.67
Nardus stricta				9				5		1	2	1		3							1	22	0.14
Polytrichum spp.					8						1				31							40	0.78
Rock													1			25						26	0.96
Sphagnum fallax							1	4	1	1	1			1			10	1		1		21	0.48
Sphagnum fimbriatum																						0	0.00
Sphagnum flexuosum																						0	0.00
Sphagnum palustre							1									1						2	0.00
Vaccinium myrtillus		1		2	2							2			1						19	27	0.70
Total	27	41	11	19	39	9	39	39	6	4	38	15	7	11	39	29	12	2	1	1	23	412	
Producer accuracy	0.93	0.68	0.73	0.11	0.36	0.56	0.64	0.54	0.50	0.50	0.11	0.33	0.86	0.27	0.79	0.86	0.83	0.00	0.00	0.00	0.83		
N (total observations)						412	Overall accuracy						0.57										
X (Sum of all correct)						236	Kappa						0.54										
Y (Sum of total user x sum of total producer)						11143																	

Table 7:6. Error matrix for Kinder. Satellite derived MS data - species.

	Bare peat	Calluna vulgaris	Cushion moss	Deschampsia flexuosa	Empetrum nigrum	Erica tetralix	Eriophorum angustifolium	Eriophorum vaginatum	Feather moss	Holcus mollis	Juncus effusus	Juncus squarrosus	Mineral soil	Nardus stricta	Polytrichum spp.	Rock	Sphagnum fallax	Sphagnum fimbriatum	Sphagnum flexuosum	Sphagnum palustre	Vaccinium myrtillus	Total	User accuracy
Bare peat	8	2	2	1	6		2	4	1			1	1		2		2					32	0.25
Calluna vulgaris	2	9		1	6		2	2			3	1		1	2						2	31	0.29
Cushion moss	3	2	3			2	4				2	3			1	2					1	23	0.13
Deschampsia flexuosa	1	1			1					1	1			1	3	3	2				1	15	0.00
Empetrum nigrum		2			2	1		1			1	1			2	1						11	0.18
Erica tetralix		1																				1	0.00
Eriophorum angustifolium	4	1		3	1	1	13	6			2	1		1	3	2	2					40	0.33
Eriophorum vaginatum	3	4	2		2		1	6			6		1		3	2	1					31	0.19
Feather moss																						0	0.00
Holcus mollis																						0	0.00
Juncus effusus		3	1	1			2	4	1	2	9	1		1	6	1		2		1	1	36	0.25
Juncus squarrosus	2	2			1	1	1	1			2	1				1					1	13	0.08
Mineral soil																						0	0.00
Nardus stricta	1	3		1	3	2	1				3			4	6	1						25	0.16
Polytrichum spp.	1	1		6	6		3	4	1		2	1			4		1					30	0.13
Rock	1	1		2	2			1	1			1	4	3		15					1	32	0.47
Sphagnum fallax			2	1	4	2	4	5	1		2	2			3		1				2	29	0.03
Sphagnum fimbriatum																						0	0.00
Sphagnum flexuosum																						0	0.00
Sphagnum palustre																						0	0.00
Vaccinium myrtillus		6		1	4		1	1		1	2	2			4		1				12	35	0.34
Total	26	38	10	17	38	9	34	35	5	4	35	15	6	11	39	28	10	2	0	1	21	384	
Producer accuracy	0.31	0.24	0.30	0.00	0.05	0.00	0.38	0.17	0.00	0.00	0.26	0.07	0.00	0.36	0.10	0.54	0.10	0.00	0.00	0.00	0.57		
N (total observations)						384	Overall accuracy						0.23										
X (Sum of all correct)						87	Kappa						0.17										
Y (Sum of total user x sum of total producer)						10188																	

Table 7:7. Error matrix for Kinder. Satellite derived pansharpened MS data - species.

	Bare peat	Calluna vulgaris	Cushion moss	Deschampsia flexuosa	Empetrum nigrum	Erica tetralix	Eriophorum angustifolium	Eriophorum vaginatum	Feather moss	Holcus mollis	Juncus effusus	Juncus squarrosus	Mineral soil	Nardus stricta	Polytrichum spp.	Rock	Sphagnum fallax	Sphagnum fimbriatum	Sphagnum flexuosum	Sphagnum palustre	Vaccinium myrtillus	Total	User accuracy
Bare peat	10	4	2		6		2	2			2	1	1		2							32	0.31
Calluna vulgaris		16		2	7		1	4			4	1	1		2						3	41	0.39
Cushion moss	2	1	3	1	1	1	1	2			2	1			1						1	17	0.18
Deschampsia flexuosa	1	2	2	2	1		1	4	1	2	2	1	2	1	4	3					2	31	0.06
Empetrum nigrum	2	1			4			1			2	2			1	2						15	0.27
Erica tetralix		1				1					1	1										4	0.25
Eriophorum angustifolium	3	3	2	1	3	3	18	3			4	1		2	3					1	1	48	0.38
Eriophorum vaginatum	2	2			1		6	5		1	3	2			4	4	2	1			3	36	0.14
Feather moss																						0	0.00
Holcus mollis																						0	0.00
Juncus effusus	1	1		3	2		1	3	1	1	5	2			4		2				2	28	0.18
Juncus squarrosus	1	3	1	2	2	3		2	1		4		1		2		1					23	0.00
Mineral soil																1						1	0.00
Nardus stricta	1			1	3			4			1	1		1	3	3	1				1	20	0.05
Polytrichum spp.	1			1	1	1	3	1	1					4	4	1	1					19	0.21
Rock				3							3		1	2		14	2				1	26	0.54
Sphagnum fallax	2				2		1	2			2	1			2		1					13	0.08
Sphagnum fimbriatum																						0	0.00
Sphagnum flexuosum																						0	0.00
Sphagnum palustre																						0	0.00
Vaccinium myrtillus		4		1	5			2	1			1		1	7			1			7	30	0.23
Total	26	38	10	17	38	9	34	35	5	4	35	15	6	11	39	28	10	2	0	1	21	384	
Producer accuracy	0.38	0.42	0.30	0.12	0.11	0.11	0.53	0.14	0.00	0.00	0.14	0.00	0.00	0.09	0.10	0.50	0.10	0.00	0.00	0.00	0.33		
N (total observations)						384	Overall accuracy						0.24										
X (Sum of all correct)						91	Kappa						0.18										
Y (Sum of total user x sum of total producer)						10365																	



Table 7:8. Error matrices for Kinder. UAV derived MS data

MFFP Group 1

	Bare peat	Bryophytes	Dwarf shrubs	Grass, sedge & rush	Mineral soil	Rock	Total	User accuracy	
Bare peat	24	1		1	1		27	0.89	
Bryophytes	3	24	11	26			64	0.38	
Dwarf shrubs		20	87	28			135	0.64	
Grass, sedge & rush		26	14	106			146	0.73	
Mineral soil		2		3	3	11	19	0.16	
Rock				2	3	18	23	0.78	
Total	27	73	112	166	7	29	414		
Producer accuracy	0.89	0.33	0.78	0.64	0.43	0.62			
N (total observations)						414	Overall accuracy		0.63
X (Sum of all correct)						262	Kappa		0.50
Y (Sum of total user x sum of total producer)						45557			

MFFP Group 2

	Bare peat	Bilberry	Cotton grasses	Heather	Mineral soil	Other bryophytes	Other dwarf shrubs	Other grasses, sedge & rush	Rock	Sphagnum	Total	User accuracy
Bare peat	23				1	1		1			26	0.88
Bilberry		8	7	4		2	8	3		1	33	0.24
Cotton grasses	1	2	35	3		10	2	12			65	0.54
Heather		3	11	31		13	2	7			67	0.46
Mineral soil	1				3	1		1	11		17	0.18
Other bryophytes	2	1	12	3		22	2	16		2	60	0.37
Other dwarf shrubs		9	4			1	33	2		1	50	0.66
Other grasses, sedge & rush			7			3		38		1	49	0.78
Rock					3			1	18		22	0.82
Sphagnum			2			3	1	7		12	25	0.48
Total	27	23	78	41	7	56	48	88	29	17	414	414
Producer accuracy	0.85	0.35	0.45	0.76	0.43	0.39	0.69	0.43	0.62	0.71		
N (total observations)						414	Overall accuracy					0.54
X (Sum of all correct)						223	Kappa					0.48
Y (Sum of total user x sum of total producer)						20532						



Table 7:9. Error matrices for Kinder. MAV derived MS data

MFFP Group 1

	Bare peat	Bryophytes	Dwarf shrubs	Grass, sedge & rush	Mineral soil	Rock	Total	User accuracy	
Bare peat	26	1	2				29	0.90	
Bryophytes		44	12	8			64	0.69	
Dwarf shrubs	1	11	94	23			129	0.73	
Grass, sedge & rush		14	4	133		1	152	0.88	
Mineral soil		3		2	6	2	13	0.46	
Rock					1	26	27	0.96	
Total	27	73	112	166	7	29	414		
Producer accuracy	0.96	0.60	0.84	0.80	0.86	0.90			
N (total observations)							414	Overall accuracy	0.79
X (Sum of all correct)							329		
Y (Sum of total user x sum of total producer)							46009	Kappa	0.72

MFFP Group 2

	Bare peat	Bilberry	Cotton grasses	Heather	Mineral soil	Other bryophytes	Other dwarf shrubs	Other grasses, sedge & rush	Rock	Sphagnum	Total	User accuracy
Bare peat	25			1		1					27	0.93
Bilberry		21		1		2	2	6			32	0.66
Cotton grasses			62			4	1	34	1	1	103	0.60
Heather	2			32		1	9	7			51	0.63
Mineral soil					6	2			2		10	0.60
Other bryophytes						30	7	11			48	0.63
Other dwarf shrubs			2	6		10	29	4			51	0.57
Other grasses, sedge & rush		2	6	1		5		21		1	36	0.58
Rock					1				26		27	0.96
Sphagnum			8			1		5		15	29	0.52
Total	27	23	78	41	7	56	48	88	29	17	414	
Producer accuracy	0.93	0.91	0.79	0.78	0.86	0.54	0.60	0.24	0.90	0.88		
N (total observations)						414	Overall accuracy			0.64		
X (Sum of all correct)						267						
Y (Sum of total user x sum of total producer)						21240	Kappa			0.59		



Table 7:10. Error matrices for Kinder. Satellite derived MS data

MFFP Group 1

	Bare peat	Bryophytes	Dwarf shrubs	Grass, sedge & rush	Mineral soil	Rock	Total	User accuracy
Bare peat	12	10	16	19	1	1	59	0.20
Bryophytes	4	19	20	50	1		94	0.20
Dwarf shrubs	3	20	46	25	1	4	99	0.46
Grass, sedge & rush	5	17	19	52		3	96	0.54
Mineral soil	2	2	5	6	3	20	38	0.08
Rock					1	26	27	0.96
Total	26	68	106	152	7	54	413	
Producer accuracy	0.46	0.28	0.43	0.34	0.43	0.48		
N (total observations)						413	Overall accuracy	0.38
X (Sum of all correct)						158		
Y (Sum of total user x sum of total producer)						34736	Kappa	0.22

MFFP Group 2

	Bare peat	Bilberry	Cotton grasses	Heather	Mineral soil	Other bryophytes	Other dwarf shrubs	Other grasses, sedge & rush	Rock	Sphagnum	Total	User accuracy
Bare peat	10	1	9	3	1	8	7	4	1	2	46	0.22
Bilberry		10	6	6		11	5	10	1	2	51	0.20
Cotton grasses	7	1	22	4	1	7	5	13	2	2	64	0.34
Heather	2	3	6	14		6	8	10	1	2	52	0.27
Mineral soil											0	0.00
Other bryophytes	3		11	4	1	4	4	16	1	2	46	0.09
Other dwarf shrubs	1	1	3	4		3	7	3	1		23	0.30
Other grasses, sedge & rush		1	3	1	1	6	2	7	2		23	0.30
Rock	1	1		1	2	1	1	7	18		32	0.56
Sphagnum	2	3	9	1		8	8	13	1	4	49	0.08
Total	26	21	69	38	6	54	47	83	28	14	386	
Producer accuracy	0.38	0.48	0.32	0.37	0.00	0.07	0.15	0.08	0.64	0.29		
N (total observations)						386	Overall accuracy	0.25				
X (Sum of all correct)						96						
Y (Sum of total user x sum of total producer)						15715	Kappa	0.16				



Table 7:11. Error matrices for Kinder. Satellite derived pansharpened MS data

MFFP Group 1

	Bare peat	Bryophytes	Dwarf shrubs	Grass, sedge & rush	Mineral soil	Rock	Total	User accuracy
Bare peat	14	11	17	15	1	1	59	0.24
Bryophytes	3	18	14	29	1	3	68	0.26
Dwarf shrubs	5	11	53	31	1	4	105	0.50
Grass, sedge & rush	4	26	20	65	1	3	119	0.55
Mineral soil					1		1	1.00
Rock		2	2	12	1	17	34	0.50
Total	26	68	106	152	6	28	386	
Producer accuracy	0.54	0.26	0.50	0.43	0.17	0.61		
N (total observations)						386	Overall accuracy	0.44
X (Sum of all correct)						168		
Y (Sum of total user x sum of total producer)						36334	Kappa	0.25

MFFP Group 2

	Bare peat	Bilberry	Cotton grasses	Heather	Mineral soil	Other bryophytes	Other dwarf shrubs	Other grasses, sedge & rush	Rock	Sphagnum	Total	User accuracy
Bare peat	13		5	6	1	7	6	5		1	44	0.30
Bilberry	1	6	6	4		9	7	5		1	39	0.15
Cotton grasses	4	1	31	3		9	5	16	4	4	77	0.40
Heather	1	5	7	17	1	6	9	11		1	58	0.29
Mineral soil											0	0.00
Other bryophytes	3		5		1	9	3	8	2	2	33	0.27
Other dwarf shrubs	1	3	6	4		2	7	6	3		32	0.22
Other grasses, sedge & rush	1	4	4	3	2	8	5	10	2	1	40	0.25
Rock		1			1			9	15	1	27	0.56
Sphagnum	2	1	5	1		4	5	13	2	3	36	0.08
Total	26	21	69	38	6	54	47	83	28	14	386	
Producer accuracy	0.50	0.29	0.45	0.45	0.00	0.17	0.15	0.12	0.54	0.21		
N (total observations)						386	Overall accuracy	0.29				
X (Sum of all correct)						111						
Y (Sum of total user x sum of total producer)						17346	Kappa	0.19				



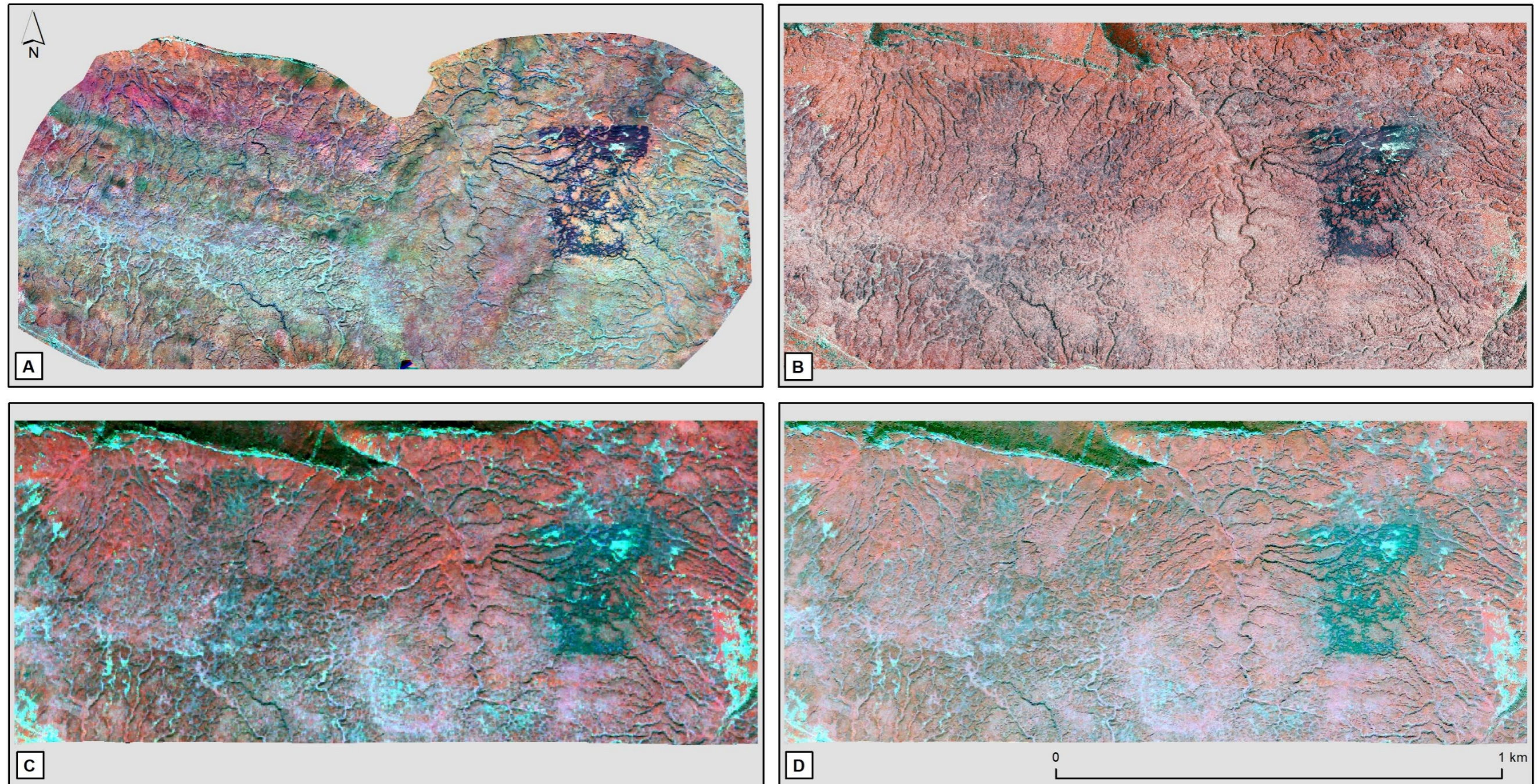


Figure 7:1. Image extents used for classification (NIR G R band composite shown). A: UAV footprint; B: MAV footprint; C: Native resolution MS WV-2 data footprint; D: Pansharpened WV-2 data footprint.

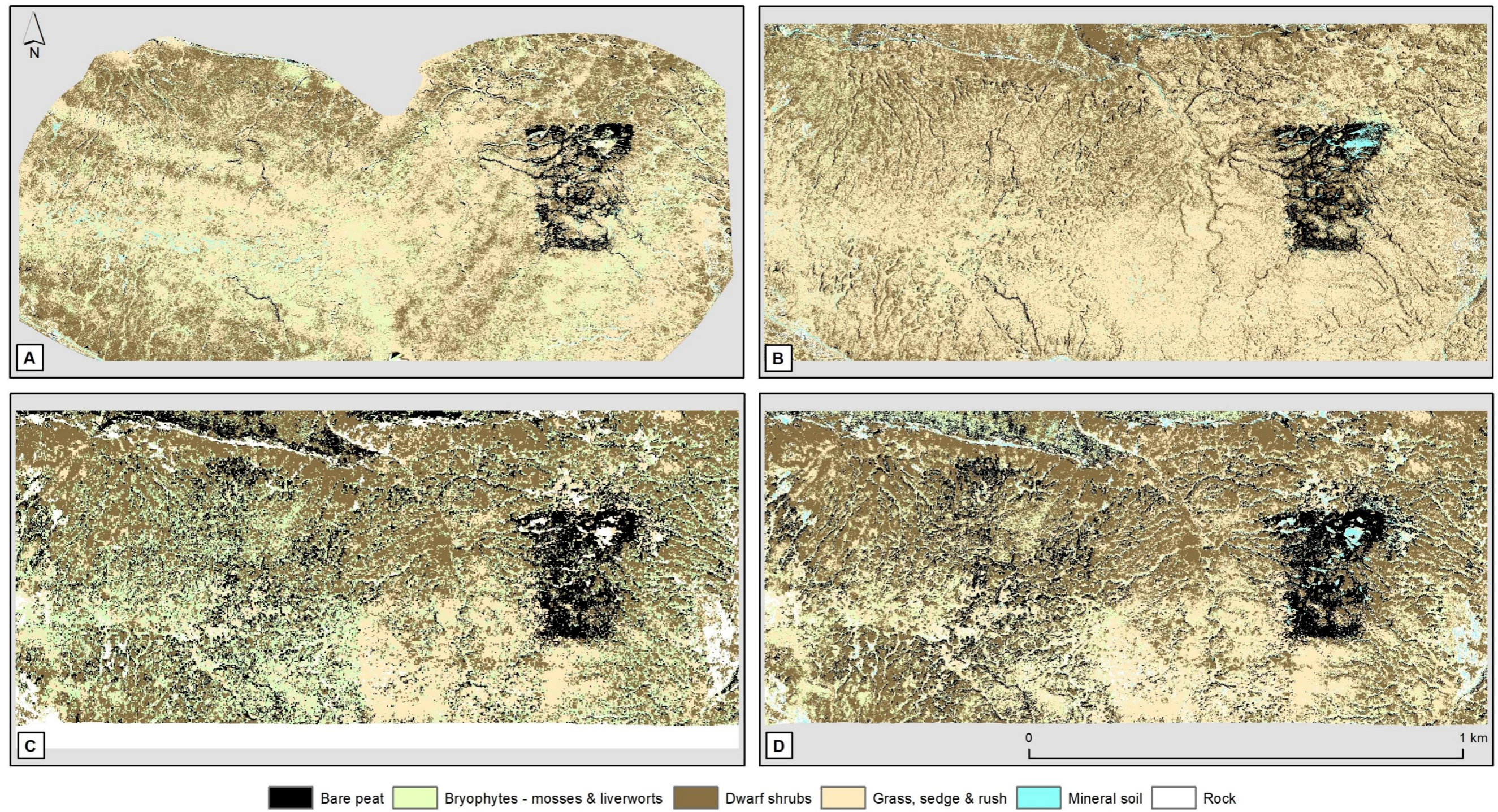


Figure 7.2. Classified outputs for each image type (MFFP Group 1). A: UAV; B: MAV; C: Native resolution MS WV-2 data; D: Pansharpned WV-2 data.



Section 8: WP 5 – Monitoring changes in surface wetness

Introduction

Work Package 5

Work package 5 is an experimental component of the project exploring the potential for thermal imagery captured using a UAV to monitor peat surface wetness. Patterns in thermal infrared imagery collected from MAV and UAV platforms have identified the location of drainage features (Luscombe et al., 2015) and near-surface flow routes (Ikkala et al., 2021). However, no direct translations of thermal measurements into an index of surface wetness have been reported.

This component aims to assess any potential relationships between near surface soil moisture and temperature (thermal emissivity) of bare peat surfaces.

Objectives of WP5

1. Collect thermal imagery at two times of day over one of the MFFP experimental catchments. This approach will enable any potential variation in thermal emission resulting from changes in sun incidence angle to be explored;
2. Collect contemporaneous samples of surface peat from locations on a hydrological gradient within the area of thermal image capture;
3. Assess any potential relationship between soil moisture and temperature recorded.

8.1 Method

8.1.1 Thermal image data

Capture. An area covering the *Sphagnum* experimental field catchment located at Birchinlee (Birchinlee 1) was flown on 08 September 2021 using a fixed-wing UAV (senseFly eBee as employed in Phase 1). The eBee was equipped with a senseFly thermoMAP which comprises a FLIR TAU 2 sensor (0.3 MP) recording longwave infrared (LWIR) wavelengths from 7500 – 13,500 nm (FLIR, 2014). The sensor has a resolution of 0.1°C and calibrates automatically during the flight. Operated in timelapse mode, the thermoMAP sensor records a continual series of images at a rate of 7.5 images per second (senseFly, 2017). As this results in significant forward overlap in imagery, every n^{th} image is typically selected for processing.

Flight parameters were programmed to capture a target area of interest (AOI) covering approximately 7 ha (Figure 8:1) and the eBee was flown at a height of approximately 75-80 m above the ground. Flights were undertaken at 11:30 and 14:45 GMT during which time wind speed ranged between 6-9 ms⁻¹ (Table 8:1). The first flight took 17 minutes, but



the second flight took 12 minutes owing to lower wind speed. At the time the flights were undertaken air temperature was between 22-23 °C.

Pre-processing. Around 2000 images were captured in each flight and every fifth image was selected for processing (Table 8:1). Images from each individual flight were processed separately using Pix4Dmapper v4.7.5. Coordinates for ground control points (GCPs), distributed on a 100 m triangular grid within the AOI (Figure 8:1), were obtained using a Trimble Geo7x DGNSS. Positional data were post-corrected in Trimble Pathfinder Office using RINEX data from the nearest OS Net base station. The mean accuracy of post-processed coordinates was reported to be 0.033 m in xy and 0.040 m in z. GCP coordinates were loaded into Pix4D and all GCPs were marked as control points to derive a model RMSE for image orthorectification.

8.1.2 Surface peat samples

Sample collection. Permission for MFFP to collect 40 peat samples from the site was granted by Natural England. Samples were collected between 13:30-14:00 GMT in four locations on a hydrological gradient following an erosion gully downslope (Figure 8:1). At each location areas of bare peat measuring >50 cm in the smallest dimension were identified and a sample of the top 10 cm of the peat was collected using a 2 cm diameter soil corer. All samples were wrapped in aluminium foil and sealed in a plastic bag for storage prior to analysis. The location of each sample was recorded using a Trimble Geo7x DGNSS and post-processed positional data achieved the accuracy reported above.

Water content. The dimensions of the peat samples were recorded and the wet peat mass measured using a Sartorius CP124S balance to a precision of 1×10^{-4} g. Samples were dried in an oven at 70°C for 48 hours and the mass of peat re-weighed. The drying and weighing process was repeated until the mean sample mass between measurements varied by <0.08%. The water content of each sample was then calculated using the final measured mass of dry peat.

Statistical analysis. Peat sample location data were intersected with both sets of thermal imagery using ArcGIS to assign the temperature value to each sample location. Surface temperature and soil moisture were entered into linear regression for both thermal datasets using SPSS v28.



8.2 Results

8.2.1 Thermal image data

Owing to the flight characteristics of fixed-wing UAVs and the field of view (FOV) of the thermal sensor the actual area of ground covered was approximately 20 ha (see Figure 8:2). The orthorectified thermal images for both flights have a comparable ground (pixel) resolution of 0.166-0.168 m (Table 8:1). The orthorectification process reported an RMSE approximately half the pixel size for both datasets indicating strong spatial alignment between sample location and the imagery.

Table 8:1. Flight details, image resolution and accuracy of orthorectification

Flight start (GMT)	Duration (minutes)	Wind speed (ms ⁻¹)	No. of images processed	Ground resolution (m)	Control point RMSE (m)	
					(x)	(y)
11:30	17	8.0 - 8.6	338	0.166	0.072	0.089
14:45	12	6.5 - 7.5	349	0.168	0.057	0.059

The thermal orthomosaics were clipped to the same extent to allow direct comparison of temperature between flights. The minimum temperature recorded between flights varied by 0.4°C, but maximum temperature increased by almost 3°C over the three-hour period (Figure 8:2). It is notable that in the first flight (11:30 GMT) east-facing slopes are showing higher temperatures across the scene, but in the later flight (14:45 GMT) west-facing slopes, particularly gully sides, show higher temperatures. The gully floors in both flights appear relatively cool indicating that they were at least in partial shade during the survey.

8.2.2 Peat samples

Mean (\pm SD) peat core length collected was 8.6 ± 1.1 cm (Table 8:2) indicating slight compression of some cores during extraction. Soil moisture content typically ranged from 67.6% - 89.6%, although was notably lower in sample 12 (25%). This sample was collected from the top of a gully and was noted in the field as being loose and dry peat.



Table 8:2. Moisture content of peat samples

Sample	Core length (cm)	Mass of wet peat (g)	Mass of dry peat (g)	Mass of water (g)	Moisture content (%)
1	10.0	9.7291	2.1578	7.5713	77.8
2	9.0	9.8013	2.1823	7.6190	77.7
3	9.4	8.6790	1.7583	6.9207	79.7
4	6.8	9.9725	2.1429	7.8296	78.5
5	10.5	8.0653	2.0945	5.9708	74.0
6	9.2	9.4972	2.2375	7.2597	76.4
7	7.2	9.6733	1.8982	7.7751	80.4
8	8.5	11.7030	2.3271	9.3759	80.1
9	6.4	5.7340	1.2886	4.4454	77.5
10	6.0	7.8938	1.6397	6.2541	79.2
11	8.6	11.5422	2.4098	9.1324	79.1
12	10.5	5.2165	3.8834	1.3331	25.6
13	7.4	15.0388	2.6273	12.4115	82.5
14	9.3	9.4441	1.6469	7.7972	82.6
15	7.5	9.9947	2.1013	7.8934	79.0
16	7.7	9.4187	1.9659	7.4528	79.1
17	9.3	12.3057	3.1196	9.1861	74.6
18	7.1	5.9584	1.5054	4.4530	74.7
19	8.3	10.7396	2.3252	8.4144	78.3
20	6.7	7.2875	1.6792	5.6083	77.0
21	10.9	11.4292	2.0385	9.3907	82.2
22	9.7	10.7941	2.0260	8.7681	81.2
23	8.4	12.2772	1.7559	10.5213	85.7
24	8.5	8.6470	2.0239	6.6231	76.6
25	9.4	12.4318	1.7152	10.7166	86.2
26	9.6	9.5781	1.6767	7.9014	82.5
27	9.1	11.3140	1.4791	9.8349	86.9
28	8.5	11.9668	1.3692	10.5976	88.6
29	8.9	13.9108	2.1144	11.7964	84.8
30	9.2	12.5641	1.9180	10.6461	84.7
31	9.7	7.9390	1.4835	6.4555	81.3
32	8.9	11.9915	2.4233	9.5682	79.8
33	8.8	10.7729	2.1514	8.6215	80.0
34	9.2	14.0265	1.4571	12.5694	89.6
35	9.2	8.1164	1.3695	6.7469	83.1
36	8.5	10.0640	1.5981	8.4659	84.1
37	8.7	11.5051	1.5494	9.9557	86.5
38	9.3	12.0515	1.6212	10.4303	86.5
39	7.9	8.0220	1.4904	6.5316	81.4
40	7.6	5.3812	1.7438	3.6374	67.6



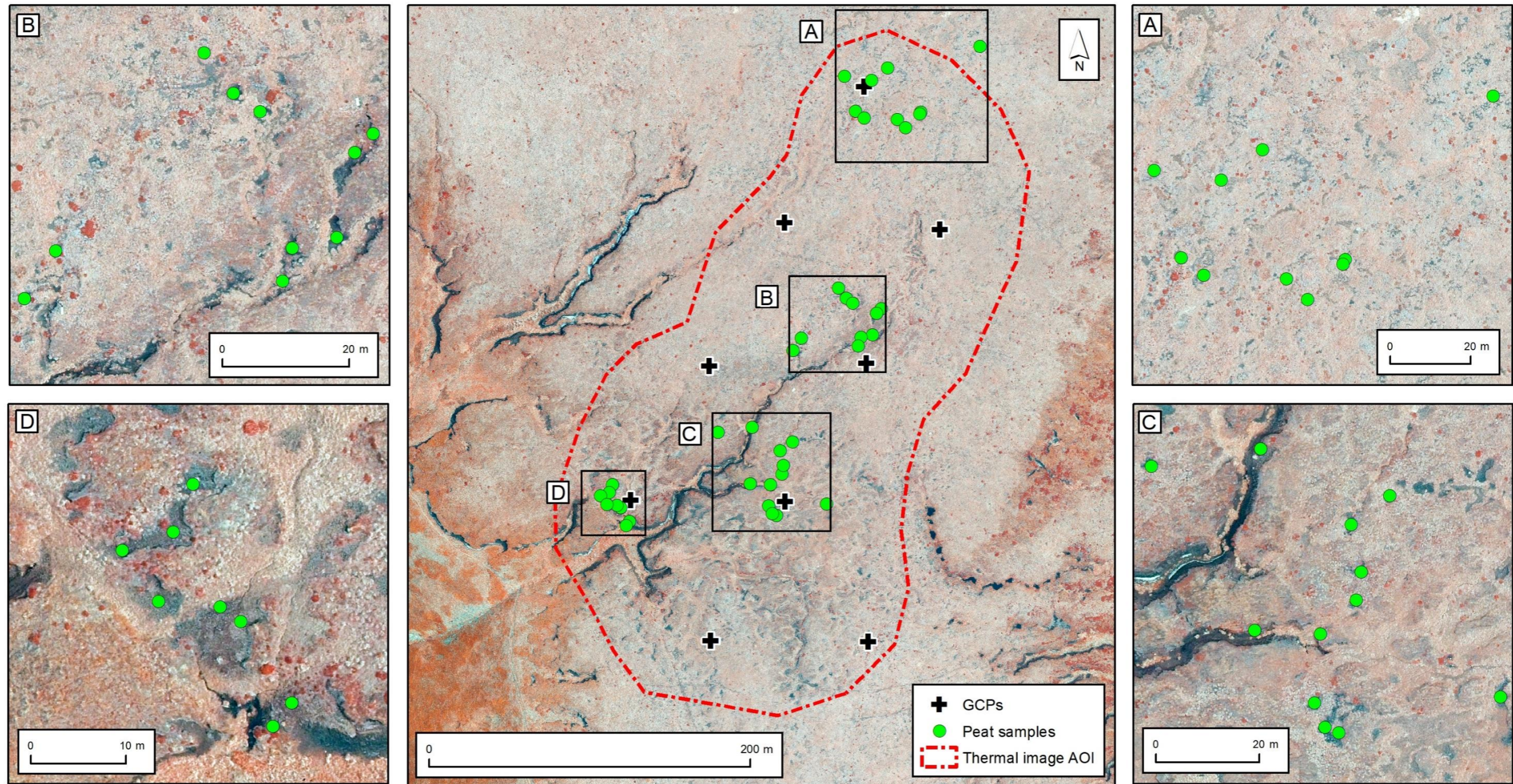


Figure 8:1. AOI of thermal capture at Birchinlee and location of peat samples.

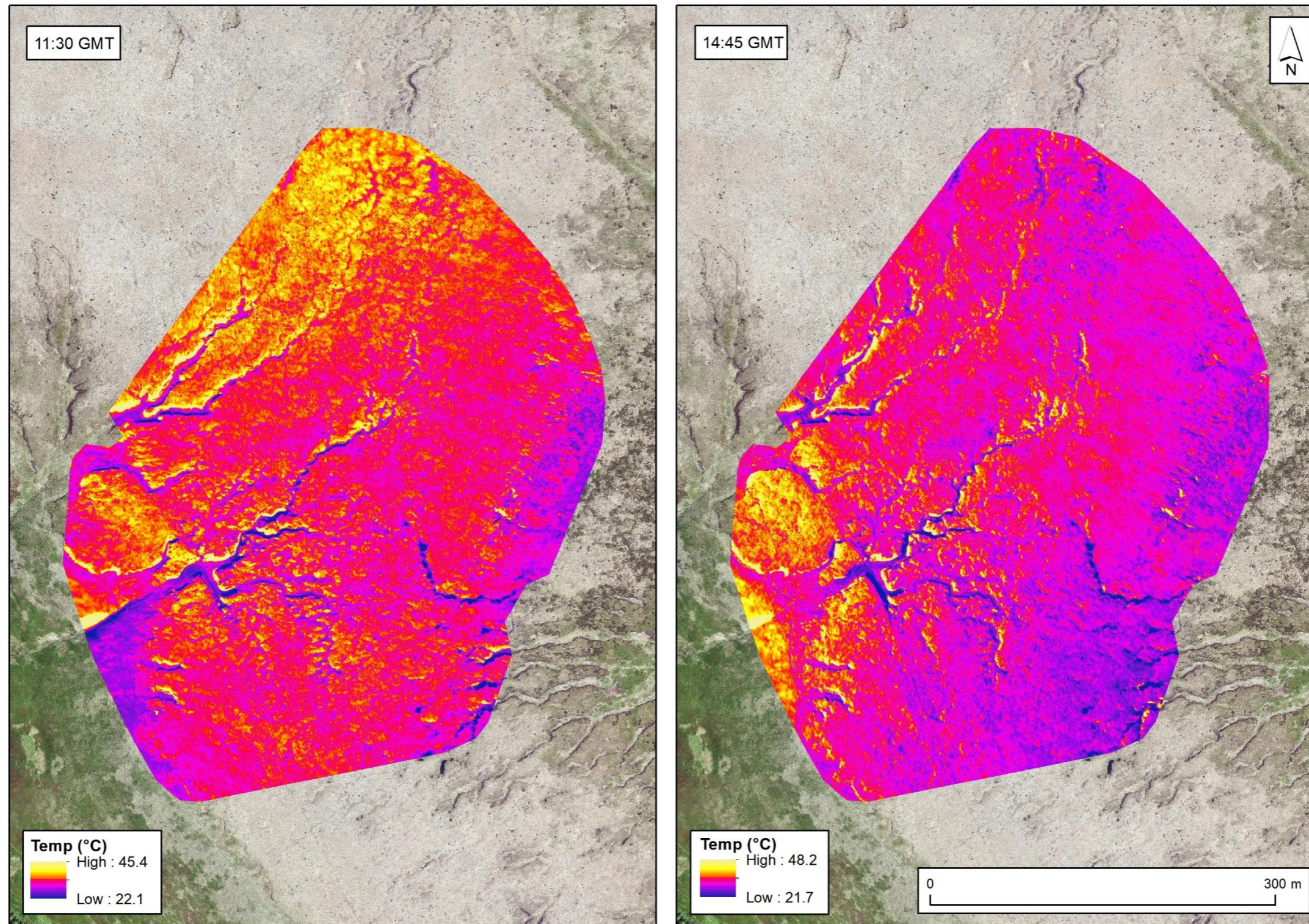


Figure 8:2. Orthorectified thermal imagery.

8.2.3 Relationship between soil moisture and temperature

Interestingly a highly significant inverse relationship between bare peat surface temperature and soil moisture was identified for both thermal image captures ($p < 0.001$ and $p = 0.009$; Table 8:3; Figures 8:3-8:4). The slopes of the regression models were not identified to be significantly different, but it should be noted that the goodness of fit is very low ($r^2 = 0.26$ and 0.17).

When 10 peat samples that were collected within gullies were excluded from analysis, the relationship between surface temperature and soil moisture using the thermal data collected at 11:30 was stronger ($r^2 = 0.41$) and still very highly significant ($p < 0.001$). In contrast, using the thermal data collected later in the day (14:45) the relationship was weaker ($r^2 = 0.13$) and only just significant ($p = 0.047$). Again the slopes of the regression models were not identified to be significantly different.

Table 8:3. Linear regressions of surface temperature against soil moisture

Flight and samples used	n	slope	r^2	p
11:30 flight – all samples	40	-2.228	0.26	<0.001
14:45 flight – all samples	40	-1.403	0.17	0.009
11:30 flight – excluding samples in gullies	30	-2.112	0.41	<0.001
14:45 flight – excluding samples in gullies	30	-1.238	0.13	0.047

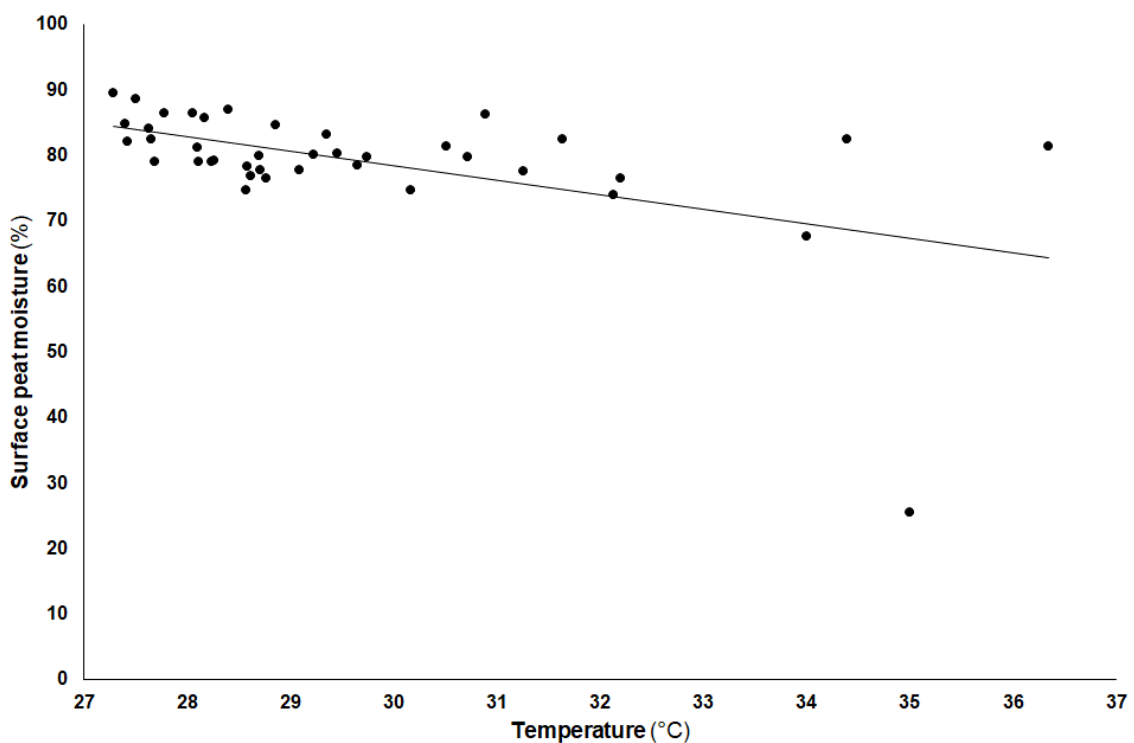


Figure 8:3. Peat surface temperature at 11:30 against peat moisture for all samples.



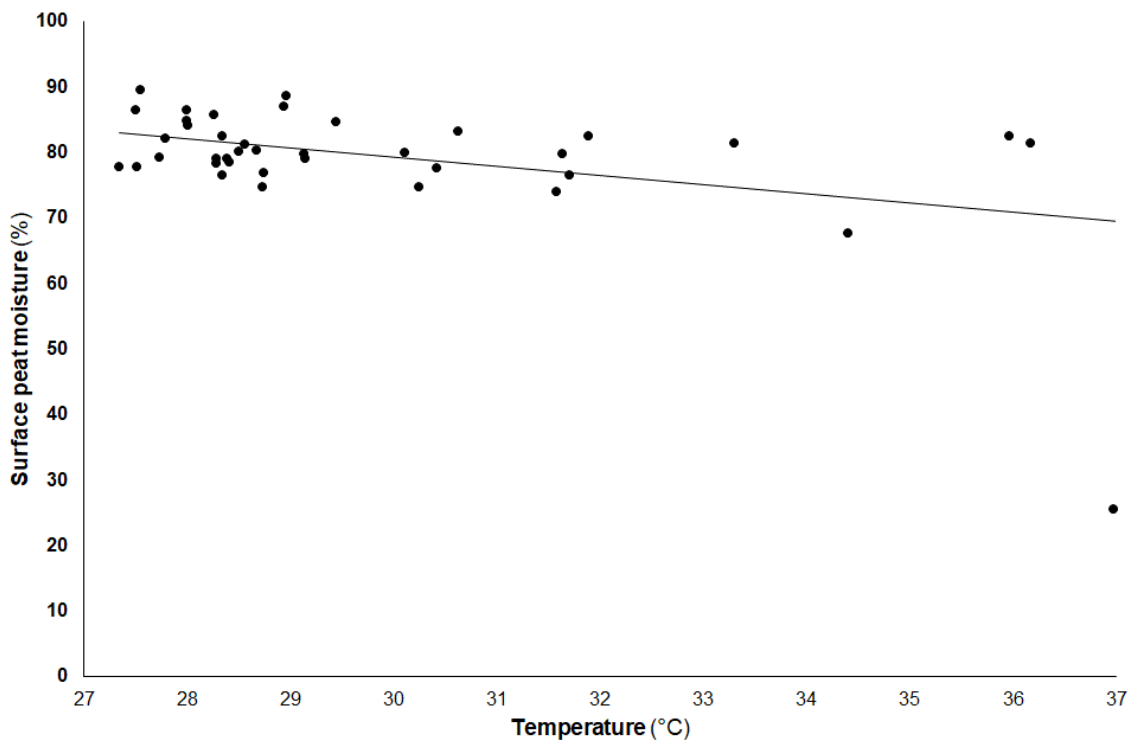


Figure 8:4. Peat surface temperature at 14:45 against peat moisture for all samples.

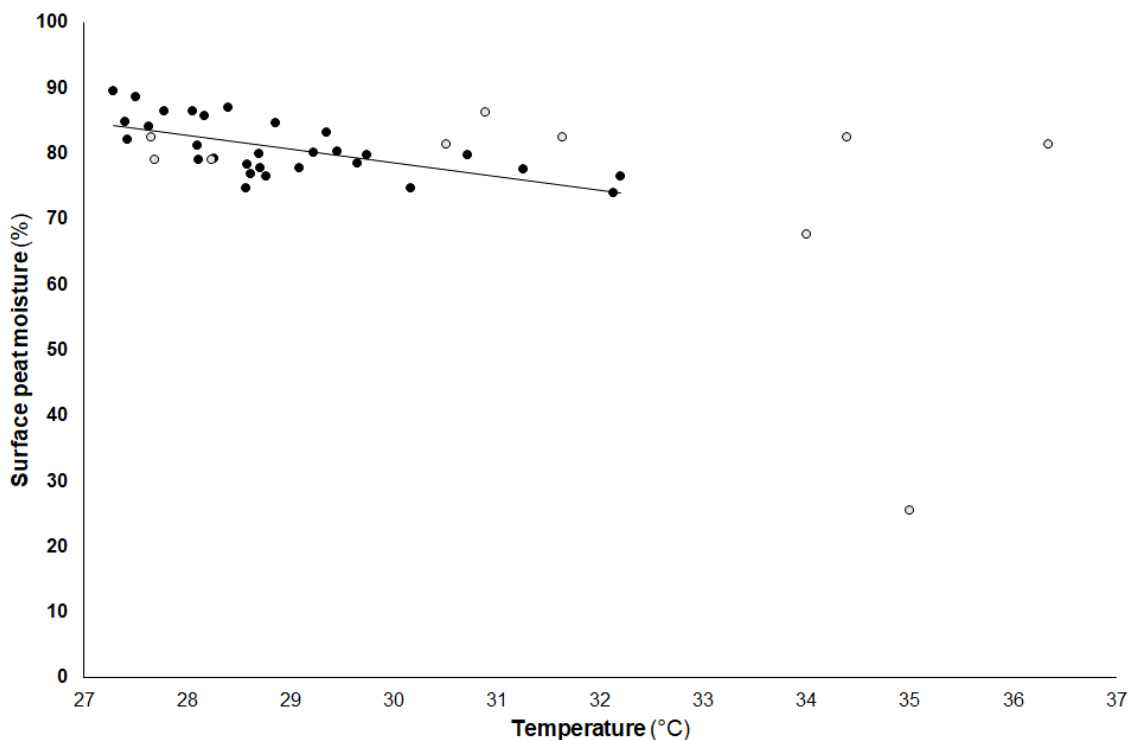


Figure 8:5. Peat surface temperature at 11:30 against peat moisture excluding samples in gullies (grey circles).

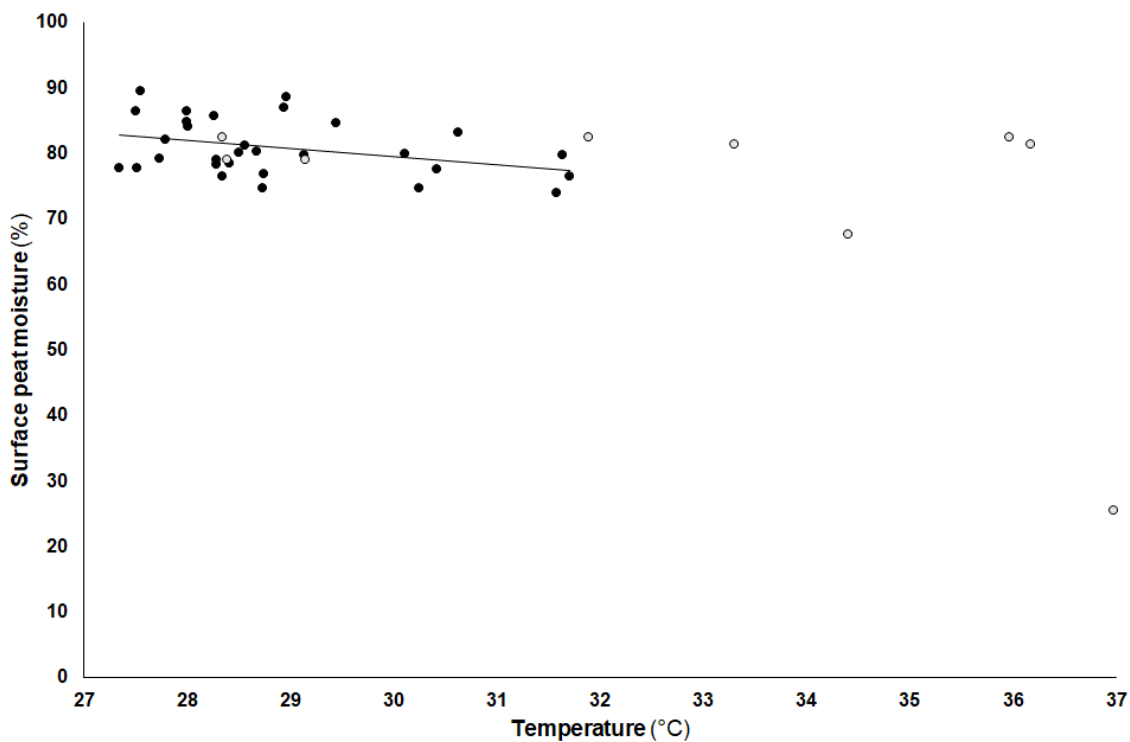


Figure 8:6. Peat surface temperature at 14:45 against peat moisture excluding samples in gullies (grey circles).



Section 9: WP 6 – Monitoring changes in erosion and accumulation

Introduction

Work Package 6

The survey approach in Phase 1 was developed to facilitate capture of UAV imagery over landscape scale areas. GCP target number and distribution was designed to produce a very high level of accuracy of orthorectification for image classification. In addition to image orthomosaics, the photogrammetric workflow creates products containing information on elevation (including 3D point cloud and DSM). These data may provide the potential to monitor localised changes in elevation over time to determine peat erosion or accumulation.

Objectives of WP6

1. Compare UAV-derived elevation data from two independent surveys to determine the viability of this data type to quantify peat erosion and accumulation.

9.1 Method

9.1.1 RGB imagery and elevation data

2018 data. RGB imagery captured for Birchinlee 1 in July 2018 were re-processed using Pix4Dmapper v4.7.5 to remove any potential differences arising from updates to software processing algorithms.

2021 capture and processing. Repeat capture of the thermal target AOI (Section 8) was undertaken with the RGB sensor on 08 September 2021 at a height of approximately 65-70 m above the ground. Images were processed using Pix4Dmapper v4.7.5 and all GCPs were marked as control points to derive a model RMSE for image orthorectification. The orthomosaic and DSM were output at the same resolution as the DSM derived in 2018 (0.021 m).

Change analysis. Elevation data in the DSM for both years were first assessed to determine compatibility of data. Both DSM datasets were clipped to the same extent for direct comparison. The elevation values determined in 2018 were then subtracted from the value determined in 2021. This process revealed that direct comparison of the DSM data is not possible (see results).

9.2 Results

The orthorectification process reported an RMSE equivalent to, or less than, the pixel size in all dimensions for both datasets (Table 9:1). The minimum and maximum elevation values recorded for both years varied by a very small amount (between 0.09 m and 0.16 m respectively; Figure 9:1). As such, the data appear comparable. However, the difference in elevation values determined between the two datasets show non-systematic variation (Figure 9:2). The northern and southern sections of the area assessed show a general trend of lower elevation in 2021. In contrast, the central section of the area (running approximately NW-SE) show a general trend of higher elevation in 2021. It is not clear what has caused this phenomenon. The pattern of variation does not align with changes in topography (Figure 9:2) and the area of difference is oriented perpendicular to the direction of flight lines in 2021. As the variation across the output is non-systematic it was not possible to apply a correction factor.



Table 9:1. Image resolution and accuracy of orthorectification

Capture	Ground resolution (m)	Control point RMSE (m)		
		x	y	z
2018	0.021	0.017	0.022	0.015
2021	0.021	0.014	0.015	0.013



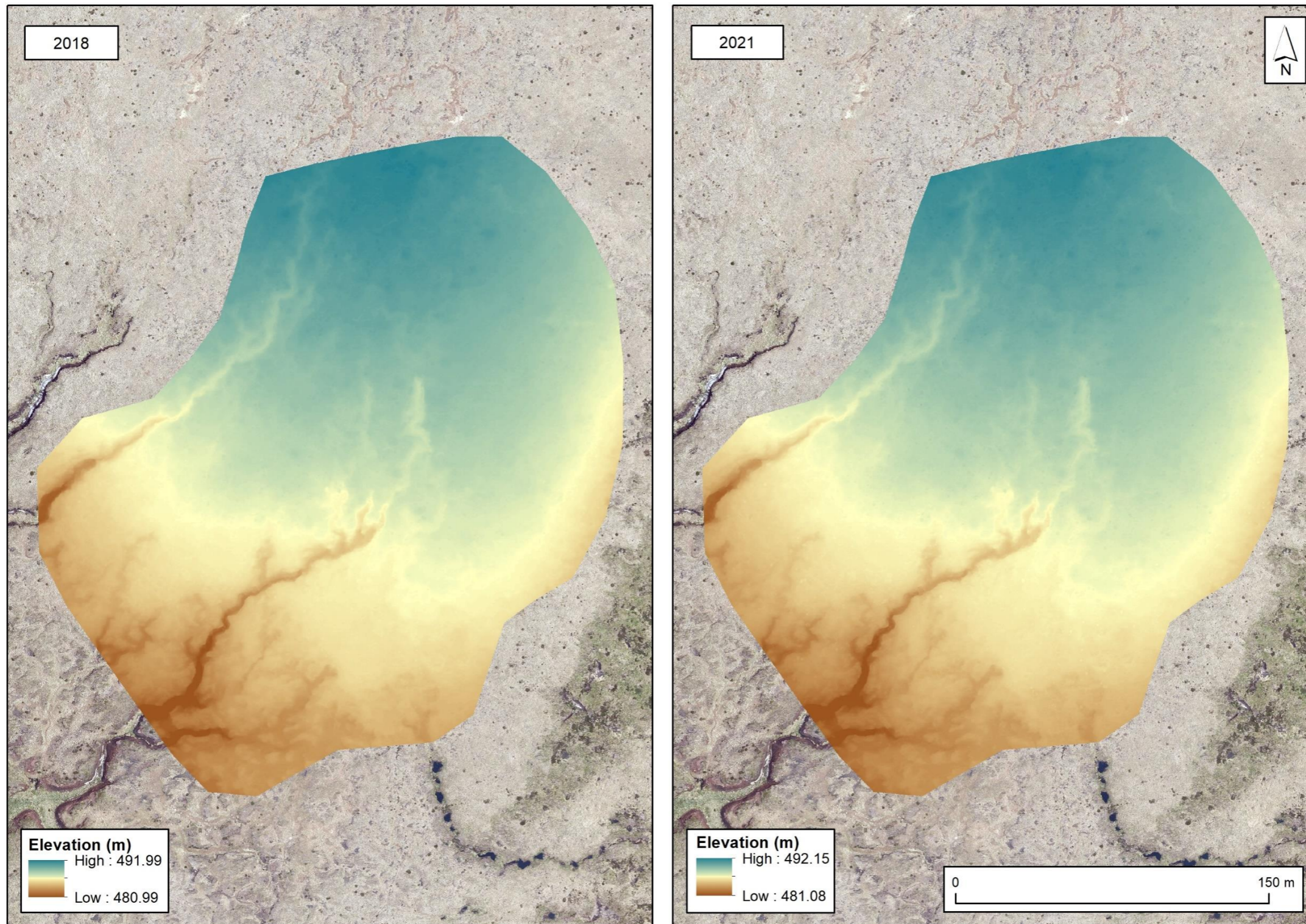


Figure 9:1. UAV-derived DSM data for 2018 and 2021.

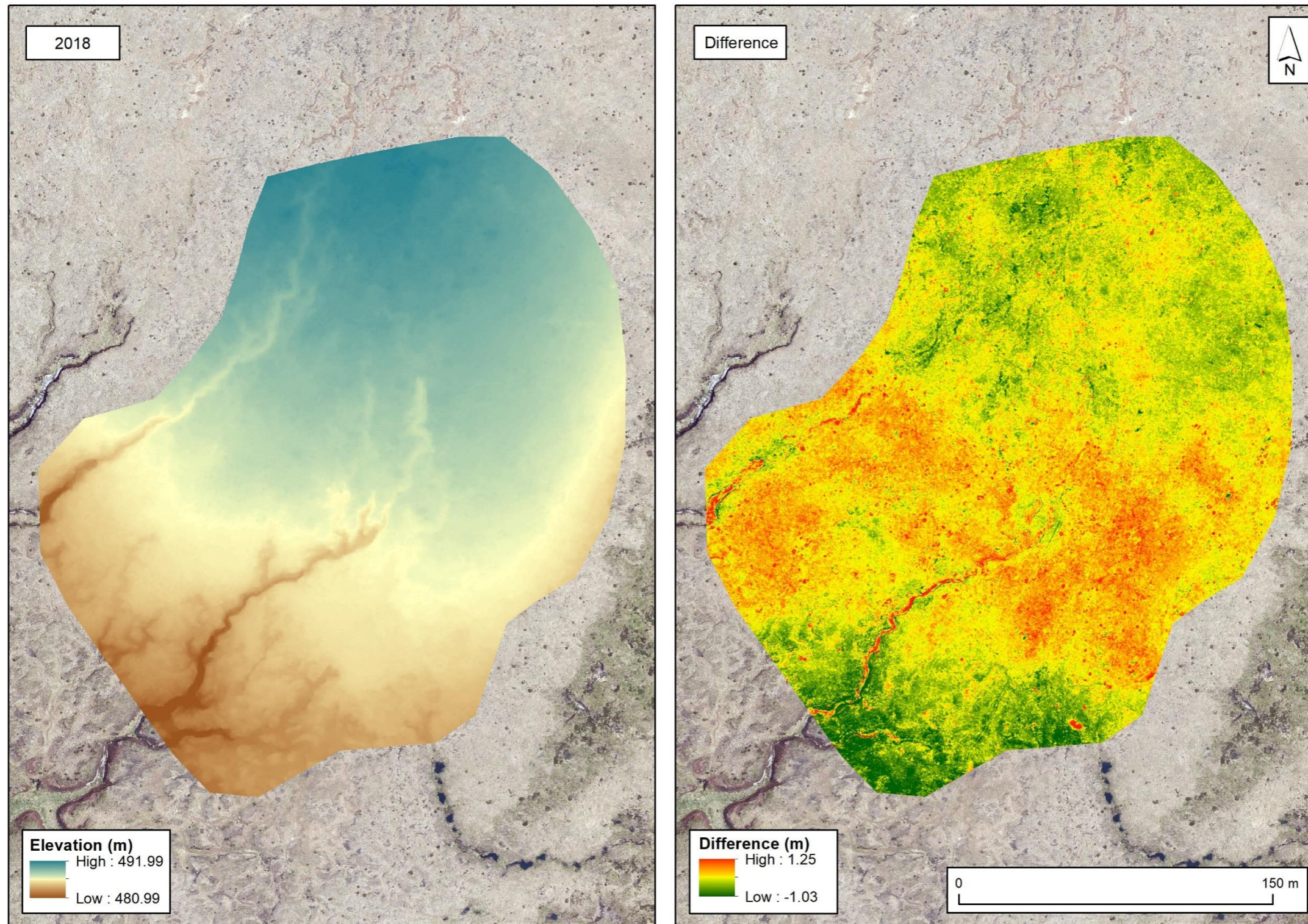


Figure 9:2. Left: UAV-derived DSM for 2018 showing topographic changes; Right: Difference in elevation between 2018 and 2021 showing non-systematic variation across the area assessed.



Section 10: Discussion, Concluding remarks and Overall Recommendations

10.1 Summary conclusions from each phase

The overall aim of 'MFF 50 2016-17 MoorLIFE 2020' has been to explore the potential role of remotely sensed data in monitoring the effectiveness of blanket bog conservation actions undertaken by MFFP.

The project comprised four annual phases of work devoted to developing techniques for mapping moorland vegetation to species level using extremely high resolution aerial imagery captured by UAV and MAV and testing these against the following objectives: to monitor land-cover change (including *Sphagnum* spp., cotton grass, purple moor grass, heather, and bare peat). The general conclusions and discussion for this work are summarised in 10.1.1 to 10.1.4 below.

Several ancillary pieces of work were undertaken in Year 4:

- i.* A direct comparison of results achieved using UAV, MAV, and orbital EO imagery data for vegetation mapping;
- ii.* An assessment of the potential for determining surface/sub-surface moisture levels using a UAV-borne thermal sensor and;
- iii.* An experiment to determine the potential for measuring topological change using DSMs extracted from UAV imagery capture.

The overall conclusion and recommendations from these pieces of work are covered in 10.1.5 and 10.1.6.



10.1.1 Phase 1 – UAV Image Capture

Phase 1 represented the first opportunity for a ‘full-up’ test of the proposed flight and field data collection protocols for baseline and monitoring data. It inevitably also provided a wealth of operational, logistical, and technical information to guide project development over the following years. This identified a number of shortcomings and vulnerabilities within the initial project assumptions and proposals. While this led to some curtailment of opportunities to fully explore the capabilities of UAV image capture during Phase 1, the lessons learned informed a considerable re-alignment of project objectives and placed it on a more solid trajectory for future years.

Operational experiences. Numerous unexpected operational and reliability issues were experienced with the planned UAV/sensor combination during work-up trials and training prior to the formal commencement of Phase 1. The most significant of these were: (i) the UAV sourced for the project experienced mechanical problems that necessitated frequent return to manufacturer, leading to loss of availability; (ii) the anticipated staff resource to ‘pilot’ the UAV anticipated during planning was not available as a result of training issues. Alongside clearly identifying the need for building in contingencies to account for such issues, these demonstrated how vulnerable planned image capture schedules can be, especially where timeframes are restricted by either intrinsic need (e.g. capturing a particular phenological stage) or extrinsic factors (e.g. access restrictions or weather). They also highlighted how easy it is during planning to both overlook potential difficulties and make over-optimistic assumptions with regard to outcomes until considerable experience and working knowledge has been gained. These points are included here to serve as useful guidance to those that follow (Crouch & Chandler 2021). To paraphrase Helmuth von Moltke the Elder ‘*no plan survives first contact*’. Contingency, and ‘plan B’, should be planned for.

In this case the issues above necessitated the use of a substitute UAV/sensor at short notice to meet the summer mapping requirements. This available replacement regrettably did not match the original project specifications in terms of spectral combinations, or spatial resolution, necessitating 2-3 flights per site to obtain the required coverage. Despite this late alteration, Phase 1 flight activities were completed and provided sufficient image data to enable appraisal as to their suitability for image processing techniques.

A second, and less resolvable, issue also occurred in the first year: unforeseen difficulties in the extensive field data collection required. Execution of this task took far longer than anticipated and ultimately the number of field samples collected fell well below the optimum. This had the effect of curtailing anticipated image-classification development



work and no complete rigorous testing of the application of UAV imagery for this sort of monitoring was ultimately possible during Phase 1.

The lessons learned from Phase 1 were particularly important in providing good insights into how the programme could be executed in future to facilitate development of image classification for monitoring.

Summary of image analysis. Although a full error-assessed classification for each site, together with an exploratory iterative ‘try, test, change’ approach as planned, was not possible during Phase 1, the examination of the image data actually produced several clear lessons.

Many UAVs, at the altitudes to which they are restricted in the UK, can produce high spatial resolutions, but of an extremely limited ‘footprint’. Combine this with a legal obligation not to fly beyond 500 m of the operator means it becomes necessary to fly numerous flight-lines to cover a significant area.

As a consequence, the time required to cover even modest areas can be considerable. Over this period, light levels, colour balance and sun angle will be changing continuously. During 2018, these issues were compounded by the need to fly each area twice using different sensors to provide the required B, G, R, RE, NIR imagery. The visible ‘striping’ and colour shift within the final mosaics used shows the impact this can have. Quantifying the negative effect this had on the accuracies of automated image-classification in Phase 1 was not possible as insufficient field data were available for error assessment.

10.1.2 Phase 2 – MAV Image Capture II

While image capture from UAV platforms undoubtedly remains the most responsive approach to monitor small areas (e.g. the MFFP field laboratory areas), following the lessons learned from Phase 1 it was decided to assess alternate sources of imagery during Phase 2. As a result, BlueSky International were contracted to undertake a bespoke flight of the study areas to capture 4-band digital imagery using a Vexcel 1 UCE on a Cessna 404. The severe limitations of undertaking UAV capture over large areas means this alternate approach is in any event probably better aligned with the broader aspirations of the project i.e. the desire to monitor at landscape scale.

Image acquisition. Airborne imagery covering all sites was captured over a period of a few minutes. From the perspective of reducing potential adverse effects from sun-angle and atmospheric effects on colour balance this is greatly superior to the days required to image the same extents when using a UAV. The spatial resolution (IFOV) of the delivered 4-band imagery was also comparable to that of multi-spectral data collected by the UAV



in 2018. From this perspective commercially contracted MAV airborne imagery seems to address the major data acquisition requirements for mapping vegetation projects such as these and appears to be an effective alternative. In addition, this approach required no MFFP staff-time commitments for flying the sites or for undertaking post-flight processing of imagery, allowing for extensive field survey tasking to be undertaken.

However, it has to be accepted that in lieu of the freedom to essentially capture ‘on demand’ enabled by UAV operations, contracting out means relying on a commercial operator with other commitments, scheduling plans and associated difficulties with weather etc. The potential impact of this was fully illustrated during Phase 2. Difficulties in obtaining clearance from ATC to fly within controlled zones for Manchester airport led to considerable delays and imagery was not captured until 02 October 2019. This was well outside of the range of dates requested and clearly highlights that the inability to control image acquisition date is a risk when using commercial airborne capture services. This was an exceptionally long delay in our experience, but the issue is generally of potential seriousness and should be discussed with an external contractor both during project planning and as soon as any issues arise. A further consideration is that slight modifications to flight parameters might facilitate more rapid acquisition (especially if ATC is an issue). Despite imagery being captured late, a full appraisal of the ability to map to species was tested during Phase 2.

Classification accuracies. The overall classification accuracies achieved during Phase 2 for all 61 species/classes recorded during the field survey were low (35%). This is below that reasonably required, making it unsuitable for even broad scale mapping let alone monitoring which requires comparison of classified map outputs. However, the full field species list included many occurring with very limited records. The original planned minimum target sample numbers for each class was around 100 (50 for training and 50 for error assessment) and this classification result is therefore not fully unexpected. Restricting the number of classes mapped to those with >70 records produced 23 species/classes for testing. This resulted in a modest increase in the overall accuracy to 46%. Although an improvement, this is still well below levels suitable for monitoring. A number of factors could possibly have driven this poor species/class separability.

Process. The techniques adopted here, individual species mapping, requires very close co-registration between field data and image pixels and if this is inadequate it could degrade classification accuracy. The choice of ‘search area’ used during signature collection will be one controllable influence on this effect, hence its role was examined. Selection of the number of adjacent pixels to be used during training is something of a trade-off. The smaller the area used the fewer pixels are ‘collected’, potentially restricting



the variability in spectral characteristics assigned to each class during training. However, it has the effect of increasing the probability of the training pixels being within the field sample collection area (in this case > 0.5m x 0.5m). If a larger 'search area' is used, then collection of a more complete range of spectral characteristics may occur, but the probability of some pixels of other classes being included increases. It is for this reason that during Phase 2 a series of training/classification/error-assessment cycles using varying training areas were performed. This process identified minimal differences in the obtained accuracy which may suggest that the orthorectification accuracy of the imagery, in this case, was less important than other factors. However, this does need to be interpreted in the context of the minimum 'pure stand' size adopted during field survey, as this protocol was specifically designed to address potential minor imagery/field data misregistration issues.

Phenology. The role of phenology, especially the variations in plant stage of individual species (or even within individual plants) in a single image is clearly important. It will serve to broaden the spectral characteristics of that species, as senesced leaves, flowers or bare stems are different colours than an 'average' leaf. Encompassing this breadth within a single class during classification training will lead to wide amorphous classes with considerable overlap, and hence little chance of good differentiation.

Prior to classification, classes such as *Pteridium aquilinum* that exhibited a range of phenological stages were visually grouped into 'green' and senesced samples. The accuracy of chlorophyllous *Pteridium* (86%) was significantly higher than that of the senesced *Pteridium* (33%). Phenological stage therefore has a clear impact on the accuracy of classification in some species. Conversely, classes such as *Eriophorum angustifolium* also produced high classification accuracy (74%) although, at the time of image capture, this species was almost completely senesced.

Shadow. The confusion observed in Phase 2 between water and other classes, especially bare peat and shadow, had a significant impact on the overall reported classification accuracies. These are classes that should be expected to achieve high classification accuracy owing to their distinct spectral signatures, particularly in the NIR. The low accuracy for water here at c.40% is unprecedented in our experience, and most probably arises entirely due to the time difference between field survey and image capture. Unless image capture dates are tied very closely to field surveys, remote sensing of transient surface phenomena is clearly always problematic and it is probable that much of the standing water identified during field survey were pools that subsequently dried before image capture. Most of these would presumably be lying over bare peat which would account for the very high level of confusion observed between these two classes.



Transiently flooded vegetated pools would also be expected to affect moorland and this probably explains the widespread confusion with nearly all species in the data. Of course, this would also apply *vice versa*, with some pools being present during image capture that were absent during field collection. It is also clear that the large areas of topographical shadow, and scattered vegetation shadow, occupy spectral space in which water and bare peat are found. The impact on the classification of these usually accurately mapped classes is clear in the error matrices. It is harder to determine the impact of shadow on the accuracy of mapped vegetation. To optimise the mapping of vegetation and bare peat, image shadow must be avoided by selecting times as close to solar noon and mid-summer as possible. In this case shadow was included in the error matrix reporting to assess classes that are spectrally confused with it but primarily to show how widespread it was. In reality, shadow is not a ground cover class and it cannot be assessed as 'right' or 'wrong'. The error statistics are therefore not entirely representative of actual classification accuracies and are included purely for illustration.

10.1.3 Phase 3 – MAV Image Capture II

Both earlier phases of this project demonstrated overall classification accuracies below the levels that would be useful for monitoring, and with poor differentiation of many target classes. However, both phases experienced considerable operational difficulties with image acquisition leading to lower than desired image quality. As this factor could readily lead to the poor results achieved, Phase 3 was tasked with determining what results were possible using commercial XHR MAV imagery free of such issues. This seemed a necessary prerequisite before definitive statements on the suitability of such imagery was made or other causes for sub-optimal accuracies being achieved could be hypothesised or tested.

Phase 3 demonstrated yet another issue with image quality (uneven spectral balancing between images for each area). This should not be seen as criticism of the quality of routine 'standard' commercially provided image data, as they are generally fit for the purposes of the vast majority of users, i.e. visual interpretation within a GIS environment. However, for the type of application desired here (automated image classification) such variation does highlight that suppliers have not always considered the more advanced uses to which their data might be put. Standards and tolerances should be negotiated and defined, so expectations and capability are better matched, something considered especially important in defining contractual obligations.

However, once a change in protocols from those planned (i.e. classifying each area separately rather than as a 'whole') was undertaken it can be considered Phase 3 did ultimately provide a realistic test of commercially sourced 5 cm resolution 4-band imagery



to meet MFFP's requirements. The results achieved were the most encouraging so far. Modest species mapping accuracies of between 20% and 55% were found for many classes with low sample numbers (e.g. *Deschampsia flexuosa*, *Juncus* spp., *Pteridium aquilinum* and *Trichophorum cespitosum*). However, many more common classes including bare peat, *Calluna vulgaris*, mineral soil, rock and *Vaccinium myrtillus* mapped with between 67% and 92% accuracy. This shows that the techniques adopted here could be utilised for landscape mapping for commonly occurring species in the upland landscape. The ability to map rare species is not testable here as their occurrence is too infrequent to provide sufficient records for training. This is not an artefact of the protocols used, rather it is part of a long understood and accepted issue with all field survey.

Within the caveats above, Phase 3 clearly demonstrates that vegetation mapping to species can achieve similar accuracies to those reported for many remote-sensing projects when using more generalised classes. This would make it suitable for landscape-scale mapping, and for baselining, with perhaps one change assessment at the end of a project being applicable.

The ability to map *Sphagnum* was a key MFFP requirement, though no ability to differentiate to species was possible here. This possibly arises from the limited number of samples of many species recorded in fieldwork or from the similarity in spectral characteristics relative to the temporal variability in each species. However, the accuracies obtained do indicate that the imagery and processes employed could be used for wide-area assay of *Sphagnum* as a group, providing a good indication of overall bog 'health' or conservation status. As with the comment above for commonly occurring species, repeated assay with these techniques for determining change, say annually, would be unsuitable as a sole monitoring method. However, if used infrequently, with comparisons perhaps every 5 years, or as part of a hybrid random field survey approach it would provide a useful tool. In the case of *Sphagnum*, such a period would be rational in any event given the likely relatively slow spread of this genus.

10.1.4 Phase 4 – Classification of Species Groupings

Species aggregations. The generally modest overall accuracies obtained during Phase 3 arise though an inability to segregate or differentiate the typology adopted within spectral space using the imagery and techniques employed. However, as the error matrices illustrate, many of the errors of omission and commission contributing to the reported overall accuracies arise from confusion between scarcer and/or less important species (from a conservation monitoring perspective). Grouping of some species might therefore be expected to result in higher overall accuracies while still retaining monitoring relevance.



Phase 4 was tasked to work in a different way to earlier phases and examined the value of such approaches by iteratively determining what classes can be mapped to higher accuracies and judging them against monitoring value. Two approaches were adopted:

- i. The first was based on two 'artificially' defined groups based solely on their conservation monitoring value to MFFP irrespective of any spectral similarities. This was anticipated to deliver lower accuracies of the two approaches but retain value through direct relevance to MFFP's monitoring needs.
- ii. The second was based on spectral commonalities i.e. grouping species that differentiated least well from each other irrespective of any taxonomic relationships. This was considered to have the greater potential to deliver higher classification accuracies, albeit by defining species groupings of unpredictable monitoring value.

To reiterate here neither of these approaches should be confused in any way with mapping of 'vegetation community' or 'habitat' types as conventionally understood as no regard is taken to the spatial proximity of pixels so grouped. Thus, unlike all other vegetation descriptors it retains all the merits of accuracy in field survey by using an unambiguous input typology i.e. plant species, but uses a simplified output typology to reduce inter-species spectral confusion during classification.

That the MFFP-defined groups improved overall classification accuracy to a higher degree than the 'natural' species clustering approaches tried is gratifying given they are considered to be of direct application to monitoring requirements (note though that the comparison is not direct, since additional species were included in the natural clusters). The increase in accuracy for the smaller Group 1 is marked and means that remote sensing of a rigorously defined and directly relevant typology, based on unambiguous field data and fully error checked is possible.

An additional result here is that bare peat is always very well separated from other species/classes meaning that, while it is often difficult to resolve individual plant species, bare peat is always distinct and easily mappable at high accuracy.

States of blanket bog. This work has mostly focussed on single species owing to the difficulty in determining communities. The groups of species used in this section do not represent classical phytosociological communities. Rather, they either form elements from within one or more community (as, for example *Sphagnum* spp within mire communities) or cross-cut several communities (dwarf shrubs, as components of both mire and heathland community types). MFFP's States of Blanket Bog (Table 10.1) partly





overlap with the MFFP-defined groups used here. However, they also include communities that draw from several of the MFFP-defined classes (e.g. State 5). One possible way of reconciling the two taxonomies might be to “assemble” communities from the building blocks of an underlying classification via a roving window. For example, a window including *Sphagnum*, *Calluna* and *Eriophorum* spp. would potentially map onto State 5. A key difficulty to consider is the classification accuracy of the building blocks of such communities.

Because bare peat is mappable with high accuracy, successful restoration would be to some extent measurable without further work, i.e. as a transition from bare peat to a vegetated surface.

Table 10.1. States of blanket bog (Moors for the Future Partnership, 2018)

State	Definition
State 2	Bare peat
State 2a	Revegetated bare peat
State 3	Dwarf shrub dominated blanket bog
State 4	Grass and/or sedge dominated blanket bog
State 5	Modified blanket bog with high dwarf shrub cover but with sphagnum and other mire species
State 6	Active hummock/hollow/ridge blanket bog

Alternative classification algorithm. A final approach included in Phase 4 was simply to determine whether the original tests and presumptions (not reported here) underpinning the choice of the appropriate classification algorithms to be adopted were still relevant at the end of a four year project and were optimising mapping accuracies. It was hoped this would also serve to ensure the current and on-going relevance of this study as newer techniques might deliver substantive improvements (e.g. Beyer et al., 2019). In this case machine-learning Random Forest classification was explored as an alternative to Maximum Likelihood.

The overall accuracy from this algorithm was no better than the techniques used for vegetation classification throughout this project, so the original choices made were considered valid.

10.1.5 Phase 5 – Comparison of UAV/MAV/EO Data

This element of the project provides a comparative test of example data from the three image sources available for conservation mapping and monitoring applications. Testing these on identical areas and extracting the same complex typologies provides a definitive assessment of the best options for a particular task.

The relatively weak performance of satellite EO imagery observed here might be considered surprising, particularly given the more expansive ‘spectral space’ available for classification created by its 8 bands. No issues with image quality or accuracy of orthorectification were noted, and the imagery was contemporaneous with the field sample data (2019).

However, it should be made clear the project typology and associated field survey protocols were not designed for, and are not ideally suited to, sensors providing the GSD of WV-2 as these were predicated on the application of XHR centimetre-resolution imagery and mapping to individual species. Few species in the upland moorland environment can be expected to exist in pure stands of the extent needed to be ‘recognised’ within the classification algorithm when using such imagery. That spatial resolution underlies the low classification accuracies achieved is supported by the improvements in classification accuracy, albeit slight, seen when using the pansharpened data. That said, it must be noted that the use of pansharpened data is not to be recommended for classification, it was used here experimentally. Resolution merge algorithms are known to preserve spatial information but distort spectral information (Oh et al., 2012).

These results should not be taken as implying that EO data can have no application for mapping peatland vegetation, rather that alternative typologies and field sample protocols beyond those used here would need adopting and testing. Field sampling areas would need to be several times the GSD (1.5-2 m), which returns to the problems of repeatability of field surveyor recording when using habitat or ‘community’-based typologies discussed in section 2.2.

UAV-derived MS data show clear potential for mapping both species and aggregated classes with moderate to good accuracies, although lower than those achieved using MAV data. While it is possible that such differences relate to sensor specifications, UAV technology has advanced significantly. Early UAV cameras used modified filters to collect NIR data and the wavelengths of bands overlapped. In contrast, the MicaSense Sequoia has a separate sensor for each band and the bandwidth of each is discrete (Parrot, 2017). The fidelity of spectral information captured by recent UAV multispectral sensors is therefore high.

However, artefacts of striping are evident in both the output image mosaic (Figure 7:1 A) and the classified product (Figure 7:2 A). This phenomenon has been attributed to changes in illumination and sun-angle during the flights (section 3.2.3). The Sequoia sensor was flown with a sun irradiance sensor and corrections of illumination were applied



during orthorectification. Unfortunately, it is clear that the technology is not flawless. It is possible that the orientation of the irradiance sensor as fixed-wing platforms counter higher wind speeds affects the measurements recorded.

It is clear that the time required to capture large areas with a UAV results in image degradation that impacts on classification performance. Irradiance sensor function may improve in the future, but currently the use of UAVs to collect imagery for classification can only be recommended for areas coverable by single flights.

In contrast, the area of Kinder examined in this section was captured in 2-3 flight lines by MAV. This likely took around 5-10 minutes. The reliability of several key groups including bare peat, dwarf shrubs and grass, sedge & rush may allow snapshot determination of site condition. Although the establishment of *Sphagnum* plugs can be visually determined in the imagery (Figure 5:1), in previous phases they did not map reliably in classification. However, this assessment demonstrates that naturally occurring *Sphagnum* can be mapped reliably. It appears therefore that *Sphagnum* plugs will need to have established for several years before automated detection can be applied.

This project indicates that MAV derived MS data are currently the best image type for mapping vegetation at landscape scale using the typologies tested.

10.1.6 Work Package 5 – Monitoring changes in surface wetness

The identification of a significant inverse relationship between surface temperature and soil moisture suggests that variation of water content in a bare peat surface is detectable in thermal imagery. However, while this may appear promising for the development of an approach to monitor soil moisture there are several confounding issues.

The thermal data assessed here were captured at two times of day just 3 hours apart. Over this short period of time the change in sun incidence angle influenced a 3°C increase in maximum temperature recorded across the AOI. As a result, the slope of the relationship between peat surface temperature and soil moisture changed. At 11:30 GMT, a 2.2°C change in surface temperature relates to a 1% change in soil moisture. Yet at 14:45 GMT, a 1.4°C change in surface temperature relates to a 1% change in soil moisture. It is therefore evident that a single direct translation of temperature into an index of soil moisture is not possible; temperature will change with time of capture and also with time of year. This issue is compounded by the fact that the increasing temperature resulting from insolation will not be homogenous across any area. Fine-scale variation in topology and slope means some areas will receive longer exposure to insolation than others and hence will have warmed more, not necessarily as a consequence of thermal capacity. A protocol for mapping soil moisture content using thermal imagery would



therefore always not only require contemporaneous soil moisture measurements but sensibly also fixed thermocouples to access continuous temperature changes. To date soil moisture probes to determine the former have not been shown to reliably measure water content in peat soils (Richard Lindsay, *pers. comm.*). The only viable approach would be to collect multiple peat samples for laboratory analysis of water content during each survey. This has associated time and logistical costs.

The stronger relationship between peat surface temperature and soil moisture identified in the earlier flight data (11:30 GMT) when areas within gullies were excluded indicates that shading resulting from topography (i.e. gully floors and walls) introduces unpredictable temperature variations. Assessment of soil moisture by this method would need to be restricted to areas of bare peat within the main peat body.

This highlights the major constraint to the use of these data, irrespective of any other issues: *it can only ever deliver information about soil surface moisture in areas of bare peat*, hopefully a small component of any bog/peatland system. As an airborne sensor cannot 'see' the ground under any canopy of vegetation it is inherently incapable of providing any soil thermal data in vegetated areas, by far the major component of the landscape.

10.1.7 Work Package 6 – Monitoring changes in peat erosion and accumulation

Non-systematic variation in elevation identified between the two surveys precluded the opportunity to extract any meaningful statistics of change. A systematic shift in elevation recorded might be expected as a result of the accuracy of the coordinates for the GCPs (± 0.04 m in z). This phenomenon was not highlighted by Glendell et al. (2017) who reported that UAV derived data can detect change within ± 0.03 m. The approach adopted by Glendell et al (2017) used RTK GPS correction achieving a reported 3D accuracy of 0.02 m. The type of UAV platform was also different (a quadcopter with gimbal) and the resolution of the imagery was at least twice as high (0.005 - 0.01 m).

Given the issues experienced here, should this technique be considered for application it needs considerable further development and, in particular, survey design and equipment need further research and development.

10.2 Concluding discussion and summary recommendations

Remote sensing is often seen by those unfamiliar with it as a kind of 'magic bullet', something able to deliver a monitoring programme cheaply without much effort. It has never been this. In the conservation sector, it is frequently executed using inappropriate or incomplete protocols with little field data support. Critically, results are usually provided



without any form of accuracy assessment so their value is impossible to gauge. The old axiom is still relevant:

‘Without accuracy assessment, remote sensing is just a pretty picture.’

There is potential that the availability of cheap, easy to use UAVs will result in an increased production of maps and data outputs of poor quality.

MFF 50 2016-17 addresses this problem directly. It set a challenging objective: to demonstrate techniques to obtain validated quantitative data, at centimetre resolution, of the distributions of vegetation cover, channel erosion and surface moisture using remotely sensed imagery and automated classification systems. These requirements are very different from simple manual visual interpretation, the predominant use to which such imagery is put in the conservation sector.

To examine this topic in breadth the project has utilised a range of image data, from orbital to UAV, and a variety of classification approaches. During its four year execution MFF 50 2016-17 experienced a considerable number of practical difficulties with acquisition of data suitable for monitoring purposes. We believe the lessons learned from these should be considered key findings of this report.



Section 11: References

Beyer, F., Jurasinski, G., Couwenberg, J. and Grenzdörffer, G. (2019) Multisensor data to derive peatland vegetation communities using a fixed-wing unmanned aerial vehicle. *International Journal of Remote Sensing*, 40:24, 9103-9125. DOI: 10.1080/01431161.2019.1580825.

Bragazza, L. (2009) Conservation priority of Italian Alpine habitats: a floristic approach based on potential distribution of vascular plant species. *Biodiversity Conservation*, 18, 2823-2835.

Breiman, L. (2001) Random forests. *Machine learning*, 45(1), 5-32.

Caporn, S. J. M., Rosenburgh, A. E., Keightley, A. T., Hinde, S. L., Riggs, J. L., Buckler, M. and Wright, N. A. (2018) *Sphagnum* restoration on degraded blanket and raised bogs in the UK using micropropagated source material: a review of progress. *Mires and Peat*, 20, 1-17.

Cherrill, A. and McClean, C. (1995) An investigation of uncertainty in field habitat mapping and the implications for detecting land cover change, *Landscape Ecology*, 10(1).5-21.

Cherrill, A. and McClean, C. (1999) Between-observer variation in the application of a standard method of habitat mapping by environmental consultants in the UK. *Journal of Applied Ecology*, 36(6), 989-1008.

Congalton, R.G. and Green, K. (2019) *Assessing the Accuracy of Remotely Sensed Data. Principles and Practices*. 3rd Edition. CRC Press. Boca Raton.

Crouch, T. and Chandler, D. (2021) A conservation practitioner's guide to the use of unmanned aerial vehicles (UAVs) for peatland monitoring and conservation: an exploration of the successes, challenges and learning of a UAV-based approach. Moors for the Future Partnership, Edale, UK.

Ferguson, P. and Lee, J. A. (1967) Past and present sulphur pollution in the southern Pennines. *Atmospheric Environment*, 17, 1131-1137.

FLIR. (2014). *Tau 2 Longwave Infrared Thermal Imaging Cameras*. FLIR Systems Inc.: Wilsonville, OR, USA.

Glendell, M., McShane, G., Farrow, L., James, M.R., Quinton, J., Anderson, K., Evans, M., Benaud, P., Rawlins, B., Morgan, D., Jones, L., Kirkham, M., DeBell, L., Quine, T.A., Lark, M., Rickson, J. and Brazier, R.E. (2017) Testing the utility of structure-from-motion



photogrammetry reconstructions using small unmanned aerial vehicles and ground photography to estimate the extent of upland soil erosion. *Earth Surface Processes and Landforms*, 42(12), 1860–1871.

Hearn, S.M, Healey, J.R., McDonald M.A., Turner, A.J, Wong, J.L.G. and Stewart, G.B. (2011) The repeatability of vegetation classification and mapping. *Journal of Environmental Management*, 92(4), 1174-1184.

Hexagon Geospatial (undated). *Evaluating signatures*. Available at: https://hexagongeospatial.fluidtopics.net/reader/uOKHREQkd_XR9iPo9Y_ljw/OD65kmNoXmbogX3mnhbhog [last accessed 4.iii.2019].

Ho, T. K. (1995). *Random decision forests*. In: Proceedings of 3rd international conference on document analysis and recognition (Vol. 1, pp. 278-282). IEEE.

Ikkala, L., Marttila, H., Ronkanen, A.-K., Ilmonen, J., Rehell, S., Kumpula, T., and Klöve, B. (2021) Thermal UAS Imaging to Monitor Restored Peatlands, EGU General Assembly 2021, online, 19–30 Apr 2021, EGU21-10582, <https://doi.org/10.5194/egusphere-egu21-10582>, 2021.

Jensen, J. R. (1996) *Introductory Digital Image Processing: A Remote Sensing Perspective*. 2nd Edition. Prentice-Hall, New Jersey.

Joosten, H. and Clarke, D. (2002) *Wise use of mires and peatlands - background and principles including a framework for decision-making*. International Mire Conservation Group and International Peat Society, Finland.

Lindsay, R., Charman, D., Everingham, F., O'Reilly, R., Palmer, M., Rowell, T. and Stroud, D. (1988) *The Flow Country: The Peatlands of Caithness and Sutherland*. Nature Conservancy Council, Peterborough, 32 pp.

Luscombe, D.J., Anderson, K., Gatis, N., Grant-Clement, E. and Brazier, R.E. (2015) Using airborne thermal imaging data to measure near-surface hydrology in upland ecosystems. *Hydrological Processes*, 29, 1656–1668.

Maskill, R., Walker, J.S, Allott, T., Evans, M. and Shuttleworth, E. (2015) *MoorLIFE: Changes to the water table and carbon budget*. Moors for the Future Report, Edale, Derbyshire.

Moors for the Future Partnership - MFFP (2013) *MoorLIFE: Active Blanket Bog Restoration in the South Pennines Moors Monitoring Programme – Mid-Term Report*. Moors for the Future Report, Edale, Derbyshire.



Oh, K-Y & Jung, H-S and Lee, K-J. (2012) Comparison of Image Fusion Methods to Merge KOMPSAT-2 Panchromatic and Multispectral Images. *Korean Journal of Remote Sensing*, 28. 10.7780/kjrs.2012.28.1.039.

Pal, M. (2005) Random forest classifier for remote sensing classification. *International Journal of Remote Sensing*, 26(1), 217-222.

Parrot. (2017) *Parrot Sequoia User guide V1.1 05/2017*. Parrot Drones SAS: Paris, France.

Rodwell, J.S. (1991) British Plant Communities. Volume 1. Woodlands and scrub. Cambridge University Press.

Rodwell, J.S. (1991) British Plant Communities. Volume 2. Mires and heaths. Cambridge University Press.

Rodwell, J. S. (1992) British Plant Communities. Volume 3. Grassland and montane communities. Cambridge University Press.

Rodwell, J.S. (1995) British Plant Communities. Volume 4. Aquatic communities, swamps and tall-herb fens. Cambridge University Press.

Rodwell, J.S. (2000) British plant communities. Volume 5. Maritime communities and vegetation of open habitats. Cambridge University Press.

Rodwell, J.S. (2006) National Vegetation Classification: Users' handbook. JNCC, Peterborough.

Scharlemann, J.P.W., Tanner, E.V.J., Hiederer, R. and Kapos, V. (2014) Global soil carbon: understanding and managing the largest terrestrial carbon pool. *Carbon Management*, 5:1, 81-91.

SenseFly. (2017) *ThermoMAP Camera User Manual*. Revision 5; senseFly Parrot Group: Cheseaux-sur-Lausanne, Switzerland.

Siddiqui, Y. (2003) *The Modified IHS Method for Fusing Satellite Imagery*. In: ASPRS 2003 Annual Conference Proceedings.

Smart, S., Goodwin, A., Wallace, H. & M. Jones (2016). MAVIS (Ver. 1.03) User Manual. CEH, Lancaster.

Tallis, J. H. (1987) Fire and flood at Holme Moss: erosion processes in an upland blanket mire. *The Journal of Ecology*, 1099-1129.



Yallop, A.R., Clutterbuck, B. and Davies, S. (2009) Burn mapping from space. In Alonso, I. ed. *Managing Heathlands in the Face of Climate Change*. Proceedings of the 10th National Heathland Conference. Natural England NECR014. ISSN 2040-5545

Yallop, A.R., Thacker, J.I., Thomas, G., Stephens, M., Clutterbuck, B., Brewer, T. and Sannier, C.A.D. (2006) The extent and intensity of management burning in the English uplands. *Journal of Applied Ecology*, 43, 1138–1148.

Yeloff, D.E., Labadz, J.C. and Hunt, C.O. (2006) Causes of degradation and erosion of a blanket mire in the southern Pennines, UK. *Mires and Peat*, 1(04), 1–18.

Yu, Z., Beilman, D.W., Froking, S., MacDonald, G.M., Roulet, N.T., Camill, P. and Charman, D.J. (2011) Peatlands and Their Role in the Global Carbon Cycle. *Eos*, 92, 12, 97-108.



Section 12: Annexes



Annex A:

Developmental groupings and species list used during Phase 2

Strim A: Exclusions

Aim to create a dataset where most samples are included except for species with very small sample numbers and unusable samples.

- 1: All <20cm samples deleted
- 2: *Agrostis* (7) deleted
- 3: *Epilobium* (2) deleted
- 4: Fern (2) deleted
- 5: *Polytrichum* (1) deleted
- 6: *flexuosum* (3) deleted
- 7: *Ulex* (1) deleted
- 8: *Juncus bulbosus* (5) deleted
- 9: *Leucanthemum* (1) deleted
- 10: Not (sic) *Pteridium* (1) deleted
- 11: *Phragmites* (2) deleted
- 12: *Rhododendron groenlandicum* (1) deleted
- 13: *Sorbus aucuparia* (3) deleted
- 14: *Vaccinium vitis-idaea* (3)
- 15: obscured selection (23) deleted
- 19: mixed species selection (53) deleted

Final size = 6889

Strim B: Exclusions

Primarily to investigate role of sample areal extent. These are in addition to those in Strim A.

- 1: <40 cm samples (518) deleted
- 2: *capillifolium* (5) deleted
- 3: *Deschampsia cespitosa* (1) deleted
- 4: *Holcus lanatus* (1) deleted
- 5: *Holcus mollis* (7) deleted
- 6: *magellanicum* (3) deleted
- 7: *tenellum* (4) deleted

Final size = 6350

Strim C: Exclusions

Primarily to investigate role of small samples. These are in addition to those in Strim A & B.

- 1: Abies deleted
- 2: Betula deleted
- 3: Pinus deleted
- 4: Rhododendron ponticum deleted
- 5: cuspidatum (16) deleted
- 6: denticulatum – (5) deleted
- 7: Erica cinerea (10) deleted
- 8: Heath brash (4) deleted
- 9: papillosum (10) deleted
- 10: squarrosus (2) deleted
- 11: subnitens (15) deleted

Final size = 6110

Table A:1. Strim D as used in 2019: 23 classes with sample record number >70

Sample	Count
Bare peat	341
Calluna	467
Calluna dead	234
Calluna flower	216
Deschampsia flexuosa	102
Empetrum nigrum	198
Eriophorum angustifolium	526
Eriophorum vaginatum	577
fallax	124
fimbriatum	85
Juncus effusus	412
Juncus squarrosus	106
Mineral soil	134
Molinia caerulea	119
Nardus stricta	245
Polytrichum spp	325
Pteridium aquilinum	73
Pteridium aquilinum senesced	111
Rock	162
Shadow	427
Trichophorum cespitosum	112
Vaccinium myrtillus	375
Water	241
Total	5712



Table A:10. Strim C Error matrix. Nearest Neighbour classification. 20cm search area. All classes.

	Bare peat	Calluna	Calluna burnt	Calluna cut	Calluna dead	Calluna flower	Chamerion angustifolium	Cladonia spp	Cushion moss	Deschampsia flexuosa	Empetrum dead	Empetrum nigrum	Erica tetralix	Eriophorum angustifolium	Eriophorum vaginatum	fallax	Feather moss	fimbriatum	Flagstone	Juncus effusus	Juncus squarrosus	Mineral soil	Molinia caerulea	Nardus stricta	palustre	Polytrichum spp.	Pteridium aquilinum	Pteridium aquilinum sen	Rock	Salix spp.	Shadow	Trichophorum cespitosum	Vaccinium myrtillus	Water	Total	User accuracy	
Bare peat	59				4									4							1		3												8	82	0.72
Calluna		82				17		1				2		1	2				1		6							1						9	123	0.67	
Calluna burnt			2		4																	2										1			9	0.22	
Calluna cut				2	1					1												1		1					1						7	0.29	
Calluna dead	1			1	36		1				2	1		1	1						4	1	1	2	2	1									55	0.65	
Calluna flower		21			2	27		1						10	1		1							2	2			1					3	4	72	0.38	
Chamerion angustifolium		1					3					5	2		14	2	2	2			8		5	2	2	4							3	9	1	88	0.03
Cladonia spp				1	1			3					1		5				2	1	1	1	2	1					1		1	2		23	0.13		
Cushion moss	1								1			1				1	1				4	1	1	8					2		4	4	2	31	0.03		
Deschampsia flexuosa	1		1		2					10					2						6	1	1	7					1					1	33	0.30	
Empetrum dead	4	1			8						6	1		1	1						3		1					1				3	1	2	33	0.18	
Empetrum nigrum		3			1							10			4	1		2			2	1									1	3	1	34	0.29		
Erica tetralix		1			2	3			1	1		2	10		3	9	1				3	1		3				2				3	10		56	0.18	
Eriophorum angustifolium						3								117	4																	1			126	0.93	
Eriophorum vaginatum												4			23	2		1							1		3			1			2		37	0.62	
fallax		1										1			1	6											9					1		21	0.29		
Feather moss									1								3								3										10	0.30	
fimbriatum									2						3	1		6									4	1					2		20	0.30	
Flagstone																			13																32	0.41	
Juncus effusus		1							1	1				1	2						3														10	0.30	
Juncus squarrosus	1	2			3	1			2	4		3			2	1					13	9		2	1		1		3			1	3	1	53	0.17	
Mineral soil			2					1		3												22													33	0.67	
Molinia caerulea		1			4					2		1	1		5		2	1			13	2	7	2	1								2	7		51	0.14
Nardus stricta					1					3					2		3				2	1	1	29					2	1	2	1			48	0.60	
palustre												1	1	1	1			2			2		1	1	2										12	0.17	
Polytrichum spp.									2			2			13	10	1	4								1									89	0.62	
Pteridium aquilinum		4							1			3			25	2							1				7	19					5		71	0.27	
Pteridium aquilinum sen		1				1					1	1	3	6																			1		30	0.37	
Rock	1																																	1	39	0.74	
Salix spp.		1					1			1			1	2	33			2			8		3	2									3	7	73	0.05	
Shadow	12	1								1		1				1	2	1	1		2						2							8	109	0.66	
Trichophorum cespitosum		7			1	9			1	2		7	3	12	4	1	1				12	2	6					4							93	0.17	
Vaccinium myrtillus		8			2	2						14	1	7	7	2	1				12	3		1			3	1	3						97	0.35	
Water	22	2										2		3	4	3					1	1	1	1		1					35			127	0.39		
Total	102	138	5	4	72	63	5	6	12	31	9	62	20	159	174	34	16	27	16	123	32	40	36	74	9	98	21	33	49	8	126	34	114	75	1827		
Producer accuracy	0.58	0.59	0.40	0.50	0.50	0.43	0.60	0.50	0.08	0.32	0.67	0.16	0.50	0.74	0.13	0.18	0.19	0.22	0.81	0.02	0.28	0.55	0.19	0.39	0.22	0.56	0.90	0.33	0.59	0.50	0.57	0.47	0.30	0.67			

N (total observations)	1827	Overall accuracy	0.43
X (Sum of all correct)	781		
Y (Sum of total user x sum of total producer)	128722	Kappa	0.40





Table A:11. Strim C Error matrix. Nearest Neighbour classification. 20cm search area. Calluna (includes Calluna, Calluna flower and Calluna dead); Pteridium (includes Pteridium and Pteridium sen) folded.

	Bare peat	Calluna	Calluna burnt	Calluna cut	Chamerion angustifolium	Cladonia spp	Cushion moss	Deschampsia flexuosa	Empetrum dead	Empetrum nigrum	Erica tetralix	Eriophorum angustifolium	Eriophorum vaginatum	fallax	Feather moss	fimbriatum	Flagstone	Juncus effusus	Juncus squarrosus	Mineral soil	Molinia caerulea	Nardus stricta	palustre	Polytrichum spp.	Pteridium aquilinum	Rock	Salix spp.	Shadow	Trichophorum cespitosum	Vaccinium myrtillus	Water	Total	User accuracy
Bare peat	59	4										4						1		3								3			8	82	0.72
Calluna	1	185		1	1	2			2	3		12	4		1	1		10	2	1	2	2	1		2		1	3	13		250	0.74	
Calluna burnt		4	2																	2							1				9	0.22	
Calluna cut		1		2				1												1		1				1					7	0.29	
Chamerion angustifolium		1			3			1		5	2		14	2	2	2		23	8		5	2	2	4	2					9	1	88	0.03
Cladonia spp		1		1		3		1			1		5				2	1		1	2	1				1	1		2		23	0.13	
Cushion moss							1			1				1	1													4		4	2	31	0.03
Deschampsia flexuosa		1	1					10					2					6	1	1		8				2				1	33	0.30	
Empetrum dead	4	9							6	1		1	1					3			1				1			3	1	2	33	0.18	
Empetrum nigrum		4								10			4	1		2		2	1					3	2		1		3	1	34	0.29	
Erica tetralix		6					1	1		2	10	3	9	1				3	1		3			2	1			3	10		56	0.18	
Eriophorum angustifolium		3							1			117	4															1			126	0.93	
Eriophorum vaginatum										4			23	2		1						1		3		1			2		37	0.62	
fallax		1								1			6											9					1		21	0.29	
Feather moss							1								3	2			1			3									10	0.30	
fimbriatum							2					3	1			6								4	1		1		2		20	0.30	
Flagstone																	13														32	0.41	
Juncus effusus		1					1	1				1	2					3													10	0.30	
Juncus squarrosus	1	6					2	4		3		2	1					13	9		2	1		1	3			1	3	1	53	0.17	
Mineral soil			2			1		3												22							5				33	0.67	
Molinia caerulea		5						2		1	1		5		2	1		13	2		7	2	1						2	7	51	0.14	
Nardus stricta		1						3					2		3			2	1	1		29				2	1	2	1		48	0.60	
palustre										1		1	1			2		2			1	1	2	1							12	0.17	
Polytrichum spp.							2			2			13	10	1	4								55					2		89	0.62	
Pteridium aquilinum		6					1			4	1	3	31	2							1		3	7	32		1	1	6		101	0.32	
Rock	1																			4		1				29		3		1	39	0.74	
Salix spp.		1			1			1			1	2	33			2		8			3	2		3	2		4		3	7	73	0.05	
Shadow	12	1					1			1				1	2	1	1	2						2				72		8	109	0.66	
Trichophorum cespitosum		17					1	2		7	3	12	4	1		1		12	2		6			4				16	5		93	0.17	
Vaccinium myrtillus		12								14	1	7	7	2	1			12	3		1			3	4		2	1	34		97	0.35	
Water	22	2								2		3	4	3				1		1	1	1		1			35		1	50	127	0.39	
Total	102	273	5	4	5	6	12	31	9	62	20	159	174	34	16	27	16	123	32	40	36	74	9	98	54	49	8	126	34	114	75	1827	
Producer accuracy	0.58	0.68	0.40	0.50	0.60	0.50	0.08	0.32	0.67	0.16	0.50	0.74	0.13	0.18	0.19	0.22	0.81	0.02	0.28	0.55	0.19	0.39	0.22	0.56	0.59	0.59	0.50	0.57	0.47	0.30	0.67		
N (total observations)																											1827		Overall accuracy	0.45			
X (Sum of all correct)																											823		Kappa	0.42			
Y (Sum of total user x sum of total producer)																											174475						

Table A:12. Strim C Error matrix. Nearest Neighbour classification. 10cm search area. All classes.

	Bare peat	Calluna	Calluna burnt	Calluna cut	Calluna dead	Calluna flower	Chamerion angustifolium	Cladonia spp	Cushion moss	Deschampsia flexuosa	Empetrum dead	Empetrum nigrum	Erica tetralix	Eriophorum angustifolium	Eriophorum vaginatum	fallax	Feather moss	fimbriatum	Flagstone	Juncus effusus	Juncus squarrosus	Mineral soil	Molinia caerulea	Nardus stricta	palustre	Polytrichum spp.	Pteridium aquilinum	Pteridium aquilinum sen	Rock	Salix spp.	Shadow	Trichophorum cespitosum	Vaccinium myrtillus	Water	Total	User accuracy		
Bare peat	60				5							2		3						2		2			1											11	92	0.65
Calluna	1	82				12						2		1	2					4							1	1			1	1	8			116	0.71	
Calluna burnt			3		8					1												3														16	0.19	
Calluna cut			1	2						1												2			1											7	0.29	
Calluna dead	6	1		1	31							2			1					3	1	1	3		2				1					1	54	0.57		
Calluna flower		19			2	29			1					11		1		1			1		4	3		2						2	7	76	0.38			
Chamerion angustifolium		2				3			1	3		7	1		21	1		1		25	8	1	4	3	1	4		2				1	11	100	0.03			
Cladonia spp				1	3			1			1		1	1	3					1	8		3	2				2					2	21	0.05			
Cushion moss									1				1				1				1				4	1			2		3		3	1	25	0.04		
Deschampsia flexuosa					2					11				1							6	1			10				1					2	35	0.31		
Empetrum dead					7		1				7	1		4	1					5	1		1					1		1	2	1	4	40	0.18			
Empetrum nigrum		1			1	1						8		6	1	1				3	1		3			3		1		1		9	40	0.20				
Erica tetralix		2			1	3		1			4	10		1	7	1	1			6	2		5			3		2			3	7	61	0.16				
Eriophorum angustifolium						5				1	1			117	3					2			1					1			2			133	0.88			
Eriophorum vaginatum												1		17	2			1								2	1			1	1	2	28	0.61				
fallax															4											8						1	14	0.29				
Feather moss									1						1		3				1				1	1	1		1					11	0.27			
fimbriatum									1						9	3		7								4	1							26	0.27			
Flagstone							1										1		14															37	0.38			
Juncus effusus													1	2						2														6	0.33			
Juncus squarrosus		2			1	1			2	3		2	1	8				2		10	7		2	2		1		1			1	3	49	0.14				
Mineral soil			1							1									1			23			1									28	0.82			
Molinia caerulea		1	1		3	1				1		1		4		1				13	1		2					2				2	3	1	38	0.05		
Nardus stricta		1			2		1		4					3		3	1			3	1	1			30				3	1	2	1	1	58	0.52			
palustre		1										1	1										1	1	2									12	0.17			
Polytrichum spp.												5		18	13	2	4									54						3	102	0.53				
Pteridium aquilinum		3										2		20	2								1			11	16	2		1	1	7	1	68	0.24			
Pteridium aquilinum sen		2			1	1	2		1				1	3	7						2	2				3	1	12					38	0.32				
Rock																						3		1					29			4		37	0.78			
Salix spp.									3					1	30		1	3		7			3	4		1		1		2			3	3	63	0.03		
Shadow	13	1					1		1							1	2		1	1		2				1					76			2	7	109	0.70	
Trichophorum cespitosum		7			5	7						9	2	11	4					11	4		5				2					16	3	1	87	0.18		
Vaccinium myrtillus		13			1	3						14	1	1	6	2	1			11	1		1			3	1	3				36	1	101	0.36			
Water	14	1									3		3	1	3							1	1			1				25			2	44	99	0.44		
Total	102	138	5	4	72	63	5	6	12	31	9	62	20	159	174	34	16	27	16	123	32	40	36	74	9	98	21	33	49	8	126	34	114	75	1827			
Producer accuracy	0.59	0.59	0.60	0.50	0.43	0.46	0.60	0.17	0.08	0.35	0.78	0.13	0.50	0.74	0.10	0.12	0.19	0.26	0.88	0.02	0.22	0.58	0.06	0.41	0.22	0.55	0.76	0.36	0.59	0.25	0.60	0.47	0.32	0.59				
N (total observations)																													1827	Overall accuracy		0.42						
X (Sum of all correct)																													761	Kappa		0.39						
Y (Sum of total user x sum of total producer)																													128032									



Table A:13. Strim C Error matrix. Nearest Neighbour classification. 10cm search area. Calluna (includes Calluna, Calluna flower and Calluna dead); Pteridium (includes Pteridium and Pteridium sen) folded.

	Bare peat	Calluna	Calluna burnt	Calluna cut	Chamerion angustifolium	Cladonia spp	Cushion moss	Deschampsia flexuosa	Empetrum dead	Empetrum nigrum	Erica tetralix	Eriophorum angustifolium	Eriophorum vaginatum	fallax	Feather moss	fimbriatum	Flagstone	Juncus effusus	Juncus squarrosus	Mineral soil	Molinia caerulea	Nardus stricta	palustre	Polytrichum spp.	Pteridium aquilinum	Rock	Salix spp.	Shadow	Trichophorum cespitosum	Vaccinium myrtillus	Water	Total	User accuracy
Bare peat	60	5										3						2		2		1						8			11	92	0.65
Calluna	7	176		1			1			4		12	3	1		1		8	1	1	3		2		4	1	1	1	3	16		246	0.72
Calluna burnt		8	3					1												3						1						16	0.19
Calluna cut			1	2				1												2		1										7	0.29
Chamerion angustifolium		2			3		1	3		7	1		21	1		1		25	8	1	4	3	1	4	2				1	11		100	0.03
Cladonia spp		3		1		1			1		1	1	3					1			3	2				2			2		21	0.05	
Cushion moss	3						1				1				1			4	1			4		1		2		3		3	1	25	0.04
Deschampsia flexuosa		2						11				1						6	1	1						1					2	35	0.31
Empetrum dead	3	7			1				7	1		4	1					5	1		1				1		1	2	1	4	40	0.18	
Empetrum nigrum		3								8			6	1		1		3	1		3			3	1		1		9		40	0.20	
Erica tetralix		6					1			4	10	1	7	1	1			6	2		5			3	2		2		3	7		61	0.16
Eriophorum angustifolium		5						1	1			117	3					2			1				1				2		133	0.88	
Eriophorum vaginatum										1			17	2		1								2	1	1	1	1	2		28	0.61	
fallax														4		1								8					1		14	0.29	
Feather moss							1						1		3	1			1			1	1	1	1	1					11	0.27	
fimbriatum							1						9	3		7								4	1		1				26	0.27	
Flagstone					1										1		14										8	1			37	0.38	
Juncus effusus											1	2						2													6	0.33	
Juncus squarrosus		4					2	3		2	1	8				2		10	7		2	2		1	1			1	3		49	0.14	
Mineral soil			1					1									1				23		1			1					28	0.82	
Molinia caerulea	1	5						1	1			4			1			13	1		2				2			2	3	1	38	0.05	
Nardus stricta	1	2			1			4				3			3	1		3	1	1		30				3	1	2	1		58	0.52	
palustre		1								1		1				4		1			1	1	2								12	0.17	
Polytrichum spp.							3			5		18	13	2	4									54					3		102	0.53	
Pteridium aquilinum		6			1	2	1	1	2	1	3	27	2					2	2		1		3	11	31	1	1		7	1	106	0.29	
Rock																				3		1				29		4			37	0.78	
Salix spp.								3				1	30		1	3		7			3	4		1	1		2				63	0.03	
Shadow	13	1			1		1						1	2		1	1	1		2			1				76		2	3	1	109	0.70
Trichophorum cespitosum		19								9	2	11	4					11	4		5			2				16	3	1	87	0.18	
Vaccinium myrtillus		17								14	1	6	2	1				11	1		1			3	4		2		36	1	101	0.36	
Water	14	1								3		3	1	3						1	1			1		25		2		44	99	0.44	
Total	102	273	5	4	5	6	12	31	9	62	20	159	174	34	16	27	16	123	32	40	36	74	9	98	54	49	8	126	34	114	75	1827	
Producer accuracy	0.59	0.64	0.60	0.50	0.60	0.17	0.08	0.35	0.78	0.13	0.50	0.74	0.10	0.12	0.19	0.26	0.88	0.02	0.22	0.58	0.06	0.41	0.22	0.55	0.57	0.59	0.25	0.60	0.47	0.32	0.59		

N (total observations) 1827
 X (Sum of all correct) 798
 Y (Sum of total user x sum of total producer) 173548
 Overall accuracy 0.44
 Kappa 0.41



Table A:14. Strim C Error matrix. Nearest Neighbour classification. 5cm search area. All classes.

	Bare peat	Calluna	Calluna burnt	Calluna cut	Calluna dead	Calluna flower	Chamerion angustifolium	Cladonia spp	Cushion moss	Deschampsia flexuosa	Empetrum dead	Empetrum nigrum	Erica tetralix	Eriophorum angustifolium	Eriophorum vaginatum	fallax	Feather moss	fimbriatum	Flagstone	Juncus effusus	Juncus squarrosus	Mineral soil	Molinia caerulea	Nardus stricta	palustre	Polytrichum spp.	Pteridium aquilinum	Pteridium aquilinum sen	Rock	Salix spp.	Shadow	Trichophorum cespitosum	Vaccinium myrtillus	Water	Total	User accuracy		
Bare peat	59				6							1		3						2		2			1											12	93	0.63
Calluna	1	82				15						2		1	2												2	1			1	1	8			122	0.67	
Calluna burnt			2		5					1												2															10	0.20
Calluna cut			1	3															1			2														8	0.38	
Calluna dead	7	1	1	1	32					1		2	1		1					4	1	2				2			1					1		60	0.53	
Calluna flower		17			2	26			1					8		1		1										1			1	2	7			68	0.38	
Chamerion angustifolium		2				1	2		1	4		7	2		21	3		1		25	6		4	4	1	5		3				2	14			108	0.02	
Cladonia spp					4			2			1		1	1	4					1	6		4	2					3				2	2		27	0.07	
Cushion moss	4				2				2			3	1				1	1					4		6	1			2		3		7	1		38	0.05	
Deschampsia flexuosa	1				2					11				1							9	1	1		5				1					2		34	0.32	
Empetrum dead	2				6						7			2						5	2		1					1			1	1	1	6		36	0.19	
Empetrum nigrum												10			7					2	1		2			4		2		1		8			37	0.27		
Erica tetralix		3			1	2			1			4	9	2	5	1	1			6	2		3			3		3		2		3	7		58	0.16		
Eriophorum angustifolium						6				1	1			119	3					2			1					1				2				136	0.88	
Eriophorum vaginatum															17	2		1		1						3				1	1	1	2			29	0.59	
fallax							1									3		2								9							1			17	0.18	
Feather moss									1						1		3	1							1	1										9	0.33	
fimbriatum									1						8	4		8								4						1	1			27	0.30	
Flagstone								1							1		1		14																	36	0.39	
Juncus effusus													1									1														2	0.00	
Juncus squarrosus		3			1	1	1		2	3		2	1		8		2				14	10		3	4		1						2			61	0.16	
Mineral soil	1		1		1					1												24		1												33	0.73	
Molinia caerulea	1	1			2	1						2			2		1				8	1		4									2	4		29	0.14	
Nardus stricta	1				2		1			4					1		3				3	1	1		32				4	1	3	1			59	0.54		
palustre		1												1				4							1	2										11	0.18	
Polytrichum spp.												4			18	12	2	3									51						3			95	0.54	
Pteridium aquilinum		3							1			1			19	1							2				11	17								61	0.28	
Pteridium aquilinum sen		2				1	1	1		1				4	6						1	1				3		1	11						33	0.33		
Rock																			1																	35	0.77	
Salix spp.										3		2	1	1	38		1	3			7		3	3		1	1			3			1	3	1	72	0.04	
Shadow	13	1					1			1						1	2					3				1						81				115	0.70	
Trichophorum cespitosum		6			5	7						9	2	12	6						10	2	6					2					17	3	1	88	0.19	
Vaccinium myrtillus		14			3							10	1	1	5	3	1				8	3	1			3		4				34	1		95	0.36		
Water	12	2			1						2			3	1	3										1				19					85	0.46		
Total	102	138	5	4	72	63	5	6	12	31	9	62	20	159	174	34	16	27	16	123	32	40	36	74	9	98	21	33	49	8	126	34	114	75	1827			
Producer accuracy	0.58	0.59	0.40	0.75	0.44	0.41	0.40	0.33	0.17	0.35	0.78	0.16	0.45	0.75	0.10	0.09	0.19	0.30	0.88	0.00	0.31	0.60	0.11	0.43	0.22	0.52	0.81	0.33	0.55	0.38	0.64	0.50	0.30	0.52				

N (total observations) 1827 Overall accuracy 0.42
 X (Sum of all correct) 763
 Y (Sum of total user x sum of total producer) 127380 Kappa 0.39



Table A:15. Strim C Error matrix. Nearest Neighbour classification. 5cm search area. Calluna (includes Calluna, Calluna flower and Calluna dead); Pteridium (includes Pteridium and Pteridium sen) folded.

	Bare peat	Calluna	Calluna burnt	Calluna cut	Chamerion angustifolium	Cladonia spp	Cushion moss	Deschampsia flexuosa	Empetrum dead	Empetrum nigrum	Erica tetralix	Eriophorum angustifolium	Eriophorum vaginatum	fallax	Feather moss	fimbriatum	Flagstone	Juncus effusus	Juncus squarrosus	Mineral soil	Molinia caerulea	Nardus stricta	palustre	Polytrichum spp.	Pteridium aquilinum	Rock	Salix spp.	Shadow	Trichophorum cespitosum	Vaccinium myrtillus	Water	Total	User accuracy	
Bare peat	59	6								1		3						2		2		1						7			12	93	0.63	
Calluna	8	175	1	1			1	1		4	1	9	3	1		1		11	1	2	2		2		4	1	2	3	16		250	0.70		
Calluna burnt		5	2					1												2												10	0.20	
Calluna cut			1	3													1			2		1										8	0.38	
Chamerion angustifolium		3			2		1	4		7	2		21	3		1		25	6		4	4	1	5	3				2	14		108	0.02	
Cladonia spp		4				2			1		1	1	4					1			4	2				3			2	2		27	0.07	
Cushion moss	4	2					2			3	1				1	1		4				6		1		2		3		7	1	38	0.05	
Deschampsia flexuosa	1	2						11				1						9	1	1		5				1				2	2	34	0.32	
Empetrum dead	2	6							7	1		2						5	2		1				1			1	1	1	6	36	0.19	
Empetrum nigrum										10			7					2	1		2			4	2			1		8		37	0.27	
Erica tetralix		6					1			4	9	2	5	1	1			6	2		3			3	3		2		3	7		58	0.16	
Eriophorum angustifolium		6						1	1			119	3					2			1				1				2			136	0.88	
Eriophorum vaginatum													17	2		1		1						3		1	1	1	2			29	0.59	
fallax					1									3		2		1						9					1			17	0.18	
Feather moss							1						1		3	1			1			1	1									9	0.33	
fimbriatum							1						8	4		8								4			1		1			27	0.30	
Flagstone						1							1		1		14					11						1				36	0.39	
Juncus effusus											1									1												2	0.00	
Juncus squarrosus		5			1		2	3		2	1		8			2		14	10		3	4		1	3				2			61	0.16	
Mineral soil	1	1	1					1												24		1				4						33	0.73	
Molinia caerulea	1	4								2			2		1			8	1		4								2	4		29	0.14	
Nardus stricta	1	2				1		4					1		3			3	1	1		32				4	1	3	1		1	59	0.54	
palustre		1										1				4		2				1	2									11	0.18	
Polytrichum spp.							2			4			18	12	2	3								51					3			95	0.54	
Pteridium aquilinum		6			1	1	1	1		1		4	25	1				1	1		2		3	11	30			1	3	1		94	0.32	
Rock																	1			2	2					27		3				35	0.77	
Salix spp.							3		2	1	1	38		1	2			7			3	3		1	1		3		1	3	1		72	0.04
Shadow	13	1					1							1	2			1		3				1				81		2	8	115	0.70	
Trichophorum cespitosum		18								9	2	12	6					10	2		6				2				17	3	1		88	0.19
Vaccinium myrtillus		17								10	1	1	5	3	1			8	3		1			3	4			3	34	1		95	0.36	
Water	12	3								2		3	1	3										1				19	2			85	0.46	
Total	102	273	5	4	5	6	12	31	9	62	20	159	174	34	16	27	16	123	32	40	36	74	9	98	54	49	8	126	34	114	75	1827		
Producer accuracy	0.58	0.64	0.40	0.75	0.40	0.33	0.17	0.35	0.78	0.16	0.45	0.75	0.10	0.09	0.19	0.30	0.88	0.00	0.31	0.60	0.11	0.43	0.22	0.52	0.56	0.55	0.38	0.64	0.50	0.30	0.52			
N (total observations)																											1827	Overall accuracy		0.44				
X (Sum of all correct)																											800	Kappa		0.41				
Y (Sum of total user x sum of total producer)																											172896							



Table A:16. Strim C Error matrix. Mahalanobis classification. 10cm search area. All classes.

	Bare peat	Calluna	Calluna burnt	Calluna cut	Calluna dead	Calluna flower	Chamerion angustifolium	Cladonia spp	Cushion moss	Deschampsia flexuosa	Empetrum dead	Empetrum nigrum	Erica tetralix	Eriophorum angustifolium	Eriophorum vaginatum	fallax	Feather moss	fimbriatum	Flagstone	Juncus effusus	Juncus squarrosus	Mineral soil	Molinia caerulea	Nardus stricta	palustre	Polytrichum spp.	Pteridium aquilinum	Pteridium aquilinum sen	Rock	Salix spp.	Shadow	Trichophorum cespitosum	Vaccinium myrtillus	Water	Total	User accuracy
Bare peat	43				4																	1							2					3	53	0.81
Calluna	1	86			19							2		1	1			1			7						2	3				1	10	134	0.64	
Calluna burnt			2		1					1												1													5	0.40
Calluna cut				1																															1	1.00
Calluna dead	3	1			24							2									3	1	2		2								1	40	0.60	
Calluna flower		15			1	22						1		10		1																2	6	58	0.38	
Chamerion angustifolium										2		1	1		4						2					2		1				4	4	31	0.00	
Cladonia spp	1	1		1	11	1		2			1		3	2	4				2		1		4	10								2	1	51	0.04	
Cushion moss	2				1				2			3	1							2			2	3								9	1	36	0.06	
Deschampsia flexuosa	3		1		8				1	11				1	1						2	1		23					4	1	2		2	76	0.14	
Empetrum dead	1				5		1				7			1	1						3	1	1					1			2	1	2	27	0.26	
Empetrum nigrum	1	8			1	3			1			11	1		4	1					7	2	5			2		3			1	10	61	0.18		
Erica tetralix					1				1				5		2	1					1	2	1									3	1	18	0.28	
Eriophorum angustifolium					4	7				1	1			126	2						2		1					1			4		149	0.85		
Eriophorum vaginatum							1					1	1		20	2					6					2	1			1	1	2	1	39	0.51	
fallax		1					1		4			10		32	11	2	10				2			1		34				3		15	2	128	0.09	
Feather moss					2		1		1	1		1	1		8		4	2			3	2	1	1	6	2	1		1		1	1	2	43	0.09	
fimbriatum									1	1					17	4				1					1	7					2			43	0.16	
Flagstone																																		22	0.50	
Juncus effusus		1											1	4				2			7	2									1	1	21	0.33		
Juncus squarrosus										3				1							5	7		1							1	2	21	0.33		
Mineral soil	4		2	2	5		1		2										1					3					4				51	0.53		
Molinia caerulea						1				1		3	3		5		1				11	1		5				3			3	1	38	0.13		
Nardus stricta	1								3						2		1		1	1	1				14				1		2	1	28	0.50		
palustre		1					1		1					1	9	1	3				7	4		2	2	2	1	3				3	41	0.05		
Polytrichum spp.												4			12	8	1										37				1	1	63	0.59		
Pteridium aquilinum		3										1			12	1							1			5	15	2		1	1	5	1	48	0.31	
Pteridium aquilinum sen		5			1	2		2	1	1		3	2	8	12						3	2			3		1	13			5	3	69	0.19		
Rock										1												4		1						28	4		38	0.74		
Salix spp.															14		1	1		5			3	2						3		1	1	32	0.09	
Shadow	19	1			1		1		1			2				1	2		1	2		4				3					89	3	10	140	0.64	
Trichophorum cespitosum		2			1	6						3		3	1						4	1	3								6	1	1	32	0.19	
Vaccinium myrtillus		8			1	1						10		1	5		2				6	2				4		2		1		24		66	0.36	
Water	23	5			1	1						4	1	5	1	3					2		1	1				1		19	6	50	124	0.40		
Total	102	138	5	4	72	63	5	6	12	31	9	62	20	159	174	34	16	27	16	123	32	40	36	74	9	98	21	33	49	8	126	34	114	75	1827	
Producer accuracy	0.42	0.62	0.40	0.25	0.33	0.35	0.00	0.33	0.17	0.35	0.78	0.18	0.25	0.79	0.11	0.32	0.25	0.26	0.69	0.06	0.22	0.68	0.14	0.19	0.22	0.38	0.71	0.39	0.57	0.38	0.71	0.18	0.21	0.67		

N (total observations) 1827 Overall accuracy 0.40
 X (Sum of all correct) 722
 Y (Sum of total user x sum of total producer) 131358 Kappa 0.37

Table A:17. Strim C Error matrix. Mahalanobis classification. 10cm search area. Calluna (includes Calluna, Calluna flower and Calluna dead); Pteridium (includes Pteridium and Pteridium sen) folded.

	Bare peat	Calluna	Calluna burnt	Calluna cut	Chamerion angustifolium	Cladonia spp	Cushion moss	Deschampsia flexuosa	Empetrum dead	Empetrum nigrum	Erica tetralix	Eriophorum angustifolium	Eriophorum vaginatum	fallax	Feather moss	fimbriatum	Flagstone	Juncus effusus	Juncus squarrosus	Mineral soil	Molinia caerulea	Nardus stricta	palustre	Polytrichum spp.	Pteridium aquilinum	Rock	Salix spp.	Shadow	Trichophorum cespitosum	Vaccinium myrtillus	Water	Total	User accuracy
Bare peat	43	4																		1								2			3	53	0.81
Calluna	4	168								5		11	1	1		1		10	1	1	2		2		5				3	17	232	0.72	
Calluna burnt		1	2					1												1												5	0.40
Calluna cut				1																												1	1.00
Chamerion angustifolium								2		1	1		4					11	2		1	2		2	1					4		31	0.00
Cladonia spp	1	13		1		2			1		3	2	4				2	1			4	10				4			2	1	51	0.04	
Cushion moss	2	1					2			3	1				1			10			2	3				1			9	1	36	0.06	
Deschampsia flexuosa	3	8	1				1	11				1	1		1			14	2	1		23				4	1	2		2	76	0.14	
Empetrum dead	1	5			1				7			1	1					3	1		1				1			2	1	2	27	0.26	
Empetrum nigrum	1	12					1			11	1		4	1				7	2		5			2	3				1	10	61	0.18	
Erica tetralix		1					1				5		2	1				1	2		1								3	1	18	0.28	
Eriophorum angustifolium		11					1	1				126	2					2			1				1				4		149	0.85	
Eriophorum vaginatum					1					1	1		20	2				6						2	1		1	1	2	1	39	0.51	
fallax		1			1		4			10			32	11	2	10		2				1		34			3		15	2	128	0.09	
Feather moss		2			1		1	1		1	1		8		4	2		3	2	1	1	6	2	1		1	1	1	2	1	43	0.09	
fimbriatum							1	1					17	4		7								7	2		1		2		43	0.16	
Flagstone															1		11					5									22	0.50	
Juncus effusus		1									1	4				2		7	2		2								1	1	21	0.33	
Juncus squarrosus							3					1						5	7		1				1				1	2	21	0.33	
Mineral soil	4	5	2	2		1		2									1			27		3				4					51	0.53	
Molinia caerulea		1	2					1		3	3		5		1			11	1		5				3				3	1	38	0.13	
Nardus stricta	1						3						2		1		1	1	1			14				1		2	1		28	0.50	
palustre		1			1			1				1	9	1		3		7	4		2	2	2	1	3				3		41	0.05	
Polytrichum spp.										4			12	8		1								37					1		63	0.59	
Pteridium aquilinum		11			2	1	1		4	2	8	24	1					3	2		1		3	5	31		2	2	5	8	117	0.26	
Rock								1												4		1				28		4			38	0.74	
Salix spp.								1				14			1	1		5			3	2					3				32	0.09	
Shadow	19	2			1		1			2				1	2		1	2		4				3				89	3	10	140	0.64	
Trichophorum cespitosum		9							3		3	1						4	1		3							6	1	1	32	0.19	
Vaccinium myrtillus		9							10		1	5			2			6	2					4	2		1		24		66	0.36	
Water	23	7							4	1	5	1	3					2			1	1				1	19	6	50	124	0.40		
Total	102	273	5	4	5	6	12	31	9	62	20	159	174	34	16	27	16	123	32	40	36	74	9	98	54	49	8	126	34	114	75	1827	
Producer accuracy	0.42	0.62	0.40	0.25	0.00	0.33	0.17	0.35	0.78	0.18	0.25	0.79	0.11	0.32	0.25	0.26	0.69	0.06	0.22	0.68	0.14	0.19	0.22	0.38	0.57	0.57	0.38	0.71	0.18	0.21	0.67		

N (total observations) 1827
 X (Sum of all correct) 761
 Y (Sum of total user x sum of total producer) 172701
 Overall accuracy 0.42
 Kappa 0.38

Annex B:

Re-examination of field data for 2020 classification

Table B:1. Samples in shadow in 2019 moved to classification in 2020 during Phase 3

Class	Shadow 2019	Shadow 2020	Added to classification	Incorrect class
<i>Agrostis</i> spp.	1			
Bare peat	118	10	108	
<i>Calluna</i> in flower	1		1	
<i>Calluna</i> no flower	7		7	
Cushion moss	2			
<i>Deschampsia flexuosa</i>	7		7	
<i>Empetrum</i> dead	2			
<i>Empetrum nigrum</i>	6		6	
<i>Eriophorum angustifolium</i>	26		26	
<i>Eriophorum vaginatum</i>	22		22	
<i>fallax</i>	15		15	
Feather moss	1			
<i>fimbriatum</i>	13		13	
Flagstone	19			1
Heather Brash	2			
<i>Holcus mollis</i>	2			
<i>Juncus bulbosus</i>	2			
<i>Juncus effusus</i>	15	1	14	
<i>Juncus squarrosus</i>	5		5	
Mineral soil	41		39	2
<i>Nardus stricta</i>	14		14	
<i>Polytrichum</i> spp.	25	1	24	
<i>Pteridium aquilinum</i>	5		5	
<i>Pteridium aquilinum</i> senesced	1		1	
Rock	16		16	
<i>Sorbus aucuparia</i>	1			
<i>Trichophorum cespitosum</i>	1		1	
<i>Vaccinium myrtillus</i>	15		15	
Water	42	1		
Total	427		339	



Annex C:

Error matrices created during spectral clustering



Table C:1. Error matrix for Kinder. Species.

	Bare peat	Betula spp.	Calluna dead	Calluna vulgaris	Chamaenerion angustifolium	Cushion moss	Deschampsia flexuosa	Empetrum nigrum	Erica tetralix	Eriophorum angustifolium	Eriophorum vaginatum	Feather moss	Juncus effusus	Juncus squarrosus	Mineral soil	Nardus stricta	Pinus spp.	Polytrichum spp.	Rock	Salix spp.	Sphagnum capillifolium	Sphagnum cuspidatum	Sphagnum denticulatum	Sphagnum fallax	Sphagnum fimbriatum	Sphagnum palustre	Sphagnum papillosum	Sphagnum subnitens	Sphagnum tenellum	Vaccinium myrtillus	Total	User accuracy	
Bare peat	36																	1														37	0.97
Betula spp.		2			5	1	2	1			5		1	1		2	3			1												24	0.08
Calluna dead			14	2		2		6		1			1																			26	0.54
Calluna vulgaris	1		4	42			2	5	3					2																		62	0.68
Chamaenerion angustifolium		3			5		4				1						2														3	18	0.28
Cushion moss	3		4			6						1	6	1													1	1	1		24	0.25	
Deschampsia flexuosa		2		2	1		4	1		1	2			2		2														1	18	0.22	
Empetrum nigrum			3	3				15		2		2	1	1			1	4														32	0.47
Erica tetralix			1	7			1	6	5				1	2			1															24	0.21
Eriophorum angustifolium								3	1	32	3	1	10					1						1				1	1			54	0.59
Eriophorum vaginatum						2	3			3	14		3	1		3	2			3	1											35	0.40
Feather moss												4												1		1						6	0.67
Juncus effusus						1		1		3		1	12	1		2		1														22	0.55
Juncus squarrosus		1		4			4	1		2	2		3	4		1	3													1	26	0.15	
Mineral soil															6				3			1		1	1							12	0.50
Nardus stricta			1				2				1					5			3													10	0.50
Pinus spp.								1								1	18			1										1	23	0.78	
Polytrichum spp.				2				7					2	1			1	36												2	51	0.71	
Rock															2				35													37	0.95
Salix spp.							1				2		1	1		1				1										1	1	9	0.11
Sphagnum capillifolium							1			2	4		1			1		1	1				1									12	0.00
Sphagnum cuspidatum										1	1				1	2							3									20	0.15
Sphagnum denticulatum							1					1							3													9	0.00
Sphagnum fallax											1										1											8	0.38
Sphagnum fimbriatum											3				2						3											17	0.00
Sphagnum palustre		1					2			1	6		2	1	1	1						1										18	0.00
Sphagnum papillosum										2	4		2			2			1				1	2					2			17	0.00
Sphagnum subnitens										1	2	1	5											1	1	1	1			1		14	0.00
Sphagnum tenellum											2												2	2		1	1					8	0.00
Vaccinium myrtillus		1		1			1	2									3	3						2							25	0.66	
Total	40	10	27	63	11	12	29	49	9	52	53	9	52	19	12	23	34	50	43	6	5	5	7	20	10	9	8	5	5	34	711		
Producer accuracy	0.90	0.20	0.52	0.67	0.45	0.50	0.14	0.31	0.56	0.62	0.26	0.44	0.23	0.21	0.50	0.22	0.53	0.72	0.81	0.17	0.00	0.60	0.00	0.15	0.30	0.00	0.00	0.00	0.00	0.00	0.74		
N (total observations)						711						Overall accuracy	0.46																				
X (Sum of all correct)						330						Kappa	0.44																				
Y (Sum of total user x sum of total producer)						23079																											

Table C:2. Error matrix for Kinder. Transformed divergence stage 2.

	Bare peat	Group 1	Calluna dead	Group 2	Chamaenerion angustifolium	Cushion moss	Empetrum nigrum	Group 3	Group 4	Feather moss	Juncus squarrosus	Mineral soil	Pinus spp.	Polytrichum spp.	Rock	Salix spp.	Sphagnum capillifolium	Sphagnum cuspidatum	Sphagnum denticulatum	Group 5	Sphagnum subnitens	Sphagnum tenellum	Vaccinium myrtillus	Total	User accuracy
Bare peat	36													1										37	0.97
Group 1	9	9			6	1		2	9		1		1										2	32	0.28
Calluna dead			14		2	2	7	4																29	0.48
Group 2	1	3	5	57			9	1			3			3										82	0.70
Chamaenerion angustifolium	8				5				1				2			1							3	20	0.25
Cushion moss	3		4			6	1	11			1									1	1	1		29	0.21
Empetrum nigrum			3	3			17	3		2	2		2	5										37	0.46
Group 3				1		1	2	48	5	2			1	1						2	1			64	0.75
Group 4		6				1		3	24		1		1			1	1	1						39	0.62
Feather moss										3						1				2				6	0.50
Juncus squarrosus		5	1	4			1	8	5		8		4										1	37	0.22
Mineral soil												7			4		1	1	1	2				16	0.44
Pinus spp.		1					1		1				19			1				1			1	25	0.76
Polytrichum spp.				3			7	3			1		1	36									2	53	0.68
Rock												2			35									37	0.95
Salix spp.		1						1	3		1					1							1	9	0.11
Sphagnum capillifolium		1						5	11					1	1	1			1					21	0.00
Sphagnum cuspidatum								1	3			1						3		12		1		21	0.14
Sphagnum denticulatum		1						2				1			3					4				11	0.00
Group 5		2						1	9	1	1	1					1		2	12	3	1		34	0.35
Sphagnum subnitens						1		11	3	1							2		1	5		1		25	0.00
Sphagnum tenellum									2										2	4				8	0.00
Vaccinium myrtillus		2		1			4						3	3						2			24	39	0.62
Total	40	39	27	72	11	12	49	104	76	9	19	12	34	50	43	6	5	5	7	47	5	5	34	711	
Producer accuracy	0.90	0.23	0.52	0.79	0.45	0.50	0.35	0.46	0.32	0.33	0.42	0.58	0.56	0.72	0.81	0.17	0.00	0.60	0.00	0.26	0.00	0.00	0.71		

N (total observations) 711
 X (Sum of all correct) 364
 Y (Sum of total user x sum of total producer) 30886
 Overall accuracy 0.51
 Kappa 0.48

Group 1 Deschampsia flexuosa, Betula spp.
 Group 2 Calluna vulgaris, Erica tetralix
 Group 3 Eriophorum angustifolium, Juncus effusus
 Group 4 Eriophorum vaginatum, Nardus stricta
 Group 5 Sphagnum fallax, S. fimbriatum, S. palustre, S. papillosum

Table C:3. Error matrix for Kinder. Transformed divergence stage 3.

	Bare peat	Group 1	Polytrichum spp.	Group 2	Juncus squarrosus	Chamaenerion angustifolium	Group 3	Group 4	Salix spp.	Feather moss	Rock	Group 5	Sphagnum capillifolium	Group 6	Sphagnum tenellum	Total	User accuracy
Bare peat	37	1	1													39	0.95
Group 1	1	82	6	1	4		6	7		1						108	0.76
Polytrichum spp.		14	39	4	1			3								61	0.64
Group 2		2	2	46		2		6	1			3				62	0.74
Juncus squarrosus		9		6	12		3	40		1					1	72	0.17
Chamaenerion angustifolium				7		9		14	1							31	0.29
Group 3	2	12					26	16		1		2			1	60	0.43
Group 4		1	1	2	1		4	57	1	2		5	2			76	0.75
Salix spp.				1				9	1							11	0.09
Feather moss								9	1	3		3				16	0.19
Rock											37	1		2		40	0.93
Group 5					1			24		1		24	3	5	3	61	0.39
Sphagnum capillifolium			1	1				27	1		1	3		1		35	0.00
Group 6								5			5	7		9		26	0.35
Sphagnum tenellum								2				9		2		13	0.00
Total	40	121	50	68	19	11	39	219	6	9	43	57	5	19	5	711	
Producer accuracy	0.93	0.68	0.78	0.68	0.63	0.82	0.67	0.26	0.17	0.33	0.86	0.42	0.00	0.47	0.00		

N (total observations)	711	Overall accuracy	0.54
X (Sum of all correct)	382		
Y (Sum of total user x sum of total producer)	48728	Kappa	0.49

- Group 1 Calluna vulgaris, Empetrum nigrum, Erica tetralix
- Group 2 Pinus spp., Vaccinium myrtillus
- Group 3 Calluna dead, Cushion moss
- Group 4 Betula spp., Deschampsia flexuosa, Eriophorum angustifolium, Eriophorum vaginatum, Juncus effusus, Nardus stricta
- Group 5 Sphagnum cuspidatum, S. fallax, S. fimbriatum, S. palustre, S. papillosum, S. subnitens
- Group 6 Mineral soil, Sphagnum denticulatum



Table C:4. Error matrix for Kinder. ISODATA species.

	Group 1	Betula spp.	Group 2	Chamaenerion angustifolium	Cushion moss	Deschampsia flexuosa	Eriophorum angustifolium	Eriophorum vaginatum	Feather moss	Juncus effusus	Juncus squarrosus	Group 3	Nardus stricta	Pinus spp.	Rock	Salix spp.	Sphagnum fallax	Vaccinium myrtillus	Total	User accuracy					
Group 1	50		13				1					1							65	0.77					
Betula spp.		2	1	5	1	2		5		1	1		2	3		1			24	0.08					
Group 2	9		132		1	2	1		2	3	4			1					155	0.85					
Chamaenerion angustifolium		3		5		5		1						2				3	19	0.26					
Cushion moss	5				7		1			7	1	3							24	0.29					
Deschampsia flexuosa		2	6	1		4	1	2			1		2					1	20	0.20					
Eriophorum angustifolium	1		4			1	34	3	1	11		3					1		59	0.58					
Eriophorum vaginatum		1			2	5	8	28		7	2	2	5	2		3			65	0.43					
Feather moss							1	1	4	1		2					2		11	0.36					
Juncus effusus			4		1		3		2	14	2	1	2						29	0.48					
Juncus squarrosus	1	1	5			4	2	2		4	6		1	5				1	32	0.19					
Group 3								1		2		28			3		5		40	0.70					
Nardus stricta	1					2		2			1		5						11	0.45					
Pinus spp.												1	1	18		1		1	22	0.82					
Rock						1						4	1		39				45	0.87					
Salix spp.						1		2		1	1	1	1			1		1	9	0.11					
Sphagnum fallax						1		6		1		20	2		1		10		41	0.24					
Vaccinium myrtillus		1	6			1								3			2	27	40	0.68					
Total	67	10	171	11	12	29	52	53	9	52	19	66	23	34	43	6	20	34	711						
Producer accuracy	0.75	0.20	0.77	0.45	0.58	0.14	0.65	0.53	0.44	0.27	0.32	0.42	0.22	0.53	0.91	0.17	0.50	0.79							
N (total observations)						711	Overall accuracy					0.58													
X (Sum of all correct)						414	Kappa					0.54													
Y (Sum of total user x sum of total producer)						48715																			
Group 1	Bare peat, Calluna dead																								
Group 2	Calluna vulgaris, Empetrum nigrum, Erica tetralix, Polytrichum spp.																								
Group 3	Mineral soil, all Sphagnum except fallax																								

Table C:5. Error matrix for Kinder. Spectral position stage 1.

	Bare peat	Group 1	Calluna dead	Calluna vulgaris	Chamaenerion angustifolium	Cushion moss	Empetrum nigrum	Erica tetralix	Group 2	Eriophorum vaginatum	Juncus effusus	Juncus squarrosus	Mineral soil	Pinus spp.	Polytrichum spp.	Rock	Salix spp.	Group 3	Sphagnum cuspidatum	Sphagnum denticulatum	Group 4	Vaccinium myrtillus	Total	User accuracy
Bare peat	36														1								37	0.97
Group 1	4	4		1		1			2	1	1			1								1	12	0.33
Calluna dead			19	5		1	8		5						1						1		40	0.48
Calluna vulgaris	1	2		40			4	3	1			3			3								57	0.70
Chamaenerion angustifolium		8			9				1	2				3			1					1	25	0.36
Cushion moss	3		4			7	2		4		8	1						1			1		31	0.23
Empetrum nigrum				3			13		2		1			1	3								23	0.57
Erica tetralix		1	2	6			5	6			1												21	0.29
Group 2		1				1			13		6							3				1	25	0.52
Eriophorum vaginatum		4				1			17	33	5	2		2			2						66	0.50
Juncus effusus				1		1	1		18	1	15				3			1			2		43	0.35
Juncus squarrosus		4	1	4			3		3	1	5	10		5									38	0.26
Mineral soil													9			3		3	1	1	1		18	0.50
Pinus spp.									1					18									19	0.95
Polytrichum spp.				2			10				2	1		1	36							2	54	0.67
Rock																36							36	1.00
Salix spp.		10			1				6	10	1	1					3					1	34	0.09
Group 3		2							3	4	1										2	5	34	0.50
Sphagnum cuspidatum									5	1	4		2					9	4	3	4		32	0.13
Sphagnum denticulatum		1									2		1			2		4		1	4		15	0.07
Group 4			1						3							2					2		8	0.25
Vaccinium myrtillus		2		1	1		3					1		3	3			2				27	43	0.63
Total	40	39	27	63	11	12	49	9	84	53	52	19	12	34	50	43	6	40	5	7	22	34	711	
Producer accuracy	0.90	0.10	0.70	0.63	0.82	0.58	0.27	0.67	0.15	0.62	0.29	0.53	0.75	0.53	0.72	0.84	0.50	0.43	0.80	0.14	0.09	0.79		

N (total observations)	711	Overall accuracy	0.50
X (Sum of all correct)	358		
Y (Sum of total user x sum of total producer)	25715	Kappa	0.48

- Group 1 Deschampsia flexuosa, Betula spp.
- Group 2 Eriophorum angustifolium, feather moss, Nardus stricta
- Group 3 Sphagnum capillifolium, S. fallax, S. fimbriatum, S. subnitens
- Group 4 Sphagnum palustre, S. papillosum, S. tenellum



Table C:6. Error matrix for Kinder. Spectral position stage 2.

	Bare peat	Group 1	Group 2	Group 3	Group 4	Group 5	Juncus effusus	Juncus squarrosus	Group 6	Salix spp.	Group 7	Group 8	Vaccinium myrtillus	Total	User accuracy
Bare peat	37			2										39	0.95
Group 1		40		1	1	6		1		2	3		3	57	0.70
Group 2		2	23	2	6	8	4		1		2			48	0.48
Group 3		1	7	2	83	18	2	4						117	0.71
Group 4			1	6	13	26	4	1	2					53	0.49
Group 5			9	3			53	8	1		3	5	1	83	0.64
Juncus effusus				1	3	3	21	22	1			2		53	0.42
Juncus squarrosus			14	4	5	1	14	7	8				2	55	0.15
Group 6			1						43		2			46	0.93
Salix spp.			1			6	1	1		1	1		1	12	0.08
Group 7			2				21	2	1	3		29	5	63	0.46
Group 8						4	4	4	8		18	6		40	0.15
Vaccinium myrtillus			9		4	3		1					28	45	0.62
Total		40	84	39	113	58	137	52	19	55	6	62	12	711	
Producer accuracy		0.93	0.48	0.59	0.73	0.45	0.39	0.42	0.42	0.78	0.17	0.47	0.50	0.82	

N (total observations)	711	Overall accuracy	0.56
X (Sum of all correct)	399		
Y (Sum of total user x sum of total producer)	48205	Kappa	0.51

- Group 1: Betula spp, Chamaenerion angustifolium, Deschampsia flexuosa, Pinus spp.
- Group 2: Calluna dead, cushion moss
- Group 3: Calluna vulgaris, Polytrichum spp.
- Group 4: Empetrum nigrum, Erica tetralix
- Group 5: Eriophorum angustifolium, E. vaginatum, feather moss, Nardus stricta
- Group 6: Mineral soil, Rock
- Group 7: Sphagnum capillifolium, S. fallax, S. fimbriatum, S. palustre, S. papillosum, S. subnitens, S. tenellum
- Group 8: Sphagnum cuspidatum, S. denticulatum

Table C:7. Error matrix for Kinder. Spectral position stage 3.

	Bare peat	Group 1	Vaccinium myrtillus	Group 2	Group 3	Group 4	Group 5	Total	User accuracy
Bare peat	39	2			2			43	0.91
Group 1	1	85		18	18			122	0.70
Vaccinium myrtillus		5	31	3	12		1	52	0.60
Group 2		17		31	40	10		98	0.32
Group 3		2	2	5	67	15	8	99	0.68
Group 4		2	1	1	54	101	13	172	0.59
Group 5					7	11	107	125	0.86
Total	40	113	34	58	200	137	129	711	
Producer accuracy	0.98	0.75	0.91	0.53	0.34	0.74	0.83		
N (total observations)								711	
X (Sum of all correct)								461	Overall accuracy 0.65
Y (Sum of total user x sum of total producer)								82447	Kappa 0.58
Group 1	Calluna vulgaris, Polytrichum spp.								
Group 2	Empetrum nigrum, Erica tetralix								
Group 3	Betula spp., Calluna dead, Chamaenerion angustifolium, Cushion moss, Deschampsia flexuosa, Juncus effusus, Juncus squarrosus, Pinus spp.								
Group 4	Eriophorum angustifolium, E. vaginatum, Feather moss, Nardus stricta								
Group 5	Mineral soil, Rock, Sphagnum capillifolium, S. cuspidatum, S. denticulatum, S. fallax, S. fimbriatum, S. palustre, S. papillosum, S. subnitens, S. tenellum								